

THE ROLE OF HER2 IN CANINE MAMMARY CANCER

A thesis submitted to the University of Kent for the degree of
Doctorate of Philosophy in Biochemistry

2012

by **Stephanie Jane Magub**

School of Biosciences

University of Kent at Canterbury



DECLARATION

No part of this thesis has been submitted in support of an application for any degree or qualification of the University of Kent or any other institute of learning.

Stephanie J. Magub

30th July, 2012

ACKNOWLEDGMENTS

This thesis would not have been made possible without the help, love and support of so many people.

Many thanks to members of the Gullick lab (past and present) for all of their advice and support, in particular my supervisor Professor Bill Gullick for his advice throughout my project and especially in writing this thesis, and also Edith Blackburn for her unending patience and advice!

I am grateful to Dr Richard C. Bird and Professor Kari Alitalo for their provisions of the CMT28 and NEN-7 cell lines respectively. Thanks also to Professor Ken Smith of the Royal Veterinary College for making samples of malignant canine mammary cancer available for use in this project.

None of this research would have been possible without the generous financial support of Pfizer Animal Health. I am particularly thankful to Dr Karen Greenwood, Dr Theo Kanellos and Christine Berger who were valuable in helping us secure funding.

I've made too many friends in Biosciences over the years to possibly thank you all – but all of you have helped me in some way, and I would never have made it this far without all the advice, the support and the laughs!

I never would have made it as far as I have if it wasn't for the unending love and support of my Mum, Dad, little sister Ally and Chris's family.

But the most special thank you goes to Chris, who has been my rock at the end of every tough day, who put the smile back on my face when I couldn't see the light at the end of the tunnel, and who held my hand and wiped away the tears when it all got a little too much. Thank you.

CONTENTS

Declaration	i
Acknowledgments.....	ii
Figure List	x
Table List.....	xiv
Abbreviations	xv
Abstract	xix

Chapter One: Introduction

1.1. Cancer	1
1.1.1. The History of Cancer.....	1
1.1.2. What is Cancer?	2
1.2. Receptor Tyrosine Kinases and Cancer.....	7
1.2.1. The Epidermal Growth Factor Receptor Family.....	7
1.2.2. EGFR Structure, Activation and Cell Signalling.....	9
1.2.3. The Type 1 Growth Factor Receptor Family and Cancer	13
1.2.3.1. HER2 and Cancer	14
1.3. Cancer Therapies	16
1.3.1. “An Ounce of Prevention is Worth a Pound of Cure”	16
1.3.2. Treating an Established Disease.....	17
1.3.2.1. Small molecule tyrosine kinase inhibitors	17
1.3.2.2. Antibody Therapies.....	18
Monoclonal antibodies	18
Immunoconjugates	19
Multistep targeted approaches	20
Current Antibody Therapies.....	20

1.2.3. Drug Resistance.....	21
1.4. Canine Cancer.....	22
1.4.1. Causes and Epidemiology.....	22
1.4.1.1. Carcinogens and Age.....	22
1.4.1.2. The Problem with Pedigree.....	23
1.4.1.3. Papillomaviruses and Canine Cancer.....	27
1.4.2. The Market in Animal Health.....	28
1.4.3. Treatment.....	29
1.4.4. Comparative Oncologies.....	31
1.5. Statement of Purpose & Experimental Aims.....	33

Chapter Two: Materials & Methods

2.1. Antibodies used in this study.....	34
2.2. Immunohistochemistry.....	35
2.2.1. Canine Tissues.....	35
2.2.2. Staining.....	36
2.3. Cell Lines and Culture.....	37
2.3.1. Cell Lines Used In This Study.....	37
2.3.2. Routine Cell Culture and Maintenance.....	38
2.3.3. Freezing Down Cell Stocks.....	39
2.4. Immunofluorescence.....	39
2.5. Small Molecule Tyrosine Kinase Inhibitors.....	40
2.6. Growth Factors.....	41
2.7. Observing Kinase Inhibition using SMTKIs.....	41
2.7.1. The Effects of TKIs on Kinase Activity.....	41
2.7.2. The Effect of Drug Vehicle on Kinase Inhibition.....	42
2.8. Creation of Cell Lysate.....	43

2.9.	SDS-PAGE and Western Blotting.....	44
2.9.1.	Bradford Assay	44
2.9.2.	SDS-PAGE	44
2.9.3.	Western Blotting	45
2.10.	Cell Proliferation Assays	47
2.10.1.	Cell Harvesting, Counting & Seeding	47
2.10.2.	Reading Cell Proliferation Assays.....	48
2.10.3.	Generation of Mammalian Cell Growth Curves.....	48
2.10.4.	Investigating the Effect of Growth Factors on Cell Proliferation.....	48
2.10.5.	Investigating the Effect of Tyrosine Kinase Inhibitors on Cell Proliferation ...	49
2.11.	siRNA Knockdown.....	49
2.11.1.	siRNA Design	49
2.11.2.	Observing siRNA Knockdown.....	50
2.11.3.	Cell Proliferation Assays Using siRNA	51
2.11.4.	Observing Apoptosis Using Propidium Iodide	51
2.12.	RNA Isolation	52
2.13.	cDNA Synthesis by Reverse Transcription	53
2.14.	PCR & Agarose Gel Electrophoresis.....	53
2.14.1.	Polymerase Chain Reaction	53
2.14.2.	Agarose Gel Electrophoresis.....	54

Chapter Three: Bioinformatical Analysis of Canine HER2

3.1.	Introduction.....	55
3.2.	Aims	58
3.3.	Results.....	58
3.3.1.	Comparisons of Human and Canine HER2	58
3.3.1.1.	Dot Plot Analysis.....	63

3.3.1.2.	Whole Protein BLAST Alignment	64
3.3.1.3.	Tendency for HER2 to form an Ordered Structure.....	66
3.3.2.	Bioinformatic Analysis of Canine HER2 Alternative Splicing.....	70
3.3.2.1.	Comparing Exons Between the Human and Canine HER2 Genes	70
3.3.2.2.	Detecting Alternative Canine HER2 Transcripts Using the EST Database ..	77
3.3.3.	Observations on Chromosome Structures.....	81
3.5.	Discussion	83
3.5.1.	Gene & Chromosome Structure Comparisons.....	83
3.5.2.	Protein Structure Comparisons.....	84
3.5.3.	Summary	84

Chapter Four: Surveying the levels of EGF Receptor and Ligand Expression in Healthy Canine Tissue Samples

4.1.	Introduction.....	86
4.2.	Experimental Aims.....	87
4.3.	Results.....	87
4.3.1.	Determining if Available Antibodies were Suitable for Use Against Canine Antigen.....	87
4.3.2.	Determining EGF Receptor and Ligand Expression in Normal Canine Tissue ...	88
4.3.2.1.	The Central Nervous System	91
	Cerebral Cortex	91
4.3.2.2.	The Respiratory System.....	94
	Lung.....	94
4.3.2.3.	The Gastrointestinal System.....	97
	Tongue	97
	Oesophagus.....	101
	Stomach	103
	Liver.....	106

Pancreas.....	109
Rectum.....	112
4.3.2.4. The Urinary System.....	115
Kidney.....	115
Bladder.....	118
4.3.2.5. Miscellaneous Tissues.....	121
Vasculature.....	121
Muscle.....	122
4.3.3. Results of Comparisons in EGF Receptor and Ligand Expression Between <i>C. familiaris</i> and <i>H. Sapiens</i>	122
EGF Receptors.....	124
Neuregulins.....	124
Amphiregulin, Epigen and TGF α	124
4.4. Discussion.....	125
4.4.1. The Expression of the EGF Family in Normal Canine Tissues.....	125
4.4.2. Comparing EGF Family Expression between Canine and Human Tissues.....	127
4.4.3. Limitations of Immunohistochemical Studies.....	127
4.4.4. The Role of Immunohistochemical Studies in Drug Development and Medicine.....	128

Chapter Five: Surveying the levels of EGF Receptor Expression in Benign and Malignant Canine Mammary Cancers

5.1. Introduction.....	129
5.2. Aims.....	130
5.3. Results.....	130
5.3.1. Determination of the EGF Receptor and Ligand Expression in Benign Canine Mammary Cancers.....	130
5.3.2. Determination of the EGF Receptor and Ligand Expression in Malignant Canine Mammary Cancers.....	133

5.4.	Discussion	137
5.4.1.	The Heterogeneity of Canine Mammary Cancer	137
5.4.2.	Statistical Analysis.....	138

Chapter Six: Observing Small Molecule Inhibitor Efficacy using a Human EGFR/Rat HER2 Chimeric Receptor

6.1.	Introduction.....	139
6.1.1.	Small Molecule Tyrosine Kinase Inhibitors and Drug Discovery.....	139
6.1.2.	Using Human Small Molecule Tyrosine Kinase Inhibitors in Dogs.....	140
6.2.	Aims	144
6.3.	Results.....	144
6.3.1.	Detecting Chimeric Receptor Phosphorylation in the NEN-7 Cell Line.....	144
6.3.2.	Determining the Suitability of SMTKIs.....	145
6.3.3.	Determining Relative Potencies of the Observed SMTKIs	150
6.4.	Discussion	150
6.4.1.	Reversible versus Irreversible Inhibitors.....	151
6.4.2.	Pharmacokinetics versus Pharmacodynamics	151
6.4.3.	Taking SMTKIs into Tests with Canine Mammary Cancer Cells	152

Chapter Seven: Characterising the CMT28 Cell Line and Determining the Role HER2 Plays in the Growth of Canine Mammary Cancer

7.1.	Introduction.....	154
7.2.	Aims	155
7.3.	Results.....	156
7.3.1.	Determining CMT28 Receptor Status by PCR	156
7.3.2.	Determining CMT28 Receptor Status by Western Blotting.....	159
7.3.3.	Using Herceptin in Canine Mammary Cancer	160
7.3.4.	Determining to What Extent Canine Mammary Cancer Relies on HER2.....	164
7.3.4.1.	Generating CMT28 Growth Curve	164

7.3.4.2. Stimulating CMT28 Growth by the Application of Growth Factors.....	165
7.3.4.3. Inhibiting CMT28 Growth by the Application of SMTKIs.....	167
7.3.4.5. Inhibiting CMT28 Growth by the Application of siRNA & Establishing how siRNA Affects CMT28 Cell Growth.....	169
Inhibiting CMT28 Cell Growth with siRNA	169
Does siRNA Induce Apoptosis in CMT28 Cells?.....	171
7.4. Discussion	174

Chapter Eight: Discussion

8.1. Results of This Project.....	177
8.2. The Future.....	182

References.....	183
------------------------	------------

Appendices..... A

Appendix I: Examples of uncropped PCR gel images and Western Blot autoradiographs	A-I
Appendix II: Image catalogue of immunohistochemical stains on normal and cancerous canine tissues.....	A-IV
Appendix III: Raw data from cell proliferation experiments.....	A-V
Appendix IV: Western Blots for HER3	A-XI

FIGURE LIST

Figure 1.1: The hallmarks of cancer	4
Figure 1.2: The 20 most commonly diagnosed cancers worldwide	5
Figure 1.3: Cancer incidences in the UK.....	6
Figure 1.4: The structure of the ErbB receptors.....	10
Figure 1.5: Comparisons of the extracellular domains of the ErbB receptors.....	10
Figure 1.6: Conformational change undergone by the ErbB receptors	11
Figure 1.7: Paracrine, autocrine and juxtacrine signalling	12
Figure 1.8: HER2 overexpression in breast cancer as determined by IHC	14
Figure 1.9: Causes of HER2 overexpression	15
Figure 1.10: Antibody therapies.....	18
Figure 1.11: Comparisons of working dogs and their show counterparts	24
Figure 1.12: Incidences of cancer in pet dogs	26
Figure 1.13: Pet insurance from high street vendors.....	28
Figure 3.1: BLAST alignments of human HER2 sequences	60
Figure 3.2: Ensembl alignments of human HER2 transcripts	62
Figure 3.3: Dot plot analysis of human and canine HER2	63
Figure 3.4: BLAST analysis of human and canine HER2 sequences.....	65
Figure 3.5: The "entropic brush" of the ErbB receptors	67
Figure 3.6: IUPRED plots comparing the tendencies for human and canine HER2 to form an ordered structure	69
Figure 3.7: Human and canine HER2 alignments with the Ensembl Gene Ontology Tool.....	71
Figure 3.8: BLAST alignments of human and canine HER2 exons.....	72
Figure 3.9: Canine exons mapped to the HER2 gene	76
Figure 3.10: tblastn alignment of canine HER2 peptide sequence against the EST library ...	77

Figure 3.11 Annotated view of the tblastn alignment of canine HER2 peptide against the EST library.....	80
Figure 3.12: Comparisons between human and canine chromosomes on which HER2 is located.....	82
Figure 4.1: Immunohistochemical stains of canine cerebral cortex	93
Figure 4.2: Immunohistochemical stains of canine lung.....	96
Figure 4.3: Immunohistochemical stains of canine tongue	100
Figure 4.4: Immunohistochemical stains of canine oesophagus	102
Figure 4.5: Immunohistochemical stains of canine stomach.....	105
Figure 4.6: Immunohistochemical stains of canine liver.....	108
Figure 4.7: Immunohistochemical stains of canine pancreas.....	111
Figure 4.8: Immunohistochemical stains of canine rectum	114
Figure 4.9: Immunohistochemical stains of canine kidney	117
Figure 4.10: Immunohistochemical stains of canine bladder	120
Figure 5.1: Examples of benign complex adenoma of canine mammary cancer stained for the four members of the EGF receptor family.....	132
Figure 5.2: Examples of malignant canine mammary cancer stained for the four members of the EGF receptor family	135
Figure 5.3: Examples of malignant canine mammary cancer stained for the presence of NRG1 α , NRG1 β , NRG2 α and NRG2 β	136
Figure 6.1: Typical timeline of the evolution of a pharmaceutical compound	139
Figure 6.2: Cartoon depiction of the construct within the NEN-7 cell line	140
Figure 6.3: BLAST analysis of kinase domains rat and dog and human and dog HER2.....	142
Figure 6.4: 3D mapping of substituted residues in intracellular canine HER2.....	143
Figure 6.5: NEN-7 cells were stimulated with four different concentrations of EGF.....	144
Figure 6.6a: Western blot of NEN-7 cells treated with Iressa.....	146
Figure 6.6b: Western blot of NEN-7 cells treated with Tyrphostin.....	146
Figure 6.6c: Western blot of NEN-7 cells treated with Canertinib.....	147
Figure 6.6d: Western blot of NEN-7 cells treated with Lapatinib	147

Figure 6.6e: Western blot of NEN-7 cells treated with Neratinib	148
Figure 6.6f: Western blot of NEN-7 cells treated with PD158780	148
Figure 6.6g: Western blot of NEN-7 cells treated with ZM260603	149
Figure 6.7: The specificity profiles of 20 separate SMTKIs against the kinome	153
Figure 7.1a: PCR experiments using MDCK cDNA	157
Figure 7.1b: PCR experiments using CMT28 cDNA	158
Figure 7.2: Western blots comparing lysate from CMT28 cells with lysates from positive control cell lines	159
Figure 7.3a: Determining if Herceptin is able to bind to canine HER2 using immunofluorescent staining	162
Figure 7.3b: 3D structure of Herceptin Fab in complex with human HER2	163
Figure 7.4: Growth curve generated for CMT28 cells	165
Figures 7.5a & b: Stimulating CMT28 cell growth by the application of ligands of the EGF family.....	166
Figure 7.6a & b: Inhibiting CMT28 cell growth by the application of Lapatinib and Neratinib to cells	168
Figure 7.7a: Knockdown of canine HER2 using siRNA.....	169
Figure 7.7b: The effect of HER2 specific siRNAs on CMT28 cell proliferation	170
Figure 7.8a: Determining the number of CMT28 cells undergoing apoptosis following treatment with siRNA.....	171
Figure 7.8b: Examples of fluorescent images obtained in the course of propidium iodide experiments	173
Figure 7.9: Graphical representation of results obtained from propidium iodide experiments	174
Figure A-1: Examples of uncropped PCR agarose gels	A-I
Figure A-2: Examples of uncropped Western Blot autoradiographs	A-II
Figure A-3: Example of uncropped Western Blot where SKBR3 lysate was compared with CMT28 lysates	A-III
Figure A-4: Example of uncropped Western Blot where CMT28 cells were treated with siRNA	A-III

Figure A-5: Example of Western Blot for HER3 A-XI

TABLE LIST

Table 2.1– Primary antibodies used throughout this study	34
Table 2.2 – Secondary antibodies used in this study	35
Table 2.3 – Experimental conditions of SMTKI inhibition tests	41
Table 2.4 – Volumes of vehicles and concentrations of SMTKIs used	42
Table 2.5 – Volumes of vehicle applied to NEN-7 cells to test for non-specific cytotoxicity	43
Table 2.6 – Concentration of SMTKIs used in cell proliferation experiments.....	49
Table 2.7 – Scaling up and down siRNA transfections with Lipofectamine 2000	51
Table 2.8 – Thermo cycling conditions	54
Table 3.1 – Ensembl entries for human ERBB2 gene	59
Table 3.2 – Canine and Human HER2 exon comparisons.....	74
Table 4.1 – Comparisons of canine antigens with respective antibody sequences.....	88
Table 4.2 - Immunoreactivity of epidermal growth factor receptors and their ligands in normal canine tissues.....	90
Table 4.3 – Immunoreactivity of epidermal growth factor receptors and their ligands in normal human tissue	123
Table 5.1 – Immunoreactivity of the epidermal growth factor family of receptors in benign canine mammary cancer specimens.....	131
Table 5.2 – Immunoreactivity of the EGF receptors and neuregulins 1 and 2 to samples of malignant canine mammary cancer.....	134
Table 5.3 – Percent of benign and malignant cases which showed strong (+++) and moderate (++) staining of the receptors.....	138
Table 6.1 – Relative potencies of observed SMTKIs.....	150
Table 7.1 – Comparison of HER2 binding residues between human and dog proteins.....	164

ABBREVIATIONS

ADEPT	Antibody-directed enzyme pro-drug therapy
AG1478	Tyrphostin
AIDS	Acquired immunodeficiency syndrome
AKT	Protein kinase B
AML	Acute myeloid leukaemia
APS	Ammonium persulphate
AREG	Amphiregulin
ATCC	American Type Culture Collection
ATP	Adenosine triphosphate
BBC	British Broadcasting Corporation
BLAST	Basic Local Alignment Search Tool
BSA	Bovine serum albumin
BTC	Betacellulin
CCDS	Consensus Coding Sequence
CCOGC	Canine Comparative Oncology and Genomics Consortium
CI-1033	Canertinib
CMT28	Canine mammary tumour cells
COPV	Canine oral papilloma virus
DAB	3,3'-Diaminobenzidine
DMEM	Dubecco's Modified Eagle Medium
DMSO	Dimethyl sulfoxide
DNA	Deoxyribose nucleic acid
dNTPs	deoxynucleotide triphosphates
DPX	N,N'-4-xylylenebis(pyridinium)
DTT	Dithiothreitol
ECL	Enhanced chemiluminescence
EDTA	Ethylenediaminetetraacetic acid
EGF	Epidermal growth factor
EGFR	Epidermal growth factor receptor
ER	Estrogen receptor
EST	Expressed sequence tag

FACS	Fluorescent automated cell sorting
FCS	Foetal calf serum
FGF	Fibroblast growth factor
FISH	Fluorescent <i>in situ</i> hybridisation
FITC	Fluorescein isothiocyanate
GIST	Gastrointestinal stromal tumour
GW-2016	Lapatinib
HB-EGF	Heparin binding EGF-like growth factor
HEK-293	Human embryonic kidney cell line
HER2	Human epidermal growth factor receptor 2
HER3	Human epidermal growth factor receptor 3
HER4	Human epidermal growth factor receptor 4
HIV	Human immunodeficiency virus
HKI-272	Neratinib
HPV	Human papilloma virus
HRP	Horseradish peroxidase
IF	Immunofluorescence
IHC	Immunohistochemistry
ISD	Information Services Division
I-TASSER	Iterative Threading ASSEmblY Refinement
IUPRED	Prediction of Intrinsically Unstructured Proteins
JM or JmD	Juxtamembrane domain
KD	Kinase domain
KRAS	V-Ki-ras2 Kirsten rat sarcoma viral oncogene homolog
MAPK	Mitogen-activated protein kinase
MDCK	Madin-Derby Canine Kidney cell line
MET	Hepatocyte growth factor receptor
NCBI	National Center for Biotechnology Information
NEN-7	Mouse fibroblast cell line stably transfected with a chimeric human EGFR/rat c-erbB2 proto-oncogene
NIH3T3	Swiss mouse embryo fibroblast cell line
NRG	Neuregulin
NRTK-1	Neurotrophic Tyrosine Kinase receptor, type 1
NSCLC	Non-small cell lung cancer

OD	Optical density
PBS	Phosphate buffered saline
PCR	Polymerase chain reaction
PDB	Protein Data Bank
PI3K	Phosphoinositide 3-kinase
PSA	Prostate serum antigen
PTEN	Phosphatase and tensin homolog
RET	Rearranged during transfection proto-oncogene
RISC	RNA-induced silencing complex
RNA	Ribonucleic acid
RTK	Receptor tyrosine kinase
RT-PCR	Reverse-transcription polymerase chain reaction
sc-FV	Single-chain variable fragment
SDS-PAGE	Sodium dodecyl sulphate-polyacrylamide gel electrophoresis
siRNA	Small interfering ribonucleic acid
SIV	Simian immunodeficiency virus
SMTKI	Small molecule tyrosine kinase inhibitor
TAE	Tris-acetate- ethylenediaminetetraacetic acid
TEMED	Tetramethylethylenediamine
TGF- α	Transforming growth factor alpha
TKI	Tyrosine kinase inhibitor
TRITC	Rhodamine
UK	United Kingdom
US	United States
USA	United States of America
UTR	Untranslated region
UV	Ultraviolet
VEGF	Vascular endothelial growth factor
WB	Western Blot

Immunohistochemical Annotations

Al	Alveoli
Bd	Bile duct

Br	Bronchiole
CL	Crypt of Lieberkühn
D	Ducts
Dt	Distal convoluted tubule
FiP	Filiform papillae
FoP	Foliate papillae
GC	Goblet cells
Gg	Gastric glands
Gp	Gastric pits
Ha	Hepatic artery
Hv	Hepatic vein
IL	Islet of Langerhaans
LP	Lamina propia
MM	Muscularis mucosae
PA	Pancreatic acinii
Pn	Pyramidal neurone
Pt	Proximal convoluted tubule
RC	Renal corpuscle
SC	Stem cells
SM	Skeletal muscle
SSE	Stratified squamous epithelium
TE	Transitional epithelium

ABSTRACT

While the role of the EGF family (in particular the HER2 receptor) has been well documented in human cancers, its role in the progression of canine mammary cancer is less well understood. Dogs have long been used as models of human disease in the development of human therapeutics, however the animal health market is only just beginning to develop animal-specific therapies. This project aimed to survey the expression of the complete family of EGF receptors and ligands in a range of normal tissues, and also in benign and malignant canine mammary cancers. In addition to this, the functional role of HER2 in maintaining transformed canine mammary cancer cells was also explored through cell proliferation assays, in which cells were treated with specific SMTKIs and siRNA. Results showed that the EGF family was well-distributed throughout normal canine tissues – in particular in the GI tract – and that inhibiting HER2 with SMTKIs and knocking it down with siRNA caused a decrease in cell proliferation, suggesting the receptor is involved in the growth of canine mammary cancer cells. These results indicate that the dog may not only be a more useful model in studying human disease than previously believed, but that the animal health market may also stand to benefit from the years of research in which companion animal disease has been somewhat overlooked – a plethora of intermediate compounds exist which have been evaluated in the search for the most suitable therapies, and which may be of use in companion animal therapeutics.

CHAPTER ONE

Introduction

1.1. CANCER

1.1.1. The History of Cancer

From modern analysis of the fossil record, there appears to be little reliable evidence to suggest that cancer afflicted ancient animals (other than some possible evidence in an Edmontosaurus fossil (Natarajan *et al.*, 2007) and other fossil remains (Capasso, 2005)) or hominids (with the exception of a single Neanderthal skull with what appears to possibly be a meningioma (Czarnetzki, 1980)) (David & Zimmerman, 2010). This has led some to suggest that cancer is possibly a modern, man-made disease – a product of our modern lifestyle and pollution (David & Zimmerman, 2010). However there is some classical evidence to suggest otherwise. The first recorded instance of cancer as a recognised disease in medical history was by the ancient Egyptians between 3000-1500 B.C, in which papyri refer to a number of tumours of the breast. Later, around 400 B.C., the Ancient Greek physician Hippocrates studied the disease and is widely credited with being the first physician to distinguish between benign and malignant tumours (Cancer Research UK, 2012).

Little more was understood about cancer for another 2000 years. It was not until the 18th century that Dr Percival Potts noticed an increased incidence of scrotal cancer in chimney sweeps, and deduced that a component in soot may be causing the disease. While at the time nothing could be done to prove this (indeed, it took another century before the carcinogen in soot could be identified) chimney sweeps were encouraged to wash more thoroughly, and over time these incidences of scrotal cancer in men dropped. In 1839, French gynaecologist Recamier described the invasion of cancer cells into the bloodstream, and coined the term metastasis. Some 50 years later, the x-ray was discovered and found to be of use in treating cancer – and still is to this day in radiotherapy (Cancer Research UK, 2012).

Despite this advance, it was not until 1953, when James Watson and Francis Crick discovered the structure of DNA that cells could begin to be truly understood at a

molecular level, and since this time there has been an enormous increase in our understanding of cancer as a disease and how we may treat it.

1.1.2. What is Cancer?

The nature of cancer as a disease is now better understood, thanks in part to our advanced understanding of cell biology. 'Cancer' is a term applied to malignant neoplasms, where cells are able to divide and grow in an uncontrolled manner resulting in the formation of a tumour. This tumorigenic growth presents a number of problems, among them:

- Tumour enlargement, where the tumour will increase in size. This is often the primary cause of symptoms in cancer patients, and can have a number of detrimental effects, from increased pressure on surrounding organs to pain and discomfort.
- Tumour invasion, where the tumour will project into nearby tissues, embedding itself more deeply into healthy areas.
- Metastasis, where cells will break off of the primary tumour and travel through the lymphatic and circulatory systems, eventually forming secondary tumours at other sites.

In order for a cell to become cancerous, it must undergo a number of transformations which confer on it a certain set of distinguishing attributes. Hanahan & Weinberg suggest that there are six hallmarks of cancer (Figure 1.1) (Hanahan & Weinberg, 2000):

1. Self-sufficiency in growth signals: growth signals are typically transferred by transmembrane receptors which bind specific classes of signalling molecules. Cancerous cells however show a greatly reduced reliance on this, instead possessing some inherent growth stimulus or producing their own growth signals. This reduces their dependence on their normal microenvironment, and enables their uncontrolled growth. Studies have also shown that the presence of fusion genes may also allow a cancerous cell to grow in an uncontrollable manner, for example gene fusion may bring about constitutive activation of receptors involved in cell growth, or a fusion may attach a promoter to a particular gene which would then upregulate its expression (Edwards, 2010).

2. Insensitivity to antigrowth signals: cancer cells are able to overcome antigrowth mechanisms, primarily through disruption of the retinoblastoma protein (pRb) which (in a healthy cell) blocks proliferation through the inhibition of transcription factors associated with taking a cell from G1 into S-phase (Weinberg, 1995).
3. Evasion of apoptosis: in order for a collection of cells to form a tumour, in addition to there being uncontrolled cell growth, there must also be a lack of cell death. In cancer cells, apoptosis is typically avoided through mutation of the p53 tumour suppressor gene (found in more than 50% of cancers), which renders its protein product inactive (Harris, 1996).
4. Limitless replicative potential: it has been shown that cells in culture appear to undergo a certain number of replications, following which they enter into senescence (Hayflick, 1997). Experiments have shown that disabling the p53 and pRb tumour suppressor proteins causes cells to avoid this senescence and go into a state termed "crisis" – characterised by massive cell death, chromosome abnormalities and the occasional emergence of a cell variant which can multiply without limit (immortalisation) (Wright *et al.*, 1989). Telomerase activation within cancerous cells is also responsible for cell immortalization, and has been observed in roughly 90% of human cancers (Shay & Bacchetti, 1997).
5. Sustained angiogenesis: in many cases, angiogenesis in tumours occurs through alteration in the gene transcription of growth factors such as vascular endothelial growth factor (VEGF) and fibroblast growth factor (FGF) which become upregulated, and/or through the downregulation of inhibitors such as thrombospondin-1 or β -interferon (Singh *et al.*, 1995; Volpert *et al.*, 1997).
6. Tissue invasion and metastasis: metastasis to distant regions of the body from their original primary sites are the cause of 90% of deaths from cancer (Sporn, 1996). It has been noted that several of the proteins involved in tethering cells to their surroundings (members of the calcium-dependant cadherin families and integrins) are altered in cells with invasive and metastatic capabilities (Aplin *et al.*, 1998), and also that extracellular proteases are upregulated in

such cells (Coussens & Werb, 1996; Chambers & Matrisian, 1997). Such proteases could alter integrin stability and facilitate cell invasion (Werb, 1997).

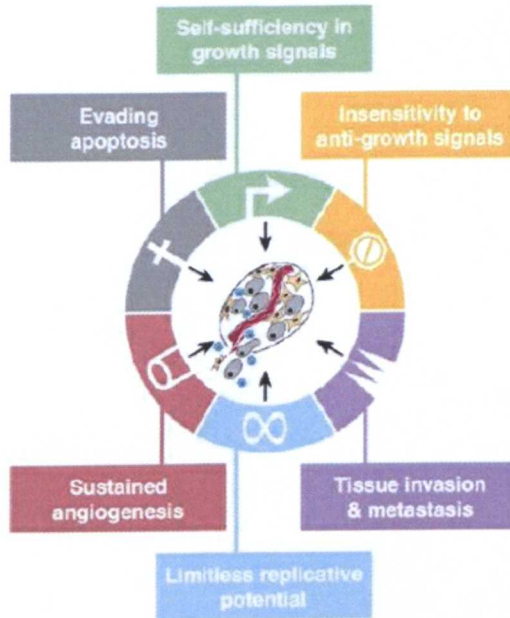


Figure 1.1: The functional changes that a cancer acquires through its development (Hanahan & Weinberg, 2000).

The World Health Organisation estimated in 2008 that 12.6 million new cases of the disease were reported (300,000 of which were in the United Kingdom), and roughly 7.6 million people died of cancer worldwide (156,000 in the United Kingdom) (Lyon, France: International Agency for Research on Cancer, 2010). Of these cancers, lung cancer is the most commonly diagnosed globally (13%) followed by cancer of the female breast (11%) (Figure 1.2), with lung, stomach and liver cancers being the most deadly cancers globally (United Nations, 2009; Lyon, France: International Agency for Research on Cancer, 2010; Ferlay *et al.*, 2010; Cancer Research UK, 2011b).

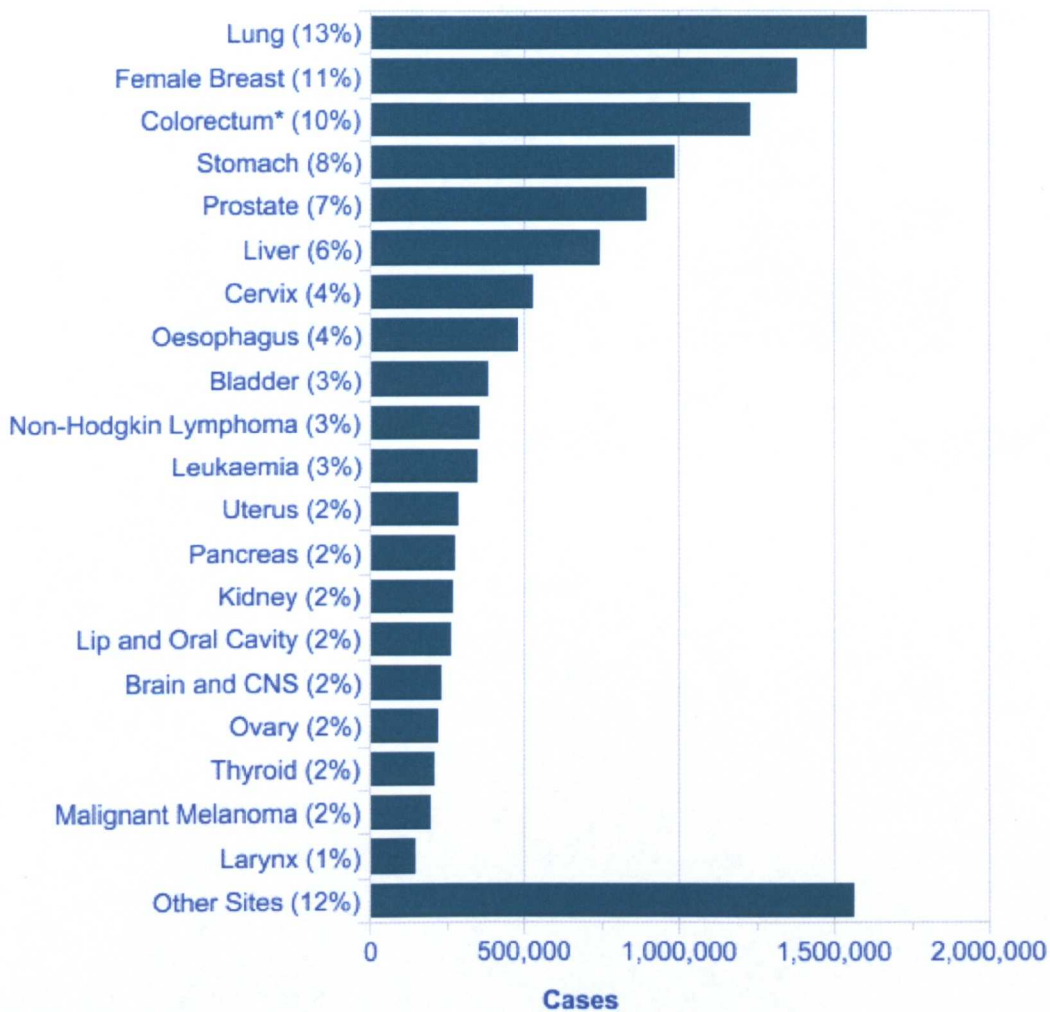
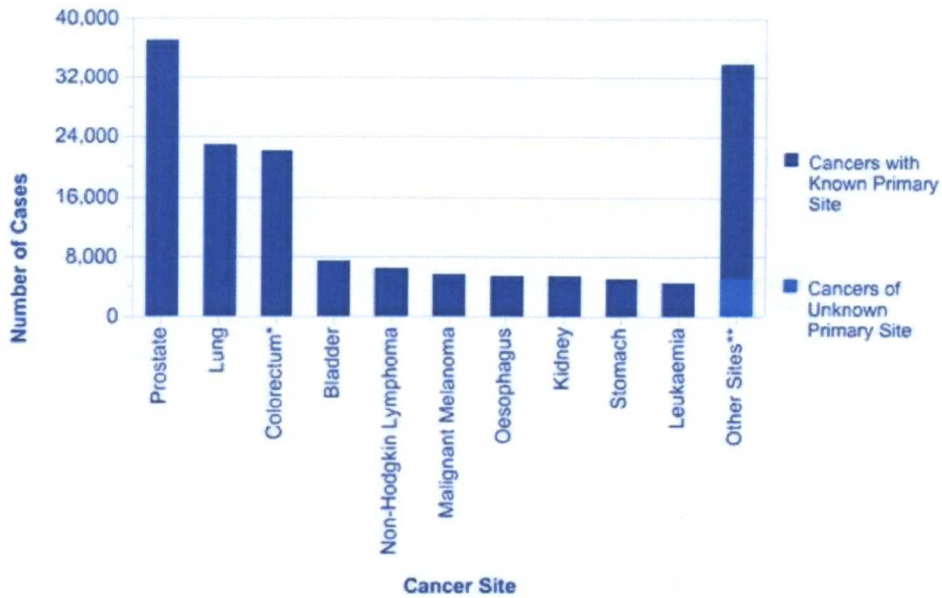


Figure 1.2: The 20 most commonly diagnosed cancer worldwide, 2008 estimates (Cancer Research UK, 2011b).

In the United Kingdom, the most commonly diagnosed cancers in males are of the prostate and lung (37,051 cases and 22,846 cases in 2008 respectively) (Figure 1.3a), while in women the most common are cancers of the breast and lung (47,693 cases and 17,960 cases in 2008 respectively) (Figure 1.3b). All in all, only four cancers account for over half (54%) of the UK's cancer burden: breast, lung, colorectal, and prostate (Northern Ireland Statistics and Research Agency, 2008; Office for National Statistics, 2010; Cancer Research UK, 2011a; ISD Scotland Online, 2011; Welsh Cancer Intelligence and Surveillance Unit, 2011).

A: men



B: women

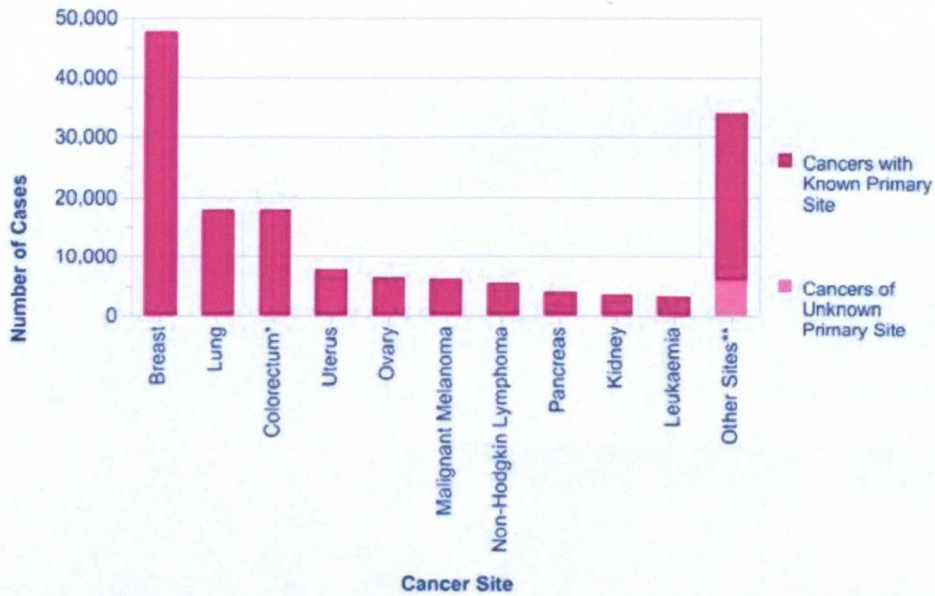


Figure 1.3: Incidences of cancers diagnosed in the UK in men (A) and women (B) (Cancer Research UK, 2011a).

* Colorectum including anus

** 3% of all male cases and 4% of all female cases are registered without specification of the primary site.

We are becoming increasingly aware of the molecular details of these cancers, and of what causes them: cancer may develop as a product of environmental factors (e.g. exposure to carcinogenic substances or harmful levels of radiation), and/or from a genetic predisposition. In recent years, survival rates for many cancers have improved. Five-year survival rates in women diagnosed with breast cancer improved by 6% every five years between 1986 and 1999 to 77%, and survival in men with prostate cancer has increased by 12% every five years between 1986 and 1999 with survival rates increasing from 42% to 65% (Cancer Research UK, 2009). However, it should be noted that some of this increased survival in prostate cancer is due to an increase in diagnosis following the implementation of the prostate serum antigen (PSA) test, which has made diagnosis of non-life threatening prostate disease more common and somewhat skewed the statistics of this disease relative to other cancers. A small group of cancers have shown little improvement (and in some cases, a fall) in survival rates, including brain tumours, multiple myeloma, oesophageal cancer, cervical cancer, laryngeal cancer, lung cancer (in men) and bladder cancer (Cancer Research UK, 2009).

1.2. RECEPTOR TYROSINE KINASES AND CANCER

1.2.1. The Epidermal Growth Factor Receptor Family

Epidermal growth factor (EGF) was originally discovered in the early 1960s, and over the next two decades further proteins were added to the family (Cohen, 1997), eventually resulting in the EGF family that we know today. The family consists of four membrane-spanning receptor tyrosine kinases (RTKs), which are widely distributed throughout the animal kingdom (Stein & Staros, 2006) and (in mammals) are coded for by four genes: ERBB1, ERBB2, ERBB3 and ERBB4. These receptor proteins which span cell surface membranes (Herbst, 2004) are activated by various ligands (termed growth factors) that bind to their extra-cellular domains. This binding brings about receptor dimerization and the activation of their cytoplasmic domains, where a kinase enzyme transfers a phosphate group from adenosine triphosphate (ATP) to tyrosine residues (Greenberg *et al.*, 1993), resulting in the initiation of specific signalling cascades within the cell itself. Until recently it has been thought that among the EGF receptors, ERBB3 was devoid of kinase activity as it lacks several key conserved residues involved in phosphorylation. However, some studies

appear to suggest that HER3 does retain some kinase activity of its own (Prigent & Gullick, 1994; Shi *et al.*, 2010).

In addition to the four receptors, there are eleven genes within the family which encode soluble ligands including transforming growth factor alpha (TGF- α), amphiregulin, betacellulin, epigen, epiregulin, EGF, heparin-binding EGF-like growth factor (HB-EGF) and the neuregulin family (NRGs 1-4). These have a high affinity for their receptors due to the presence of an EGF-like binding domain within their structure, containing six cysteine residues that are characteristically spaced, so that they form three disulphide bridges within the ligand (Linggi & Carpenter, 2006; Fuller *et al.*, 2008). These ligands are synthesised as membrane proteins that are inserted into the plasma membrane, and subsequently cleaved by cell surface proteases to release the mature form of the protein (Harris *et al.*, 2003). The cleaved, mature ligands bind specifically to certain combinations of EGF receptors (Table 1.1), and depending on which ligand binds to which receptor (and the resulting dimer), the outcome of the signalling cascade will differ.

Table 1.1 – Growth factor binding specificities in the EGF family

Ligand	EGFR	HER2	HER3	HER4
TGF- α	✓	x	x	x
Amphiregulin	✓	x	x	x
Betacellulin	✓	x	x	✓
Epigen	✓	x	x	x
Epiregulin	✓	x	x	✓
EGF	✓	x	x	x
HB-EGF	✓	x	x	✓
NRG1	x	x	✓	✓
NRG2	x	x	✓	✓
NRG3	x	x	x	✓
NRG4	x	x	x	✓

(Linggi & Carpenter, 2006)

Alternative splicing within the family gives rise to a number of isoforms of both receptors and ligands. For example there are at least 15 known isoforms of NRG1 (Buonanno & Fischbach, 2001; Falls, 2003a), and a number of isoforms of the HER4 receptor: JM-a, -b, -c and -d (which are generated through alternative splicing of exons 16 and 15b), and these may be combined with CYT-1 and -2 (which, through the alternative splicing of exon 26,

may or may not encode a 16 amino acid signalling motif) (Veikkolainen *et al.*, 2011). These different isoforms can confer different functions on the receptor. For instance, JM-a CYT-2 is capable of ligand-independent activation and promotion of cell growth, while its non-cleavable counterpart JM-b CYT-2 is not (Sundvall *et al.*, 2010). When expressed in cultured cells the JM-a CYT-2 isoform also promotes survival in serum-starved rat fibroblasts, while the JM-b CYT-2 isoform stimulates (rather than suppresses) starvation-induced apoptosis (Määttä *et al.*, 2006; Sundvall *et al.*, 2010). Furthermore, the p95HER2 isoform (which lacks the extracellular portion of the receptor and the Trastuzumab binding epitope) has also been described, and is present in 60% of tumours (Molina *et al.*, 2002; Anido *et al.*, 2006; Scaltriti *et al.*, 2007).

While some isoforms are examples of splicing occurring as a normal process, they may also be the product of an aberrant event within the cell. An example of such aberrant splicing has given rise to an oncogenic form of HER2: HER2 Δ 16. This isoform, originally detected in several HER-overexpressing breast cancer cell lines (Kwong & Hung, 1998; Siegel *et al.*, 1999) and primary tumours (Siegel *et al.*, 1999; Castiglioni *et al.*, 2006), harbours enhanced transforming activity when compared with wild type HER2, and is associated with Trastuzumab resistance (Mittra *et al.*, 2009).

1.2.2. EGFR Structure, Activation and Cell Signalling

The family of four EGF receptors are closely related in their structure, with each composed of an extracellular domain, a transmembrane domain, a juxtamembrane domain, an intracellular tyrosine kinase domain, and a C-terminal regulatory region (Burgess *et al.*, 2003). The extracellular domain consists of two homologous L domains, and two cysteine rich (CR) domains (Ward & Garrett, 2001): arranged in the order L1-CR1-L2-CR2. These are also typically annotated as domains I-II-III-IV (Lax *et al.*, 1988) (Figure 1.4). For EGFR, HER3 and HER4, the inactive conformation is oriented in such a way that the dimerization arm of region II is unavailable for binding to a partner (it is “tethered” to domain IV), preventing the formation of homo or heterodimers among the receptors. This is not the case with HER2, which (in its equivalent inactive state, in the absence of a ligand) has its domains I and III aligned in close proximity (Figure 1.5). This makes ligand binding impossible, and explains why HER2 has no ligand.

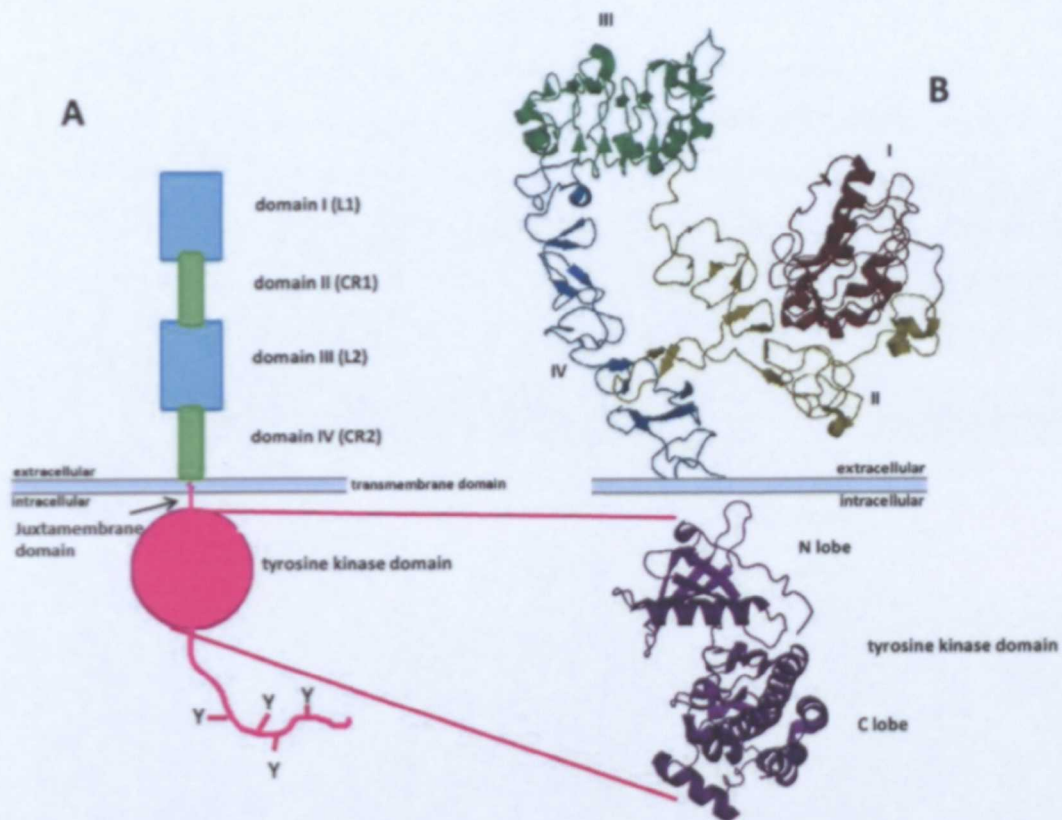


Figure 1.4: The structure of the ErbB receptors. **A:** simplified cartoon representation of basic domain organisation; **B:** structural representation of EGFR showing the organisation of the extracellular domain in its inactivated form, and the structure of the tyrosine kinase domain.

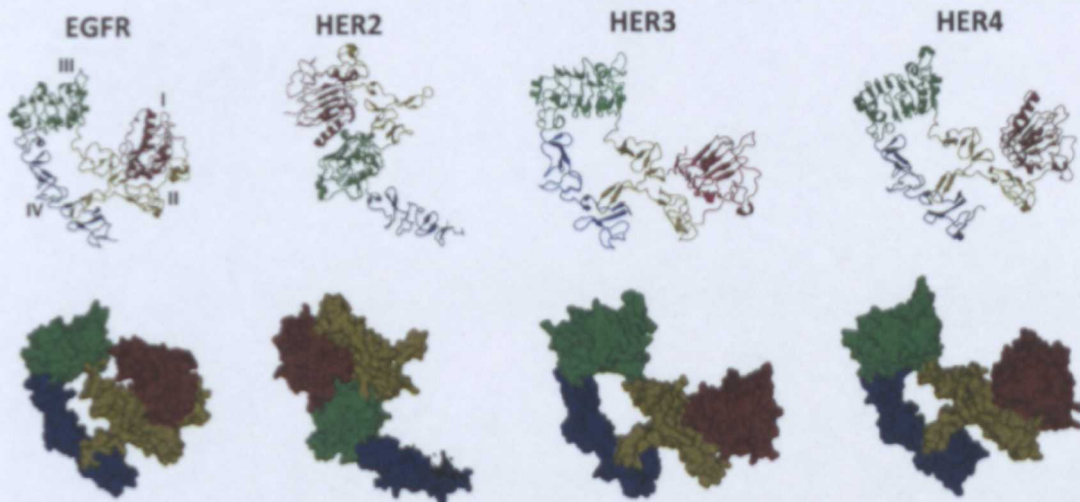


Figure 1.5: Comparison of extracellular domains of the human ErbB family of receptor tyrosine kinases in the inactive conformation, from left to right: EGFR (Ferguson *et al.*, 2003a), HER2 (Cho *et al.*, 2003), HER3 (Cho & Leahy, 2002) and HER4 (Bouyain *et al.*, 2005). Domains I (red), II (yellow), III (green) and IV (blue) are indicated. Top: ribbon diagrams; bottom: surface views.

During the activation process (Figure 1.6) ligand binding between domains I and III causes a rigid body rotation within the extracellular portion of the receptor, where the two L domains (I and III) rotate roughly 130° counter-clockwise, exposing the first CR domain, or dimerization arm (domain II) (Burgess *et al.*, 2003). This rotational movement of the extracellular domain breaks the intramolecular tether between the two CR domains II and IV, while the ligand binding to the two L domains lends this extended configuration greater thermostability. Upon contact with another similarly activated receptor, the two CR1 domains (domain II) interact intermolecularly and “hook together” to form a dimer (Burgess *et al.*, 2003).

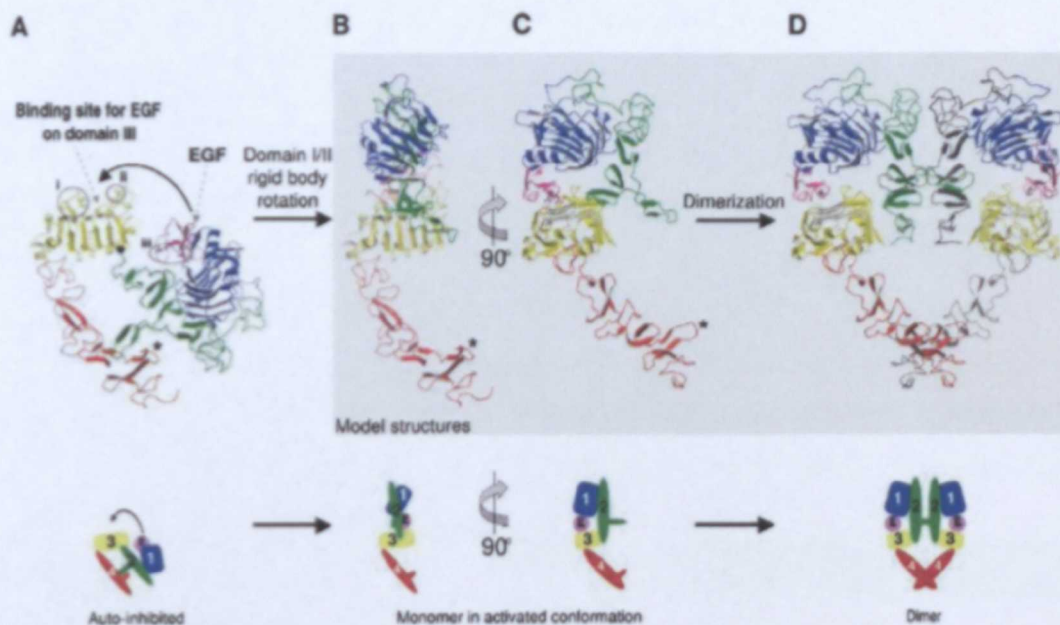


Figure 1.6: Conformational change in the extracellular portions of members of the EGF receptor family following activation by a ligand. **A:** Ligand binding between domains I and III; **B, C, D:** a rotation of 130° occurs in the extracellular portion and exposes the dimerization hook so that two receptors may bind together. **Top:** ribbon diagram; **bottom:** cartoon diagram (Ferguson *et al.*, 2003b).

Activation of the intracellular kinase region is not yet fully understood, but ligand binding to the extracellular domain has been shown to be necessary to elevate the receptor’s tyrosine kinase activity (Jorissen *et al.*, 2003). It is believed that the rigid body rotation brought about by the ligand binding previously described may serve to appropriately orientate the L1, CR1 and L2 domains (domains I, II and III respectively), which subsequently re-orientate the intracellular domains to form an active configuration for the

intracellular kinase and CR2 (IV) domains (Jorissen *et al.*, 2003). Following such activation, autophosphorylation of specific tyrosine residues occurs at the intracellular C-terminal domain, and downstream signalling pathways (including Ras/Raf/ mitogen-activated protein kinase (MAPK) and the phosphatidylinositol 3-kinase (PI3K)/Akt pathway, among others) are activated. Interestingly, the EGF receptor does not require phosphorylation for full enzymatic activity, while some tyrosine kinases (such as insulin receptor, fibroblast growth factor (FGF) receptor and hepatocyte growth factor receptor (MET)) do (Gotoh *et al.*, 1992; Hubbard *et al.*, 1998).

Once activated, the receptors of the EGF family are able to transmit signals from the extracellular environment to the inside of the cell. This signalling is able to occur through three mechanisms: paracrine, autocrine and juxtacrine signalling (Figure 1.7).

A prominent example of paracrine signalling in the EGF family is found in the development of the heart. In normal cardiac morphogenesis, the endocardium signals to the myocardium. However, these layers of tissue are separated by connective tissue and not in direct contact within the heart. In foetal heart, NRG1 is produced in endocardial endothelial cells while its receptor HER4 is expressed in the cells of the myocardium. This requires paracrine signalling between the two cell types. In mouse models in which NRG1 has been deleted, normal trabeculation of the ventricles is absent (Gassmann *et al.*, 1995). It should be noted that in addition to this role in formation of foetal heart, NRGs also play a

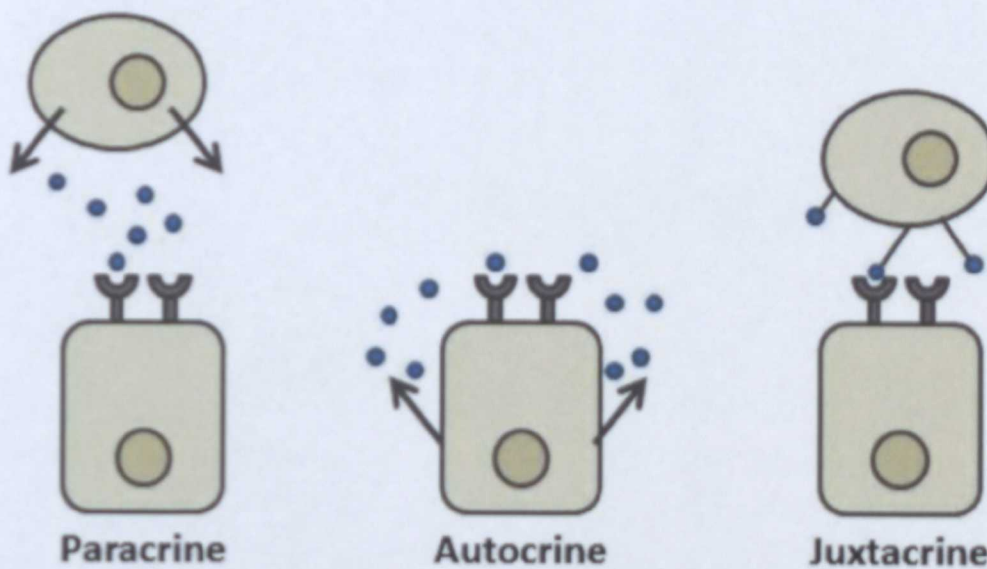


Figure 1.7: Paracrine, autocrine and juxtacrine cell signalling. Adapted from (Abe, 2000).

prominent role in signalling in adult heart and in the nervous system (Gullick, 2001; Falls, 2003b).

Autocrine signalling has been well documented amongst the NRGs in a number of cell types, such as developing muscle where NRG1 activation of HER2 and HER3 on the cell surface generates a signal which activates synaptic expression of acetylcholine receptor. This would suggest that autocrine signalling plays a role in regulating neuromuscular synapse development (Moscoso *et al.*, 1995). Autocrine signalling of NRGs has also been observed in transformed cells (Gollamudi *et al.*, 2004), in a number of breast cancer cell lines (Lupu *et al.*, 1996) and in a great deal of ovarian and colon cancer cells (Gilmour *et al.*, 2001).

Juxtacrine signalling amongst members of the EGF family has also been shown to occur. The membrane-tethered precursor ProHB-EGF can only act in a juxtacrine fashion via cell-cell interactions with neighbouring cells. Once cleaved by ectodomain shedding however, HB-EGF is able to diffuse to distant sites and act in a paracrine fashion (Higashiyama *et al.*, 2008; Higashiyama *et al.*, 2011). Similarly, experiments have also shown that the membrane-anchored form of TGF α (proTGF α) is biologically active through a juxtamembrane mechanism (Brachmann *et al.*, 1989; Wong *et al.*, 1989; Anklesaria *et al.*, 1990).

1.2.3. The Type 1 Growth Factor Receptor Family and Cancer

It is now apparent that alterations to oncogenes, tumour suppressor genes and micro RNA genes can collectively lead to cell transformation. One class of these are the members of the epidermal growth factor family which can be activated by overexpression and/or mutation. Mutations within the extracellular transmembrane or kinase domain of RTKs can stimulate ligand-independent activation of the receptor (Zwick *et al.*, 2001). Tumour suppressor genes on the other hand normally inhibit the formation of tumours in a healthy individual (Zhang *et al.*, 2007), however inactivating mutations in these genes can cause them to lose their inhibitory effect that they normally provide and contribute to the development of various cancers. Gene fusions have also been observed in kinases of other families (notably RET and NRTK1 in thyroid carcinomas (Alberti *et al.*, 2003)) and it has been suggested that fusions within tyrosine kinases may cause constitutive receptor activation through the creation of receptors which are constitutively dimerized (Edwards,

2010). Literature searches currently show no evidence of gene fusions within the EGF receptors, however chromosome translocations have been observed in NRG1 where translocation has fused the 3' end of NRG1 (including the receptor-binding domain) downstream of ODZ4. This fusion creates a secreted protein (known as γ -Heregulin) which shows biological activity (Schaefer *et al.*, 1997; Liu *et al.*, 1999; Wang *et al.*, 1999).

1.2.3.1. HER2 and Cancer

The role of HER2 has been well documented in human disease. The receptor is known to be overexpressed in roughly 15%-20% of breast cancers, and its presence is strongly associated with aggressive disease and recurrence (Slamon *et al.*, 1987) (Figure 1.8). HER2 overexpression has also been observed in cancers of the ovary (Hellström *et al.*, 2001), stomach (Kameda *et al.*, 1990; Lemoine *et al.*, 1991), bladder (Simon *et al.*, 2003; Latif *et al.*, 2004; Krüger *et al.*, 2005; Matsubara *et al.*, 2008) and aggressive cancer of the uterus, such as endometrial carcinoma (Santin, 2003; Santin *et al.*, 2005; Díaz-Montes *et al.*, 2006).

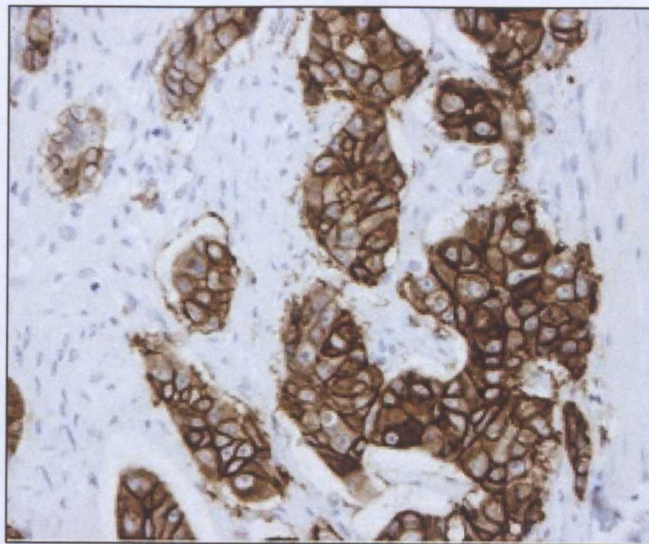


Figure 1.8: HER2 overexpression in human breast cancer determined by immunohistochemical staining, (Moelans *et al.*, 2011).

Overexpression and/or over activity of the HER2 receptor is caused by a number of mechanisms (Figure 1.9):

- Gene amplification: where additional copies of the HER2 gene are produced.
- Increased transcription: leading to increased mRNA levels.

- Point mutations: which may lead to the constitutive activation of the receptor.

In addition to the above direct mechanisms of over expression, over activity of HER2 may also be caused by over expression of a ligand which targets a receptor for which HER2 is a binding partner. These mechanisms have been documented in both cases of human cancer and in cultured cells. Gene amplification has frequently been shown to occur in the tumours of patients with breast cancer (Harbeck *et al.*, 1999; Lyon *et al.*, 2001; Meng *et al.*, 2004; Page *et al.*, 2011) and in cultured cell lines such as T-47D and SKBR3 (Lyon *et al.*, 2001). Similarly, cultured cells have been valuable in demonstrating the effect of mutation on the HER2 receptor. Often these mutations can bring about constitutive activation, not requiring a ligand for receptor phosphorylation (Shigematsu *et al.*, 2005; Wang *et al.*, 2006), essentially meaning the receptor is continually signalling to the cell.

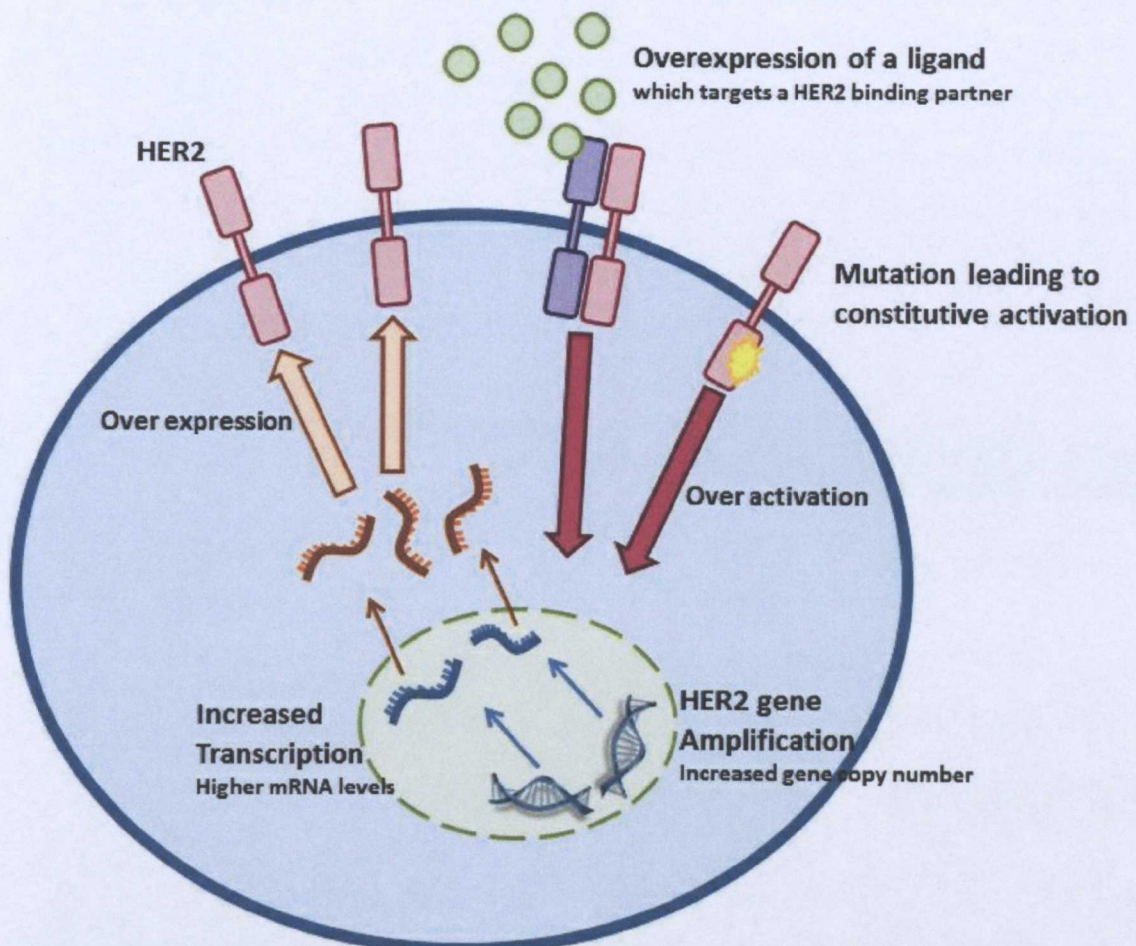


Figure 1.9: Causes of HER2 overexpression and over activation: gene amplification, increased transcription, point mutations leading to constitutive activation, overexpression of a ligand which targets a binding partner for HER2.

1.3. CANCER THERAPIES

1.3.1. “An Ounce of Prevention is Worth a Pound of Cure”

– Benjamin Franklin (1706-1790)

To prevent disease is always a better way to manage health than to treat a patient who is already ill. It is not only more cost effective to both the patient and any insurance or public healthcare service available to them, but will also prevent the need for distressing or painful therapies which may cause harm to undiseased tissues through their adverse effects.

Recent years have seen the advent of a number of vaccines and public health campaigns encouraging patients to take measures which could prevent them developing or acquiring cancers. It is estimated that every year, over 500,000 cases of cervical cancer (caused by strains of the human papillomavirus [HPV]) are reported globally, resulting in an estimated 200,000 deaths, thus making cervical cancer the second-most common cause of female cancer mortality worldwide (World Health Organisation, 2009). The first HPV vaccine (called Gardasil), for example, was initially researched in the 1980s and eventually developed by Merck. It was approved for marketing in 2006 by the United States Food and Drug Administration (United States Food & Drug Administration, 2006) and as of 2007 was approved in over 80 countries. The subsequent Cervarix vaccine from GlaxoSmithKline was approved for use in September 2007 by the European Union and Australia (Reuters, 2007) and in the United States in 2009 (United States Food & Drug Administration, 2009). The vaccines are aimed at young women with the aim to prevent infection with papillomaviruses that have been shown to cause cervical dysplasias (which may progress to cervical cancers), genital warts and other rarer types of HPV-associated cancers.

Globally, public health campaigns have addressed the fact that we encounter numerous carcinogenic substances on a daily basis which we can control our intake of. Smoking has long been known to be a cause of lung cancer, poor diets (such as those low in fibre or vitamins and minerals) and alcoholism have been linked to incidences of colon and liver cancer respectively, and exposure to ultraviolet rays through sunbathing or (increasingly) the use of tanning beds have been linked to the development of melanomas.

However there is only so much an early warning will achieve: old habits are hard to break, and eventually there comes a point where cancer prevention becomes an exercise in social

change. In cases where people may not heed the warnings, or in some cases feel they cannot (for example where a patient may have a prior addiction to a substance such as alcohol or nicotine), if a cancer develops the disease must be treated.

1.3.2. Treating an Established Disease

Surgery and radiotherapy are most commonly used to treat patients suffering from cancer, to excise any tumours and destroy any remaining cells. Chemotherapy is generally used when it is either known that or there is a fear that a cancer may have metastasised, and is generally a prolonged treatment with numerous cytotoxic adverse effects. A number of different types of chemotherapeutics exist, which can broadly be grouped into two categories: therapies which target generic processes (such as alkylating agents, anti-metabolites, plant alkaloids and topoisomerase inhibitors) and targeted agents (including small molecule drugs and biologicals – of which antibody therapies are the most common).

1.3.2.1. Small molecule tyrosine kinase inhibitors

The EGF receptors have been extensively studied in human cancers, and consequently many target-specific therapies have been developed to combat their effects. There is now a growing class of anti-cancer agents aimed at inhibiting the action of the RTKs which are often over-expressed, or are overactive through the increased expression of ligands, or through activating mutations. These drugs are known as tyrosine kinase inhibitors (TKIs), and many have only recently been approved for clinical use in the past decade following early work in the 1980s.

Small molecule drugs have lost some popularity amongst pharmaceutical companies, as many early ones still carried side effects with them. Biological drugs (such as antibodies) showed fewer side effects whilst still being effective (Herceptin shows few adverse effects, other than occasional cardiotoxicity). There is, however, a greater focus now on producing small molecule drugs which are as effective with fewer side effects, so that a patient may continue to live their normal day-to-day life whilst therapy is on-going – in essence, the patient would be living with their cancer.

TKIs may operate as competitors with either ATP (such as Canertinib – an inhibitor of EGFR, HER2 and HER4 (Slichenmyer *et al.*, 2001)), or as competitors with a phosphorylating entity or a substrate, or they may function as allosteric inhibitors, by binding outside of the active

site and inducing or prohibiting conformational change (such as CI-1040 – an inhibitor of MEK1 and MEK2 (Ohren *et al.*, 2004)).

1.3.2.2. Antibody Therapies

Other therapies that may target the EGF family of receptors include monoclonal antibodies, which despite having a different mechanism of action to small-molecule tyrosine kinase inhibitors also inhibit the proliferation of cancerous cells. Such antibodies can be broadly categorised into three therapies (Figure 1.10).

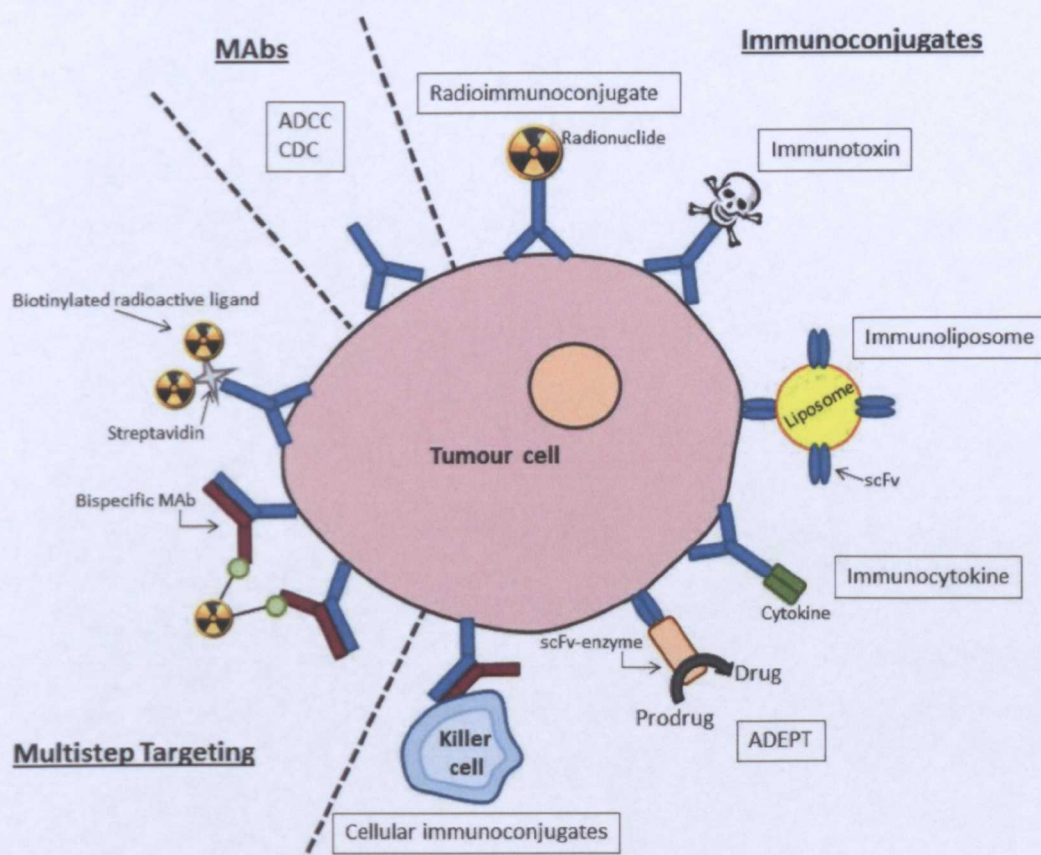


Figure 1.10: Antibody therapies. Three primary therapeutic areas exist: monoclonal antibodies, immunoconjugates and multi-step targeted approaches.

Monoclonal antibodies

Monoclonal antibodies are those which lack any kind of conjugate (for example, Herceptin and Pertuzumab). The binding of these naked antibodies to a cell surface antigen may induce antibody-mediated toxicity within the patient, where macrophages and natural killer cells are attracted to the cancerous cells to which the antibodies have bound. The immune system then destroys the cells associated with the tumour. Naked monoclonal

antibodies may also act by inhibiting the activation of certain receptors through steric hindrance. This is the case with Pertuzumab, where binding of the antibody to the extracellular domain of HER2 prevents the formation of hetero- or homo-dimers with other receptors and inhibiting receptor phosphorylation (Schaefer *et al.*, 1997; Agus *et al.*, 2002; Mendoza *et al.*, 2002; Jackson *et al.*, 2004; Takai *et al.*, 2005). While numerous possibilities for Herceptin's mechanism of action have been postulated (including the initiation of antibody-mediated cell cytotoxicity (Clynes *et al.*, 2000), the suppression of angiogenesis and HER2 ectodomain cleavage (Albanell *et al.*, 2003)), the mechanism is still not yet fully understood.

Immunoconjugates

Immunoconjugates may take many forms, but all share one common feature – the antibody in question is conjugated to a cytotoxic agent, or an agent which is capable of converting a non-toxic agent into a cytotoxic agent (as is the case with antibody-direct enzyme prodrug therapy [ADEPT]). Toxins (such as ricin, diphtheria toxin (Esworthy & Neville, 1984) or pseudomonal exotoxin (Bjorn *et al.*, 1986)) may be conjugated to monoclonal antibodies specific to antigens associated with a tumour, which destroy the cancerous cells upon their internalisation. However the risk that monoclonal antibodies may not be specific enough to prevent adverse effects brought about by the destruction of healthy cells has precluded many therapies of this type from being licensed. There is currently only one such therapy available for treatment: gemtuzumab ozogamicin makes use of a highly cytotoxic agent from the calicheamicin class and is used to treat patients over the age of 60 in first relapse suffering from acute myelogenous leukaemia (AML) (Bross *et al.*, 2001). The toxin cleaves double-stranded DNA, eventually leading to apoptosis (Ikemoto *et al.*, 1995).

Alternatively, a radionuclide may be conjugated to the antibody. This has proven effective in the treatment of lymphomas due to their sensitivity to radiolabels (Park & Press, 2007). Radioactive isotopes with short half-lives (typically around 7-8 days) are chosen and conjugated to murine antibodies, as these are rapidly cleared from the patient's body.

In ADEPT, a drug-activating enzyme is conjugated to a monoclonal antibody through either chemical or recombinant methods. The antibody-enzyme conjugate is administered intravenously to a patient, whereupon it binds to specific targets on tumour cells. Several hours later an inactive form of a cancer drug is administered. The enzyme conjugated to

the antibody allows for the prodrug to be converted to its active state in close proximity to the cells (Bagshawe *et al.*, 1994). Advantages of this therapy are that the drug can be targeted directly to cells, rather than having a biologically active therapeutic flowing throughout the entire body, where it may have a greater chance of affecting healthy tissues.

Other immunoconjugates include immunoliposomes (where a liposome containing a therapy is conjugated to a single-chain variable fragment antibody [sc-Fv]) (Park *et al.*, 2001; Park *et al.*, 2002; Mamot *et al.*, 2003), immunocytokines (where a cytokine is conjugated to an antibody and can stimulate an immune response against a tumour) (Lode *et al.*, 1998; Gillies *et al.*, 2005) and cellular immunoconjugates (where an antibody is conjugated to a natural killer cell) (Shiraiwa *et al.*, 1991).

Multistep targeted approaches

Similarly to immunoconjugates, multistep targeted approaches rely on the addition of cytotoxic substances to antibodies in order to exert their antiproliferative effects. However they differ from immunoconjugates in that the cytotoxic substances are not conjugated directly to the antibody, but through the application of intermediate binding agents which have a high affinity for each other (for example, streptavidin and biotin). Radionuclides can be applied to cancerous growths in this manner (Schuhmacher *et al.*, 1995).

Current Antibody Therapies

While these therapies may seem varied and promising, few have yet to reach the market. Thus far, simple monoclonal antibody therapies have had the most success with drugs such as Herceptin (Trastuzumab), Erbitux (Certuximab) and Rituxan/MabThera (Rituximab) to name but a few. Of the other immunotherapies described in this chapter, only radioimmunoconjugates have reached promising stages in clinical trials with Ibritumomab tiuxetan (Shipley *et al.*, 2009) and Tositumomab (Kaminski *et al.*, 2005) having shown some promise. It also worth mentioning the newly-developed therapy Trastuzumab emtansine (T-DM1), in which Trastuzumab has been conjugated to a microtubule polymerization inhibitor (Girish *et al.*). Phase II studies have shown that T-DM1 has response rates of 26%-35% in patients with metastatic breast cancer who have previously received HER2 therapies (Girish *et al.*; Burris *et al.*, 2011).

1.2.3. Drug Resistance

Despite the advances which have brought such effective drugs to the market, many cancers have been able to develop resistance to these therapies. Such resistance may exist as a *de novo* mutation, or be acquired through exposure to a chemotherapeutic agent a result of the selective pressure of TKIs following an initially responsive treatment. *De novo* resistance to doxorubicin has been documented in patients with p53 mutations (Aas *et al.*, 1996), while acquired resistance has been observed with the T790M mutation of EGFR, which has been documented in non-small cell lung cancer (NSCLC). The mutation affects a specific threonine residue (known as the “gatekeeper” residue) which is substituted with a methionine, and it is believed that its mutation blocks the TKI binding site, preventing inhibitor binding (Kwak *et al.*, 2005; Pao *et al.*, 2005). However the fact that other drugs have been documented binding to this mutant (Carter, 2001; Greulich *et al.*, 2005; Kwak *et al.*, 2005; Sequist, 2007), would suggest that other mechanisms are in play. It has been suggested that this mutant may have an increased affinity for ATP compared to the wild type (Yun *et al.*, 2008), and that the problem with this mutant may not be its inability to bind TKIs, but rather its increased affinity for ATP relative to those TKIs. Cancers which express this mutant are normally responsive to therapy in the first instance – Gefitinib and Erlotinib have been shown to be active against non-small cell lung cancers with mutations which confer anti-apoptotic properties (Pao *et al.*, 2004; Sordella *et al.*, 2004) – however the subsequent T790M mutation renders the cells resistant to treatment with these drugs.

Such resistant effects have also been observed in antibody therapies, including Trastuzumab (Herceptin). Only 33% of patients who receive single agent Trastuzumab with metastatic breast cancers which overexpress HER2 respond to treatment (Vogel *et al.*, 2002). Numerous theories for this resistance have been proposed, such as the presence of compensatory and/or aberrant signalling pathways within the cells. It has also been demonstrated that Trastuzumab cannot inhibit tumour cell proliferation in cells which are EGFR-activated through autocrine signalling (Lane *et al.*, 2000), or prevent ligand-induced signalling from heterodimers of which HER2 is a component (Motoyama *et al.*, 2002). Experimental results suggest that ligands of the EGF family make it possible for cells to overcome Trastuzumab-inhibition by activating alternative combinations of homo- and heterodimers, which is made further possible when one considers that the antibody binds to a region of HER2 that is not involved in the formation of dimers.

Often, therapeutic resistance correlates with the downregulation of intracellular EGF-family signalling such as the mitogen-activated protein kinase (MAPK) and phosphoinositide 3-kinase-protein kinase B (PI3K-AKT) pathways. It has been suggested that the aberrant signalling of these pathways could account for resistance against both Trastuzumab and EGF-receptor targeted therapies (Janmaat *et al.*, 2003). To further lend credence to this, it has been observed that activation of AKT, or the loss (or mutation) of phosphatase and tensin homolog (PTEN – the negative regulator of PI3K) have been found to be causes of tumour cell resistance (She *et al.*, 2003). This would further suggest that mutation within these pathways may have an important role in the efficacy of anti-tumour therapies.

1.4. CANINE CANCER

1.4.1. Causes and Epidemiology

A quarter of all dogs will develop cancer at some time in their life, with this figure rising to 50% in dogs which live to ten years of age or older (European Society of Veterinary Oncology, 2010). This is twice the incidence of cancer in humans – the reason for which is not yet understood, although numerous possibilities exist.

1.4.1.1. Carcinogens and Age

Exposure to carcinogens in our day to day lifestyle frequently has a greater impact on our pets than us. Many pet owners frequently spray fertilizers on their lawns, which pets will interact with to a greater extent and subsequently be exposed to the carcinogens that they contain. Some studies have shown that pet foods may contain mutagens and carcinogens (such as heterocyclic amines) as a by-product of high temperatures associated with pet food production, that could potentially be harmful to companion animals (Knize *et al.*, 2003). Dogs are also vulnerable to the effects of passive smoking by their owners, and the longer filtration systems found in their nasal cavities can make dogs more likely to be affected by the deposition of carcinogenic particles found in the air which are associated with tobacco smoke and car exhaust (Kelsey *et al.*, 1998).

Advances in veterinary care have also lead to an increase in the life expectancy of many companion animals. Cancers typically associated with old age in humans, such as prostate cancer, are being increasingly diagnosed in our geriatric pets (Waters *et al.*, 1996).

1.4.1.2. The Problem with Pedigree

Typically a dog population must meet three criteria in order to be considered a distinct breed (Arman, 2007):

1. They should be descended from a particular ancestry;
2. They should have a utility for which they serve humans; and,
3. They should be of a distinct type which lends all members of the breed a similar physical appearance.

Over the course of the 19th century, the governing bodies of the Kennel Club and the various breed societies have focused these requirements primarily on ancestry and typology, with little regard for the utility of a breed or its health (Arman, 2007). This has led to pedigrees of dog undergoing stringent selective breeding in order to produce dogs which adhere to these standards, with this breeding increasingly being conducted from a limited gene pool of “suitable” dogs. Consequently, pedigree show dogs are often much different in appearance to their working ancestors (Figure 1.11).

In 2008, a BBC documentary “Pedigree Dogs Exposed” (BBC Television, 2008) highlighted and investigated the health and welfare issues that pedigree dogs in the United Kingdom currently face. It was found that in the UK a worrying degree of inbreeding was taking place owing to the diminishing gene pools which were considered “pure” enough by Kennel Club standards to breed suitable show dogs from. This problem has been further compounded by some breeders culling puppies for cosmetic reasons (although this is now banned by the Kennel Club). This caused breeders to mate dogs in manners that included mother/son and father/daughter pairings, meaning that it is not uncommon for a dog to be both father and grandfather to a puppy (although the Kennel Club revised their breed standards and banned this practice in 2009 (Kennel Club, 2009)). These common sires or bitches which are used in breeding may carry unnoticeable recessive genetic disorders, which could then be expressed in the offspring. With some breeds, the problem in the UK has become worrying: a recent study by University College London found that although there are roughly 10,000 pugs in the country, there are essentially only 50 genetically unique individuals among them (BBC News, 2008).



A
Bulldog painting from 1790
(Philip Reinagle)



Modern show Bulldog



B
Old-style Neapolitan
Mastiff



Modern show
Neapolitan Mastiff



C
Early 20th century
Basset Hound



Modern show Basset Hound



D
Bull Terrier circa 1915



Modern Bull Terrier

Figure 1.11: Working dogs and their show counterparts. It can be seen how selective breeding for cosmetic purposes has severely altered the appearance of many breeds. **A:** the original Bulldog was taller, and lacked the flat face, bowed legs and under bite of its modern-day counterpart; **B:** the Neapolitan Mastiff was originally a war dog bred for strength, but selective breeding has brought about exaggerated skin folds on the face; **C:** the original basset hound was higher off of the ground, with less excess skin around the jaws and face; **D:** the original Bull Terrier had a concave snout shape and was higher off the ground than its modern counterpart, which is lower set in its hind legs and has an “egg-shaped” snout and triangular eyes.

Sources: **A:** Bulldog (left) painting by Philip Reinagle, 1790, (right) from the British Bulldog Club (British Bulldog Club Inc, 2011); **B:** Neapolitan Mastiff (left) from breeder’s website (Tornabene’s Bandogge Mastiffs and Performance Neapolitan Mastiffs, 2011), (right) from the UK Neapolitan Mastiff Club (UK Neapolitan Mastiff Club, 2005), **C:** Basset Hound (left) from “Il Basset Hound” by Ernesto & Giovanna Capra (Capra & Capra, De Vecchi, 1991), (right) from the UK Basset Hound Club (The Basset Hound Club, 2011; Cancer Research UK, 2011b); **D:** Bull Terrier (left) from “Dogs of All Nations” by Walter E. Mason (Mason, Kessinger Publishing, 1915; BBC Television, 2008), (right) from the Bull Terrier Club UK (The Bull Terrier Club, 2002).

While this degree of inbreeding frequently produces dogs with the strict physical exaggerations that are often required in the show world, it is easy to see from a genetic point of view what detrimental effects this could have on breed health as a whole. Indeed, the BBC documentary highlighted a number of physical conditions and diseases which had become breed specific through generations of inbreeding, including:

- High incidences of syringomyelia in Cavalier King Charles Spaniels: a condition in which the brain is essentially too large for the cranium and may herniate, causing a blockage in the flow of cerebrospinal fluid. A recent study found that 70% of Cavalier King Charles Spaniels over the age of 6 could be affected by the condition (Parker *et al.*, 2011). In addition it is estimated that 40% of this breed may be affected by heart murmurs, with mitral valve disease being the cause of 93% of murmurs (Chetboul *et al.*, 2004).
- Increased incidences of juvenile kidney disease and heart disease were detected in pedigree Boxers with common, inbred ancestry.
- Pugs were found to suffer from a catalogue of physical defects including slipped kneecaps, hiatus herniae of the stomach, collapsed larynxes, palate dysmorphias, narrow nasal passages, dermatitis and infections in the skin folds of the face, in-rolling of the lower eyelids and curvatures of the spine which are partly caused by the desire for pugs to have a “double twist, corkscrew” tail.
- Dalmatians had lost a gene over the course of their evolution which allowed them to produce the uricase enzyme which breaks down uric acid. This causes Dalmatians to suffer from hyperuricemia, which can cause urate stone disease – a problem which can have sudden and fatal consequences. Urologic disease accounts for 10.7% of all reported disease in the UK Dalmatian population, with urate stones being the second most common cause of such disease (The British Dalmatian Club, 2009). Some work has been carried out to replace this gene: a Dalmatian was first crossed with an English Pointer to replace the gene, and subsequently back crossed with pure Dalmatians for several generations to bring back the distinctive breed phenotype.

Along with the physiological issues and diseases highlighted above, pedigree dogs may also be vulnerable to certain cancers (the most common of which are summarised in Figure 1.12 and Table 1.2). Studies have shown that in bitches, the most common cancer appears to be of the mammary gland, with this accounting for 51%-70% of diagnosed disease. In male dogs, cancers of connective tissues and Non-Hodgkin's lymphoma are fairly common with incidences of 13%-17% and 10%-20% respectively (Dorn *et al.*, 1968; Kelsey *et al.*, 1998; Merlo *et al.*, 2008).

Dogs* (1963–1966)		Male Dogs* (1963–1966)	
Cancer	% of total	Cancer	% of total
Breast	51	Connective tissue	17
Connective tissue	9	Testis	16
Malignant melanoma of skin	8	Malignant melanoma of skin	14
Lymphoma	6	Mouth and pharynx	10
Mouth and pharynx	5	Lymphoma	10
Biliary passages and liver	2	Bone	4
Bone	2	Stomach and intestines	3

Figure 1.12: Incidences of cancer in pet dogs (left: female; right: male). Data from Californian pets, 1963-1968. Adapted from (Dorn *et al.*, 1968; Kelsey *et al.*, 1998).

Table 1.2 – Incidences of cancer in pet dogs, as found by the Animal Tumour Registry of Genoa, Italy (1985-2002)

Site	Male %	Female %
Lip, oral cavity, pharynx	10.5	2.6
Digestive organs, peritoneum	5.2	2.6
Respiratory, intrathoracic organs	1.9	1.0
Bones and articular cartilage	3.6	2.0
Skin (excluding melanoma)	19.2	3.8
Connective tissue and other soft tissue	13.2	4.6
Skin melanoma	0.7	0.2
Mammary	2.2	70.5
Female genitourinary organs	N/A	1.6
Prostate	0.7	N/A
Male genitourinary organs	16.8	N/A
Non-Hodgkin's lymphoma	20.1	8.4
Other sites	6.0	2.6

Adapted from (Merlo *et al.*, 2008)

In some cases, there appears to be some degree of breed predisposition to certain malignancies. Pointers, Poodles and Cocker Spaniels have shown high incidences of mammary cancers (Ostrander *et al.*, 2000) and brachycephalic breeds such as Pugs, Boxers and Shar-Peis have higher incidences of primary brain tumours (Merck, 2010). When the extensive inbreeding of pedigree dogs is considered, it is easy to see how recessive genes may be passed down and accumulated within a breed, leading to these breed-specific disease tendencies.

Some breed specific cancers may also develop as a consequence of the phenotype for which the breeding has selected - large and giant breeds such as Great Danes and Saint Bernards frequently develop osteosarcomas (Ostrander *et al.*, 2000) for example. These are often found near the growth plates of bones, suggesting that they are perhaps a product of the extreme levels of growth that large breed dogs must undergo to attain their size. Osteosarcomas are also regularly seen in Greyhounds, with one study showing that the leading cause of death in retired Greyhounds was cancer (with 25% of those cancers being osteosarcomas) (Lord *et al.*, 2007), perhaps owing to their delicate skeletal structure which is often subject to great stresses upon their musculoskeletal tissues in racing.

Despite recent changes to Kennel Club standards, the problems that inbreeding and selective breeding cause are still rife amongst the canine population. As it stands in the UK, there is as yet no legislation preventing the inbreeding of dogs or the culling of puppies for cosmetic reasons and so the situation is unlikely to change anytime soon.

1.4.1.3. Papillomaviruses and Canine Cancer

Dogs are also vulnerable to various papillomaviruses, which can induce the growth of viral plaques in dogs. Certain breeds, such as Pugs and Miniature Schnauzers, appear to be predisposed to this plaque growth, while in most other breeds they only appear in immunosuppressed dogs. These plaques may eventually become *in situ* or invasive carcinomas, although this neoplastic transformation is relatively rare (Munday & Kiupel, 2010). Canine oral papillomavirus (COPV) induces the growth of papillomas in the oropharynx of dogs, which can occasionally progress to squamous cell carcinomas (Nicholls & Stanley, 1999; Campo, 2002).

1.4.2. The Market in Animal Health

Chemotherapy is well-known to be an expensive treatment in humans, and some individuals may find justifying such an expense for a pet difficult. However, the market for pet insurance has made these costs more manageable for pet owners. Since the first pet insurance premium was sold in Britain in 1947, the UK's pet insurance market has grown substantially with some 23% of pets now being insured, and is now second only to Sweden in terms of policies sold (Kroger Pet Insurance, 2012). In the UK, pet insurance is widely available to buy not only from specialist insurance companies but also from many high street outlets and shops (Figure 1.13).

Figures show that in 2005, 34% of all UK pets insured were dogs – making them the most commonly insured pets (Intel Reports Summary, 2005). In the United States, pets are also frequently insured: in 2008, it was estimated that roughly 800,000 pets were insured (0.52% of the estimated US pet population), with a total direct premium across the country of US\$272 million – this represented a growth of 18% between 2003 and 2008 (Embrace Pet Insurance, 2009). Recent reports have also suggested that US pet owners are also

The figure displays four distinct advertisements for pet insurance:

- Top Left (Tesco):** A blue background with the Tesco logo and the text "Pet Insurance". Below it, it says "Buy Tesco Pet Insurance online and get 20% discount." A black and white dog is shown on the right. A red button at the bottom left says "GET A QUOTE".
- Top Right:** A dark background with the text "MORE TH>N PET INSURANCE" in green and white. A ginger and white cat is on the left. A red speech bubble on the right says "20% OFF when you buy online". A green button at the bottom right says "Get a Quote >".
- Bottom Left (Argos):** A white background with the Argos logo and "Pet Insurance". The text reads "Vets bills are so expensive". It features a black and white dog and a brown cat. A red button at the bottom right says "Save up to 15% >".
- Bottom Right:** An orange background with "Pet Insurance" at the top. It shows a dog and a cat in a circular frame. A blue circle on the right says "3 months free*". A smaller blue circle below it says "PLUS 15% online discount". A red button at the bottom right says "Find out more".

Figure 1.13: Pet insurance is widely available in the UK from high street vendors.

spending more than ever on their pets: the American Pet Products Association reported that general spending (including pet accessories, and services such as grooming, pet sitting and walking) on US pets surpassed US\$50 billion in 2011 (American Pet Products Association, 2012), with spending on pet insurance in the same year estimated at US\$450 million (BBC News, 2012) (a 65% increase since 2008) and further forecast to reach US\$664 million by 2012 (a further 44% increase) (Embrace Pet Insurance, 2009).

This rapidly growing market in pet insurance has helped to spur on growth in the animal health industry (Mintel Reports Summary, 2008), and lead to the development of a number of pet-specific therapies, from de-worming and anti-parasite treatment, to motion sickness tablets, to the more recently emerging chemotherapeutics: Palladia, Masivet and Oncept.

1.4.3. Treatment

Canine cancers are treatable, although until recently most treatments revolved around simple excision surgeries and radiotherapies. Using chemotherapeutics to treat canine malignancies is a relatively new practice, and there is still no firmly established standard of care for their use. Currently chemotherapeutics designed for humans have been most commonly used to treat dogs, with canine mast cell tumours being the cancer most commonly treated with chemotherapeutics described in literature. Studies have shown that human therapies such as imatinib mesylate (Gleevec) can be both safe and effective treatments for canine mast cell tumours (Hahn *et al.*, 2008), as are Vinblastine (Thamm *et al.*, 1999), Lomustine (Rassnick *et al.*, 1999) and Chlorambucil (Taylor *et al.*, 2009). However this chemotherapy was only reserved for dogs with inoperable tumours or with tumours where radiotherapy was not feasible, as an adjunct to these treatments, or where dogs presented with advanced (grade III) cancers (Hahn *et al.*, 2008). Recently though, pharmaceutical companies have realised the potential for generating profit in this area of animal health, and as such research and development into these areas has increased. There are now three dog-specific anti-cancer therapies on the market:

- Palladia (Toceranib phosphate): the first drug which from design through to marketing has been developed specifically to treat malignancies in dogs. This small molecule drug targets members of the split-kinase family and is designed to inhibit angiogenesis involved in the growth of canine mast cell tumours (Yancey *et al.*, 2010).

- Kinavet/Masivet (Masitinib phosphate): Masivet works similarly to Palladia, in that it targets members of the split kinase family and is used to treat canine mast cell tumours, and is also in trials as a therapy for gastrointestinal stromal tumours (GIST) (Le Cesne *et al.*, 2010).
- Oncept: revolutionarily, Oncept is the first treatment of its kind in any species – a therapeutic DNA vaccine which treats canine melanoma (particularly oral melanoma). The vaccine is composed of an antigen of interest (in the case of Oncept, a tyrosinase antigen that is required in melanin production) that is cloned into a bacterial expression plasmid with a constitutively active promoter (Bergman *et al.*, 2006). The portion of DNA cloned into the plasmid is not that of the species to be treated – this has been shown to be ineffective at eliciting an immune response. Instead, orthologous DNA from a different species is used to create a xenogeneic vaccine. The small differences in the sequence are sufficient to recruit antigen presenting cells and stimulate an immune response against the cancer and induce tumour immunity (Weber *et al.*, 1998; Wolchok *et al.*, 1998). In trials, Oncept was able to extend long-term survival in nine dogs with a Kaplan-Meier median survival time of 389 days, with one dog with stage IV disease showing a complete clinical response in multiple lung metastases for 329 days (Bergman *et al.*, 2003).

However dogs are not invulnerable to the side effects commonly associated with these drugs (such as gastrointestinal disorders and haematological abnormalities like neutropenia and thrombocytopenia (Hahn *et al.*, 2008) along with more readily-associated side effects of chemotherapy such as alopecia (Chun *et al.*, 2007)), so veterinarians and pet owners may be reluctant to treat their dogs knowing that they could undergo certain degrees of discomfort. Many of the more modern drugs have focused on reducing the severity of these side effects, and trials with Oncept showed few side effects – and in those patients which did display adverse effects, these were primarily depigmentations (Bergman *et al.*, 2006) which would cause little discomfort to the patient. Furthermore, studies with drugs such as Palladia have shown that should any side effects be noticed, a short treatment break often allows for the effect to clear up on its own, and frequently the adverse effect does not reappear once treatment is resumed (London *et al.*, 2003).

1.4.4. Comparative Oncologies

Animal cancers, particularly in mammals, show many similarities to those found in humans and for many years animal models have been used to study the disease in the hope that we might improve our understanding of cancer and its progression (LeRoy & Northrup, 2009). Such models have already been used to study cancers such as lymphoma, mammary gland carcinoma, soft-tissue sarcoma, osteosarcoma, and melanoma (Vail & MacEwen, 2000), all of which also commonly occur in humans. However, there have thus far been relatively few studies which seek to find some clinical benefit for animals themselves suffering from the disease, as opposed to using them simply as *in vivo* models for drugs being developed for humans.

Generally among mammalian species, there is a high degree of conservation in gene sequences. This has made it possible for drugs designed for humans to be trialled in these animals. Dogs have proven to be an excellent model system for *in vivo* studies and drug trials for numerous reasons. We as humans are genetically more similar to dogs than we are to rodents owing to the lesser degree of nucleotide divergence between our species. This makes the dog a better model for cancer than rodents or pigs – more traditional laboratory models. Dogs are also much more accessible as laboratory animals than our closest ancestors – primates – which are difficult to come by for research in Britain. This is due in part to governmental regulations (experiments on higher apes [chimpanzees, bonobos, gorillas and orangutans] have been formally banned since 1998 (The Independent, 2006)) and also due to increasing pressure from animal-rights groups which have deterred airlines from flying primates directly into Britain (Goodman & Check, 2002). Despite this, the number of primates being imported has not decreased, but the animals must endure over 50 hours of combined air and sea travel to reach their ultimate destination in the British Isles (Goodman & Check, 2002) – ultimately causing them to become more stressed, making their suitability as lab models questionable, in addition to raising ethical questions.

But it is not only Britain and Europe that has trouble securing primate models. Experiments on chimpanzees have largely stopped in the United States following years of unsuccessful experiments in which chimps were infected with human immunodeficiency virus (HIV). These chimpanzees did not develop acquired immunodeficiency syndrome (AIDS) and macaques were found to be better models when infected with simian immunodeficiency

virus (SIV). Subsequent reports of the use of chimpanzees in developing HIV vaccines further proved the ape to be a poor model owing to its inability to accurately predict a human response (Bailey, 2008). Consequently, chimpanzees were deemed to be unsuitable for further research into HIV and AIDS.

These difficulties in securing primates in a humane, sustainable and economical manner, combined with the drawbacks of the more common murine models, may encourage laboratories to look to other mammals (such as dogs) as model systems, at least for certain trials and tests – although with regards to areas of research such as neuroscience (Parkinson's disease and Alzheimer's disease for example), primates are still much better suited as animal models than any other lab model (Chiavaras & Petrides, 2000).

Given that dogs are a popular choice of companion animal, there is a large enough patient population to fuel drug trials (the canine population in the United States is estimated to be 78.2 million (American Pet Products Association, 2012), and 10.5 million in the UK (Murray *et al.*, 2010)), and the fact that we care for them into older ages means they may develop more age-specific or spontaneous cancers that are rarely seen in other lab models – in fact, dogs are the only other animal known to spontaneously develop prostate cancer (Rivenson & Silverman, 1979). Companion dogs also possess an intact immune system, which allows for drugs to be trialled in a patient where they must work alongside the body's natural defences to fight disease, and also allows for observation of any hypersensitivity reaction which may occur as an adverse reaction of a therapy.

The scientific community is beginning to take notice of both the benefits that using dogs as a model system can bring, and also the financial benefits of dog-specific cancer therapies to the pharmaceutical market. In June 2004, a group of veterinary and biomedical professionals began the Canine Comparative Oncology & Genomics Consortium (CCOGC) with the aim of improving the current knowledge with regard to companion animal cancers, and to develop novel technologies which would benefit the studies of cancer biology and therapy (CCOGC, 2004). Since 2007, the Consortium has been working in conjunction with Pfizer to build up a repository of normal and diseased canine tissue samples which represent not only disease found in companion dogs, but also those which are of significant comparative value in treating human cancer. Such resources are helping to drive studies into canine cancers – previously tumour samples were difficult to come by and precious, often relying on tissue collected through veterinary institutions for study.

Cultured cell lines of canine disease are also becoming more widely available through individual groups and culture collections such as the American Type Culture Collection (ATCC).

1.5. STATEMENT OF PURPOSE & EXPERIMENTAL AIMS

This thesis aims to explore the role of HER2 (a receptor which is prominently involved in breast and other cancers in humans) in canine mammary cancer. By establishing this, it is possible to explore the possibility of using human therapies (those which both have and haven't made it to market) in pets, and also to put the dog forward as a more suitable model for human disease than mice and rats. This will be established through a number of methods, outlined below.

1. Exploring the distribution of the EGF receptors and ligands in normal canine tissues, benign mammary cancers and malignant mammary cancers.
2. Exploring the expression of the EGF receptors in a canine mammary cancer cell line by PCR and Western Blotting.
3. Exploring the role that HER2 plays in maintaining a malignant phenotype in canine mammary cancer through the application of specific small molecule drugs and siRNAs to canine mammary cancer cells in culture.

CHAPTER TWO

Materials & Methods

2.1. ANTIBODIES USED IN THIS STUDY

The majority of antibodies used throughout this project were available in the laboratory from affinity purified stocks. Where this is not the case, the appropriate reference or manufacturer's details have been supplied (Table 2.1.1).

Table 2.1– Primary antibodies used throughout this study

Antibody/Cat #	Directed against	Species and clonality	Application(s)
56AR (Saeki <i>et al.</i> , 1992)	Amphiregulin	Rabbit polyclonal	IHC
97BTC (Srinivasan <i>et al.</i> , 1999)	Betacellulin	Rabbit polyclonal	IHC
F4 (Gullick <i>et al.</i> , 1986)	EGFR	Mouse monoclonal	IHC, WB
AF1127 (R&D Systems [Oxfordshire, UK])	Epigen	Goat polyclonal	IHC
AF1195 (R&D Systems)	Epiregulin	Goat polyclonal	IHC
111HB (Chobotova <i>et al.</i> , 2002)	HB EGF	Rabbit polyclonal	IHC
20N (Gullick <i>et al.</i> , 1987)	HER2	Rabbit polyclonal	WB, IF
21N (Gusterson <i>et al.</i> , 1987)	HER2	Rabbit polyclonal	IHC, WB, IF
CB11 (Abcam [Cambridge, UK])	HER2	Mouse monoclonal	WB
Herceptin –(Roche [Hertfordshire, UK])	HER2	Humanised monoclonal	IF
RTJ-2 (Hunt <i>et al.</i> , 1995)	HER3	Mouse monoclonal	IHC
HFR-1 (Srinivasan <i>et al.</i> , 1998)	HER4	Mouse monoclonal	IHC
NRG1- α (Normanno <i>et al.</i> , 1993)	NRG1- α	Rabbit polyclonal	IHC
NRG1- β (Srinivasan <i>et al.</i> , 1999)	NRG1- β	Rabbit polyclonal	IHC
NRG2- α (Dunn <i>et al.</i> , 2004)	NRG2- α	Rabbit polyclonal	IHC
NRG2- β (Dunn <i>et al.</i> , 2004)	NRG2- β	Rabbit polyclonal	IHC
122NRG3 (Dunn <i>et al.</i> , 2004)	NRG3	Rabbit polyclonal	IHC
123NRG4 (Dunn <i>et al.</i> , 2004)	NRG4	Rabbit polyclonal	IHC
PY20 (Sigma [Poole, UK])	Phosphotyrosine	Mouse monoclonal	WB
GF10 (Calbiochem [Nottingham, UK])	TGF- α	Rabbit polyclonal	IHC
TAT (Woods <i>et al.</i> , 1989)	α -Tubulin	Mouse monoclonal	WB

Antibodies were available either as affinity purified stocks, or were purchased. (IHC = immunohistochemistry; IF = immunofluorescence; WB = western blotting; IP = immunoprecipitation).

Unless otherwise stated, primary antibodies were diluted in 1% bovine serum albumin (BSA [Sigma]) dissolved in 1x phosphate-buffered saline (PBS [from a 10x stock made from 80g NaCl, 2 g KCl, 14.4g Na₂HPO₄, 2.4g KH₂PO₄ dissolved in 1 litre of distilled water and adjusted to pH 7.4]).

Secondary antibodies were all purchased from manufacturers, and in some instances were supplied in particular kits. These are listed in Table 2.1.2.

Table 2.2 – Secondary antibodies used in this study

Antibody	Application(s)
Rabbit anti-mouse horseradish peroxidase (HRP)-tagged* (DAKO [Cambridgeshire, UK])	WB
Goat Anti-mouse HRP (Sigma)	WB
Swine anti-rabbit HRP (DAKO)	WB
Goat Anti-rabbit HRP (Sigma)	WB
*Biotinylated goat anti-rabbit & anti-mouse (Diagnostic BioSystems, [California, USA])	IHC
Biotinylated rabbit anti-goat (DAKO)	IHC
Goat anti-rabbit FITC (Sigma)	IF
Goat anti-human TRITC (Zymed [California, USA])	IF

(IHC = immunohistochemistry; IF = immunofluorescence; WB = western blotting)
 * Biotinylated secondary was directed against both rabbit and mouse primaries and available as part of a kit (Cat #: KP-500)

2.2. IMMUNOHISTOCHEMISTRY

2.2.1. Canine Tissues

Normal canine formalin-fixed paraffin-embedded tissue arrays were purchased from Zyagen Laboratories (California, USA). The tissues had been fixed in 10% buffered formalin and cut to 5-7µm in thickness, and two sections of tissue were mounted on slides treated for adhesion. The following tissues were purchased: bladder, cerebral cortex, kidney, liver, lung, oesophagus, pancreas, rectum, stomach and tongue.

Benign cancerous canine specimens were a gift of Heather Colhoun of Pfizer Animal Health (Kalamazoo, Michigan). These tissues were originally from paraffin-embedded, formalin-fixed samples available in the Pfizer Canine Comparative Oncology Genomics Consortium (CCOOG) Biospecimen Repository.

Malignant canine mammary cancer specimens were provided by Professor Ken Smith of the Royal Veterinary College. These were delivered as microtomed sections of samples that had previously been formalin-fixed and paraffin embedded.

2.2.2. Staining

Unless otherwise specifically mentioned in this thesis, all solutions were used at room temperature. Tissue sections were stained using the Universal HRP Immunostaining Kit for Mouse and Rabbit Primary Antibodies (Diagnostic BioSystems, Catalogue number: KP-500). This kit contained both a biotinylated secondary antibody which was directed against mouse and rabbit primary antibodies (called the "Linker" reagent), and a streptavidin-peroxidase conjugate (called the "Tracer" reagent).

As epigen and epiregulin were stained using a polyclonal goat antibody, the biotinylated antibody of the Kit was substituted with a biotinylated rabbit anti-goat HRP (DAKO, Cambridgeshire, UK) used at a 1 in 500 dilution in PBS.

Staining was performed according to the streptavidin-biotin complex method. In brief, paraffin sections were dewaxed in three four-minute Histo-Clear II (National Diagnostics, Georgia, USA) washes, and then rehydrated in a series of three four-minute graded ethanol washes (two absolute ethanol washes followed by one 70% ethanol wash). The tissues were then washed in distilled water for 5 minutes, and PBS for five minutes. Endogenous peroxidase activity was blocked by incubating tissues with a 3% hydrogen peroxide solution (diluted from 30% hydrogen peroxide [Sigma] in distilled water) for ten minutes. Tissues were again washed in distilled water for 5 minutes and PBS for 5 minutes before being incubated with the appropriate primary antibody diluted in 1% BSA (Sigma)/PBS for one hour at room temperature, or at 4°C overnight in a moist chamber. Tissues were again washed in distilled water and 1X PBS, and subsequently incubated with biotinylated secondary antibody from the staining kit for 20 minutes at room temperature. Tissues were washed as before and then incubated with a Streptavidin/HRP complex, also from the kit for a further 20 minutes. Again, the tissues were washed and then stained using 3-3'-diaminobenzidine (DAB [Diagnostic BioSystems], diluted into the supplied substrate according to the manufacturer's instructions) as the chromagen, washed for 5 minutes in running distilled water and counterstained with Gill's Haematoxylin (MERCK [Darmstadt, Germany], diluted 1:1 v/v with distilled water) for 60 seconds before being 'blued' by rinsing in running tap water for 5 minutes. Finally, tissues were dehydrated in a

series of three four-minute washes in graded ethanol (one 70% ethanol wash followed by two washes in absolute ethanol), two four-minute and one final ten-minute wash in Histo-Clear II (National Diagnostics) before being mounted in Di-n-butylPhthalate (DPX [Fischer Scientific, Leicestershire, UK]) under 22x22mm or 22x50mm coverslips (Menzel-Gläser, Braunschweig, Germany) according to the size of the tissue.

Primary antibody negative controls and peptide block controls (where the primary antibody was incubated with its complimentary peptide [15µl of 10mg/ml peptide with every 150µl antibody] at room temperature for 30 minutes on an SB1 Blood Tube Rotator (Bibby Stuart Scientific, [Staffordshire, UK]) prior to adding it to the tissue) were also carried out on select tissues. Haematoxylin-only controls were also carried out, where slides were processed as described above, with the exception of the steps involving hydrogen peroxide, antibodies and chromagen staining, which were omitted.

Images of stained tissues were obtained using a Leitz DMRB microscope (Leica) fitted with a Leica DC 300F digital camera.

2.3. CELL LINES AND CULTURE

2.3.1. Cell Lines Used In This Study

Madin-Darby Canine Kidney (MDCK) cells were originally isolated in 1958 from an apparently normal adult female cocker spaniel by S.H. Madin and N.B. Darby (Gauth *et al.*, 1966). SKBR3 cells are derived from a human breast cancer and significantly overexpress HER2. A431 cells were originally derived from an epidermoid carcinoma of the vulva of an 85 year old female patient and express abnormally high levels of EGFR. These cell lines were available from laboratory stocks (with the exception of the stably transfected cell lines, which were engineered in the laboratory), originally derived from the American Type Culture Collection (ATCC).

HEK-293/HER3 cells are derived from HEK-293 (human embryonic kidney) cells, which were stably transfected to overexpress the HER3 receptor. The c-erbB-3 clone used in this transfection was a kind gift of Dr. G. D. Plowman (Plowman *et al.*, 1990). NIH3T3 and NIH3T3/HER4 cells were originally obtained from Swiss mouse embryo tissue, with the latter having been stably transfected to overexpress HER4, and were a kind gift of Dr. B. D. Cohen (Cohen *et al.*, 1996). The NEN-7 cell line is a mouse fibroblast cell line originally

engineered from the NIH-3T3 cell line which contains a chimeric human EGFR/rat c-erbB2 proto-oncogene. This allows for EGF to stimulate c-erbB2 tyrosine kinase activity (Lehväslaiho *et al.*, 1989). The cell line was a kind gift of Dr. K. Alitalo.

The CMT28 cell line (Ahern *et al.*, 1996) is a canine mammary cancer cell line which expresses HER2 at higher levels than in normal mammary cells. The cell line was a kind gift of Dr. R.C. Bird, University of Auburn (Alabama, USA).

2.3.2. Routine Cell Culture and Maintenance

Cell lines were routinely grown in 25cm² polystyrene cell culture flasks from Sarstedt (North Carolina, USA), and in 35mm x 10mm 'Cellstar' polystyrene petri dishes, 24-well plates or 96-well plates (all from Greiner Bio One [Frankenhausen, Germany]) depending on the experiment at hand.

Cells were grown in high glucose Dulbecco's Modified Eagle Medium (DMEM [Sigma]). This DMEM contained Earle's salts and NaHCO₃, to which 10% heat inactivated foetal calf serum (FCS), 1% L-glutamine and 1% Penicillin G (sodium salt)-Streptomycin sulphate (to a final concentration of 100,000 units/L) in saline solution (to a final concentration of 100mg/L) were also added (please note that throughout this thesis unless otherwise specifically stated, "DMEM" will refer to the media and added supplements described in this paragraph). Flasks were filled with 5ml of media, while 35mm x 10mm plates were filled with 3ml, 24-well plates were filled with 1ml/well and 96-well plates were filled with 100µl/well.

Cell lines were grown from stocks available in the laboratory. The selected cell line was identified from a liquid nitrogen cryostat, removed and thawed in a water bath heated to 37°C. Once the last of the ice had thawed, the cryotube (Nunc, via Thermo Scientific [Leicestershire, UK]) they were frozen in was sterilised by wiping it with 70% ethanol before introducing it to the tissue culture flow hood. The aliquot of cells was then immediately diluted into 5ml of pre-warmed DMEM.

Cells were incubated at 37°C in 95% air and 5% CO₂. Standard cell culture techniques were applied and media was changed every two days or as required.

Cell lines were passaged when they attained 90% confluence by the addition of 1X Trypsin-ethylene diamine tetra acetic acid (EDTA) solution (0.05% trypsin, 0.53mM sodium EDTA,

from GIBCO [Paisley, UK]). Cells were then diluted in 5 ml of DMEM (Sigma) and aliquotted into fresh flasks, which were topped up with fresh media to a final volume of 5ml.

2.3.3. Freezing Down Cell Stocks

Stocks of cell lines were routinely frozen down to ensure that a renewable source of cells was available. To prepare these stocks, confluent (circa 80%) cells were trypsinised by the addition of 0.3ml of trypsin EDTA. The cells were then resuspended in 5ml of DMEM with dimethyl sulfoxide (DMSO, Sigma [Dorset, UK]) added to a final concentration of 10%. Cells were then aliquotted into 1.8ml cryotubes which were labelled and sealed.

These tubes were then bunched together with a rubber band and left on ice for 20 minutes. Following this period, the tubes were insulated with several layers of white tissue and placed in a plastic beaker. The beaker was then left at -80°C overnight. The purposes of this stepped cooling and insulation is to lower the temperature of the cells gradually, to prevent the formation of ice crystals which would otherwise harm cellular membranes. Finally, cell stocks were stored in liquid nitrogen and their location recorded. Care was taken at all stages to minimise the thawing of the stocks, as this (combined with rapid freezing) could cause damage to the cells.

2.4. IMMUNOFLUORESCENCE

Cells to be immunofluorescently stained were trypsinized from the flasks in which they grew. From these flasks, 500µl of cells were seeded onto sterile glass coverslips which had been placed in the wells of 'Cellstar' 24-well plates (Greiner). To this, 500µl of DMEM was added to maintain the cells which were then left to adhere and grow at 37°C and 5% CO₂ until they reached 30-40% confluence.

Media was then aspirated from each well and coverslips were subjected to three separate 5 minute washes in PBS before being fixed with 1ml of 4% paraformaldehyde (pH 7.4) in PBS or 1ml of ice cold 100% methanol for 10 minutes. Coverslips were again subjected to three 5 minute PBS washes, and subsequently (where required) permeabilised with 1ml of 0.1% Triton X-100 (Sigma) for 10 minutes (note that where methanol was used as a fixative, cells did not require an additional permeabilisation step).

Coverslips were then incubated in 500µl of 5% BSA (Sigma) in PBS for 30 minutes at room temperature to block non-specific binding. This buffer was drained from the coverslips onto

fibre-free paper before being incubated with 50µl of primary antibody (at an appropriate dilution in 1% BSA/PBS) by pipetting the antibody onto Parafilm (Alcan Packaging [Wisconsin, USA]) and carefully overlaying the coverslip cell-side-down onto the aliquot. Coverslips were incubated in this way for 1 hour at room temperature (or 4°C overnight) in a humidified chamber, before the primary antibody was drained away onto fibre-free paper and the coverslips were again subjected to three separate 5 minute washes in PBS.

Coverslips were then incubated with 50µl of fluorescently-tagged secondary antibody (at an appropriate dilution in 1% goat serum [Sigma]/1% BSA in PBS) in the same manner as the primary antibody was applied. Coverslips were left to incubate for 1 hour in a humidified chamber in the dark at room temperature before being rinsed three times in separate 5 minute PBS washes.

Samples were mounted onto glass slides (Menzel-Gläser via Thermo Scientific) with Histomount mounting medium (National Diagnostics via Thermo Scientific), and left to set overnight at 4°C. Slides were stored wrapped in foil, and stored in the dark at 4°C to preserve the fluorescent probes.

Peptide block controls were carried out by incubating 15µl of appropriate peptide with every 150µl of primary antibody used for 30 minutes at room temperature on a SB1 Blood Tube Rotator (Bibby Stuart Scientific).

Primary antibody negative controls were also carried out, where the primary antibody was omitted from the protocol and coverslips were instead incubated with 50µl of 1% BSA (Sigma)/PBS.

2.5. SMALL MOLECULE TYROSINE KINASE INHIBITORS

Canertinib (CI-1033) and Palladia (SU11654) were both provided by Pfizer (Sandwich, UK) and solubilised in DMSO to give 10µM stock solutions. AG1478 (Tyrphostin) was obtained from Sigma and solubilised in absolute ethanol to give a working stock of 1mM. CGP59326 was originally obtained from Novartis Pharmaceuticals (Surrey, UK) and PD158780 from Parke-Davis (now Pfizer). Both were available as stocks in the laboratory which had been solubilised in absolute ethanol to obtain stocks of 35.5µM and 30.2µM respectively. ZD1889 (Gefitinib/Iressa) and ZM260603 were both originally obtained from AstraZeneca (Hertfordshire, UK) and were available as stock in the laboratory which had been

solubilised in DMSO to obtain stocks of 22.87 μ M and 25 μ M respectively. Lapatinib and Neratinib were purchased from Chemie Tek (Indianapolis, USA) and Selleck Chemicals (Suffolk, UK) respectively, and both dissolved in DMSO to give stocks of 100 μ M.

All drug stocks were stored in the dark at 4°C.

2.6. GROWTH FACTORS

Receptor grade EGF derived from mouse submaxillary glands was sourced from Sigma to give a working concentration of 1x10⁻⁵M, dissolved in PBS and stored at -20°C. Recombinant *Escherichia coli*-derived human NRG1- β 1 was sourced from R&D Systems (Abingdon, UK) and reconstituted according to the manufacturer's instructions in sterile-filtered PBS supplemented with 0.1% BSA.

2.7. OBSERVING KINASE INHIBITION USING SMTKIS

2.7.1. The Effects of TKIs on Kinase Activity

NEN-7 cells were plated into seven 35x10 mm CellStar plates (Greiner) in 3ml of DMEM and left to adhere overnight. These seven dishes contained different experimental conditions (Table 2.7.1).

Table 2.3 – Experimental conditions of SMTKI inhibition tests

Dish	Treated with drug or vehicle?	Stimulated?
1 Negative control	Untreated	No – EGF substituted for 1X PBS
2 Positive vehicle control	Treated with vehicle only	Yes – EGF at 1x10 ⁻⁷ M
3 Positive control	Untreated	Yes – EGF at 1x10 ⁻⁷ M
4-7 TKI test dishes	Treated with various TKI concentrations	Yes – EGF at 1x10 ⁻⁷ M

One hour prior to carrying out the experiment, dishes were refreshed with 1ml of new DMEM. Following this period, the appropriate TKI was added to dish 4 to a suitable final concentration, and this was then serially diluted through to dish 7 so that a concentration dependent effect could be observed (Table 2.7.2). To dish 2, a volume of vehicle equivalent

to that used in dish 4 (as this was the dish with the highest volume added) was added to act as a vehicle control (Table 2.7.2).

Table 2.4 – Volumes of vehicles and concentrations of SMTKIs used

SMTKI	Vehicle in dish 2 and volume		Dish number and concentration of SMTKI (M)			
			4	5	6	7
Canertinib (CI-1033)	DMSO	10 μ l	1×10^{-7}	1×10^{-8}	1×10^{-9}	1×10^{-10}
CGP59326	EtOH	140 μ l	5×10^{-6}	5×10^{-7}	5×10^{-8}	5×10^{-9}
Iressa (ZD1889)	DMSO	50 μ l	1×10^{-6}	1×10^{-7}	1×10^{-8}	1×10^{-9}
Lapatinib	DMSO	10 μ l	1×10^{-6}	1×10^{-7}	1×10^{-8}	1×10^{-9}
Neratinib	DMSO	10 μ l	1×10^{-6}	1×10^{-7}	1×10^{-8}	1×10^{-9}
Palladia (SU11654)	DMSO	10 μ l	1×10^{-7}	1×10^{-8}	1×10^{-9}	1×10^{-10}
PD-158780	EtOH	30 μ l	1×10^{-6}	1×10^{-7}	1×10^{-8}	1×10^{-9}
Tyrphostin (AG1478)	EtOH	10 μ l	1×10^{-5}	1×10^{-6}	1×10^{-7}	1×10^{-8}
ZM260603	DMSO	40 μ l	1×10^{-6}	1×10^{-7}	1×10^{-8}	1×10^{-9}

The dishes were left to incubate at 37°C in 5% CO₂ for 2 hours. EGF was then added to dishes 2 through 7 to a final concentration of 1×10^{-7} M for five minutes. An equivalent volume of 1 x PBS was added to dish 1 to act as a negatively stimulated control.

Cells were then lysed (as described in section 2.8), taking care to make sure that phosphatase inhibitor cocktail (Sigma) had been added to the lysis buffer. Lysate was analysed by Western Blotting (Section 2.9). Gels were run in duplicate, and one probed for the presence of HER2 using the CB11 antibody, and other probed for phosphotyrosine using the PY20 antibody.

2.7.2. The Effect of Drug Vehicle on Kinase Inhibition

NEN-7 cells were plated in six 35x10mm CellStar petri dishes and left to adhere overnight. Cells were left to grow until they had reached roughly 70% confluence.

One hour prior to the experiment being carried out, the media was aspirated and replaced with 1ml of fresh DMEM. Following this, drug vehicles (absolute ethanol or DMSO) were added to the dishes in varying volumes (Table 2.7.3) and left for two hours at 37°C in 5% CO₂, before the addition of EGF to a final concentration of 1×10^{-7} M for five minutes.

Table 2.5 – Volumes of vehicle applied to NEN-7 cells to test for non-specific cytotoxicity

Dish & Conditions		Volume of abs EtOH	Volume of DMSO	Stimulated?
1	Negative control	Nil	Nil	No – PBS used
2	Positive control	Nil	Nil	EGF – $1 \times 10^{-7} \text{M}$
3	 Increasing volume of vehicle	1 μl	1 μl	EGF – $1 \times 10^{-7} \text{M}$
4		10 μl	5 μl	EGF – $1 \times 10^{-7} \text{M}$
5		100 μl	10 μl	EGF – $1 \times 10^{-7} \text{M}$
6		150 μl	50 μl	EGF – $1 \times 10^{-7} \text{M}$

Cells were then lysed as described in Section 2.8, and the lysate analysed by Western Blotting (Section 2.9). Gels were run in duplicate, and one probed for the presence of HER2 using the CB11 antibody, and other probed for phosphotyrosine using the PY20 antibody.

2.8. CREATION OF CELL LYSATE

The cell line to be lysed was grown in 35x10mm Cell Star petri dishes until sub-confluent (roughly 70%). Medium was then removed from the dish and discarded before performing two 1ml washes with ice-cold PBS containing 2mM EDTA. Cells were then incubated for 1-2 minutes in 200 μl of lysis buffer (0.05M Tris HCl pH 7.4, 1% Triton-X 100, 5M EDTA, 0.15M NaCl, 0.5% protease inhibitor, 1% phosphatase inhibitor [both Sigma, reconstituted following manufacturer's instructions]). The resulting lysate was collected in 1.5ml Eppendorf tubes and centrifuged at 14,000rpm for 10 minutes at 4°C in a Genofuge 16M centrifuge (Techne [Cambridge, UK]) to remove cell debris. The supernatant was decanted into fresh Eppendorf tubes, and the pellet discarded. Finally, the lysate was combined with Laemmli's sample buffer (from a 2X stock composed of: 2.5ml 0.5M Tris-HCl pH 6.8, 2ml glycerol, 4ml 10% sodium dodecyl sulphate [SDS] and 0.5ml bromphenol blue, made up to a final volume of 10ml with ultra pure water – β -mercaptoethanol was added to the buffer as required to a final concentration of 5%) (Laemmli, 1970) to a 1X concentration and heated to 60°C, before being stored at -20°C.

2.9. SDS-PAGE AND WESTERN BLOTTING

2.9.1. Bradford Assay

In instances where cells had been treated with agents that could affect their cell number and thus the total amount of protein available for analysis, Bradford Assays (Bradford, 1976) were performed to determine the total protein concentration of each sample.

Bradford Assays were performed using an Eppendorf® Biophotometer (Eppendorf [Cambridge, UK]), which had been pre-calibrated using 50µl BSA standards (containing 0, 100, 200, 300 and 400µg of BSA) mixed with 1ml of Bradford Agent (BIORAD [Hertfordshire, UK]). Standards were vortexed briefly and left to stand for ten minutes at room temperature before being used to calibrate the spectrophotometer at 580nm.

Cell lysate samples were diluted 1:10 with ddH₂O to a final volume of 50µl. To this, 1ml of Bradford reagent was added, briefly vortexed and left to react at room temperature for 10 minutes. Samples were then decanted into a plastic cuvette (Thermo Scientific), and the OD measured at 580nm.

From these readings, total protein was calculated and appropriate lysate dilutions were performed to ensure that equal quantities of protein were loaded onto acrylamide gels.

2.9.2. SDS-PAGE

Acrylamide gels were cast in the Hoefer Mighty Small Multiple Gel Caster from AP Biotech (Little Chalfont, UK), using 70x80mm gel plates. These plates were cleaned with distilled water and then rinsed with acetone and left to dry before being assembled according to the manufacturer's instructions. A total volume of 30ml of 7.5% acrylamide resolving gel (capable of resolving 17-210kDa) was prepared in a 50ml Falcon tube by the addition of the following reagents (in the following order): 5.6ml 2M Tris-HCl pH 8.8, 7.5ml 30% acrylamide/bis (BIORAD), 300µl 10% SDS in dH₂O. The solution was made up to 30ml using distilled water, covered and inverted twice. To polymerize the mixture, 10µl tetramethylethylenediamine (TEMED [Sigma]) and 300µl 10% ammonium persulphate (APS [BIORAD]) were added. The mixture was again covered and inverted twice, before being quickly poured into the gel caster leaving a 3 centimetre gap for the stacking gel. A thin layer of water saturated iso-1-butanol was poured over the top of each gel using a Pasteur pipette and left to set for approximately 20 minutes.

Once set, the layer of iso-1-butanol was poured away and the surface of each gel washed thoroughly with distilled water. The gel caster was dismantled and gel plates were assembled in the 'Mighty Small II' SE250 mini-vertical gel unit (AP Biotech) as per the manufacturer's instructions. Any resolving gels not immediately required were stored wrapped in tissue (moistened with the same 2M Tris pH 8.8 that was used to make the gels) at 4°C for up to 2 days. Stacking gel (3.75% acrylamide) was prepared in a 15ml falcon tube by the addition of the following reagents (in the following order): 1.25ml 30% acrylamide/bis solution (BIORAD), 1.25ml Tris-HCl pH 6.8, 0.1ml 10% SDS in dH₂O. The solution was made up to 9.5ml with dH₂O, covered and inverted twice. To this, 10µl TEMED (Sigma) and 500µl APS (BIORAD) was added. The mixture was again covered and inverted twice before quickly being poured around the stacking comb using a Pasteur pipette to the top of the gel plate, taking care not to introduce any air bubbles. The gel was left to set for approximately 5 minutes.

The reservoirs and spaces behind the plates of the gel running apparatus were then filled with 1X running buffer (diluted down from a 10X stock composed of 0.25M Tris pH 8.6, 1.92M glycine and 10% SDS in dH₂O made up to 1L with dH₂O). The stacking combs were carefully removed and 30µl of protein samples were loaded into each of the lanes using a 200µl Pipetman (Gilson [Wisconsin, USA]) – 1X sample buffer was loaded into unused wells to maintain a constant potential difference across the sample front during electrophoresis and all gels were run with high range (10-250kDa) dual colour Precision Plus Protein Standards (BIORAD). Initially 60 volts were applied to the apparatus with the 'Power-Pac 200' (BIORAD) whilst the dye front ran through the stacking gel, and this was increased to 120 volts as the samples passed through the resolving gel. The power pack was switched off once the dye front reached the bottom of the gel.

2.9.3. Western Blotting

Proteins separated through SDS-PAGE were transferred onto nitrocellulose membranes for antibody probing using the Trans-Blot® Electrophoretic Transfer Cell (BIORAD). The following materials were soaked in transfer buffer (250ml 10X SDS running buffer [see section 2.9.2], 250ml methanol and 25ml 10% SDS made up to a final volume of 2.5 litres with dH₂O): 2 pieces of filter paper (cut to the size of the transfer cassette), Hybond ECL nitrocellulose membrane (AP Biotech [Buckinghamshire, UK]) and 2 scotch pads (BIORAD). These were then assembled in the following order on the bottom electrode of the transfer apparatus: 1 scotch pad, 1 filter paper, nitrocellulose paper, gels (directly on top of the

nitrocellulose paper and cut in one corner for orientation), 1 filter paper and 1 scotch pad. A razor blade was used to trim away any excess nitrocellulose paper from around the gels, in order to maintain a constant and equal flow of electrical current through the apparatus. A Pasteur pipette was rolled over the 'sandwich' throughout assembly of each layer to remove any air bubbles. The cassette was closed and locked before being loaded into the transfer tank and run at 400mA for 3 hours, or 100mA overnight.

Once transfer was complete, the apparatus was disassembled. The gels were stained with Coomassie Blue (2.5g Coomassie stain, 450ml methanol, 100ml acetic acid and 450ml dH₂O) and then destained (10% acetic acid in dH₂O) to determine the level of protein transfer. Meanwhile blots were stained with 0.1% Ponceau S (Sigma) in 0.5% acetic acid to detect protein. Ponceau S stain was removed from the blot by repeated washing in 1X PBS/0.1% Tween 20 (Fischer [Loughborough, UK]).

Blots were blocked for 1 hour at room temperature in blocking buffer (175ml 1X PBS, 6.25g non-fat milk powder [Marvel, UK] and 62.5 µl Tween 20). Blots were then rinsed once using 1X PBS/0.1% Tween 20 and subsequently incubated with primary antibody diluted in blocking buffer at room temperature for 1.5 hours (or overnight at 4°C) with constant shaking. Blots were subjected to 5 separate 5 minute washes using 1X PBS/0.1% Tween 20 before being incubated for one hour with secondary antibody, again diluted in blocking buffer, with constant shaking. Blots were again washed (as above) before being developed using enhanced chemiluminescent (ECL) reagents (prepared in the lab and composed of two separate solutions, the first containing: 1ml of 250 mM luminol [Sigma] in DMSO, 440µl 90 mM coumaric acid [Sigma] in DMSO, 10ml 1M Tris-HCl pH 8.5 and distilled water to a final volume of 100ml; and the second: 64µl hydrogen peroxide, 10ml 1M Tris-HCl pH 8.5 and distilled water to a final volume of 100ml). ECL solutions were combined in a 1:1 ratio and applied to the blot. Signals were detected on Hyperfilm ECL (AP Biotech) in a dark room, which were then developed using a Compact X4 Film Processor (Xograph [Gloucester, UK]).

2.10. CELL PROLIFERATION ASSAYS

2.10.1. Cell Harvesting, Counting & Seeding

Several flasks of confluent (circa 80%) cells were trypsinised, resuspended in 5ml DMEM and centrifuged at 1000 rpm for 5 minutes in a Centaur 2 Bench Top centrifuge (MSE [London, UK]). The trypsin-containing media was aspirated from the pellet, which was then resuspended in 2-5ml of fresh DMEM. Cells clumps were broken up by gentle pipetting up and down.

To 40 μ l of this cell suspension an equal volume of Trypan Blue (Sigma) was added, and gently pipetted up and down to mix. A haemocytometer (Marienfeld [Germany]) was prepared by placing a thick glass cover slip (Marienfeld) tightly against the counting chambers. This haemocytometer consisted of a thick glass microscope slide with two counting chambers engraved onto one surface. Each chamber was divided into nine squares, each of which had a surface area of 1mm². The cover slip was supported 0.1mm over the chambers, giving each square a total volume of 0.1mm³.

To count the cells, 20 μ l of the cell/Trypan Blue solution was pipetted onto the join of the cover slip and the haemocytometer and the solution was drawn into the counting chambers by capillary action. Care was taken not to overfill the counting chambers and cause leakage. The haemocytometer was placed on an Olympus CKX31 inverted microscope for cell counting.

Cells which did not stain blue (as the dye is excluded from live cells possessing an intact cell membrane) were counted. The number of these live cells in five individual 0.1mm³ squares was counted in each chamber (making a total count of ten 0.1mm³ squares), from which the average number of cells per square was derived. Cells which lay on a boundary between squares were only counted where those cells intersected two square boundaries. If over 10% of the cells represented were in clumps all steps were repeated, avoiding aggregates.

The number of cells per ml was calculated using the formula:

$$\text{cells ml}^{-1} = \text{average cell number} \times 10^4 \times \text{dilution factor}$$

Further calculations were carried out to determine the dilution factors required to obtain the appropriate number of cells for seeding.

2.10.2. Reading Cell Proliferation Assays

WST-1/ECS dye (Millipore, [Watford, UK]) was prepared following the manufacturer's instructions by dissolving the supplied lyophilized WST-1 reagent with 5ml of the supplied Electro Coupling Solution.

To each well of the 96-well plate 10 μ l of WST-1/ECS was added and left to develop for between 30 minutes to 1 hour. Plates were then read on a Multiskan Ascent plate reader (Thermo Fisher Scientific, [Essex, UK]) with the measurement filter set at 450nm and the reference filter set at 620nm. Plates were shaken on a medium setting for one minute prior to reading.

2.10.3. Generation of Mammalian Cell Growth Curves

Cells were first harvested and counted (see section 2.10.1) and then seeded into a 96-well plate with 100 μ l of DMEM using a repeating pipette. These cells were seeded at varying concentrations: 750 cells/well, 1500 cells/well, 2500 cells/well, 5000 cells/well and 10000 cells/well. The outermost wells of the plate were not used for cell seeding, and were instead filled with 100 μ l of DMEM to prevent media loss in the plate by evaporation whilst in the incubator.

Cells were left to grow for 7 days before reading the plate (as described in section 2.10.2).

From the results, a growth curve was generated from which a suitable number of cells for seeding in future experiments was determined by observing the log phase of growth. For CMT28 cells this was determined to be 600 cells/well.

2.10.4. Investigating the Effect of Growth Factors on Cell Proliferation

The effects of EGF (Sigma) and NRG1 β (R&D Systems) growth factors on cell growth were determined by first seeding an appropriate number of cells (as determined from the growth curve – see previous section) in 100 μ l DMEM. Cells were left to adhere for 24hrs, before the media was aspirated and replaced with serum-reduced DMEM (containing only 0.1% FCS). Cells were then serum-starved in this way for 24 hours before a range of concentrations (1x10⁻⁶M, 1x10⁻⁷M, 1x10⁻⁸M and 1x10⁻⁹M) of growth factor were added (also diluted in reduced-serum DMEM). One row of cells was left as an untreated control.

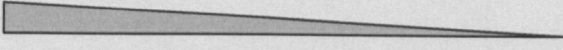
Cells were then left at 37 °C in 5% CO₂ and 100% humidity for seven days before reading the plates as described in section 2.10.3.

2.10.5. Investigating the Effect of Tyrosine Kinase Inhibitors on Cell Proliferation

Cells were counted and seeded at 600 cells/well (as described previously in section 2.10.1) and left to adhere overnight. The following day, the serum-containing media was aspirated and replaced with a reduced-serum media for 24 hours in order to serum starve the cells.

Tyrosine kinase inhibitors (diluted in reduced-serum media) were added at a range of concentrations to the cells (Table 2.10.1), making sure to leave an untreated row of cells and a media-only row as controls. After 7 days, the plates were read as described previously by WST-1 assay.

Table 2.6 – Concentration of SMTKIs used in cell proliferation experiments

SMTKI	Final concentration				Negative control (media only)
					
Lapatinib (Tyverb/Tykerb)	1x10 ⁻⁶ M	1x10 ⁻⁷ M	1x10 ⁻⁸ M	1x10 ⁻⁹ M	OM
Neratinib (HKI-272)	1x10 ⁻⁶ M	1x10 ⁻⁷ M	1x10 ⁻⁸ M	1x10 ⁻⁹ M	OM

2.11. siRNA KNOCKDOWN

2.11.1. siRNA Design

Specific small interfering ribonucleic acids (siRNAs) against the canine HER2 mRNA were designed using the Invitrogen Block-iT RNAi Designer (<https://rnaidesigner.invitrogen.com/rnaiexpress/>), which predicts siRNAs likely to be effective at protein knockdown and BLASTs the results against the appropriate species database to check for specificity. siRNAs were designed to be 21-mers and to have 3' overhangs of two deoxythymidines to enhance RNA-induced silencing complex (RISC) loading and make the siRNA more resistant to exonuclease activity.

siRNA 1: GCAGGGCUAUGUGCUCAUU-dTdT (sense) and AAUGAGCACAUAGCCUGC-dTdT (antisense); siRNA 2: CCCAGCUCUUUGAGGACAA-dTdT (sense) and

UUGUCCUCAAGAGCUGGG-dTdT (antisense); siRNA 3: CCUACAACACGGACACCUU-dTdT (sense) and AAGGUGUCCGUGUUGUAGG-dTdT (antisense).

Two controls consisting of the scrambled sequences of siRNAs 1 and 2 were also designed, BLASTed and purchased:

siRNA Control 1: GCAAUCGGUGUCUCGGAUU-dTdT (sense) and AAUCCGAGACACCGAUUGC-dTdT (antisense); siRNA Control 2: CCCUCUCAGUUAGGGACAA-dTdT (sense) and UUGUCCCUAACUGAGAGGG-dTdT (antisense).

These sequences were synthesised by Eurofins MWG Operon (Ebersberg, Germany). siRNAs were reconstituted following the manufacturer's instructions in 5X siMAX buffer (provided by MWG) diluted to a 1X solution with RNase-free water.

2.11.2. Observing siRNA Knockdown

In order to first observe HER2 knockdown using siRNA, cells were plated in 7 separate 35x10mm dishes (enough for 3 test siRNAs, 2 scrambled control siRNAs, and a mock transfection control and an untreated control) in 2ml of DMEM supplemented with 10% FCS, 1% L-glutamine but lacking penicillin-streptomycin. Cells were left overnight to adhere and grown to roughly 50% confluence.

All transfection steps were carried out in a Class II Tissue Culture Hood. siRNA transfection was carried out using Lipofectamine 2000 transfection reagent (Invitrogen) following the manufacturer's instructions. Briefly, the appropriate siRNA was diluted in 250µl Opti-MEM® I Reduced Serum Media (Invitrogen), so that the final concentration when the full transfection complex was added to the cells would be 33nM (that is, 33nM siRNA in 2500µl media - 2000µl plating media, and 500µl of transfection complex). The solution was mixed by gently flicking. In a separate tube, 5µl of Lipofectamine 2000 transfection reagent was added to 250µl of OPTI-MEM media. This was also mixed gently by flicking, and left to incubate at room temperature for 5 minutes. Following this, 250µl of Lipofectamine 2000 and 250µl of siRNA were combined, gently mixed and left to incubate at room temperature for 20 minutes in order to form oligomer-Lipofectamine 2000 complexes. The full 500µl of this complex was added to the appropriate dish of cells, and mixed by gently rocking back and forth. The media was changed after 6 hours and replaced with DMEM containing 0.1% FCS and 1% L-glutamine but still lacking penicillin-streptomycin, to minimise non-specific transfection agent cytotoxicity.

It should be noted that elsewhere in this chapter, Lipofectamine 2000 is used in a variety of tissue culture vessels. The manufacturer's instructions were followed when scaling these transfections up and down, and the volumes of plating media and transfection agent used are summarised in Table 2.11.1.

Cells were incubated at 37°C in 5% CO₂ for 24 hours and 36 hours, before they were lysed (Section 2.8). Lysate protein concentration was determined by Bradford Assay and protein knock-down assayed for by SDS-PAGE and Western Blot (see Section 2.9) using the 20N antibody. Tubulin loading controls were also probed for on the same blot.

Table 2.7 – Scaling up and down siRNA transfections with Lipofectamine 2000

Vessel	Volume of plating medium	Volume of dilution medium µl per well (or dish)	Volume of Lipofectamine 2000
96-well plate	100	2 x 25	0.25
24-well plate	500	2 x 50	1
35x10mm dish	2000	2 x 250	5

Note: In all cases, siRNA was transfected to a final concentration of 33nM/well (or dish)

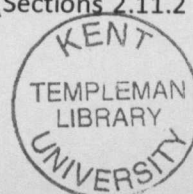
2.11.3. Cell Proliferation Assays Using siRNA

Where this technique was applied in proliferation assays, CMT28 cells were again seeded at 600 cells/well. The transfection was performed as previously described (Section 2.11.2), following the manufacturer's instructions for scaling down the transfection. Cells were also given 6 hours to transfect, after which time the media was aspirated and replaced with DMEM containing 0.1% FCS and 1% L-glutamine but still lacking penicillin-streptomycin. Cells were left for 7 days before the results were read by WST-1 assay (Section 2.10.2).

2.11.4. Observing Apoptosis Using Propidium Iodide

Cells were harvested and counted as described previously and plated at a concentration of 4000 cells/well into 7 wells of a 24 well plate (enough for three test siRNAs, two scrambled controls, and one mock transfected and one untransfected well of cells), each well of which contained a glass coverslip.

Cells were left to adhere overnight, and transfected with siRNA as previously described (Section 2.11.2) to a final concentration of 33nM siRNA/well, following the manufacturer's instructions for scaling down the transfection. The siRNA: Lipofectamine 2000 ratio was kept the same as in knockdown observation and proliferation (Sections 2.11.2 and 2.11.3



respectively) experiments. After 6 hours, the media was changed to minimise any cytotoxic effects caused by prolonged exposure to the transfection reagent. Cells were then left for 3 days at 37°C and 5% CO₂.

Following this 3 day incubation, the media was aspirated from each well and each was then washed three times with 1ml of 1x PBS. Cells were then fixed with 1ml of ice-cold methanol per well at room temperature for 10 minutes, and subsequently washed again with three separate 1ml 1X PBS washes. Cells were then incubated for 7 minutes with 1ml of propidium iodide ([Sigma] dissolved in 1X PBS to 20µg/ml) at room temperature in the dark, and again washed in three separate 1ml PBS washes.

Coverslips were mounted cell-side down onto glass slides using Histomount mounting medium (National Diagnostics via Fischer Scientific) and left to set over night at 4°C in the dark.

Fluorescence was observed using a Leitz DMRB microscope (Leica) fitted with a Leica DC 300F digital camera.

2.12. RNA ISOLATION

RNA was isolated from the MDCK and CMT28 cell lines using the RNeasy kit (Qiagen [Sussex, UK]), following the manufacturer's instructions. Owing to the easily degradable nature of RNA, care was taken at all times to minimise the chance of contamination by using full personal protective equipment and by regularly decontaminating gloved hands and bench top equipment with RNase-Away[®] (Sigma).

Final RNA concentration was determined by spectrophotometric analysis using a BIO-RAD 'SmartSpec 3000' (BIORAD) reading absorbance at 260nm. RNA was diluted in 10mM Tris HCl pH7.5 to obtain accurate values. A₂₆₀ readings should be greater than 1.5. Pure RNA should exhibit A₂₆₀/A₂₈₀ ratios of 2.0, however due to variations between starting materials and in performing the procedure ratios of 1.7-2.0 were deemed acceptable. Cuvettes were washed with 0.1M NaOH, 1mM EDTA, followed by a wash with RNase-free water.

Stocks of RNA were stored at -80°C.

2.13. cDNA SYNTHESIS BY REVERSE TRANSCRIPTION

cDNA was synthesised from RNA isolated from cell lines using reverse transcription (RT). To 1µg of total cellular RNA, 1µl of Oligo(dT)₁₂₋₁₈ primer (Invitrogen [Paisley, UK]) was added and the total volume made up to 10µl with Rnase-free water. This mixture was incubated at 70°C for 10 minutes before the addition of 10µl of reverse transcription 'mastermix', consisting of: 4µl 5X RT buffer (Invitrogen), 2µl 0.1mM dithiothreitol (DTT [Invitrogen]), 2µl 5mM deoxynucleotide triphosphates (dNTPs), 1µl RNasin (Promega [Dublin, Ireland]) and 1µl Superscript II RT (Invitrogen). Enough 'mastermix' was added to make a total reaction volume of 20µl. This was then incubated at 37°C for 90 minutes and the cDNA product stored at -20°C.

2.14. PCR & AGAROSE GEL ELECTROPHORESIS

2.14.1. Polymerase Chain Reaction

Polymerase chain reactions (PCRs) were carried out using primer pairs designed to be specific for the four canine EGF-receptors, EGFR: 5'-TCTGACAGCTACGAGGTGGA-3' (forward) and 5'-TCGACGTGCAGTTTTTGAA-3' (reverse); HER2: 5'-AGCCAAGTGAGGCAGATCC-3' (forward) and 5'-GGTCTCCATTGTCCAGCAC-3' (reverse); HER3: 5'-GGGAGCCGCTTCCAGACT-3' (forward) and 5'-CCGTACTGTCCGGAAGACAT-3' (reverse); HER4: 5'-CATGGCCTTCCAAGTACTGACT-3' (forward) and 5'-CACCTGCCATCACAAGTGTTC-3' (reverse).

Primers were designed using the publicly available canine genomic sequences, and the online [Primer3: WWW Primer Tool](http://biotools.umassmed.edu/bioapps/primer3_www.cgi) (http://biotools.umassmed.edu/bioapps/primer3_www.cgi). Primers were synthesized by Eurofins MWG and purified through High Purity Salt Free (HPSF[®]) purification.

PCRs were carried out with the following reagents: 10x PCR Reaction Buffer, Taq DNA Polymerase (both Roche [Hertfordshire, UK]) and 20mM dNTPs, all of which were used at concentrations recommended in the manufacturers' instructions. Throughout the preparation of PCRs, care was taken to ensure there was no cross-contamination between

samples. The volume of each reaction was adjusted as necessary using distilled water to a final volume of 50 μ l.

Samples were thermo cycled in a 'GeneAmp PCR System 9700' from Applied Biosystems (Warrington, Cheshire, UK). General conditions used for thermo cycling are described in Table 2.14.1.

Table 2.8 – Thermo cycling conditions

	Step	Temperature	Time	
35 cycles	1	94°C	3 min	Initial denaturation step
	2	94°C	1 min	Denature double stranded DNA
	3	*52.2-56°C	1 min	Primer annealing
	4	72°C	1 min 30s	DNA extension
	5	72°C	7 min	Final extension to ensure DNA synthesis is complete
	6	4°C	∞	To preserve DNA at the end of thermo cycling

* At this stage, the temperature required depended on the primer set being used

2.14.2. Agarose Gel Electrophoresis

DNA products were resolved on 3% agarose gels, made up using Certified Molecular Biology Agarose (BIORAD) dissolved in 50ml 1X tris-acetate EDTA (TAE) buffer (diluted from a 50X stock composed of 242g Tris, 57.1ml glacial acetic acid and 18.6g EDTA adjusted to 1 litre with dH₂O) stained with 5 μ l SYBR Safe DNA Gel Stain (Invitrogen), and then cast in the Flowgen (Nottingham, UK) 10cm x 7cm Mini Gel Tank. All gels were run with a 25bp DNA ladder from Invitrogen. DNA samples and ladders were made visible to the naked eye by the addition of Blue/Orange 6x loading dye (Promega) to a final concentration of 1X. Electrical current was applied to the gels using a 'Power-Pac 200' (BIORAD) at 60 volts for roughly 30 minutes, or until the dye front was three quarters of the way down the gel.

Gels were visualised and photographed under UV light using a Kodak Gel Logic 100 Imaging System.

CHAPTER THREE

Bioinformatical Analysis of Canine HER2

3.1. INTRODUCTION

In recent years, human genes and proteins have been extensively analysed, sequenced and studied, culminating in the publishing of the human genome. Not only did this represent a milestone in our understanding of human origins, but it also allowed for many scientific investigations of human genes and disease to be carried out *in silico*. This achievement has since been followed by the publication of the genomes of a number of other organisms, among them the dog. Before embarking on the laboratory portion of this project, it was important to investigate the scope of information relating to the EGF family already available. Bioinformatics provides a number of tools and databases which provide an opportunity to learn more about a particular species' genetic make-up through cross-genomic comparisons, which is particularly useful in species which are closely related, such as *H. sapiens* and *C. familiaris*.

With regard to the EGF family (with which this project is concerned), some members have been shown in the laboratory and through bioinformatical analysis to have a number of different gene products. The resulting isoforms of these gene products may have significantly different structures and activities, which possibly not only affect their role in cell signalling, but also to what extent therapies targeted against them may be successful as alterations in protein structure can affect receptor dimerization, trigger constitutive activation and mask drug binding sites.

There are several different mechanisms through which various gene products are produced:

- Posttranslational modifications, where the addition of biochemical function groups (such as carbohydrates, acetates, phosphates and lipids) can alter the chemical nature of a peptide or bring about structural changes (for example the creation of disulphide bonds or proteolytic cleavage);
- Alternative initiation due to the presence of alternative initiation codons within the mRNA;

- Gene splicing, which can splice exons in or out of sequence and, in some cases, splice in alternative exons.

Before embarking on an analysis of these processes in the canine EGF family, it was important to review what is already known in human cases. A number of examples of the mechanisms described above are found in the EGF receptors in humans.

One such example is the presence of a truncated form of HER2 (also known as p95-HER2) which lacks the extracellular regions of the receptor. This truncated form arises either through a process of proteolytic shedding of the extracellular domain (Christianson *et al.*, 1998; Codony-Servat *et al.*, 1999), or through alternative initiation of translation from two methionine residues that are located before and after the transmembrane domain, (611 and 687 respectively) (Anido *et al.*, 2006).

It has been shown *in vitro* that this truncated form of HER2 in breast tumours will not bind Herceptin, although it is still vulnerable to phosphorylation inhibition by SMTKIs such as lapatinib (Scaltriti *et al.*, 2007).

Expression of p95-HER2 has been shown to be present in up to 30% of human breast tumours with HER2 overexpression (Molina *et al.*, 2001), and its presence may in part be the reason why not all patients treated with Herceptin respond to therapy. Truncated p95-HER2 has also been associated with aggressive disease and high risk of lymph node metastatic progression (Christianson *et al.*, 1998; Sáez *et al.*, 2006), and is considered a marker of negative prognosis.

Another example of a more recently identified isoform, is one in which exon 16 is spliced out of HER2, giving rise to a particular gene product known as $\Delta 16$ HER2. Research has shown that there is an in-frame deletion in this gene product in the same region that is mutated in neu or HER2 proto-oncogene ERBB2 mice, which removes extracellular cysteine residues involved in maintaining protein structure in HER2. This subsequently disrupts disulphide bonds within the protein, and leaves any unpaired cysteine residues available for intermolecular bonding (Marchini *et al.*, 2011), resulting in this isoform of HER2 being constitutively active.

This isoform was originally detected in a number of HER2-overexpressing breast cancer cell lines (Kwong & Hung, 1998; Siegel *et al.*, 1999) and primary tumours (Siegel *et al.*, 1999; Castiglioni *et al.*, 2006). Studies have shown that in breast cancers which have spread to

local lymph nodes and which are HER2 positive, $\Delta 16\text{HER2}$ is present in 89% of patients (Mitra *et al.*, 2009). It has been reported that this isoform also possesses enhanced transforming activity (Kwong & Hung, 1998; Siegel *et al.*, 1999), promotes receptor dimerization and cell invasion, and breast cancers expressing this isoform *in vitro* seem to have increased resistance to Herceptin therapy (Mitra *et al.*, 2009).

Similarly the RET (rearranged during transfection) proto-oncogene which encodes a receptor tyrosine kinase belonging to the glial cell line-derived neurotrophic factor family (Knowles *et al.*, 2006) undergoes splicing to give rise to a number of gene products: isoforms RET59, RET43 and RET9 (where the numbers in their nomenclature correspond to the number of amino acids in their C-terminal tails)(Myers *et al.*, 1995).

Activating point mutations within these RET isoforms give rise to genes whose products cause ligand-independent activation of the receptor, and which can cause patients to develop multiple endocrine neoplasia (MEN) type 2 hereditary cancer syndromes, of which there are three subtypes: MEN2A, MEN2B and familial medullary thyroid carcinoma (FMTC) (Vita *et al.*, 2000). To date, more than 100 mutations have been reported in RET (Knowles *et al.*, 2006). Of those that account for the gain-of-function mutations associated with MEN type 2 cancer syndromes, the mutations are grouped into those present in the cysteine rich regions of the receptor, and those within the RET kinase domain. The most common residue mutated in MEN2A patients is cysteine 634, where one-half of an intramolecular disulphide bond is removed, allowing for the formation of an intermolecular disulphide bond with a second mutant molecule. This arrangement leads to constitutive receptor dimerization and aberrant signalling (Knowles *et al.*, 2006). Mutations within the kinase domain have much more varied mechanisms, but are not known to give rise to constitutive receptor dimerization (Knowles *et al.*, 2006).

At the time of writing, literature searches showed no studies into the presence (or lack thereof) of splice variants within the canine ERBB2 gene. Knowledge of whether HER2 isoforms exist in dogs could be valuable in considering what therapies to administer to a veterinary patient, and could be taken into consideration in future drug discovery programs. This knowledge may also further encourage the scientific community to use the dog as a useful model for disease and in drug trials.

One method of investigating the presence of these isoforms in canine sequences is through bioinformatical analysis. Using sequence comparisons and alignments, and mapping intron and exon boundaries, it is possible to speculate on what isoforms may be present in dogs simply through the application bioinformatical tools and analysis to publicly available protein and gene sequences.

To this end, this chapter describes a number of genetic and protein comparisons that were drawn between canine and human HER2 using various bioinformatic tools.

3.2. AIMS

1. To compare canine and human HER2 through sequence alignments, dot plot analysis and observations on protein structure;
2. To compare intron and exon boundaries between the two species and investigate splice variation in the canine gene.

3.3. RESULTS

3.3.1. Comparisons of Human and Canine HER2

Before conclusions can be drawn with regard to the presence of isoforms in canine HER2, comparisons must first be made between the protein and genetic sequences of canine and human HER2. To this end, the publicly available sequences for canine and human HER2 were compared, first through preliminary dot plot analysis (which provides a general idea of regions of homology between sequences) and then through more detailed sequence alignment using BLAST (Basic Local Alignment Search Tool) analysis (available from the National Centre for Biotechnology Information [NCBI]). Protein structure was also analysed through observation of how likely it tended towards structural disorder.

The canine genomic and protein sequences encoding HER2 were retrieved from the Ensembl genome browser (ID: ENSCAFG00000016351). Examination of this entry showed

that (at the time of writing) the gene is located on chromosome 9 and is 24,116 bases long (starting at base 26,088,707 and ending at 26,112,823) and contains 27 exons.

The human genomic and protein sequences encoding HER2 were also available from Ensembl (ID: ENST00000406381). Annotations on this entry showed that the gene is located on chromosome 17, is 40,522 bases long (starting at base 37,844,393 and ending at 37,884,915) and contained 29 exons.

In addition to having the exons annotated onto the gene, these sequences have also had their 5' upstream and 3' downstream untranslated sequences identified.

It should be noted that the Ensembl entry for human HER2 had a number of transcripts available for analysis. This entry showed that there were six different human HER2 transcripts (see Table 3.1), although only 3 of these were consensus coding sequences (CCDS [the CCDS project is a collaborative effort to identify a core set of protein coding regions that are consistently annotated and of high quality (Pruitt *et al.*, 2009), making these sequences more reliable]).

Table 3.1 – Ensembl entries for human ERBB2 gene

Name	Transcript length (bp)	Exons	Peptide length (aa)	CCDS?
ERBB2-201	4624	27	1255	CCDS32642
ERBB2-202*	4806	29	1225	CCDS45667
ERBB2-203	3238	21	979	-
ERBB2-204	2147	15	603	-
ERBB2-205	4624	27	1225	CCDS45667
ERBB2-206	4341	27	1240	-

* This transcription was used in bioinformatic comparisons in the rest of this chapter, as it was the longest and most completely annotated.

To compare these sequences, the cDNAs of each of these transcripts were BLAST aligned against ERBB2-202 (Figure 3.1a). This alignment showed that while all the transcripts were able to fully align with the longest (ERBB2-202) sequence, none were the same length. Alignments ERBB2-201, 205 and 206 all had the same percentage query coverage (89%) owing to their similarities in length and exon numbers (indeed, ERBB2-202 and ERBB2-205 appear to actually be identical entries as they share the same CCDS identifier). ERBB2-203

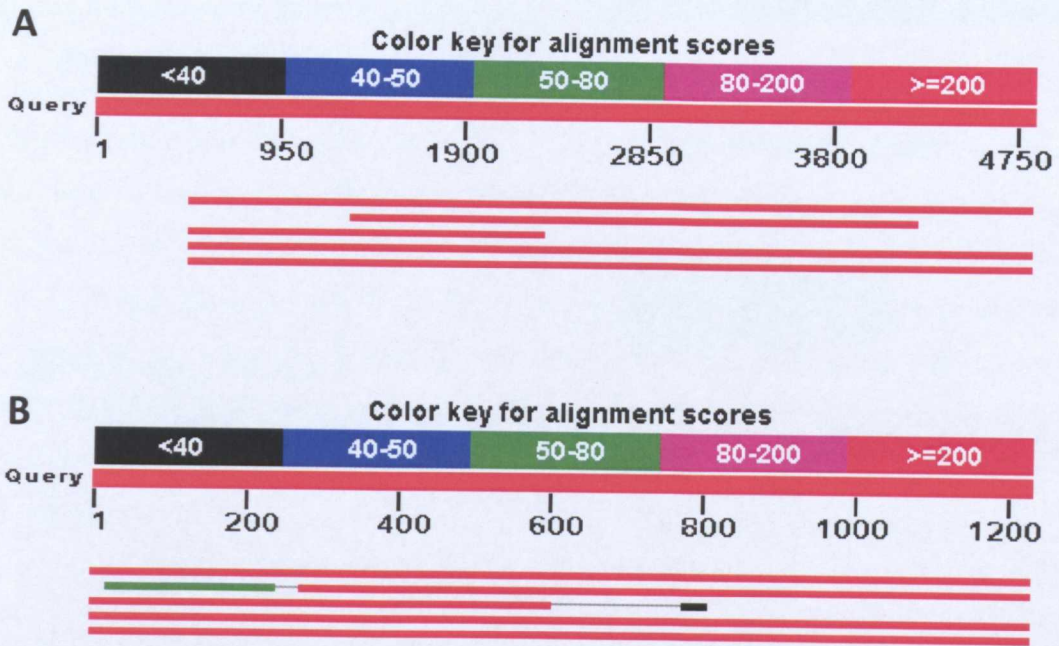


Figure 3.1: BLAST alignments of Ensembl entries for human HER2. **A:** cDNA alignments; **B:** peptide alignments. In each case, the Query sequence is ERBB2-202. The other sequences are (from top to bottom: ERBB2-201, ERBB2-203, ERBB2-204, ERBB2-205 and ERBB2-206).

aligned in the middle portion of the query (ERBB2-202) sequence, but not at either the 5' or 3' ends, and ERBB2-204 aligned with the beginning of sequences ERBB2-201, 205 and 206.

Reasons for these differences can be explained by looking at the exon structures of the sequences (Figure 3.2). The sequences which align the most (ERBB2-201, 205 and 206) with full-length (ERBB2-202) ERBB2 lack the first two exons of the longer sequence (and have their first exon in a different location), but other than that are predominantly conserved. ERBB2-203 also lacks these first three exons, but in addition to this lacks a further five at the beginning of its sequence. ERBB2-204 is the smallest of these sequences and contains only 15 exons, which align with the beginning of the shorter sequences (ERBB2-201, 205 and 206).

A further BLAST alignment was performed on the proteins of these sequences to determine how they were related to one another (Figure 3.1b). Results from this showed that all sequences (except ERBB2-203) aligned well at the beginning of the sequence. This would suggest that the initial 2 exons at the beginning of ERBB2-202 which all the other sequences lack are not particularly relevant to protein coding. Indeed further analysis of

the exonic sequence of ERBB2-202 shows that the first three exons are composed entirely of untranslated sequence.

Similarly to the cDNA alignment, ERBB2-203 and 204 are rather different from the other transcripts. In the case of ERBB2-204, the peptide aligns with the beginning of the sequence, as exon 4 (where translated protein sequence appears to begin) is conserved. However as this sequence consists of only 15 exons, the alignment is significantly shorter (aligning only up to roughly residue 600 of ERBB2-202). Further along the alignment of ERBB2-204, there is a small and very low-scoring alignment (black bar on the graph in Figure 3.1b). Given that this alignment is so short (only 34 residues), only has a percent identity of 28% and a very high e-value of 6.3, it is likely that this alignment occurred by chance, rather than being a “true” alignment.

With ERBB2-203, it can be seen that there is a strong alignment for most of the sequence, with there being an alignment with a lower score at the beginning (green line on graph in Figure 3.1b). From looking at the exon boundaries in Figure 3.2, it would be expected that there would be a strong alignment for the latter portion of this transcript as it lacks five exons at the beginning of the sequence. The presence of the less strong (green) alignment is unexpected, and corresponds to a low-scoring alignment with 25% identity between the two sequences. Further exonic alignments were carried out between ERBB2-202 and 203 to investigate this. It was found that ERBB2-203 only aligned with exons 10 through 29 of ERBB2-202, and not anywhere earlier in the sequence, which the protein BLAST alignment would seem to suggest. Further analysis of this alignment using Artemis showed that it was protein sequence from exons 10 through 16 which was aligning at the beginning of the sequence. However closer inspection of the BLAST results showed large gaps in this alignment which combined with the low percent identity (25%) between the two sequences, the relatively short length of the alignment and a relatively high error score of 2×10^{-15} compared to the other alignments (which all scored 0) would suggest that this alignment happened perhaps by chance (similarly to that of the short alignment at the end of ERBB2-204) rather than being a “true” alignment.

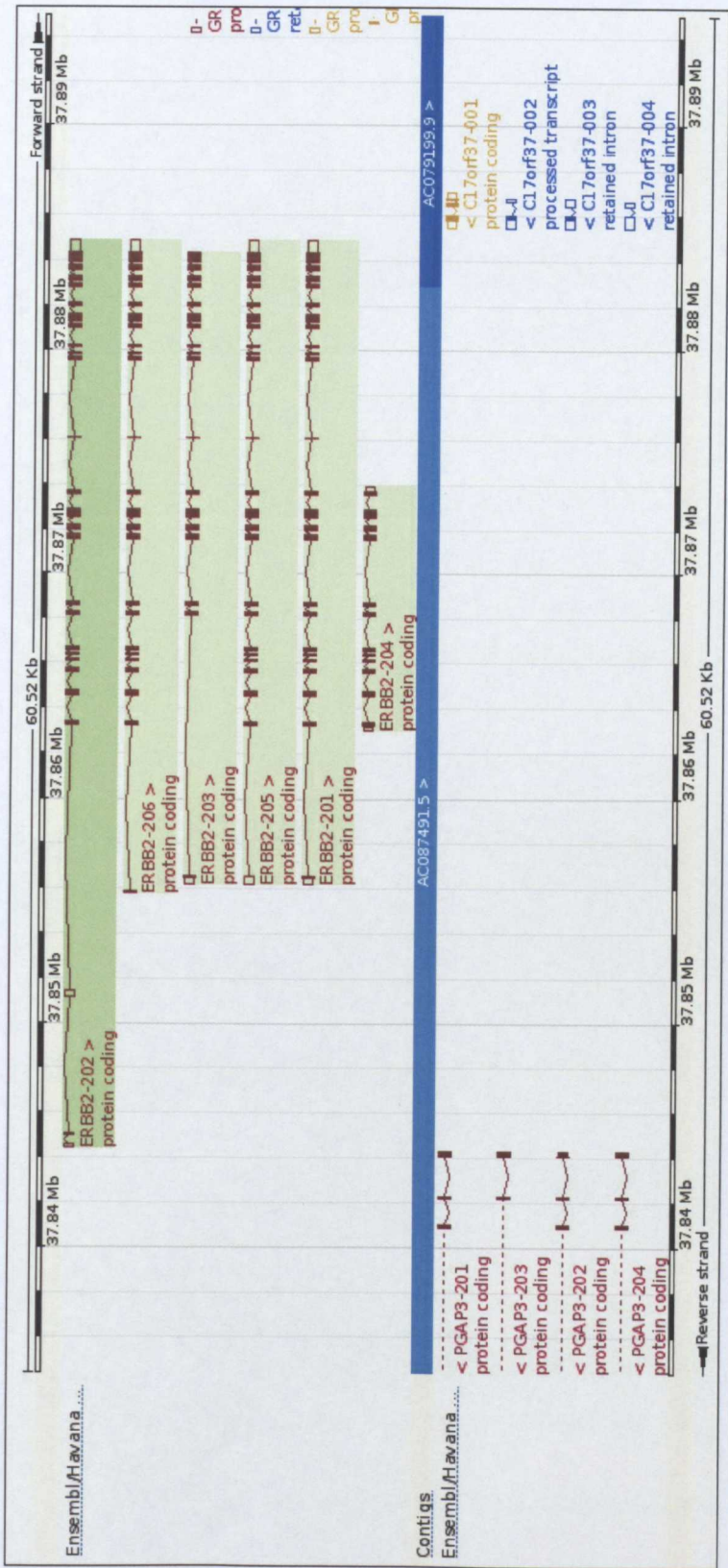


Figure 3.2: Ensembl alignments of transcripts of the human HER2 showing exons (red boxes). This alignment shows that ERBB2-202 is significantly longer than the other transcripts, owing to the presence of two extra exons at the beginning of its sequence. Further exonic analysis showed that these exons coded for untranslated regions, which were not present in the other transcripts. Transcripts ERBB2-201, 205 and 206 are highly similar to each other. While ERBB2-203 shows a similar nucleotide length to these sequences, it is missing five exons from the beginning of its sequence, making its peptide length somewhat shorter. ERBB2-204 is the shortest of the sequences, lacking exons at both 5' and 3' ends, however it still retains the exons which contain translated protein sequence so it aligns with the beginnings of each of the other peptide transcripts (see Figure 3.1b).

3.3.1.1. Dot Plot Analysis

From the dot plot analysis (carried out using Dotlet [<http://myhits.isb-sib.ch/cgi-bin/dotlet>], Figure 3.3) it can be seen that canine and human sequences are highly similar. Attention should be paid to several areas of this dot plot. Firstly, the diagonal line which spans the plot. In dot plots, the closeness of two sequences in similarity determines how close this diagonal line is to graphically demonstrating a direct relationship. The presence of a strong, straight line shows that these two sequences are very closely matched. Secondly, in the upper left corner of the plot, a number of areas of darker shading can be seen around the diagonal line. These shaded areas are representative of repeated protein domains which are shared between the two sequences, in the N-terminal region of the protein. The presence of these shaded areas shows that there are four repeating domains in each protein (highlighted in blue and red in Figure 3.3), which themselves are made up of a number of smaller repeats (represented by the stronger, smaller black lines within the shaded areas). Given what is already known regarding the structure of receptors in the EGF family, and by observing the residue numbers within these shaded regions, these areas

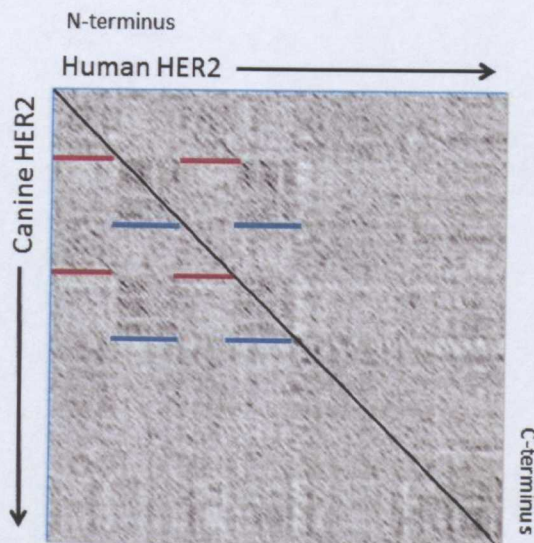


Figure 3.3: Dot plot analysis of human (horizontal axis) and canine (vertical axis) HER2. The strong diagonal line denotes a high degree of similarity between the two species. The sequences also share a number of repeating protein regions, made up of a number of smaller repeats. The areas highlighted by **blue lines** correspond to CR regions of the extracellular portion of HER2 (domains II and IV), while the areas highlighted by **red lines** are L regions (domains I and II).

Dotlet specifications: Matrix: Blosum62; Sliding window: 15; Zoom: 1:4; Grayscale: 72%-15%

represent protein domains rich in repeats, corresponding to extracellular domains I-IV of HER2 (Flynn *et al.*, 2009).

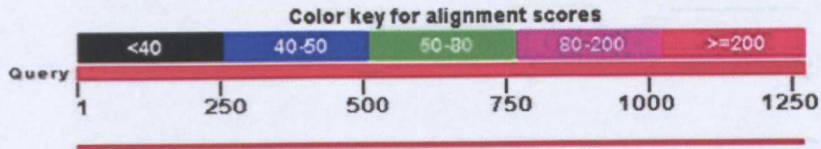
3.3.1.2. Whole Protein BLAST Alignment

Further protein sequence analysis carried out through BLAST alignments also shows that canine and human HER2 are closely related, with 93% of identical residues overlapping between the two sequences (Figure 3.4).

BLAST analysis also showed that the alignment produced a high bit score of 2340 bits (where a higher score denotes a better alignment), with an E-value of 0 (where a lower E-value also denotes a better alignment).

It should also be noted that sequence alignments show that the key methionine residues (described in Section 3.3.2) involved in alternative initiation which results in p95-HER2 isoform being produced are conserved between dog and human species.

Figure 3.4: BLAST analysis of canine (query) and human (subject) HER2 sequences. **A:** Graphic summary of BLAST hits against the query sequence. Graph **A** shows that the length of the alignment has a high bit score exceeding 2000 bits. **B:** Alignment produced by BLAST (note that the full alignment continues on the next page).

A**B**

>lcl|61949 unnamed protein product
Length=1255

Score = 2340 bits (6065), Expect = 0.0, Method: Compositional matrix adjust.
Identities = 1170/1260 (93%), Positives = 1209/1260 (96%), Gaps = 5/1260 (0%)

Query	4	MELAANCWGLLLALLPSGAAGTQVCTGTDMLRLPASPETHLDMLRHLHYQGCQVQGNL	63
		MELAA CRWGLLLALLP GAA TQVCTGTDMLRLPASPETHLDMLRHLHYQGCQVQGNL	
Sbjct	1	MELAALCRWGLLLALLPPGAASTQVCTGTDMLRLPASPETHLDMLRHLHYQGCQVQGNL	60
Query	64	ELTYLPANASLSFLQDIQEVQGYVLIHNSQVRQIPLQRLRIVRGQTQLFEDNYALAVLDNG	123
		ELTYLP NASLSFLQDIQEVQGYVLIH+QVRQ+PLQRLRIVRGQTQLFEDNYALAVLDNG	
Sbjct	61	ELTYLPTNASLSFLQDIQEVQGYVLIAHNQVRQVPLQRLRIVRGQTQLFEDNYALAVLDNG	120
Query	124	DFLEGGIPAPGAAPGGLRELQRLSLTEILKGGVLIQRSPQLCHQDTILWKDVFHKNNQLA	183
		DPL P GA+PGLRELQRLSLTEILKGGVLIQR+PQLC+QDTILWKD+FHKNNQLA	
Sbjct	121	DPLNNTTIPVTGASPGGLRELQRLSLTEILKGGVLIQRNPQLCYQDTILWKDIFHKNNQLA	180
Query	184	LTLIDTNRSRACPPCSPACKDAHCWGASSGDCQSLTRTVCAGGCARCKGPQPTDCCHEQC	243
		LTLIDTNRSRAC PCSP CK + CWG SS DCQSLTRTVCAGGCARCKGP PTDCCHEQC	
Sbjct	181	LTLIDTNRSRACHPCSPMCKGSRGWESSEDCQSLTRTVCAGGCARCKGPLPTDCCHEQC	240
Query	244	AAGCTGPKHSDCLACLHFNHSGICELHCPALVTYNTDTFESMPNPEGRYTFGASCVTSCP	303
		AAGCTGPKHSDCLACLHFNHSGICELHCPALVTYNTDTFESMPNPEGRYTFGASCVT+CP	
Sbjct	241	AAGCTGPKHSDCLACLHFNHSGICELHCPALVTYNTDTFESMPNPEGRYTFGASCVTACP	300
Query	304	YNYLSTDVGSCTILVCPLNQEVTAEDGTQRCEKCSKPCARVCYGLGMEHLREVRVTSAN	363
		YNYLSTDVGSCTILVCP+L+NQEVTAEDGTQRCEKCSKPCARVCYGLGMEHLREVRVTSAN	
Sbjct	301	YNYLSTDVGSCTILVCP+LHNQEVTAEDGTQRCEKCSKPCARVCYGLGMEHLREVRVTSAN	360
Query	364	IQEFAGCKKIFGSLAFLPESFEGDPASNTAPLQPEQLRVFEALEEITGYLYISAWPDSLP	423
		IQEFAGCKKIFGSLAFLPESF+GDPASNTAPLQPEQL+VFE LEEITGYLYISAWPDSLP	
Sbjct	361	IQEFAGCKKIFGSLAFLPESFDGDPASNTAPLQPEQLQVFETLEEITGYLYISAWPDSLP	420
Query	424	NLSVFQNLRVIRGRVLDHGDAYSLSLTLQGLGISWLGRLSLRELGSGLALIHNRNARLCFVHTV	483
		+LSVFQNL+VIRGR+LH+GAYSLSLTLQGLGISWLGRLSLRELGSGLALIH N LCFVHTV	
Sbjct	421	DLSVFQNLQVIRGRILHNGAYSLSLTLQGLGISWLGRLSLRELGSGLALIHHTHLCFVHTV	480
Query	484	PWDQLFRNPHQALLHSANRPEEFCVGEGLACYPLCAHGHCWGPFTQCVNCSQFLRGQEC	543
		PWDQLFRNPHQALLH+ANRPE+ECVGEGLAC+ LCA GHCWGPFTQCVNCSQFLRGQEC	
Sbjct	481	PWDQLFRNPHQALLHTANRPEDEFCVGEGLACHQLCARGHCWGPFTQCVNCSQFLRGQEC	540
Query	544	VEECRVLQGLPREYVKDRYCLPCHSECQPQNGSVTCFGSEADQCVACAHYKDPFFCVARC	603
		VEECRVLQGLPREYV R+CLPCH ECQPQNGSVTCFG EADQCVACAHYKDPFFCVARC	
Sbjct	541	VEECRVLQGLPREYVNRHCLPCHPECQPQNGSVTCFGPEADQCVACAHYKDPFFCVARC	600
Query	604	PSGVKPDLSFMPWKFADDEEGTQCPQPCINCTHSCADLDEKGCPAEQRASPVTSIIAAVVG	663
		PSGVKPDLS+MPIWKF DEEG CQPCPINCTHSC DLD+KGCPAEQRAS+TSII+AVVG	
Sbjct	601	PSGVKPDLSYMPIWKFDEEGACQPCPINCTHSCVDLDDKGCPAEQRASPLTSIIAAVVG	660

Figure 3.3 continued

Query	664	ILLAVVVLGVLGILIKRRRQKIRKYTMRRLLQETELVEPLTPSGAMPNQAQMRILKETEL	723
Sbjct	661	ILLVVVLGVVFGILIKRRQKIRKYTMRRLLQETELVEPLTPSGAMPNQAQMRILKETEL	720
Query	724	RKVKVLGSGAFGTVYKGIWIPDGENVKIFVAIKVLENTSPKANKEILDEAYVMAGVGSF	783
Sbjct	721	RKVKVLGSGAFGTVYKGIWIPDGENVKIFVAIKVLENTSPKANKEILDEAYVMAGVGSF	780
Query	784	YVSRLGICLTSTVQLVTQLMPYGCLLDHVREHRGLSGDQLLNWCQIAKGMSYLEDVR	843
Sbjct	781	YVSRLGICLTSTVQLVTQLMPYGCLLDHVRENHRGLSGDQLLNWCQIAKGMSYLEDVR	840
Query	844	LVHRDLAARNVLVKS PNHVKITDFGLARLLDIDETEYHADGGKVPFKWMALESILRRRFT	903
Sbjct	841	LVHRDLAARNVLVKS PNHVKITDFGLARLLDIDETEYHADGGKVPFKWMALESILRRRFT	900
Query	904	HQSDVWSYGVTWELMTFGAKPYDGI PAREIPDLLEKGERLPQPPICTIDVYIMVVKCWM	963
Sbjct	901	HQSDVWSYGVTWELMTFGAKPYDGI PAREIPDLLEKGERLPQPPICTIDVYIMVVKCWM	960
Query	964	IDSECRPRFRELVAEF SRMARDPQR FVVIQNE DLGPASPLDSTFYRSLEDDDDMGDLVDA	1023
Sbjct	961	IDSECRPRFRELVSEF SRMARDPQR FVVIQNE DLGPASPLDSTFYRSLEDDDDMGDLVDA	1020
Query	1024	EEYLV PQQGF FCP EPTPGAGGTAHRRHRSSSTRSGGGELTLGLEPSEEEPPKSP LAPSEG	1083
Sbjct	1021	EEYLV PQQGF FCP DPAPGAGGMVHRHRSSSTRSGGGDLTLGLEPSEEEAPRSP LAPSEG	1080
Query	1084	AGSDVFDGDLGMGAAGLQSLPSQDPSPLQRYSEDPTVPLPPETDGYVAPLTCSPQPEYV	1143
Sbjct	1081	AGSDVFDGDLGMGAAGLQSLP+ DPSPLQRYSEDPTVPLP ETDGYVAPLTCSPQPEYV	1140
Query	1144	NQPEVWPQPPSPLEGPLPPSRPAGATLERPKTILSPKTLSPGKNGVVKDVFVAFGSAVENPE	1203
Sbjct	1141	NQP+V PQQPSP EGPLP +RPAGATLER PKTILSPGKNGVVKDVFVAFG AVENPE	1195
Query	1204	YLAPRGRAAPQPHPPPAFSPA FDNLYYWDQDP SERGSPSTFEGTPTAENPEYLGLDVFPV	1263
Sbjct	1196	YL P+G AAPQPHPPPAFSPA FDNLYYWDQDP ERG+PPSTF+GTPTAENPEYLGLDVFPV	1255

3.3.1.3. Tendency for HER2 to form an Ordered Structure

Further observation on protein structure and similarity were made by analysing the tendency for HER2 to form an ordered structure in both species. Protein FASTA sequences were obtained from Ensembl, and submitted to IUPRED (Dosztányi *et al.*, 2005a; Dosztányi *et al.*, 2005b). The IUPRED server recognises regions of protein which have “no well-defined tertiary structure in their native, functional state”. It recognises these regions based on the estimated pairwise energy content of the amino acid sequence. The resulting plot generated gives an idea of whether a protein (in its entirety or merely a portion of it) has a tendency to form a structured or unstructured protein.

It should be noted that while the extracellular, juxtamembrane and kinase domains have all had been crystallized and their structures determined the C-terminal region as yet has not had any definitive structure reported.

The method by which receptor phosphorylation occurs in the EGF family is not yet fully understood. However it is believed that the C-terminus of the protein exists in a fluid and relatively unstructured form, which is able to move more freely than its neighbouring regions, creating a kind of “entropic brush”. This freedom of movement allows the tyrosine residues within this region to be highly flexible in space, so that they may come into contact with the kinase domains of their receptors and any available residues can be phosphorylated by ATP. This brush may then continue to wave about to maximise the chance of binding and recruiting intracellular signalling proteins (Figure 3.5). It would be expected that such a feature of a protein would have a tendency to be unstructured and disordered, and that this should be visible when plotted by IUPRED.

In the case of human and canine HER2, both plots show that the proteins have a tendency to remain structured until residues 1022 and 1020 (in dog and human respectively), whereupon they both suddenly seem to lose structure as their tendency towards disorder increases (Figure 3.6). These figures correlate with the region of the protein expected to be involved in this “entropic brush” structure, which begins roughly 950 residues into the structure of HER2 (Flynn *et al.*, 2009).

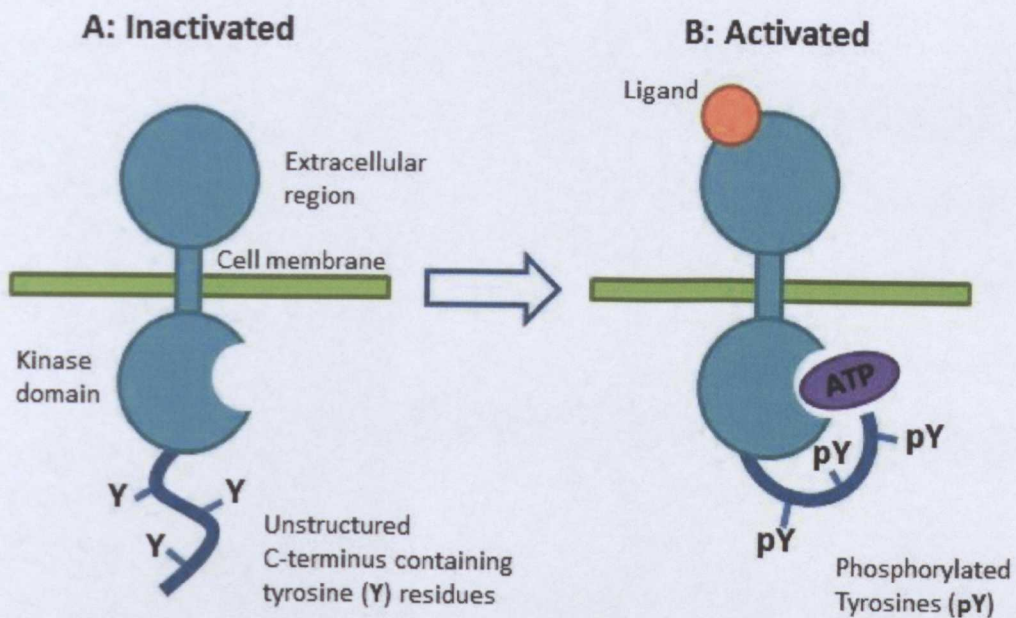


Figure 3.5: The relatively unstructured “entropic brush” of the EGF receptors allows for tyrosine residues to be brought into close proximity with the kinase domain which binds ATP. Tyrosine residues are then phosphorylated and then resume their flexibility in order to recruit downstream signalling proteins.

Having determined that full-length human and canine HER2 protein are highly similar, it was next necessary to investigate if the canine form also undergoes splice variation at the genomic level in the same way that our human form does.

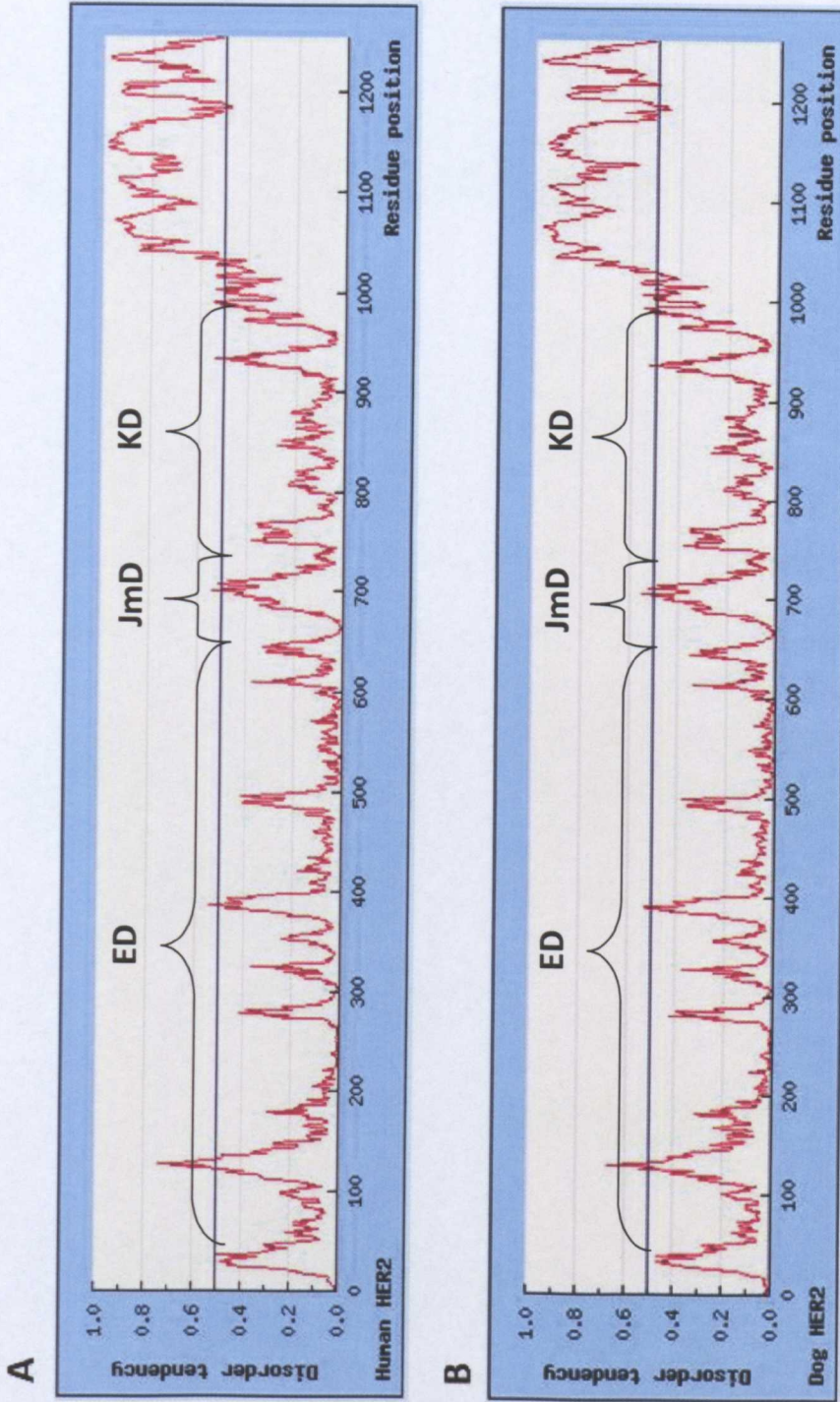


Figure 3.6: IUPRED plots comparing the tendency for HER2 to form an unstructured protein in (A) human and (B) dog primary sequences. Both plots show that up until roughly the 1000 residue mark, the protein has a tendency to be structured. Beyond this however, the disorder tendency increases significantly. ED = extracellular domain, JmD = Juxtamembrane domain, KD = kinase domain.

IUPRED specifications: Prediction type: long disorder; Output type: generate plot; Window size: 2000

3.3.2. Bioinformatic Analysis of Canine HER2 Alternative Splicing

Following the general sequence comparisons described in the previous section, it was next necessary to apply further bioinformatical tools to the gathered sequence data in order to determine if any splice variation occurs in the canine gene.

This was accomplished first through exon comparisons between species to gauge the likelihood that the gene was able to undergo splice variation, and later through comparing the available sequence to the canine expressed sequence tag (EST) library to attempt to detect any isoforms which may have already been reported through whole-genome shotgun and cDNA sequencing.

3.3.2.1. Comparing Exons Between the Human and Canine HER2 Genes

In order to gauge whether canine HER2 could possibly undergo splice variation similarly to the human gene, it was first necessary to compare human and canine intron and exon boundaries. This was first carried out by observing gene structure using the Ensembl Ontology Tool, which generates a graphical comparison of gene structure (Figure 3.7).

Using this alignment, it could be seen that overall the sequence and the structure of the gene were highly conserved, particularly in the 3' regions. However, it can be seen that the human gene appears to be somewhat larger and has a slightly different structure at its 5' end, as well as containing two extra exons compared to its canine counterpart.

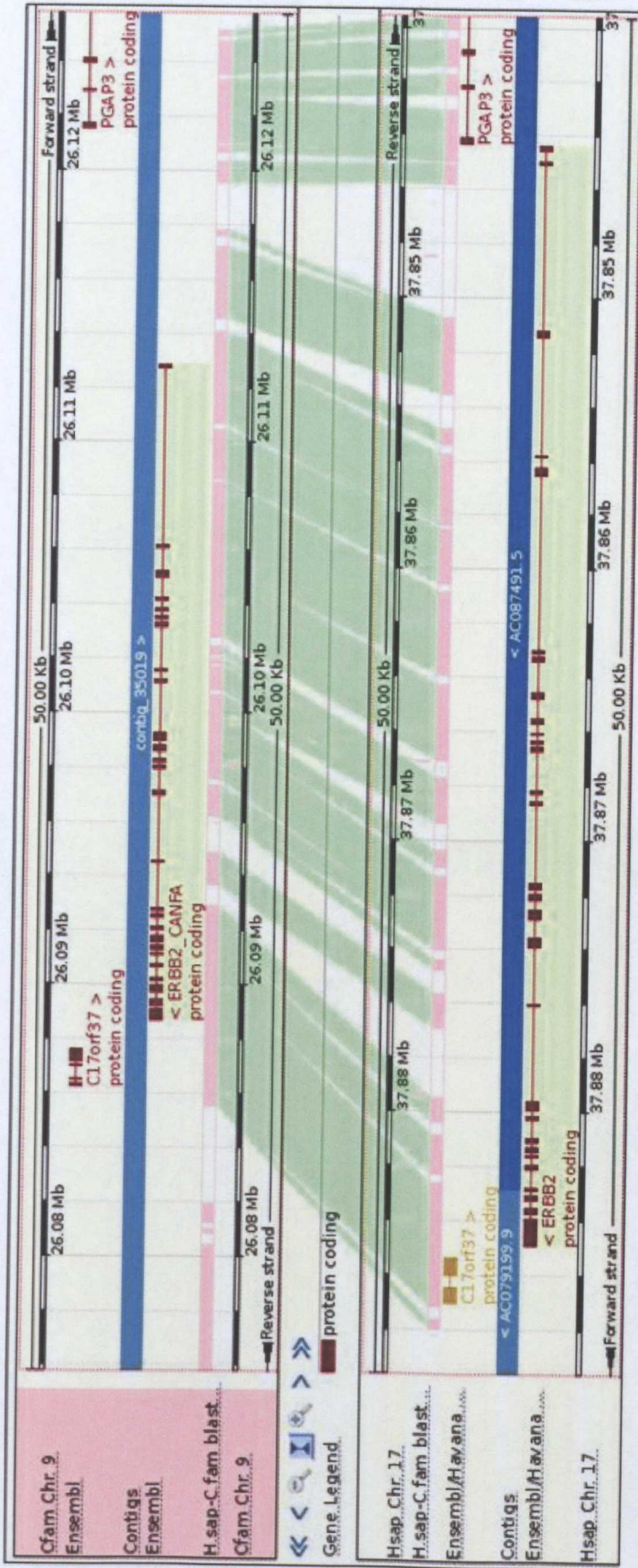


Figure 3.7: Multi-species alignment view of HER2 using the Ensembl Gene Ontology Tool.

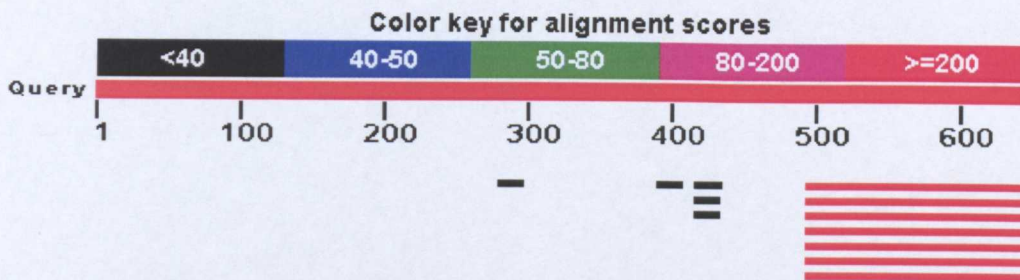
Top panel: canine HER2; Bottom panel: human HER2. Regions of alignment are indicated on the pink bar, with these being connected between species by the green shading.

Using this tool, it can be seen that the two sequences align with a high degree of similarity, with the exception of one end of the sequence, where the human gene appears to be somewhat longer, due in part to the presence of two additional exons at its 5' end when compared to its canine equivalent.

In order to determine why these differences exist, the two cDNA sequences of the HER2 genes were aligned using BLAST. This alignment showed that while the full canine cDNA (consisting of 3792 bp) aligned with the human cDNA (consisting of 4624 bp) and gave 100% query coverage, there was more genetic information available for the human gene which simply was not present in the canine equivalent.

Further analysis was carried out by aligning portions of the 5' and 3' ends of the human HER2 gene (exons 1 through to 4 – a total of 645bp; and exons 27-29 – a total of 1416bp) with the canine genome (Figure 3.8) using BLAST.

A: human 5' end BLAST against canine genome



B: human 3' end BLAST against canine genome

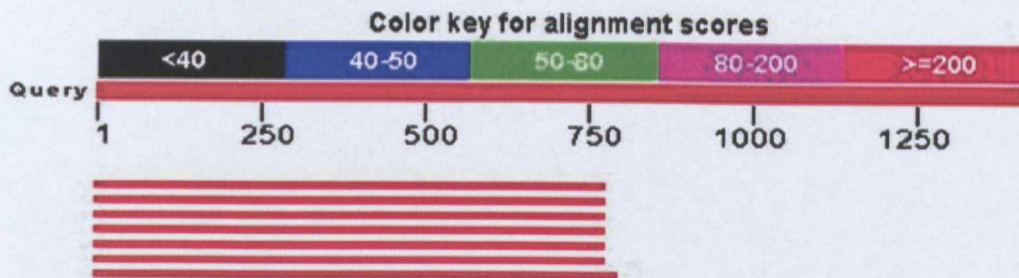


Figure 3.8: BLAST results of aligning human 5' and 3' HER2 exons with the canine genome. Results showed that 7 entries aligned with high identity at both 5' and 3' ends and that all of these were entries for canine HER2. However none of these alignments exceeded 153bp in length at the 5' end or 798bp at the 3' end. Further investigation showed that these canine sequences stopped just before the untranslated region begins

Results from this alignment gave 7 hits, all related to the canine HER2 gene. While these hits all showed strong alignments to the original 645bp and 1416bp queries, none was longer than 153bp or 798bp respectively. Further investigation of these alignments showed that the sequences showed high identities up until the presence of the untranslated region

(UTR) in the human sequence (found in exon 29), indicating that the canine sequence lacked this UTR.

In order to further investigate and compare exon structure between species, BLAST alignments were carried out looking specifically at exonic sequences. Canine exons were exported from Ensembl in FASTA format and saved as a .txt file in Microsoft Notepad. This file was then NCBI BLAST aligned against the human exons for HER2 (also exported in FASTA format and saved as a .txt file) and the identity between the exons was observed and recorded (Table 3.2).

It was found that all the 27 canine exons with the exception of the first aligned with the human exons 4 through to 29. In the course of observing the results of these alignments, it was found that all the exons between both species have the same length, with the exception of the last (canine exon 27 and human exon 29). This is due to differences in untranslated regions of these exons, with the human exon containing a large chunk of untranslated material (618 bp). Exons also showed a high degree of similarity between species with 91% identity between species on average, with identities ranging from 76% between canine exon 5 and human exon 7, and 97% between canine exons 22 and 23 and human exons 24 and 25 respectively.

It seemed unusual that all the canine exons should align to their human equivalents with the exception of exon 1. To further investigate this difference, the canine exons were again aligned by BLAST, except in this instance they were aligned to the entire human HER2 gene as opposed to the human HER2 exons only. Results from this alignment showed that there was a hit for canine exon 1 within the human HER2 gene, and that is scored highly in terms of both query coverage and percent identity (100% and 94% respectively). Further analysis of this alignment showed that while it did not match any known exonic human HER2 sequence, it was present within human intron 3. While this may at first seem odd given that the rest align so closely, it should be considered that the structure of the canine gene is more similar to the human ERBB2-201 transcript (see section 3.3.1) than it is to the ERBB2-202 which was used as a comparison in these analyses. In the human ERBB2-201 transcript, the first exon also aligns within in intronic sequence of ERBB2-202 (see Figure 3.2). In this instance, it seems a similar event has occurred within the canine gene.

Table 3.2 – Canine and Human HER2 exon comparisons

Dog Exon	Dog Length (bp)	% ID	% Query Coverage	Human Exon	Human Length
1	82	No align†	N/A	N/A	N/A
2	152	92%	100%	4	152
3	215	90%	100%	5	214
4	135	92%	100%	6	135
5	69	76%	91%	7	69
6	116	92%	100%	8	116
7	142	92%	100%	9	142
8	120	92%	100%	10	120
9	127	90%	100%	11	127
10	74	91%	100%	12	74
11	91	92%	96%	13	91
12	200	92%	99%	14	200
13	133	94%	100%	15	133
14	91	87%	100%	16	91
15	161	93%	100%	17	161
16	48	92%	100%	18	48
17	139	86%	100%	19	139
18	123	95%	100%	20	123
19	99	96%	100%	21	99
20	186	94%	100%	22	186
21	156	92%	100%	23	156
22	76	97%	100%	24	76
23	147	97%	98%	25	147
24	98	89%	97%	26	98
25	189	89%	100%	27	189
26	253	90%	100%	28	253
27	371	87%	100%	29	974*

* Difference in size here is caused by a large portion of the exon being composed of untranslated regions

† While this canine exon did not align with an equivalent human exon, further BLAST analysis aligning canine exons to the whole human *gene* found that the canine exonic sequence did align with a high degree of similarity (94%) to a portion of human HER2 - found to be in intron 3.

Further analysis using the UCSC Genome Browser (<http://genome.ucsc.edu/>) mapped the canine ERBB2 exons to the gene (Figure 3.9). Similarly to the exon analysis summarised in Table 3.2, the beginning and end exons of human and dog HER2 shows some differences, while the rest remain largely similar.

With it being apparent that the two species share a similar gene structure, it was reasonably assumed that canine HER2 could splice in a similar manner to its human counterpart. The next stage in this investigation was to determine if additional transcripts of canine HER2 had been published, but not identified as belonging to the gene.

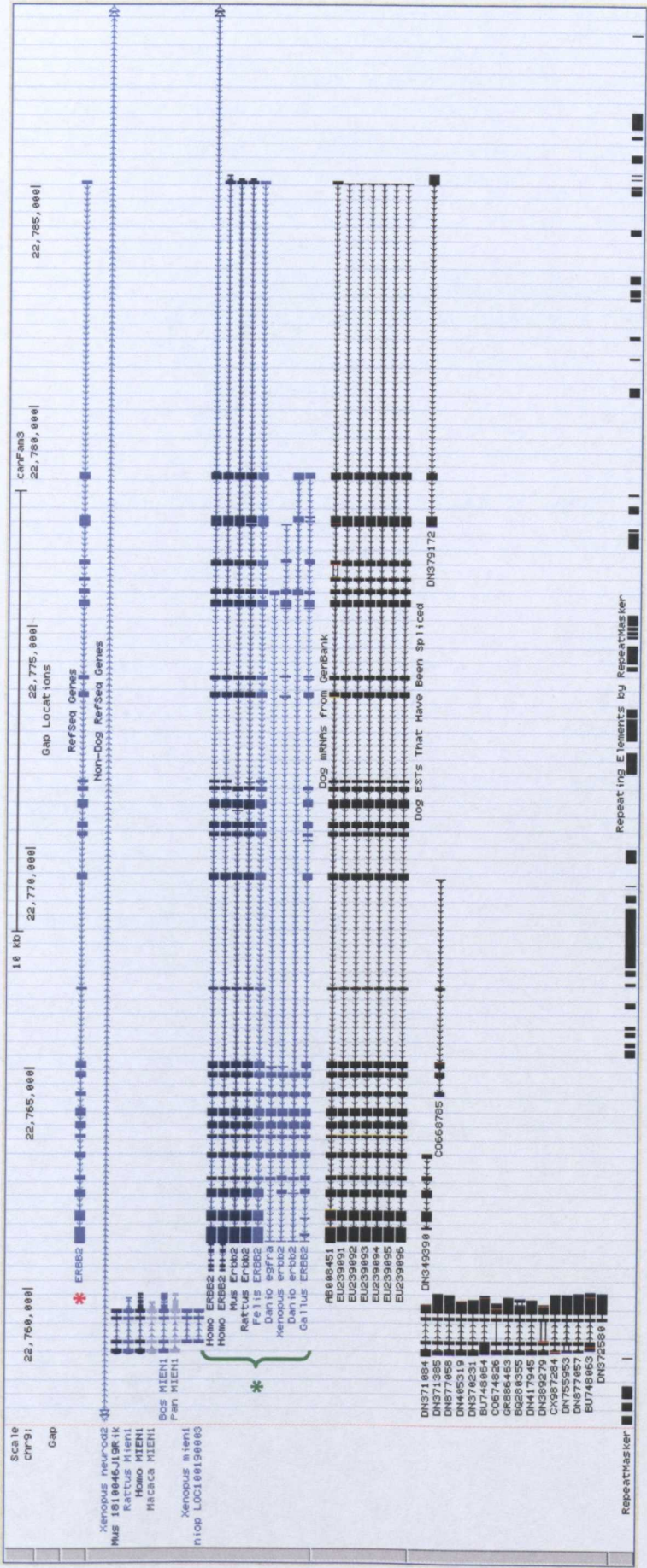


Figure 3.9: The canine ERBB2 exons (indicated with *) mapped to the genome using the UCSC Genome Browser. The ERBB2 exons of other species are also mapped below (indicated with *) for comparative purposes.

3.3.2.2. Detecting Alternative Canine HER2 Transcripts Using the EST Database

The canine HER2 protein sequence was aligned with the canine expressed sequence tags (EST) database using a tblastn search (Altschul *et al.*, 1997) available from the NCBI. This alignment produced 107 hits (Figure 3.10), although none had greater query coverage than 33%, and only two had a total alignment score exceeding 200 bits.

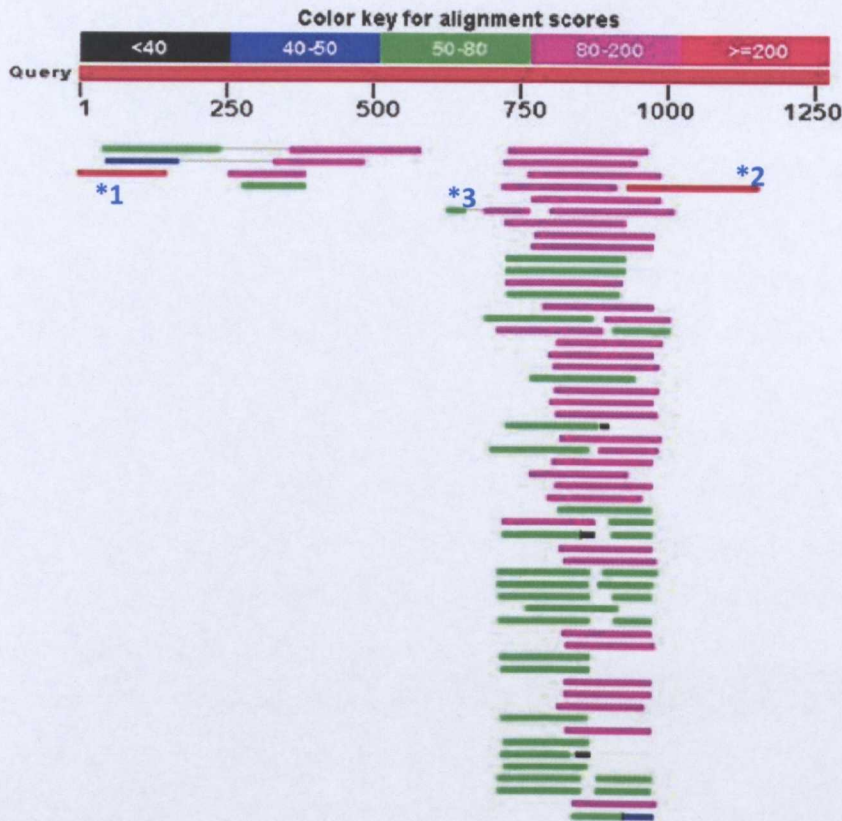


Figure 3.10: Graphical representation of tblastn alignment of canine HER2 peptide sequence against the canine EST library to detect alternative transcripts of canine HER2. Only three of these were found to be matches to HER2 (highlighted with *). The majority of the hits were in the region of residues 620-1000 which coincides with the transmembrane and kinase domain of the protein, and which tends to be highly conserved within the proteome.

Three of these alignment hits were found to be a match to canine HER2 (these are highlighted with blue asterisks [*] on Figure 3.9). To begin with, the two highest scoring alignments (*1 and *3) were investigated. Both hits were a match for canine HER2 on the UniGene database, and each had a high identity (99%) for their alignments with canine HER2 inputted to the search.

The first sequence matched the first 151 residues of canine HER2 and was identical except for serine residue 147, which was substituted for an asparagine. The mRNA from this sequence had been isolated from canine synovium. HER2 has been reported in cases of human cancers (particularly those of the head and neck) arising from the synovium (Nuciforo *et al.*, W B Saunders, 2003; Olsen *et al.*, 2005) so to detect HER2 in this tissue is not unusual.

The second high-scoring hit (the mRNA of which was obtained from canine thyroid) matched residues 929 to 1149 and was identical with the exception of glutamic acid residue 1141 which was substituted for an unknown amino acid. Similarly to the synovium, HER2 has also been detected in the thyroid (Hague *et al.*, 2002; Ensinger *et al.*, 2003).

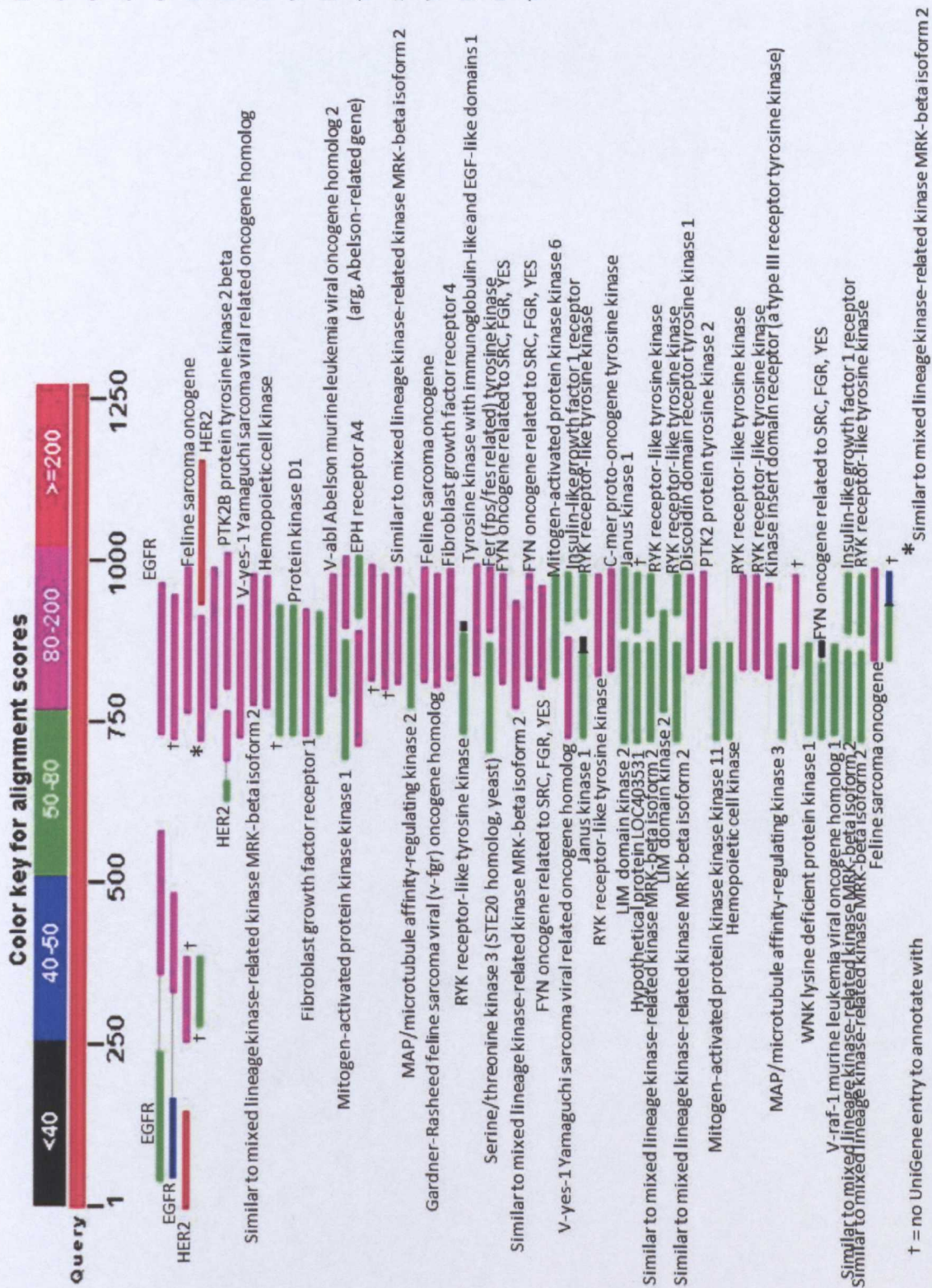
The third hit for HER2 (*2) consisted of two small alignments within the same hit. This sequence for this hit (GeneBank ID: CO668785.1) came from a cDNA isolated and sequenced from canine aorta. Interestingly, the first (and smallest) alignment is found in the region of exon 16 (which is involved in the creation of the $\Delta 16$ HER2 described earlier). To investigate if similar mutations to the human $\Delta 16$ HER2 were present in the canine sequence, the relevant exonic protein sequence was first determined using Artemis to compare genomic exon sequence with its translated peptide. This peptide sequence was found to be: CADLDEKGCPAEQRA (beginning at residue 636), and was subsequently searched for against the tblastn results.

Only this hit was found to contain the specific exon 16 residue sequence, and this was a short alignment consisting of only 30 residues. This sequence was identical to the published canine HER2 with the exception of the penultimate alanine, which is substituted with an unknown amino acid (this is possibly due to sequencing error from the cDNA the EST was derived from). Within this hit there was also a second, longer alignment which was found to fully align with residues 688 to 766 of the HER2 peptide sequence. However none of the cDNA sequence this hit supplied contained the relevant portion of HER2 which contains the mutations associated with constitutively active $\Delta 16$ HER2, and conclusions could not be drawn about the presence of this isoform in the dog.

All but eight of the 107 hits provided by the tblastn search aligned roughly between residues 620 to 1000, which coincides with the transmembrane and kinase domain of the receptor – a region which is heavily conserved among many proteins and could be expected to produce a number of alignments with a reasonable degree of similarity –

although none of these alignments exceeded a total score of 199 bits. Further investigation of the UniGene entries for these hits showed that these sequences were recorded as being from various protein kinases within the dog genome, with only three hits belonging to the EGF family (Figure 3.11).

Figure 3.11: An annotated view of the canine HER2 peptide aligned against the canine EST library using a tblastn search. It can be seen that the majority of the hits were in the tyrosine kinase region, and that the UniGene entries showed these hits were in fact other protein kinases not related to the EGF family.



3.3.3. Observations on Chromosome Structures

Through the course of the previous investigations of this chapter, it was noticed that the canine sequence was inverted compared to its human equivalent. This prompted a study of the structures of the two species' chromosomes.

HER2 is found on chromosomes 17 and 9 in humans and dogs respectively. Human chromosome 17 was retrieved from Ensembl. Using the Ensembl comparative genomics tools, its synteny with the equivalent dog chromosome (chromosome 9) was observed (Figure 3.12). From these results, it became apparent that at some point in evolution, the canine chromosome 9 had become inverted to form the bulk of the long q-arm of human chromosome 17.

The shorter "p" arm appears to have been involved in a recombination event, where a large portion of chromosome five has been inserted into the chromosome 9 sequence on the p-arm. There also appears to be a much smaller insertion just above the centromere.

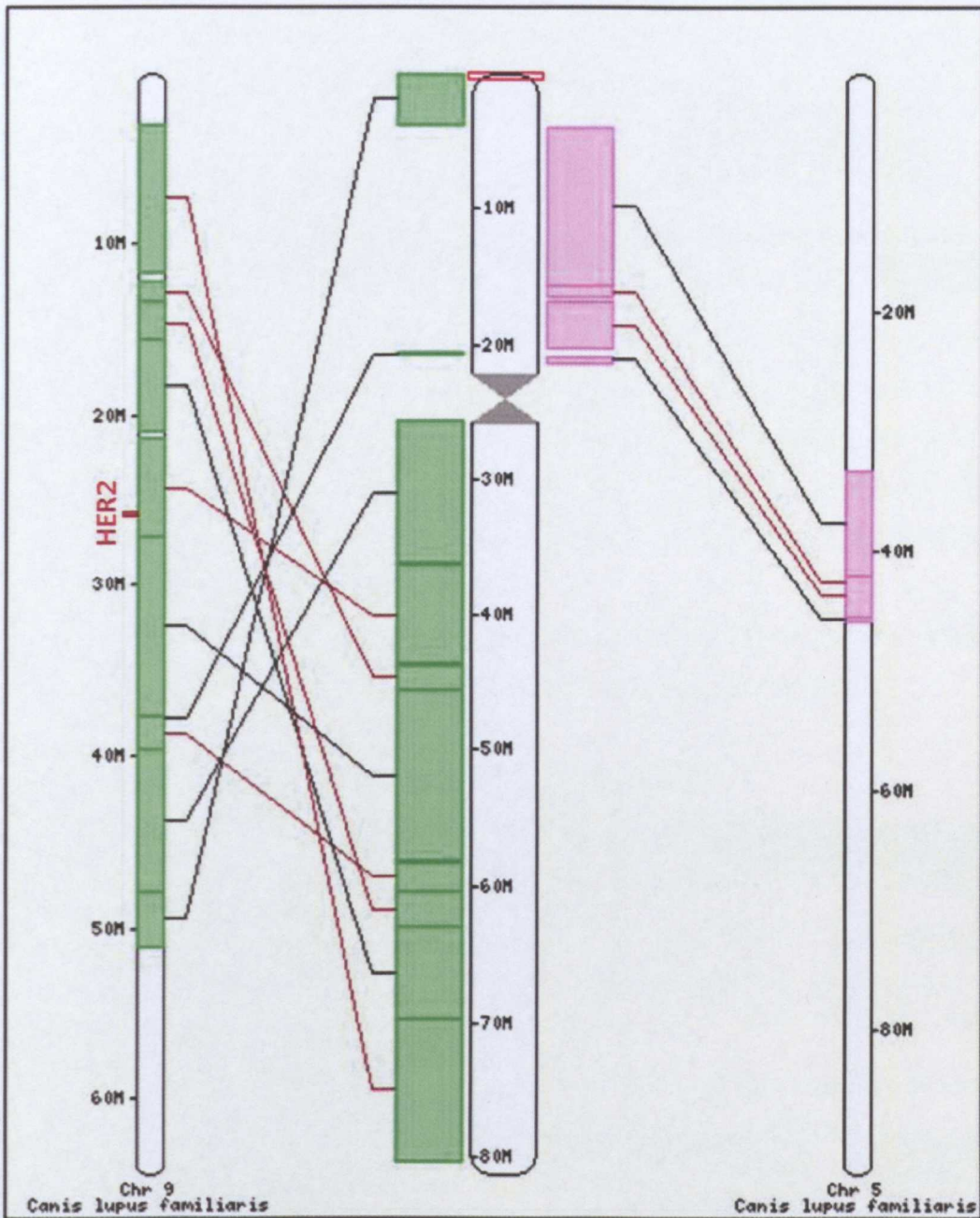


Figure 3.12: Comparisons between canine (left and right) and human (middle) chromosomes on which HER2 is found. Human chromosome 17 is largely composed of an inverted portion of canine chromosome 9, which has undergone a recombination event with an uninverted portion of canine chromosome 5. The approximate location of the HER2 gene is marked on canine chromosome 9 (**HER2**).

3.5. DISCUSSION

These results would suggest that at present no cDNAs have been submitted that would identify the presence of alternative splicing in the canine HER2 gene, despite its significant protein and gene similarities with its human counterpart which have been described in this chapter.

However this does not mean that isoforms of HER2 do not exist within the dog, simply that no sequences have yet been submitted which would lend credence to the theory. Canine mammary cancer has only relatively recently become a subject for study and scrutiny, whilst studies into human breast cancer have been on-going for a significantly longer period of time. It is also worth noting that of the ESTs found to be similar in the tblastn search carried out none had been derived from mammary tissue (either normal or healthy) which is the primary tissue with which this study is interested. Mammary tissue (particularly that from cancerous patients) is arguably where one may be most likely to observe splice variants and isoforms of HER2.

What has been confirmed in this chapter is that canine HER2 appears to have a highly similar structure to its human equivalent, in both its gene and protein structure.

3.5.1. Gene & Chromosome Structure Comparisons

Each gene had a similar exonic structure, with the dog gene having 27 known exons and human having 29 known exons. These exons were not only similar in number, but aligned with each other well. There was one exception to this, which was canine exon 1 which was found to match human intronic sequence. This can be explained by observing the alignments carried out with the various human sequences.

It was found in the human case that while there was one long sequence (ERBB2-202) which was used throughout this chapter for comparisons to the canine gene, there were also five other transcripts. Three of these transcripts (ERBB2-201-, 205 and 206) were shorter, and lacked the first two exons that the longer sequence had. However, all of their remaining exons aligned with the exception of the first, which aligned within intronic sequence of ERBB2-202 – this is also what was observed in comparing the canine and human exons with each other. In the course of comparing these exons using both Ensembl's Gene Comparison tools and through BLAST analysis of exported exonic sequence, it was also noticed that human exon 29 is significantly longer than its canine counterpart (exon 27). Further BLAST analysis aligning the 5' and 3' ends of human ERBB2 with the canine genome showed that

reasons for this were due to there being extensive information with regard to untranslated sequences in the human gene which to some extent were also present at the 5' end in dog, but were absent in the 3' end.

Throughout these analyses, it was noticed that the canine ERBB2 gene was inverted compared to the human gene. Chromosome analysis showed that at some point in evolution, a large portion of canine chromosome 9 (on which ERBB2 is found) had been inverted on human chromosome 17. There also appeared to be a recombination effect where a portion of canine chromosome 5 had been inserted within the inverted chromosome 9.

3.5.2. Protein Structure Comparisons

The canine protein showed a highly similar structure to human HER2 in a number of ways. The most basic comparison made was a simple alignment of the primary structures of the protein via BLAST analysis, which showed that the canine and human HER2 proteins were highly similar, sharing 93% identity with the alignment producing a high bit score exceeding 2000 bits.

Structure of the HER2 protein was also compared through dot plot analysis and by observing the tendency for HER2 to form an organised protein structure. In these instances, it was again found that canine and human proteins shared some common features. For example the dot plot was able to identify that the CR and L domains of the protein appear to be conserved in the canine receptor, and observations on protein organization showed that both sequences were formed an ordered structure up to the end of the kinase domain, after which their tendency to be disorganized increased. This can be explained by the theory that the C-terminal end of receptors in the EGF family may be able to freely move in space in order to phosphorylate its tyrosine residues, which would necessitate a highly flexible and disorganized structure.

3.5.3. Summary

All of the factors described in this chapter which suggest that canine HER2 is highly similar to human HER2 would perhaps allow us to reasonably assume that the canine gene should undergo similar posttranslational modifications. From these modifications, we could expect to see the production of a number of isoforms that are seen in the human gene.

However this does not appear to be the case. Investigations in this chapter show that at present no alternative gene forms or protein products can be detected with what knowledge is currently available regarding the canine genome. While the dog has had its genome sequenced, studies in dogs have been on-going for a significantly shorter period of time than they have been in humans and they possesses a much smaller EST library than humans (at the time of writing 8,315,272 EST entries for humans versus 382,629 for the dog).

Considering this, the presence of alternative gene products of ERBB2 in the dog should not be ruled out. In the future, more cDNAs may be added to the canine EST library, which could allow for similar studies to then identify alternative gene products.

CHAPTER FOUR

Surveying the levels of EGF Receptor and Ligand Expression in Healthy Canine Tissue Samples

4.1. INTRODUCTION

There is extensive knowledge on receptor and ligand expression of the EGF family in both healthy and diseased states in humans, and as a result cancers are being increasingly defined by their molecular criteria. Work in this field has allowed the scientific community to better establish which members of this family are involved in disease progression and are associated with metastasis and/or a negative prognosis. There is, however, comparatively little known about the levels of expression of this receptor family in dogs, in either a healthy or diseased state. In order for the level of understanding of canine cancers to improve, and for the dog to become a more widely accepted model for treating human cancers, a better understanding of this system in *C. familiaris* is required. Further knowledge on the expression profiles of various canine cancers would also allow veterinarians to better tailor therapeutic regimens to animal patients.

Immunohistochemistry is widely used in a pathological setting to determine the levels of expression of particular antigens associated with cancers, in order that the most suitable therapies may be administered to patients. Examples of such directed therapies are Herceptin (Trastuzumab), where detection of HER2 at a level of at least grade 2 is required before therapy will be administered, and Erbitux (Cetuximab) – used to treat metastatic colorectal cancers – will only be administered after the detection of EGFR and wild-type KRAS in a patient's tumour histology (Dutra *et al.*, 2004). When these therapies are so costly, it is important that only the patients who will most likely benefit from them are singled out for treatment. Immunohistochemical analysis is able to distinguish these patients from those who may benefit from other chemotherapies, saving public health services and insurance companies' money, and saving the patient any psychological distress and unnecessary toxic side-effects they could potentially endure.

In this project immunohistochemistry was carried out using antibodies which were either available in the laboratory, or purchased from R & D Systems. All antibodies were raised to either human or rat antigen sequences (with the exception of antibodies against epigen and epiregulin, which were purchased from R&D systems and both directed against the mouse antigen). Bioinformatic analysis showed that in the majority of cases the antigen sequences between dog and human or rat were identical or only differed by one residue. In the latter case it was reasonably assumed that the antibodies would successfully cross-react between species.

4.2. EXPERIMENTAL AIMS

1. To determine if the antibodies available in the laboratory were suitable for use against canine antigens.
2. To survey the levels of expression of the EGF receptors and ligands in a healthy canine system, and to compare this expression to that which has already been observed in humans.

4.3. RESULTS

4.3.1. Determining if Available Antibodies were Suitable for Use Against Canine Antigens

Before immunohistochemistry could be carried out, it was necessary to determine if antibodies available in the laboratory would cross-react with their equivalent antigens on canine tissues. In order to accomplish this, immunising sequences (where they were available) were BLAST aligned with their equivalent canine peptide to determine how similar the sequences were (Table 4.1).

Table 4.1 – Comparisons of canine antigens with respective antibody sequences

Target Protein	<i>C. familiaris</i>	Immunising sequence	Species raised against
EGF Receptors			
EGFR	DVVDAD EYLIPQ	DVVDAD EYLIPQ	Human
HER2	AENPEYLGLDVPV	AENPEYLGLDVPV	Human
HER3	ELEPEL L DLDLLE	ELEPEL D DLDLLE	Human
HER4	RSTLQH PDYLQEYST	RSTLQH PDYLQEYST	Human
EGF ligands			
TGF α	CHSGYVG A RCEHADLLA	CHSGYVG V RCEHADLLA	Rat
Amphiregulin	VTC Q CHQDYFGERCGEK	VTC H CHQDYFGERCGEK	Rat
Betacellulin	CDEGYIGARCERVDLFY	CDEGYIGARCERVDLFY	Human
HB EGF	SCICHPGYHGERCHGLSL	SCICHPGYHGERCHGLSL	Human
Epigen	Antibody purchased	Antibody purchased	-
Epiregulin	Antibody purchased	Antibody purchased	-
Neuregulins			
NRG1 α	CQPGFTGARCTENVPMK	CQPGFTGARCTENVPMK	Human
NRG1 β	CPNEFTGDRCQNYVMAS	CPNEFTGDRCQNYVMAS	Human
NRG2 α	CPVGYTGDRCCQFAMVN	CPVGYTGDRCCQFAMVN	Human
NRG2 β	CPNGFFGQRCLEKLPLRL	CPNGFFGQRCLEKLPLRL	Human
NRG3	*Incomplete sequence	CKEGYQGVRCDQFLPKTDS	Human
NRG4	No canine sequence	CIENYTGARCEEVFL	Human
Differences between sequences are highlighted in blue.			
* Only one entry exists for canine NRG3, which is half as long as the largest human NRG3 transcript.			
For more details with regard to these antibodies, see Chapter Two: Materials and Methods.			

BLAST alignments showed that for the majority of the antibodies, the equivalent sequences were identical between species, with only HER3, TGF α and amphiregulin showing one residue difference between the immunising sequence and the canine antigen. In these instances, it was reasonably assumed that the antibodies would still bind. This approach was also taken where comparisons couldn't be made due to the antibody having been purchased (and the immunising sequence was not supplied) or there not being a complete or available canine sequence.

4.3.2. Determining EGF Receptor and Ligand Expression in Normal Canine Tissue

Having determined that the antibodies were suitable for use against canine antigens, these were then used to detect the four receptors and ten ligands on a range of ten normal canine tissues.

The overall results for the intensities of the observed stains on each tissue with each antibody are summarised in Table 4.2. The results for individual tissue stains are grouped together by the organ systems with which they are associated, and the staining patterns are described in more detail with example images of the stains later in this chapter. Unless otherwise referenced, histology was interpreted using the Boston University Histology Learning System (Boston University, 2001) and Wheater's Functional Histology (Young *et al.*, Churchill Livingstone Elsevier, 2006).

Notes to the reader regarding the figures presented here

- Due to the volume of images that have been collected during the course of the tissue staining, the full library of images can be found in the DVD which accompanies this thesis.
- These figures have abbreviated annotations on them, which are described in the text which precedes them, and not in the figure legend itself.
- When observing these results, staining was only described for structures which are specific to each organ. Other structures (i.e. vasculature and muscle tissue) which are common to many organs are described in a separate miscellaneous section.
- I have referred to the results throughout this section as “stains” as opposed to “expression”. This is due to the fact that the signal achieved in immunohistochemistry provides a non-linear result, and as such observed staining intensity is not directly proportional to true expression levels.

Table 4.2 - Immunoreactivity of epidermal growth factor receptors and their ligands in normal canine tissues

Tissue	EGFR	HER2	HER3	HER4	NRG1 α	NRG1 β	NRG2 α	NRG2 β	NRG3	NRG4	AREG	BTC	Epigen	Epiregulin	TG α	HB EGF
Digestive Tract																
Tongue	+++	++	++	+++	++	+	+	++	++	++	++	+++	+	+	+	+
Oesophagus	++	+++	++	+++	+++	+++	+	+	+	+	+	+++	++	+++	+	++
Stomach	++	+	++	+++	+++	+++	-	+	+	++	-	+++	++	+++	+	++
Rectum	+++	++	+++	++	++	++	+	+	++	++	-	++	++	+++	+	+
Liver	++	++	++	++	+++	++	++	++	++	++	-	+++	++	+++	++	++
Pancreas	++	+	+	++	++	+	++	+	+++	++	-	+++	+++	++	+	+
Urinary Tract																
Kidney	+++	++	+	++	++	++	+	+	++	+++	-	+++	+	++	++	+
Bladder	++	+	+	++	++	++	++	+	+++	+++	-	+++	++	+++	++	+
Respiratory Tract																
Lung	+++	++	+	++	+	+	++	+	+++	+++	-	+++	+++	+++	+	++
Nervous System																
Cerebral Cortex	+	++	+	+++	++	+	+++	+	++	+++	-	+	++	++	++	++
Miscellaneous																
Vasculature	+	++	++	++	+++	+	-	-	+	++	-	+	-	+/+++	++	+
Smooth muscle	++	++	+	++	+++	++	-	-	+	++	-	+++	+	+++	+	+
Skeletal muscle	+++	+	++	+++	++	++	-	-	+	++	+	+++	+	+++	+++	+

Tissues were scored on a semi-quantitative scale based on the intensity of staining observed: negative (-); weakly positive (+); moderately positive (++) ; strongly positive (+++). In cases where multiple scores are separated by "/" this denotes the presence of different intensities of staining in separate areas of the tissue.

4.3.2.1. The Central Nervous System

Cerebral Cortex

See Figure 4.1

The cerebral cortex is a sheet of neuronal tissue connected to the cerebellum in mammalian brains. It consists of six distinct layers, each of which contains a different composition of neurons. These layers are (from the outermost to the inner most) (Shipp, 2007):

Layer I: Molecular (plexiform) layer: is almost entirely devoid of neuronal cell bodies and consists mainly of extensions of apical dendrites of pyramidal neurons as well as some horizontally-oriented axons.

Layer II: Outer granular layer: contains some pyramidal and but mostly stellate neurons.

Layer III: Pyramidal cell layer/Internal granular layer: contains small to medium-sized pyramidal neurons, and non-pyramidal Martinotti neurons with vertically-oriented axons which extend into Layer I.

Layer IV: Inner granular layer: contains various stellate and few pyramidal neurons.

Layer V: Ganglionic layer/Internal pyramidal layer: contains large pyramidal neurons (Pn) and some fusiform cells.

Layer VI: Multiform/polymorphic cell layer: so named as this layer contains a wide variety of cells, including: small pyramidal cells, Martinotti cells, stellate cells and fusiform cells.

The cerebral cortex lacks white matter (which primarily contains myelinated axons) and is largely composed of grey matter which contains the neurons described above, along with a network of capillaries.

HER4 showed the strongest staining out of the receptors, with most of the grey matter showing a moderate staining which is slightly stronger in the outer layers. HER4 also showed staining of the pyramidal neurones. Similarly, HER2 shows a similar staining pattern to HER4 with there being a moderate stain in the grey matter, and some staining of the pyramidal neurones within it. HER3 also showed a moderate staining of the grey matter, although there was less staining of the neurones than for the other receptors. In general

amongst the receptors there was a tendency for staining intensity to decrease in the innermost layers of the cerebral cortex. The exception for this was HER2 which appears to show the inverse of the other members of the EGF receptor family: in this case, staining is weakest in the outer layers and slightly stronger in the innermost layers.

NRG1 α showed light staining of the grey matter in the inner layers, which was stronger in the outer layers. There was little staining of the neuronal bodies. Similarly there was no staining of the neuronal bodies with NRG1 β , and the entirety of the grey matter stained weakly. NRG2 α showed moderate staining of the innermost layers, which was stronger in the outer layers with moderate staining of the neuronal bodies. Meanwhile NRG2 β showed weak staining in the outer layers, which became almost completely negative in the inner layers and showed no staining on the neuronal bodies. NRG3 showed light to moderate staining throughout the layers, with irregular staining of the neuronal cell bodies. Staining for NRG4 varied the most within the tissue, ranging for quite strong staining to almost negative staining, with an absence of staining in the neuronal cells.

Amphiregulin stained negatively throughout the tissue. Betacellulin showed moderate staining throughout the grey matter and in the neurones. When staining for epigen, the grey matter stained weakly and rather discontinuously and there was a complete absence of any staining in the neuronal cells. Similarly, epiregulin also showed a weak stain which was also discontinuous but less so than that of epigen and which also showed a complete lack of staining in the neuronal cells. TGF α showed generally weak staining throughout the grey matter, with a similar level of staining in the neuronal cells. HB EGF showed mostly weak staining, which was stronger in the outermost layers, but was discontinuous and showed no staining of the neuronal cells.

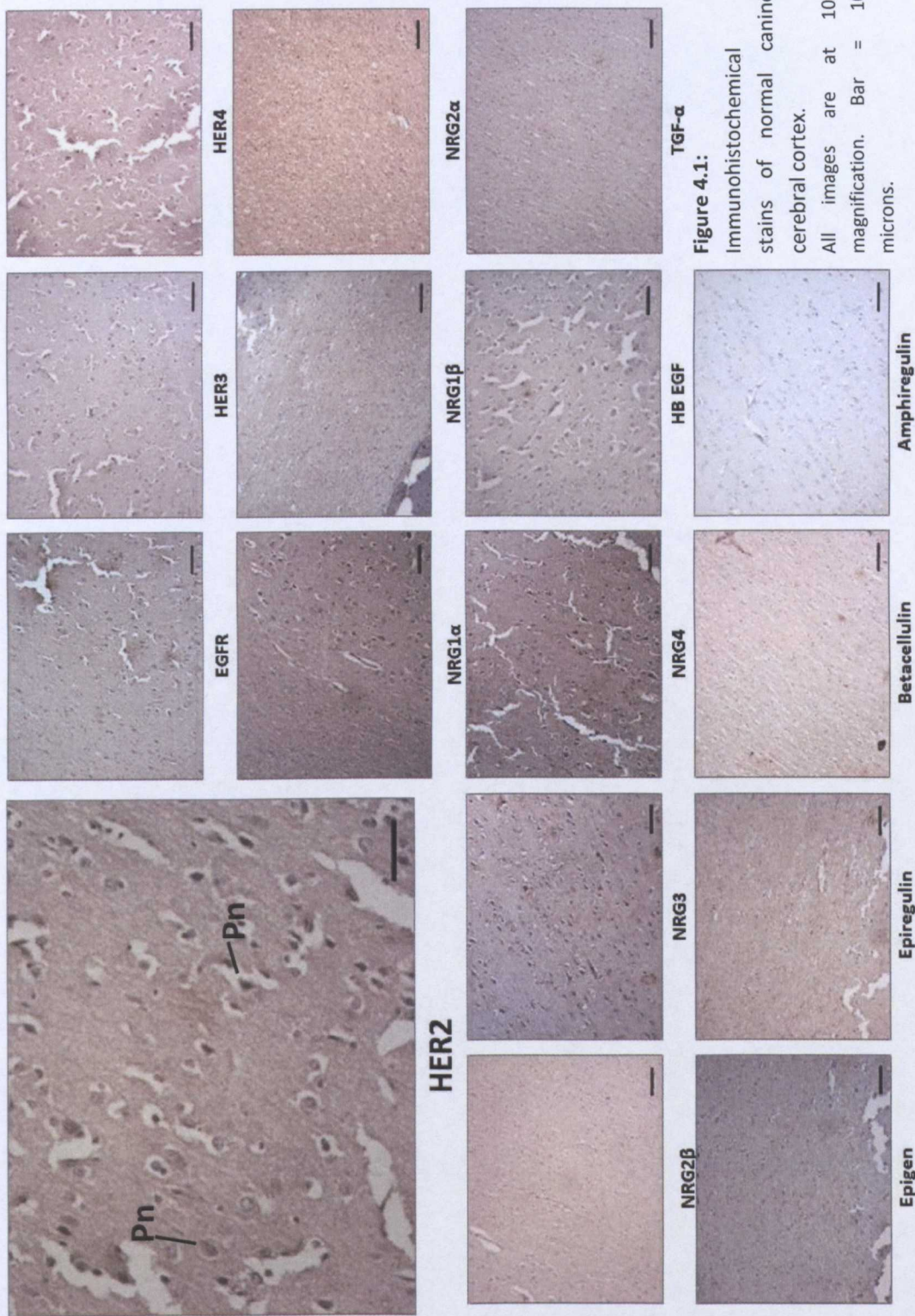


Figure 4.1: Immunohistochemical stains of normal canine cerebral cortex. All images are at 10x magnification. Bar = 10 microns.

4.3.2.2. The Respiratory System

Lung

See Figure 4.2

Lungs are involved in the gaseous exchange of oxygen and carbon dioxide between inspired air and the blood. Air enters the lungs via a system of cartilage-ringed tubes which become progressively smaller as they permeate the organ. The first divisions of these tubes from the trachea are known as the bronchi, with smaller progressive tubes being known as bronchioles. From the bronchioles (Br) stem the alveoli (Al) of the lung – small sacks lacking any cartilaginous structures, which dramatically increase the surface area of the available for necessary gaseous exchange. These alveoli form the bulk of lung tissue, and lend it an overall spongy texture.

EGF receptor and HER4 showed quite strong expression around the lining of the bronchioles, with moderate staining throughout the alveoli, with a similar staining pattern being observed for HER2 although the signal was much weaker by comparison. In contrast, HER3 showed virtually no staining of the alveolar structures, with only some slight staining around the cells which line the bronchioles.

NRG1 α showed predominantly negative staining of the structures within the lungs, with there being some light to moderate staining in the cells lining the bronchioles. A similar pattern was observed for NRG1 β although in this case there were some patchy areas of staining amongst the alveolar tissue. NRG2 α and NRG4 showed weak staining throughout the alveolar tissue and the lining of the bronchioles, with a similar pattern being observed for NRG3 although in this case the staining was stronger throughout the tissue and there was noticeable staining of the connective tissue which surrounds the bronchioles. In contrast to the rest of the neuregulin family NRG2 β showed mostly negative staining throughout both the alveolar and bronchiole tissue.

Betacellulin showed strong to moderate staining in the alveolar tissue, and moderate staining of the bronchioles and the connective tissue which surrounds them. Amphiregulin showed no staining throughout the lung tissue. Epigen, epieregulin and HB EGF showed a similar staining pattern, which was strong in the lining of the bronchioles, and moderate in

the connective and alveolar tissue which surrounds them (it should be noted that the alveolar staining was lighter in the case of HB EGF). TGF α showed very weak staining throughout the alveolar tissue, which was slightly stronger in the lining of the bronchioles.

4.3.2.3. The Gastrointestinal System

Tongue

See Figure 4.3

The tongue consists of an upper epithelium which contains the papillae, a layer of lamina propria (LP) and a large amount of skeletal muscle (SM). In humans, papillae are distributed along the anterior surface (dorsum) of the tongue, and include:

- **Fungiform papillae (not shown):** these are mushroom-shaped papillae, found at the apex and sides of the tongue.
- **Filiform papillae (FIP):** long, thin V-shaped papillae. These lack any taste function, but are the most numerous and involved in mechanical digestion. They are often characterised by increased keratinisation compared to other papillae.
- **Foliate papillae (FoP):** are characterised as being a series of ridges and found on the posterior part of the tongue. These are rudimentary in humans.
- **Circumvallate papillae (not shown):** in humans, only 10 to 14 of these papillae exist on the tongue. They are present at the most posterior part of the tongue, and contain most of the taste buds. It should be noted that taste buds and papillae are distinctly different features, with taste buds being a separate structure containing a pore on the surface of the tongue which secretes a serous fluid capable of dissolving food components, the tastes of which are then detected by gustatory cells. Taste buds are mostly found clustered in the troughs which surround the circumvallate papillae.

These papillae are conserved in dogs (fewer varieties are found in cats as they are obligate carnivores, while dogs are classed as omnivores), although it has been reported that dogs only have one sixth of the taste buds that humans do, and that most are clustered around the tip of the tongue (Whitehead *et al.*, Barnes & Noble Books, 1999). Some differences also exist in the structure of the filiform papillae in the dog. In dogs (and to a greater extent in cats), these papillae have long extensions in their posterior process, combined with a sharp tip (Kobayashi *et al.*, 2003) which gives them their rasping texture, which is important in grooming. In addition, some sources (Kainer & McCracken, Teton NewMedia, 2002) also describe additional papillae in the dog, both of which also lack any taste function:

- **Marginal papillae:** found at the very front edges of the canine tongue. These are present in neonatal puppies and aid in suckling. These papillae regress as diet changes in the animal.
- **Conical papillae:** these are found at the most posterior portion of the tongue, behind the circumvallate papillae.

Owing to the role of the tongue in mechanical digestion, it contains a large amount of skeletal muscle. These muscle fibres are often arranged perpendicular to each other, which allows the tongue its great motility. Amongst this muscle, the lingual salivary glands are also present.

In the course of observing the canine tongue tissue available in this project, only filiform and foliate papillae could be reliably observed. Some structures which appear to be circumvallate papillae were present, however these were either underdeveloped, or the tissue had been cut in an orientation which made observation of the core of the circumvallate papillae difficult. Fungiform papillae could not be observed, perhaps owing to the portion of the tongue from which the tissue was taken, as these papillae are found at the tongue's apex.

All four receptors were present in the tongue in varying amounts. EGFR, HER3 and HER4 showed strong staining throughout the filiform papillae with HER4 showing some cellular membrane staining. By contrast, HER2 showed overall weak, patchy staining of the filiform papillae which was cytoplasmic and entirely absent in cell membranes. In addition, HER2 was only present in the supporting tissue core of the papillae and not in the keratinous surface projections. Overall, staining of the keratinised areas was strongest with HER4, although it was also present to a slightly lesser extent with EGFR and HER3.

NRG1 α showed weak to moderate cytoplasmic staining (which was completely absent in cell membranes) in both the cores of the papillae and to some extent in the keratinous projections. NRG1 β showed a similar pattern although this was much weaker. Both NRG2 α and NRG2 β stained negatively. NRG3 showed moderate cytoplasmic staining in the cores of the papillae, with this extending to a certain degree into the keratinous layers. In contrast to the rest of the neuregulin family members, NRG4 showed moderate staining in the papillae, which became stronger the nearer the tips.

HB EGF and TGF α showed similar staining patterns (although HB EGF was slightly stronger), which staining being most present in the portion of the papillae nearest to the lamina propria, with staining being almost entirely absent in the uppermost keratinous portions. Epigen showed an overall negative stain, and epiregulin gave a moderate staining of the papillae. Betacellulin showed quite strong staining of the cores of the papillae but no staining in the keratinous layers. Amphiregulin only stained weakly in the papillae.

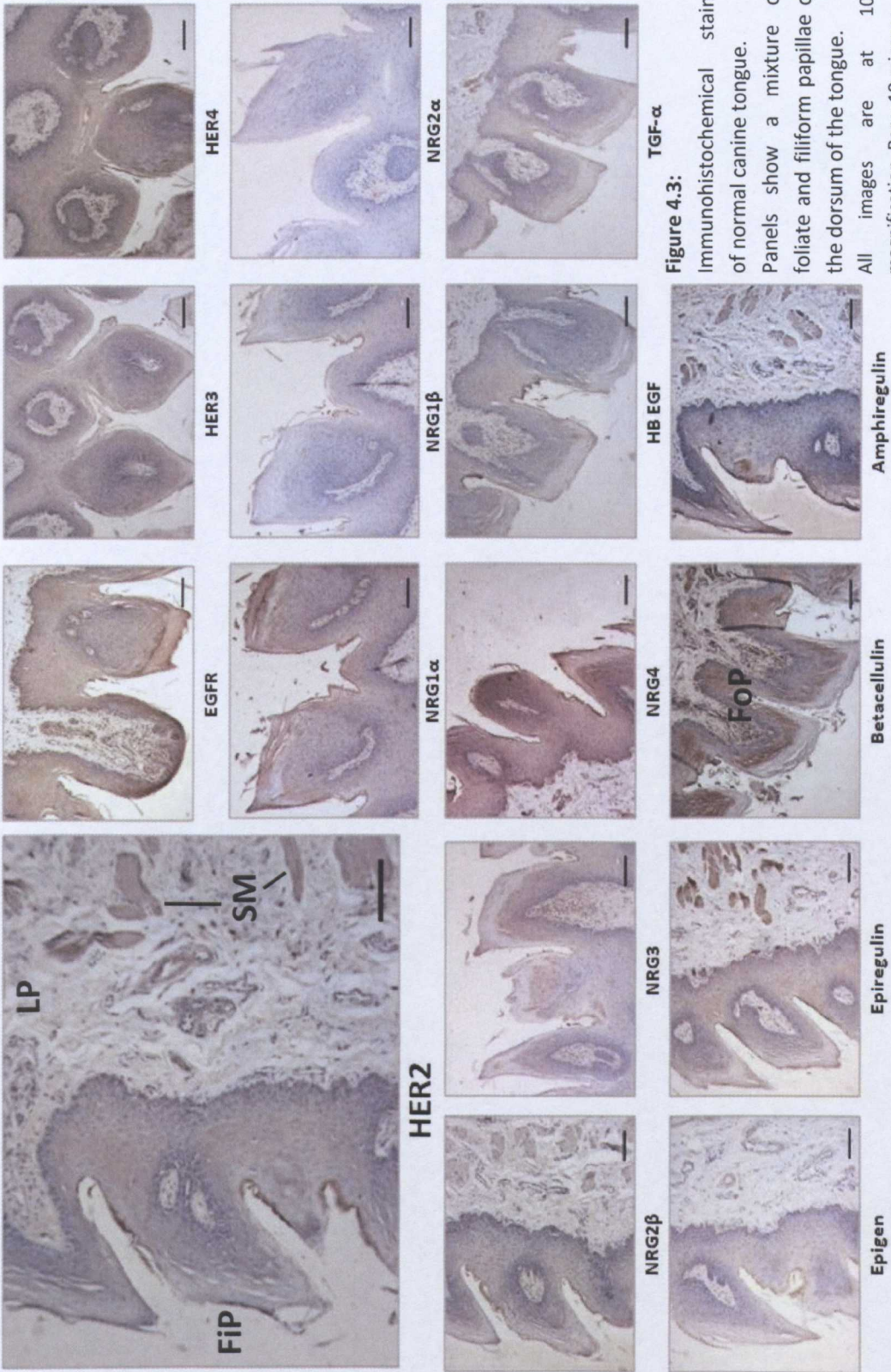


Figure 4.3: Immunohistochemical stains of normal canine tongue. Panels show a mixture of foliate and filiform papillae of the dorsum of the tongue. All images are at 10x magnification. Bar = 10 microns

Oesophagus

See Figure 4.4

The oesophagus is a long tube, through which the food bolus passes after chewing. This tube is lined with stratified squamous epithelium (SSE) which has a high turnover, beneath which is a layer of submucosa (SM). The oesophagus is lubricated by the secretion of mucus, which aids in the movement of the bolus towards the stomach. A bolus is passed along the oesophagus by means of waves of contractions of a number of muscles which line its length in a process known as peristalsis. The composition of muscle varies along the length of the oesophagus, with the superior portion consisting of skeletal striated muscles, transitioning to a mix of skeletal muscle and smooth muscle in the middle portion, and the inferior portion consisting of smooth muscle.

In the oesophagus, each of the receptors showed strong cytoplasmic staining of the stratified squamous epithelium with little or no staining of either the lamina propria or the submucosa. This staining was weakest with HER2, where staining weakened as it progressed further away from the lumen.

Epigen, amphiregulin, HB EGF and NRG2 β each showed a similar staining pattern to HER2, although the signal was weaker, and the absence of staining in the cell membranes was more noticeable.

Epiregulin showed very strong, highly cytoplasmic staining of the epithelia, with there being a significant, noticeable absence of staining from cell membranes.

TGF α showed an overall weak stain in the mucosa and lamina propria. Betacellulin showed strong staining throughout the tissue in the epithelia, which was much weaker in the lamina propria. There was also a lack of this staining from cell membranes in the epithelial layer, and staining was also slightly weaker where the epithelium met the lamina propria.

NRG1 α showed strong staining of the epithelium, with moderate to weak staining of the submucosa. A similar, but weaker, pattern was seen in NRG1 β and NRG3 although staining was absent from the submucosa and the lamina propria. NRG2- α showed strong cytoplasmic staining of the epithelium (with a notable absence of staining from the cell membranes) and moderate to strong staining throughout the submucosa and the lamina propria. With NRG4, the staining was weak in the epithelium of the mucosa, with some areas of cells showing stronger cytoplasmic staining than others.



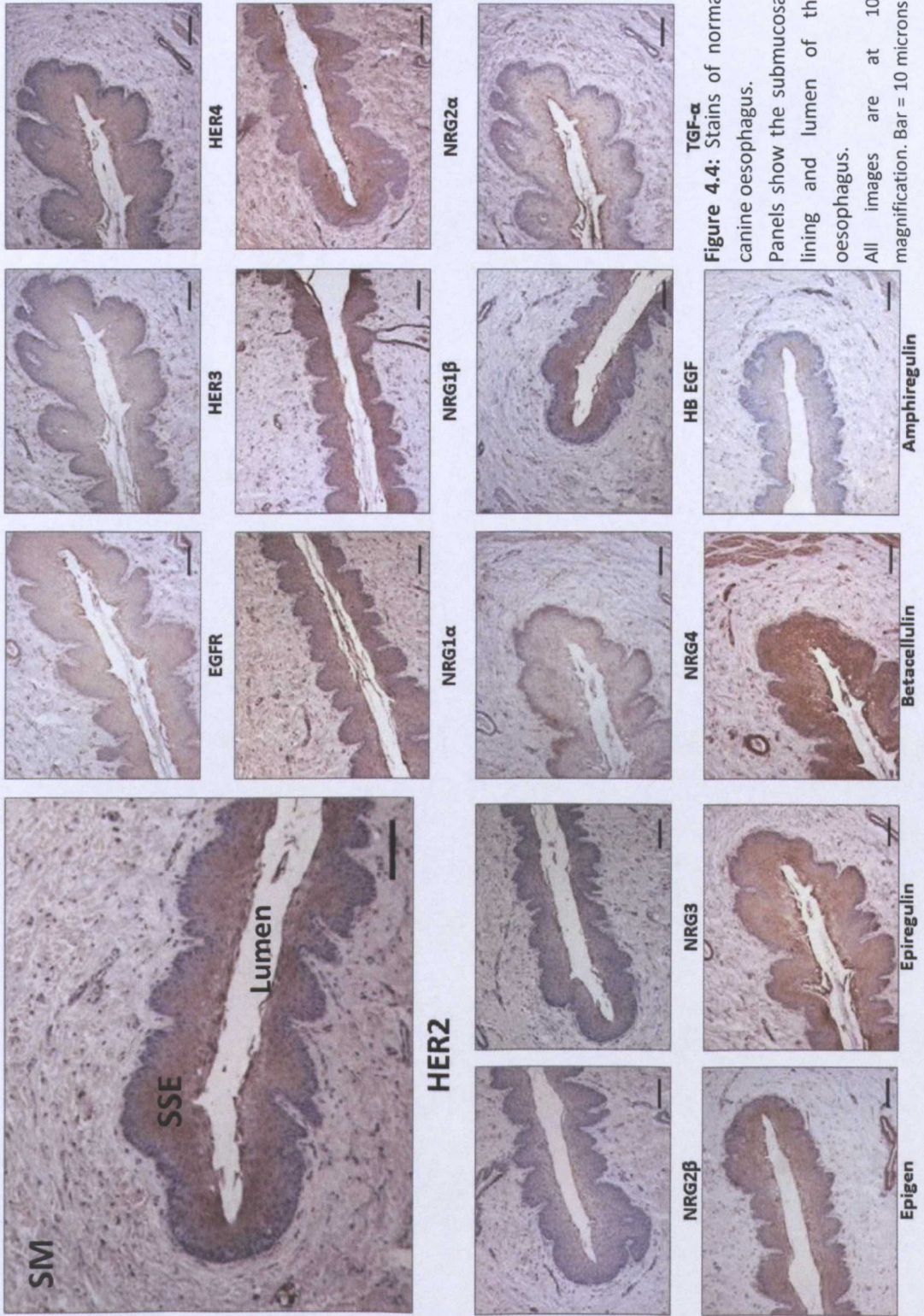


Figure 4.4: Stains of normal canine oesophagus. Panels show the submucosa, lining and lumen of the oesophagus. All images are at 10x magnification. Bar = 10 microns

Stomach

See Figure 4.5

The stomach is involved in the digestion of food, and like many other organs in the alimentary canal, can be broadly divided into the mucosa, muscularis mucosa (MM), submucosa, muscularis externa and the serosa. The mucosa of the stomach consists of two layers:

- Gastric pits (Gp): indentations in the lining of the stomach from which the gastric juices are secreted.
- Gastric glands (Gg): specialised cells within these glands synthesise and secrete hydrochloric acid and pepsinogen (used in the chemical and enzymatic breakdown of food) and mucus (used to protect the lining of the stomach from corrosive activity of the gastric acid).

The stomach is also able to mechanically digest food through a churning action brought about by peristalsis.

The stomach showed strong staining for EGFR, HER3 and HER4. This was strongest in the gastric glands and the gastric pits and was mostly visible in the cytoplasm, although some weak membranous staining of the mucous neck cells could be seen for EGFR. Extensive moderate staining of the cytoplasm of the cells in the submucosa and the muscularis mucosae was also visible in these stains. In contrast, HER2 showed no staining in the gastric glands or pits, but did have some weak staining in the muscularis mucosae and the outer longitudinal layers of muscle.

Epiregulin showed strong staining of the gastric pits and glands. This was most evident in the surface mucosal cells, but this was weaker (and in some cells, absent) from mucosal cells of the necks of the gastric glands. Epiregulin also showed moderate, granular staining of the cytoplasm of the outer longitudinal layers of muscle of the stomach.

Epigen stained predominantly negatively throughout the tissue, with some weak staining being visible in the mucosal cells of the gastric pits, and throughout the muscle of the stomach.

Amphiregulin and HB EGF stained entirely negatively throughout the gastric pits and glands, with weak staining only being visible in the submucosa and lamina propria for HB EGF.

Betacellulin showed strong staining within the gastric pits, and moderate patchy staining in the lamina propria. There also appeared to be some stained areas within the gastric pits. TGF α showed weak to moderate staining of the gastric pits, and weak staining surrounding the gastric glands.

NRG1 α showed moderate staining throughout the lamina propria, and some patchy, weak staining of the mucosal cells of the gastric glands. A similar staining pattern was observed with NRG1 β with the only difference being the presence of stronger staining in the tips of the gastric pits.

NRG2 α , NRG2 β and NRG3 showed overall negative staining throughout the entirety of the tissue, with NRG1 α and NRG3 displaying some very weak staining of the lamina propria.

NRG4 showed strong staining in the gastric pits, but less in the area of the lamina propria which surrounds the gastric glands. This was strongest at the base of the gastric pits, and less intense at the tip of the pits.

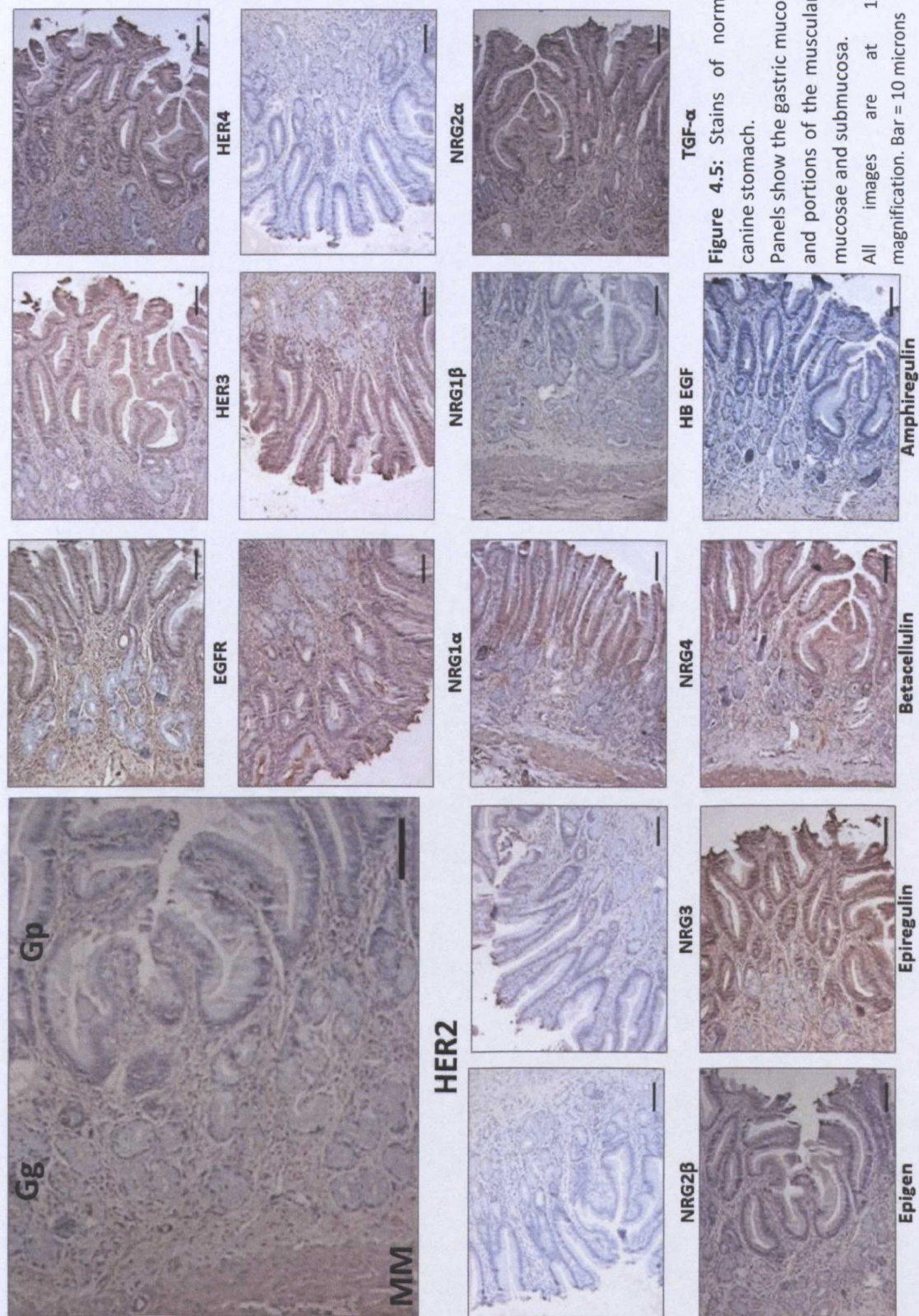


Figure 4.5: Stains of normal canine stomach. Panels show the gastric mucosa and portions of the muscularis mucosae and submucosa. All images are at 10x magnification. Bar = 10 microns

*Liver***See Figure 4.6**

The liver serves several functions: detoxification, protein synthesis, the production of some of the chemical components of digestion (including bile) and is a major site of glycogen storage.

The primary histological features of the liver are the portal triads. These are distinct groups of tissues found within the liver and contain (primarily) a branch each of the hepatic artery (Ha) and hepatic portal vein (Hv) and a bile duct (Bd), alongside a number of lymphatic vessels. Often these triads are embedded in a ring of connective tissue.

The most numerous cell type in the liver is the hepatocyte, and running amongst these are numerous bile canaliculi, which transport bile made by these hepatocytes to the bile ducts in the portal triads.

Staining for receptors in the liver showed a similar moderate to strong pattern throughout the cytoplasm of hepatocytes, with this increasing in intensity with proximity to portal tracts when stained for HER3 and (to a lesser extent) for HER2. HER3 also showed strong staining of the membranes of the epithelium of the bile ducts in the portal tract – this staining was present for the other receptors, but was significantly weaker.

Similar staining to that of the receptors was seen for HB EGF and epigen, with staining increasing in intensity closer to the triads. Epiregulin and TGF α both showed moderate, even staining of the hepatocytes surrounding the portal triad, and lacked the graduated effect seen in the receptors.

Betacellulin showed significant strong staining throughout the hepatocytes, with some strong staining of the epithelium which lines the bile duct of the portal tract. Amphiregulin stained negatively throughout the tissue.

NRG1 α showed a similar staining pattern to that of the receptors with a moderate stain throughout the hepatocytes which increased with intensity towards the portal tract. NRG1 β showed predominantly even, moderate staining throughout the cytoplasm of the hepatocytes, with less noticeable change in stain intensity with proximity to the portal tract. NRG2 α and - β showed a similar stain, although instead of there being a gradual increase in intensity, there appears to be a distinctly stronger stained ring of hepatocytes one layer deep surrounding the portal tract. NRGs 3 and 4 showed uniform staining

throughout the hepatocytes, with only NRG3 showing some weak to moderate staining of the epithelium of the bile ducts in the portal tract.

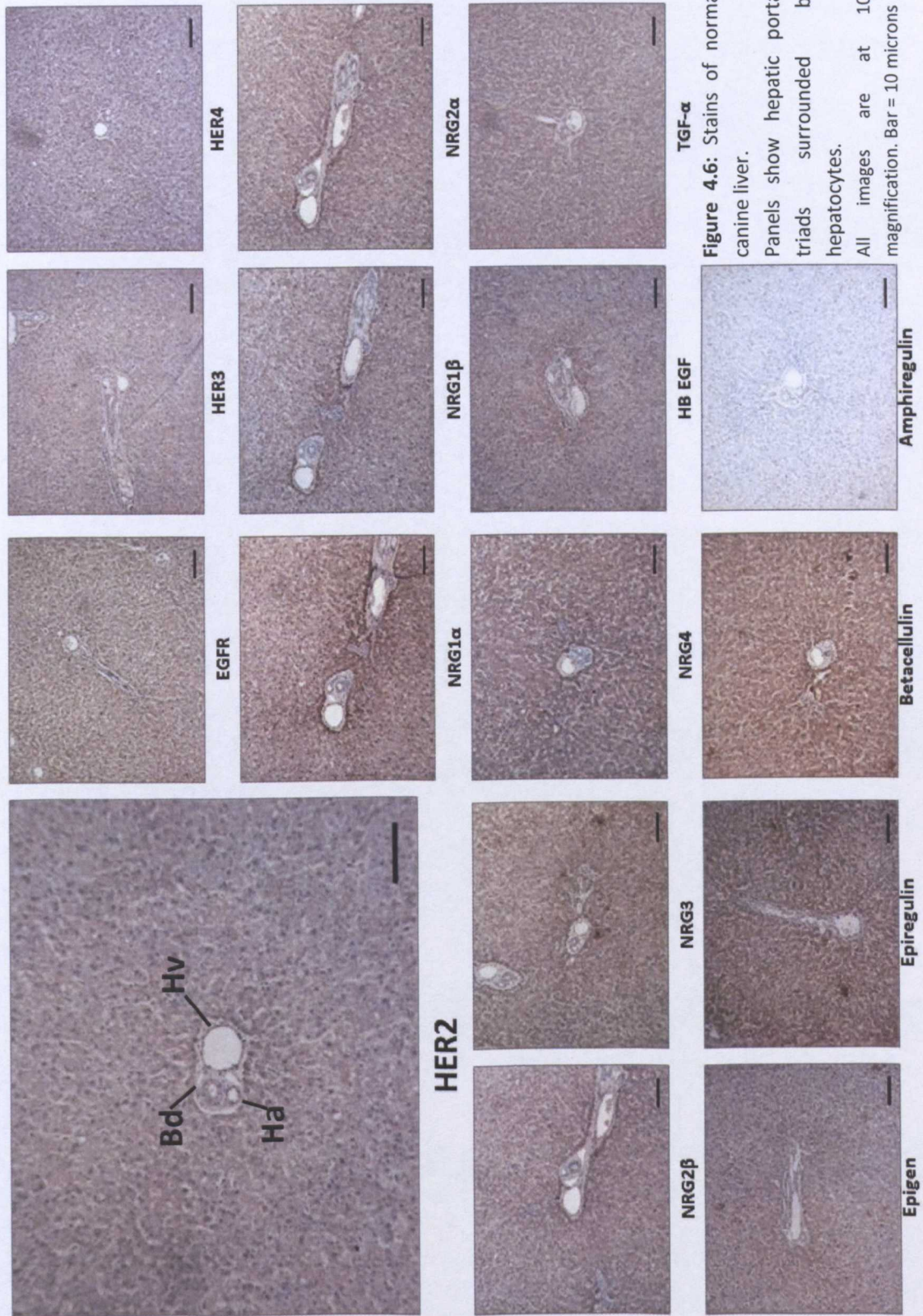


Figure 4.6: Stains of normal canine liver. Panels show hepatic portal triads surrounded by hepatocytes. All images are at 10x magnification. Bar = 10 microns

Pancreas

See Figure 4.7

The pancreas acts as both an endocrine gland (owing to its production of hormones such as insulin and glucagon) and a digestive organ (as it produces and secretes pancreatic juices containing enzymes which are involved in the chemical breakdown of food).

The hormones of the pancreas are produced by the various cell types found within the Islets of Langerhans (IL). These islets consist of five cell types, each of which is involved in the production and secretion of a separate hormone:

- Alpha cells: secrete glucagon
- Beta cells: secrete insulin and amylin
- Delta cells: secrete somatostatin
- PP cells: secrete pancreatic polypeptide
- Epsilon cells: secrete ghrelin

Pancreatic acini (PA) are responsible for production of digestive enzymes, which run into the gastrointestinal tract via a series of ducts (D) which permeate the tissue.

Receptors in the pancreas show the same generalised staining patterns. Uniform cytoplasmic staining was visible in both the pancreatic acinii and in the islets of Langerhans for each receptor. HER4 showed the strongest signal of the four in the islets, while HER3 was strongest in the acinii. EGFR and HER2 displayed moderate staining throughout the tissue. All of the receptors also displayed cytoplasmic staining of the epithelium lining the intercalated ducts.

Betacellulin (which was originally isolated from an islet beta carcinoma cell line (Rungsipat *et al.*, 1999)) showed strong staining of the islets, with some patchy weak to moderate staining of the acinii and stronger areas of staining around the nuclei of the central acinar cells.

Amphiregulin stained negatively throughout the tissue. Epiregulin showed strong to moderate grainy staining of the cytoplasm of the cells in the islets of Langerhaans, with considerably weak to negative staining throughout the cytoplasm of the acinar cells. Epigen showed moderate staining of the cytoplasm of the cells in the islets, with some patchy weak to moderate staining of the acinii. Epigen also showed moderate to strong staining of the intercalated ducts.

HB EGF showed moderate staining throughout the cytoplasm of islet cells, with this being much weaker in the surrounding acinii and ducts. TGF α showed weak staining of the islets with this being slightly weaker in the acinii.

NRG1 α showed moderate to strong staining of the cells on the islets of Langerhaans. Staining levels throughout the acinar tissue varied from moderate in the acinar cells immediately surrounding the islet, to strong levels in other areas. NRG1 α also showed very strong levels of staining of the epithelia lining the ducts within the tissue.

This strong staining of the ducts was also visible in stains for NRG1 β ; however in contrast staining of the acinar cells was significantly weaker. Cells in the islets showed an overall weak to moderate level of staining, with certain cells within the islets themselves showing much stronger signals than their surrounding histology. Further investigation into which cells NRG1 β was specifically highlighting through the use of double immunofluorescent staining with antibodies directed against hormones with known cellular origins would allow for the identification of these cells, unfortunately due to time constraints this was not possible.

NRG2 α showed moderate to strong staining of the entirety of the islets, this being surrounded by weaker, grainy, cytoplasmic staining within the acinar cells. NRG2 β showed moderate staining of the whole of the islet, with there being an absence of staining in the surrounding acinar cells. NRG2 β also exhibited moderate staining of the intercalated ducts. NRG3 showed moderate staining throughout the islets of the pancreas, with this extending to certain patches of surrounding acinar tissue. NRG4 and betacellulin showed strong staining throughout the islets, and moderate staining in the acinar cells.

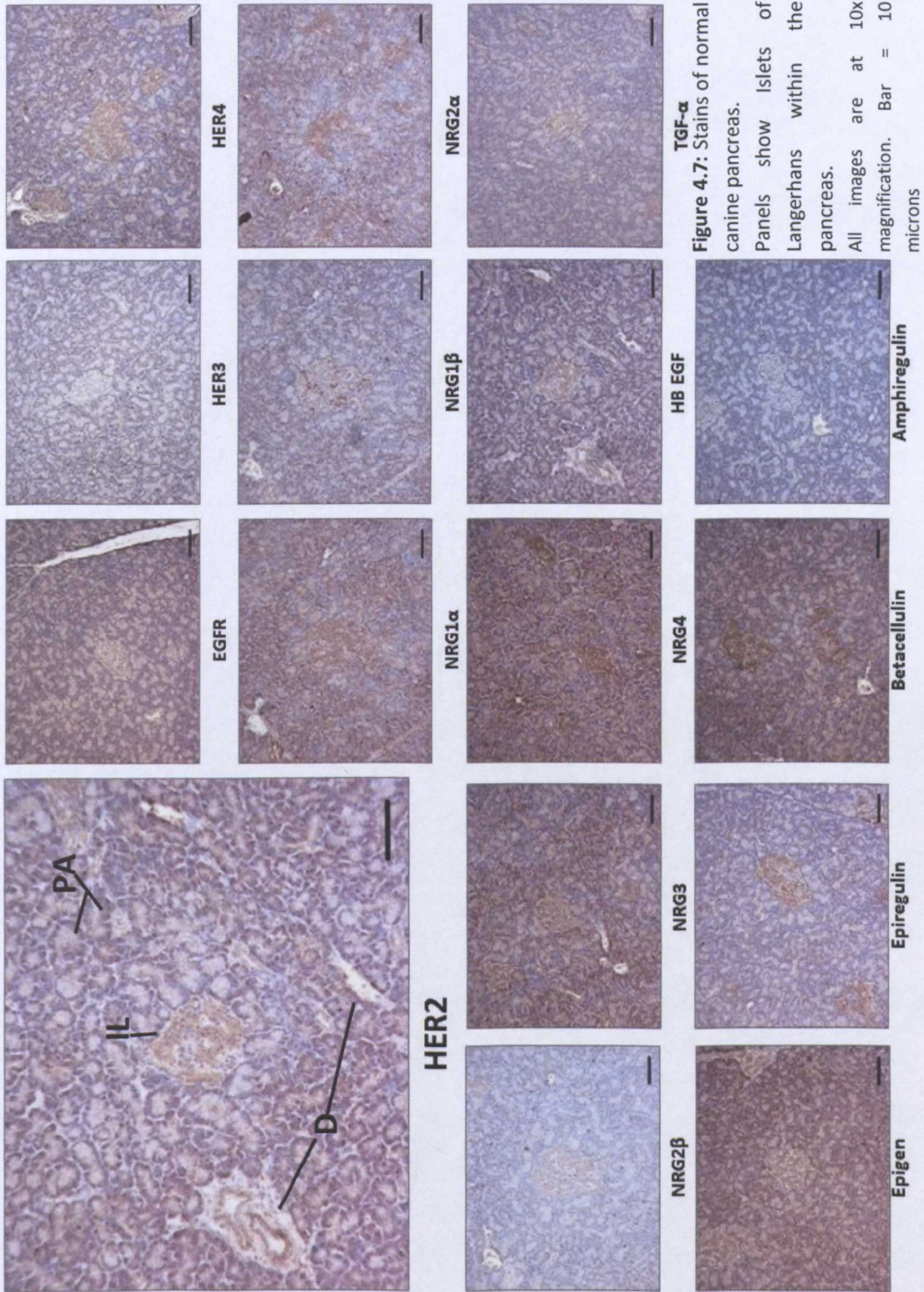


Figure 4.7: Stains of normal canine pancreas. Panels show Islets of Langerhans within the pancreas. All images are at 10x magnification. Bar = 10 microns

Rectum**See Figure 4.8**

The rectum is the final portion of the gastrointestinal tract; it is responsible for the storage of faecal matter. Stretch receptors present in the rectum stimulate the need to defecate once full, and peristalsis helps to push faeces through the anus.

In cytological structure the rectum is similar to the colon, in that the surface of the rectal lining is covered with many tubular invaginations. These are the Crypts of Lieberkühn (CL), which permeate the mucosa of the rectum and contain some specialised cells:

- **Goblet cells (GC):** responsible for the production of mucus which helps to lubricate the gastrointestinal tract.
- **Stem cells (SC):** found at the base of the crypts and are responsible for replacing the superficial epithelial cells which are frequently sloughed off as food passes through the bowel.

In the rectum, the four receptors of the EGF family generally showed moderate to strong signals around the goblet cells which line the crypts of the rectum. With the exception of HER2, the receptors also showed moderate to strong staining of the rectal mucosa. Moderate to strong staining was also visible in the submucosa for all four receptors, although there was a lack of staining in the regions of the crypts which house the stem cells.

Many of the ligands showed similar trends in their staining patterns, with staining being mostly concentrated around the goblet cells surrounding the crypts and there being a general absence of staining in the locations of the stem cells. This was the case for TGF α , betacellulin and epiregulin, where there was also moderate to strong staining present in the lamina propria. Similar staining was observed for HB EGF and epigen although the signal was weaker in these cases. Amphiregulin showed no staining in the rectum.

NRG1 α , NRG1 β and NRG3 showed strong staining within the crypts of the rectum and within the goblet cells. This was not the case with NRG1 β and NRG3 which lacked mucosal staining, and had much lower signals in the sub mucosa. NRG4 showed strong staining around the goblet cells and moderate staining of the lamina propria between the crypts.

NRG2 α showed moderate staining around the goblet cells of the crypts, although this staining did not extend into the area of the lumen. There was little staining of the

mucosa, but moderate staining of the sub-mucosa. This did not however persist into the longitudinal or circular muscle of the bowel, which showed much weaker levels of staining. NRG2 β showed little staining throughout the mucosa, but stronger staining in the submucosa.

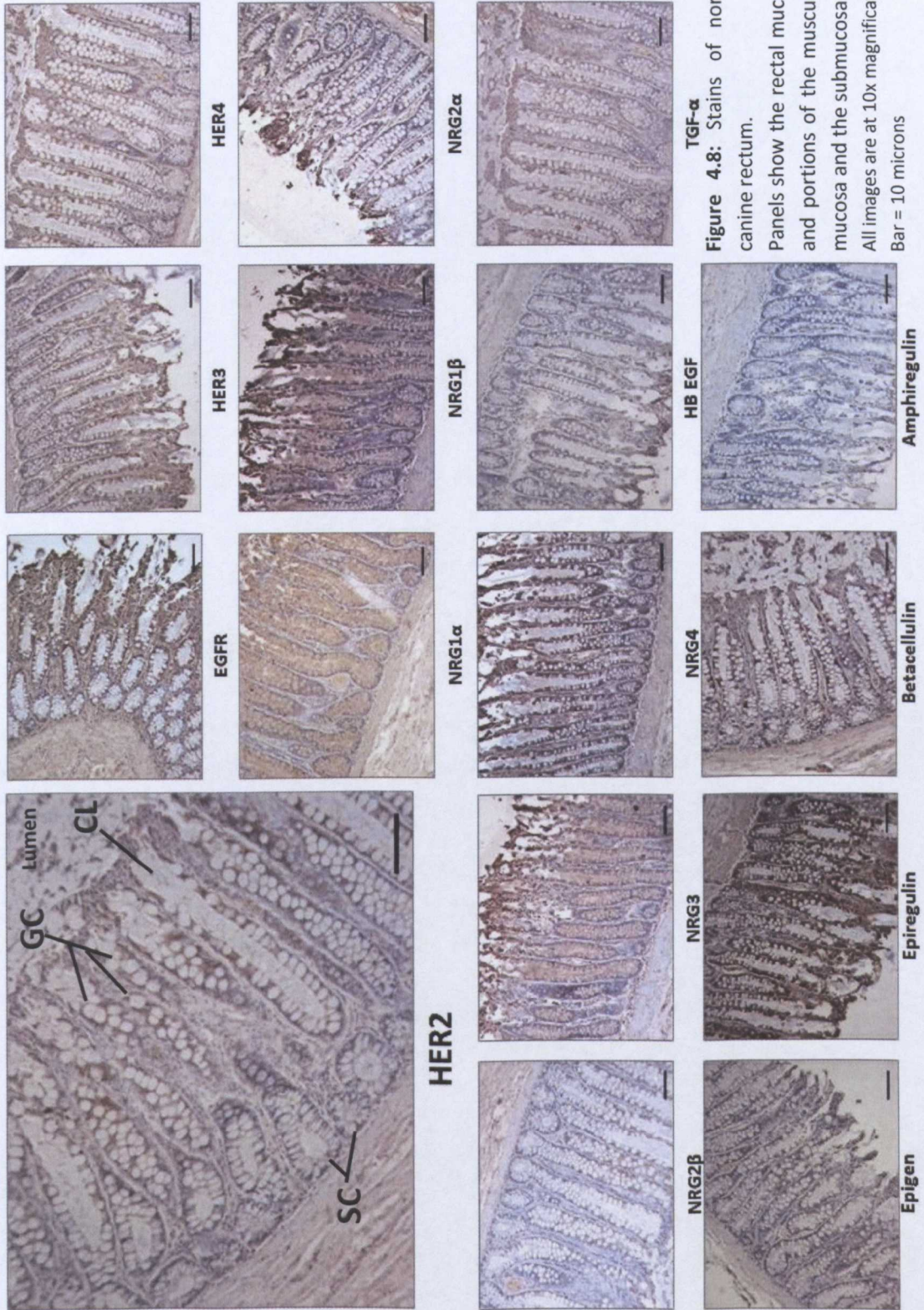


Figure 4.8: Stains of normal canine rectum. Panels show the rectal mucosa, and portions of the muscularis mucosa and the submucosa. All images are at 10x magnification. Bar = 10 microns

4.3.2.4. The Urinary System

Kidney

See Figure 4.9

The histology of the kidney can be divided into two main sections: the cortex and the medulla. The cortex of the kidney contains the renal corpuscles (RC) which consist of the glomerulae (blood supply to the corpuscle) and Bowman's Capsules (which contain podocytes that wrap around the capillaries of the glomerulae). Renal corpuscles are involved in the ultrafiltration of blood to extract the various components of urine: it removes waste products (urea) and excess water, whilst retaining glucose and sufficient mineral components to maintain homeostasis. The cortex also contains the proximal (Pt) and distal (Dt) convoluted tubules, the former of which are responsible for carrying waste filtered by the Bowman's capsules to the loop of Henle, and the latter of which regulates pH, calcium and salt ion levels before draining into the collecting ducts of the medulla. Also present in the cortex is a portion of the loop of Henle, the descending limb of which is permeable to water, allowing for its reabsorption from the urine back into the blood. Meanwhile, the ascending limb is impermeable to water, but salt ions are reabsorbed into the blood by active transport.

The medullary portion of the kidney also contains a section of the Loop of Henle, which carries some minor anatomical differences but which is functionally similar to the cortical portion. Also present in the medulla are a number of collecting tubules, which are involved in transportation of the filtered urine to the ureter.

The cortex of the canine kidney shows a largely similar pattern throughout the EGF receptors, with staining in the glomerulae being less visible than that in the surrounding tubules. EGFR, HER2 and HER4 show staining of both the proximal and distal convoluted tubules in the cortex. However HER3 shows staining primarily in the proximal convoluted tubules of the cortex, with there being less staining visible in the distal tubules. In the medulla all the receptors generally showed moderate to strong levels of staining, with EGFR and HER2 showed stronger staining of the proximal tubules than the distal tubules, whilst HER3 and HER4 appeared to show equal levels of staining for both sets of tubules.

NRG1 α and NRG1 β stained the proximal tubules and distal tubules in the cortex with a moderate intensity, however while there was a lack of staining in the corpuscles with NRG1 α , there were some areas of staining in these structures with NRG1 β . NRG1 α also moderately stained the proximal and distal convoluted tubules of the medulla, whilst NRG1 β stained the proximal tubules moderately and distal tubules more weakly. NRG2 α and NRG2 β stained negatively throughout the kidney, although NRG2 α showing some very weak staining of the proximal tubules in the medulla. NRG3 showed moderate staining of the proximal and distal tubules in the cortex, with this also being present in some cells of the renal corpuscles. In the medulla, the proximal tubules stained moderately, although the intensity of staining appeared to be somewhat reduced in the distal tubules. NRG4 showed strong to moderate staining of all the tubules in both the cortex and medulla, with there being some cells in the corpuscles also staining moderately.

Betacellulin showed strong staining of the tubules in the cortex and the medulla with there being an absence of staining in the corpuscles. TGF α showed moderate staining of the proximal tubules in the cortex and medulla with the distal tubules staining more lightly, and there being an absence of staining in the corpuscles. Amphiregulin stained negatively throughout the kidney. Epigen showed weak staining of the tubules in the cortex which became stronger in the proximal tubules in the medulla, and staining was absent in the corpuscles. Epiregulin showed weak to moderate staining of the tubules in the cortex and medulla with some individual cells staining in the corpuscles. TGF α displayed moderate staining of the tubules in the cortex, although in the medulla only the proximal tubules showed any moderate staining, with the distal tubules being predominantly negative. TGF α did not stain the renal corpuscles. HB EGF showed largely negative staining throughout the cortex, with only the proximal tubules showing any weak to moderate staining in the medulla.

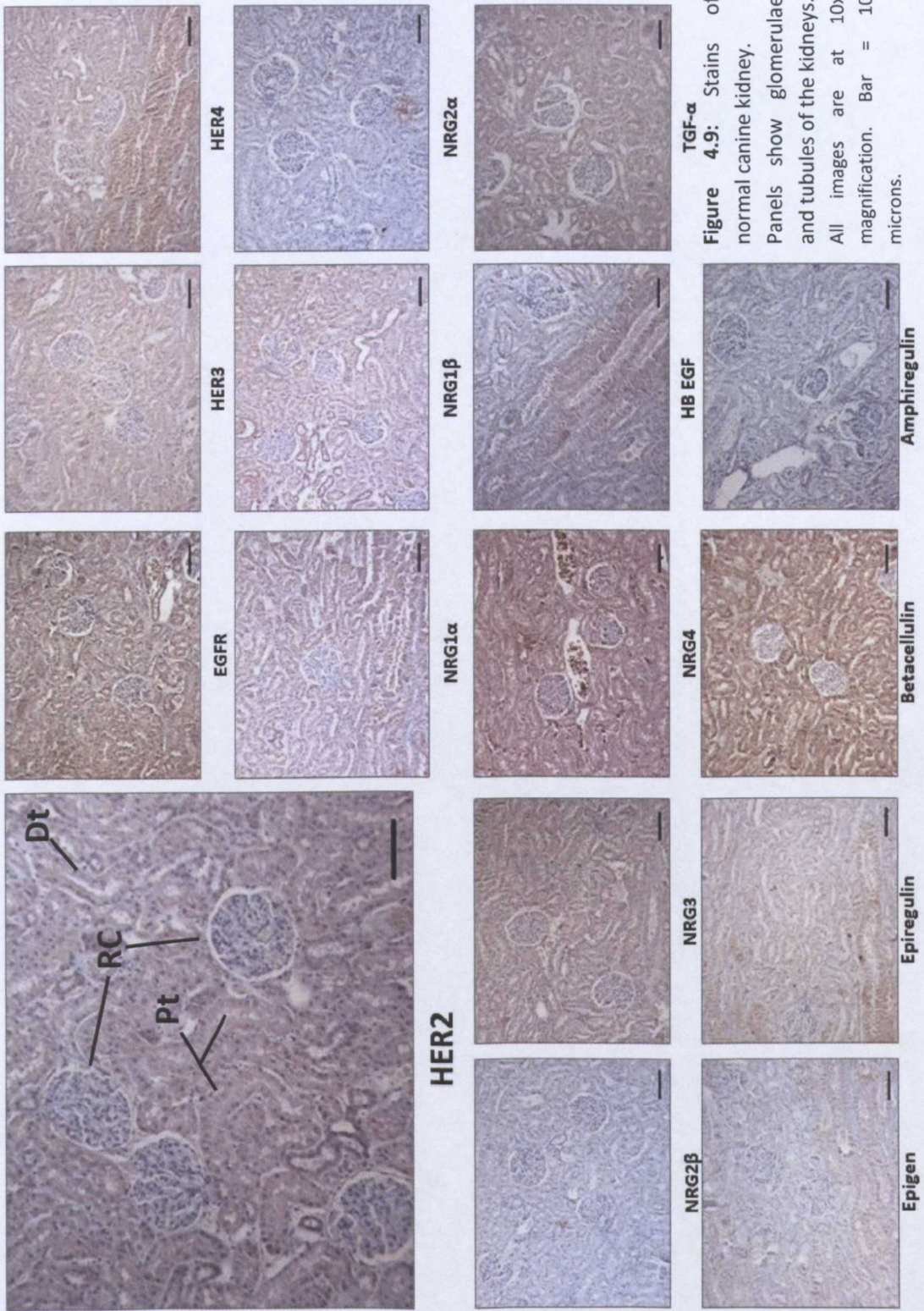


Figure 4.9: Stains of normal canine kidney. Panels show glomerulae and tubules of the kidneys. All images are at 10x magnification. Bar = 10 microns.

Bladder**See Figure 4.10**

The bladder serves to store urine that is filtered from the blood by the kidneys before it is removed from the body via the urethra. It is a highly elastic organ, which has a comparatively simple histology to other organs. The mucosa is composed of a layer of transitional epithelium (TE) (which does not produce mucus), beneath which is a thick layer of muscularis (MM), which lends the bladder its elastic quality. The bladder possesses a muscle known as the detrusor muscle, which when relaxed allows the bladder to fill and when contracted expels urine from the organ. The detrusor is composed of a number of smooth muscle fibres, and contraction of them is controlled by the parasympathetic nervous system which signals for contraction when the bladder begins to distend with urine.

When relaxed, the mucosa of the bladder has a crinkled appearance (as in the panels in Figure 4.10) which appears smoother and more flat when the bladder is full and distended.

EGF receptor and HER4 showed the strongest staining of the transitional epithelia out of all of the receptors, with staining in this region being slightly weaker with HER2 and HER3. In the case of EGFR and HER4, this staining also appeared to be present in the lamina propria to some extent.

NRG1 α and NRG1 β each showed some staining on the transitional epithelium near the lumen, with very weak staining of the lamina propria beneath. A similar pattern was seen in the stains for NRG2 α and NRG3, although in these cases the staining was more intense and more noticeable in the lamina propria. NRG2 β showed only very weak staining of the transitional epithelium, with the lamina propria appearing largely negative. NRG4 gave the strongest result of the neuregulin family, staining the full length of the transitional epithelium strongly, while leaving the lamina propria only very weakly stained.

Betacellulin, epiregulin and TGF α showed moderate to strong staining in both the entirety of the transitional epithelium and the lamina propria. Epigen showed weak to moderate staining in the transitional epithelium, with the lamina propria only staining weakly beneath it. HB EGF showed staining patterns more similar to members of the neuregulin family, with only the top portion of the transitional epithelium showing some weak

staining, and little or no staining of the lamina propria. Amphiregulin showed no staining on the bladder tissue.

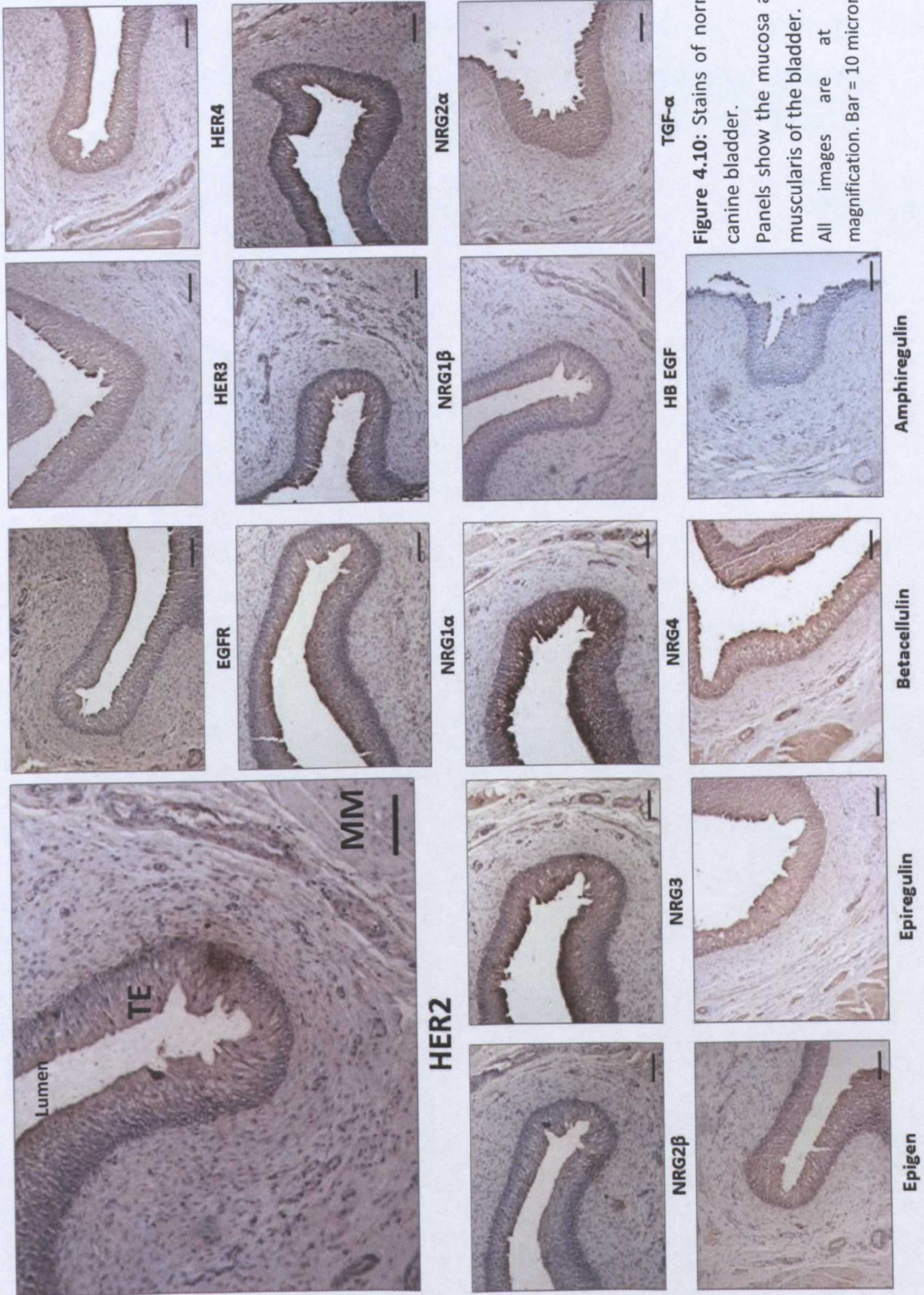


Figure 4.10: Stains of normal canine bladder. Panels show the mucosa and muscularis of the bladder. All images are at 10x magnification. Bar = 10 microns.

4.3.2.5. Miscellaneous Tissues

While no tissues were exclusively selected to observe any cardiovascular or muscular receptor or ligand expression, components of the vascular system (arteries, veins and capillaries) and smooth and skeletal muscles are common throughout the organs of mammals, and so were routinely observed in the course of this study.

Vasculature

Mammalian vasculature transports blood through a series of networks of arteries, veins and capillaries. Arteries are typically characterised by having a thick wall made up of three components:

- Tunica intima: composed of an endothelial cell wall and connective tissue.
- Tunic media: composed of elastic and muscle fibres.
- Tunica adventitia: composed of elastic and loose connective tissue, throughout which fibroblasts which secrete a mixture of collagenous and elastic fibres.

This thick wall, combined with a small lumen allows the arteries to circulate blood from the heart at a high pressure. In contrast, the veins (which carry blood at a much lower pressure back to the heart) have much smaller wall (of the same composition as that of an artery, albeit much thinner) and a large lumen. Capillaries are the smallest division of the circulatory system, and are composed of a single layer of endothelial cells surrounded by a basement membrane – as they are so small and difficult to observe, they have not been considered in this analysis. No cardiac tissue was observed in this study. It should be noted that collagen has a tendency to produce non-specific staining with immunohistochemistry, and so any staining observed within the tunica adventitia is not being considered in this analysis.

EGF receptor and HER3 showed weak staining of the tunica media, whilst HER2 showed a general lack of staining in this region. In contrast to the other receptors, HER4 showed strong staining in the tunica media.

NRG1 α and betacellulin showed strong staining of the tunica media, while NRG1 β , NRG3, TGF α and HB EGF showed weak staining of tunica media. NRG4 also showed a weak stain in the tunica media, but this had a patchy pattern when compared to the other ligands. Epiregulin showed moderate staining of the tunica media, and NRG2 α , NRG2 β , epigen and amphiregulin showed no staining of any vascular structures.

Muscle

The majority of the muscle observed in this study was smooth muscle which lined the gastrointestinal tract, although some skeletal muscle was observed in the tongue.

In skeletal muscle, EGF, HER4, betacellulin, epiregulin and TGF α all showed strong staining; HER3, NRG1 α , NRG1 β and NRG4 showed moderate staining; HER2, NRG3, amphiregulin, epigen and HB EGF all showed weak staining; and NRG2 α and NRG2 β showed no staining.

In smooth muscle, NRG1 α , betacellulin and epiregulin showed strong staining; EGF receptor, HER2, HER4, NRG1 β and NRG4 showed moderate staining; HER3, NRG3, epigen, TGF α and HB EGF stained weakly; and NRG2 α , NRG2 β and amphiregulin showed no staining.

4.3.3. Results of Comparisons in EGF Receptor and Ligand Expression Between *C. familiaris* and *H. Sapiens*

Comparisons were made between the results obtained from staining canine tissues with human tissues which had already been stained. In order to achieve this, the Human protein Atlas (<http://www.proteinatlas.org>) was used in combination with results from previously published studies (Gusterson *et al.*, 1984; Damjanov *et al.*, 1986; Press *et al.*, 1990; Prigent *et al.*, 1992; Srinivasan *et al.*, 1998). The Human Protein Atlas was set up as part of the Swedish Human Proteome Resource Program, with the aim to explore the human proteome using antibody-based proteomics. The Atlas allows for a user to search for a gene of interest, and observe immunohistochemical stains for a number of different healthy and cancerous tissues in humans.

It should be noted that the Human Protein Atlas lacked any data for stains of the tongue and vasculature, and had no data at all for betacellulin, epiregulin or HB EGF. Data for NRG1 and NRG2 was not available for separate isoforms – these stains were grouped together under the umbrella headings of NRG1 and NRG2. Collected results for staining in human tissues are summarised in Table 4.3.

Table 4.3 – Immunoreactivity of epidermal growth factor receptors and their ligands in normal human tissue

Tissue	EGFR *	HER2 **	HER3 †	HER4 ‡	NRG1§	NRG2§	NRG3§	NRG4§	AREG§	Epigen§	TGFα§
Digestive Tract											
Tongue	ND	ND	ND	ND	ND	ND	ND	ND	ND	ND	ND
Oesophagus	++	+	++	++	-	+	++	-	+++	-	++
Stomach	-	-	++	++	-/++	++	+++	++	+++	+/++	+++
Rectum	+++§	+\$	+++	+\$	-	++	+++	+	+++	n/a	+++
Liver	++	-	++	++	-/+++	-/+	++	-/+	+	+/+++	-/+++
Pancreas	++	-	-/+	+/+++	-/+++	-/+	+++	-/+	++	+/+++	+/+++
Urinary Tract											
Kidney	-/+	+	+/++	-/+/+++	-/+++	-/+	+++	-/++	+/++	-/++	-/+++
Bladder	+	+	+	++	-	++	++	+	+++	+++	++
Respiratory Tract											
Lung	++	++	++	++	-/+	-	+/+++	+/++	+/++	-/++	+/+++
Nervous System											
Cerebral Cortex	+\$	-\$	+/+\$	-\$	-	-	++	-/+++	-/+++	-/+	+/+++
Miscellaneous											
Vasculature	ND	ND	ND	ND	ND	ND	ND	ND	ND	ND	ND
Smooth Muscle	+++§	-\$	+++	+/+++§	+	-	+++	+	+/++	-	+
Skeletal Muscle	+++§	+/+++§	-\$	+/+++§	-	-	+++	+	+/+++	-	++

Tissues were scored on a semi-quantitative scale based on the intensity of staining observed: negative (-); weakly positive (+); moderately positive (++); strongly positive (+++). In cases where multiple scores are separated by "/" this denotes the presence of different intensities of staining in separate areas of the tissue. ND = not determined. *EGFR immunoreactivity as reported by (Damjanov *et al.*, 1986) and (Gusterson *et al.*, 1984); ** HER2 immunoreactivity as reported by (Press *et al.*, 1990); †HER3 immunoreactivity as reported by (Prigent *et al.*, 1992); ‡ HER4 immunoreactivity as reported by (Srinivasan *et al.*, 1998); § = determined using the HPA.

EGF Receptors

When comparing the expression of the EGF receptors between human and canine species, the results appear to be largely similar. This similarity was particularly visible in the cases of HER3 and HER4, which showed noticeably strong and moderate levels of staining in both species. The receptor which appears to differ most between species is HER2, which gave less strong results in the human tissues than the canine, in some cases being entirely absent in humans while the canine tissues gave weak or moderate stains. EGF receptor appeared to show an overall slightly stronger level of staining in the dog than in human.

Neuregulins

NRG1 showed some similarities between species, with most tissues displaying similar intensities of staining. One notable exception was observing scores for the cerebral cortex, where canine tissues showed some moderate levels of expression (2+ and 1+ for NRG1 α and NRG1 β respectively), whereas human tissues were reported to be devoid of NRG1. Isoforms of NRG1 did also show some strong staining in the gastrointestinal tract, which was also seen in dogs. In experiments with canine tissues, NRG2 isoforms rarely scored above 2+ for intensity, and this effect was mirrored in the human results.

In humans NRG3 showed overall very strong results across the bulk of the tissues, with no stains showing anything less than moderate (2+) staining. In the dog, while there were some strong stains, many of the tissues showed either weak or moderate expression – giving the dog tissue an overall lower level of expression than the human. This situation was reversed when observing the results for NRG4, with canine tissues showing overall very strong levels of staining (all tissues showed 2+ or 3+ staining with the exception of one which was 1+) whilst the human tissues scored largely weak stains, with only the cerebral cortex showing high NRG4 expression.

Amphiregulin, Epigen and TGF α

Amphiregulin seemed to be largely absent from canine tissues, with only the tongue, oesophagus and skeletal muscle showing some moderate to low-level staining. In human, this effect is completely the opposite, with many tissues showing very high expression levels and only a few showing any stain less than 2+ in intensity. Epigen showed similar stains between the two species, with tissues in the gastrointestinal tract, urinary tract and the lung showing moderate and strong levels between both species. However in the dog, the muscular tissues showed little staining, which was stronger in human tissues. TGF α

showed almost exclusively strong staining in many of the human tissues, whilst in the dog there were a mixture of staining intensities ranging from weak (1+) to strong (3+).

4.4. DISCUSSION

4.4.1. The Expression of the EGF Family in Normal Canine Tissues

The results of the immunohistochemical stains in canine tissues show that the EGF family is widely expressed in canine tissues. All the proteins probed for showed some degree of presence within the canine tissues observed here. One notable exception to this was amphiregulin, which showed quite strong levels of expression in humans and yet was almost entirely absent in the canine tissues. It was unexpected that a protein which features so prominently in the human tissues would be almost entirely absent in the dog (especially considering the relatively high degree of similarity with regard to other protein members). In this case, the reason for this discrepancy may be down to an unsuitable antibody – that is, either the antibody was out of date or hadn't been stored appropriately previously, or (as there was one residue difference between the canine antigen sequence and that which was used in immunization) the antibodies may not have been similar enough to the canine antigen to bind effectively. However, given that other antibodies which also had one residue different between the canine sequence and the immunizing sequence (HER3 and TGF α) gave positive results (which were similar in the human and dog tissues), this seems unlikely. Also, amphiregulin did show some staining in the tongue and oesophagus, suggesting that there was not a problem with antibody binding. It could simply be that the ligand occurs at naturally low levels, which the antibody lacks the affinity to bind to sufficiently for detection.

Overall, the region of the canine body which showed the most consistently strong expression of the members of the EGF family was the gastrointestinal system. This could partly be explained by the fact that the epithelia of the mucosa of these organs are exposed to frequent mechanical stresses as food passes from the mouth to the rectum. This gives rise to a high turnover of cells as they are easily sloughed off, which would require a degree of cell signaling that could be provided by ligands and receptors of the EGF family.

Organs within the urinary system also showed moderate to strong expression in the dog. These tissues are involved in the creation of urine: a process which removes urea (a

product of protein digestion and excretion), water, glucose and salts from the blood. This filtration process occurs constantly and at a high hydrostatic pressure as blood passes through the kidneys, and so the glomerulae and tubes which filter and concentrate urine are often exposed to urine which flows through the tubules. This constant flow of urine may necessitate a high cellular turnover, similarly to in the gut, which could be facilitated by the presence of both EGF receptors and ligands.

The lungs also showed some strong staining, particularly of a number of the EGF ligands. This is perhaps due to the lungs function in breathing, which not only passes air (potentially containing contaminants in it) through the tissue, but also requires a degree of elasticity within the tissue. The repetitive nature of breathing would perhaps cause the lung tissue to suffer some damage, which could be repaired through cell signaling by the EGF receptors and their ligands.

Of some interest was the presence of neuregulins on the cerebral cortex. Studies have shown that neuregulin and its receptor (HER4) appear to play a role in schizophrenia: it has been reported that in mice with a decrease in the function of this receptor in the central nervous system (CNS) exhibit symptoms similar to mice which have decreased NRG1 levels in their CNS (Gerlai *et al.*, 2000; Stefansson *et al.*, 2002). Further studies report that when ERBB4 or ERBB2 are deleted in mice, there is no gross change to the morphology of the brain. However observations on behavior show that these mice still exhibit schizophrenia-like symptoms, and the maturation of the dendrites of certain cells is inhibited (Barros *et al.*, 2009). Results in the canine studies presented here show that both HER4 and NRG1 isoforms are present in the canine cerebral cortex, with HER4 showing strong staining levels, and NRG1 isoforms showing moderate to weak staining. While no studies have been carried out to show conclusively that schizophrenia exists in dogs, it has been suggested by veterinary professionals that the disease could occur in domestic pets which can show behavioral symptoms typical of the disease (PetPages, 2010). The potential for schizophrenia to exist in dogs along with evidence from previous studies investigating the role of HER4 and NRG1 in schizophrenia supports the observation from this study that both these proteins are present in the canine cerebral cortex.

The vasculature and smooth muscle generally showed moderate to weak staining, whilst skeletal muscle (which is more heavily involved in strenuous activity) showed some strong staining, which would perhaps be consistent with the need for repair in this tissue.

4.4.2. Comparing EGF Family Expression between Canine and Human Tissues

When making comparisons between the results for human and canine immunohistochemical stains, the results were similar in the case of the digestive tract with receptors and ligands showing generally moderate to strong staining. An exception to this was HER2 which showed little expression in the digestive tract in comparison with the canine results.

Also similarly to the canine results, there was some strong staining in the kidney and the skeletal muscle, and the observation in the canine results that ligands stained more strongly in the lungs than the receptors was also seen in the human lung. The bladder and smooth muscle generally showed lower levels of expression than the equivalent canine stains.

Oddly, there was no observed staining for HER4 or NRG1 on the human cerebral cortex, despite the reported role of these two proteins in schizophrenia (see section 4.4.1 for further detail). However, other studies have shown that HER4 is present in the brain of the Rhesus monkey (*Macaca mulatta*), including in the cerebral cortex (Neddens & Buonanno, 2011).

4.4.3. Limitations of Immunohistochemical Studies

While immunohistochemistry has proven to be a valuable tool in both research and disease diagnosis/prognosis, there are some inherent limitations in the method, and in the experiments presented here.

As previously described, immunohistochemistry cannot provide a direct measure of protein expression, owing to the non-linear results it presents. Whilst this makes quantification of results difficult, it does still provide an indication of where proteins are expressed. Further experiments utilising techniques which can be considered more quantifiable (such as fluorescent staining) could be used to compliment the results presented here. However, due to time constraints and the availability of sufficient material, such experiments were not carried out here.

There is also some degree of difficulty when comparing the results between canine and human results. As the experiments on human tissue were carried out by other groups (with the exception of those for HER4), it is difficult to vouch for the specificity of the antibodies

used in these instances, and different antibodies and protocols were likely used which may have some effect on the intensity of staining observed.

A specific limitation of this study is the lack of normal mammary tissue which was stained. As these the tissues in this chapter were purchased early in the study (and before any contact was made with other researchers in the field of veterinary oncology) we were somewhat limited in what tissues we could choose. An obvious implication of this limitation is that it does not allow for a baseline comparison to be made between healthy canine mammary tissue, and the tissue in its diseased state. This is particularly relevant when one considers that the aim of this thesis is to explore the role of HER2 in this particular cancer, and information gained from studies of healthy mammary tissue could have further validated HER2 as a drug target in companion dogs. Had more time been available later in this project, attempts would have been made to procure normal canine mammary tissues for comparative purposes.

4.4.4. The Role of Immunohistochemical Studies in Drug Development and Medicine

While it has already been highlighted that IHC plays a role in determining the molecular profile of a cancer, it is also important in the drug development process. IHC catalogues, like that presented in this thesis, provide researchers with an index of specific organs and tissues which may heavily express protein which a potential drug may be designed to target. Using this catalogue, it is possible to predict possible adverse effects which could be observed in drug trials. Having observed extensive staining of the EGF family in the GI tract, possible adverse effects that could be anticipated would include diarrhea and vomiting.

CHAPTER FIVE

Surveying the levels of EGF Receptor Expression in Benign and Malignant Canine Mammary Cancers

5.1. INTRODUCTION

The role of immunohistochemistry in the understanding of diseases (including cancer) is well documented. As described in the previous chapter, the technique is often used in characterising a cancer to determine appropriate therapies; however IHC also plays an important role in characterising diseases for research purposes.

Understanding the EGF receptor profile in cancers of model organisms helps to not only identify potentially useful models for drug trials, but can also have veterinary implications. SMTKIs specific to dogs have already been released to the market, some of which will only be administered in the presence of a particular protein. Masitinib (Masivet) is one such drug – it is only administered upon the detection of a mutated form of c-kit within the tumours of severe (grade 2 or 3) mast cell cancers (European Medicines Agency, 2010; Hahn *et al.*, 2008), although typically this analysis is performed by RT-PCR on tumour specimens. In many cases IHC is also a viable method for the detection of particular markers of cancer.

While work on canine mast cell tumours has highlighted the importance of members of the split-kinase receptor family in dogs, less investigation has been carried out into the role of the EGF receptors in canine cancers – particularly cancers of the mammary gland, in which members of this receptor family have been shown to play a role in human disease.

To this end, this chapter aims to investigate the expression of the EGF receptors in benign and malignant cases of canine mammary cancer, and also the expression of neuregulins 1 and 2 in the malignant cases as these ligands are those which primarily bind to HER2 and HER3 – the receptors most involved in breast cancer.

5.2. AIMS

1. To observe the expression of the four EGF receptors in eleven cases of benign mammary cancer.
2. To observe the expression of the four EGF receptors and neuregulins 1 and 2 in nine cases of malignant canine mammary cancer.
3. To compare these expression levels with those observed in human disease.

5.3. RESULTS

Antibodies (which have been previously described in Chapter Two: Materials & Methods) were used in the staining carried out in this chapter.

As with the immunohistochemistry carried out on normal tissues, the full range of images obtained from the study of these diseased cases is available on the DVD which accompanies this thesis.

5.3.1. Determination of the EGF Receptor and Ligand Expression in Benign Canine Mammary Cancers

Staining results for the benign mammary cancer samples are summarised in Table 5.1, with examples of stains from one case in Figure 5.1.

Overall, it was noticed that while these cancers were classed by the pathologist as benign, they still showed highly disorganised histologies with features typical of those found in cancers in humans, including large prominent nuclei and groups of cells which lack any defined structure.

Benign mammary tumours showed little in terms of extremes of expression in their histologies, with most cases showing only weak to moderate expression levels. When observing the stains for HER2 (with which this project is primarily concerned) only one case (CRXBGM) showed strong HER2 expression, and this was composed of a simple adenoma and a (non-neoplastic) sebaceous hyperplasia.

Table 5.1 – Immunoreactivity of the epidermal growth factor family of receptors in benign canine mammary cancer specimens

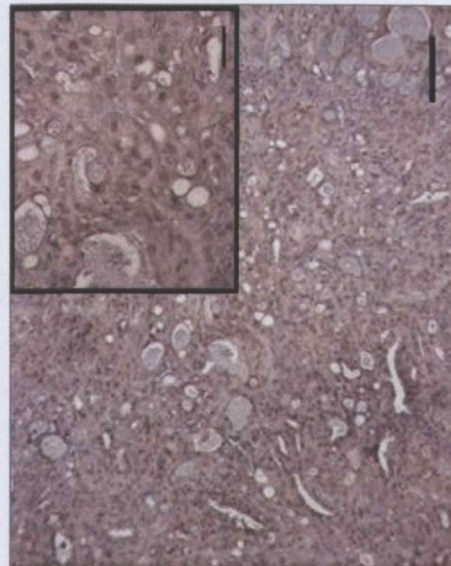
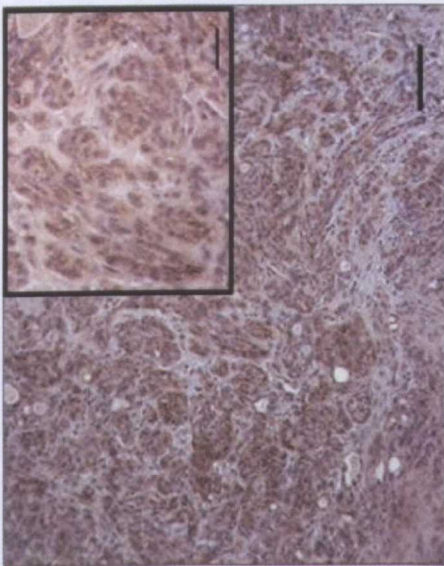
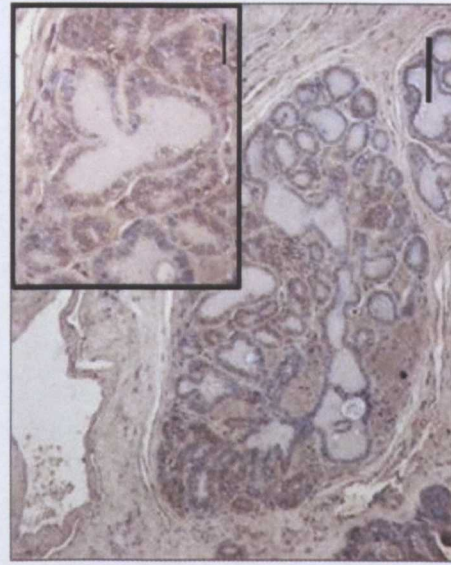
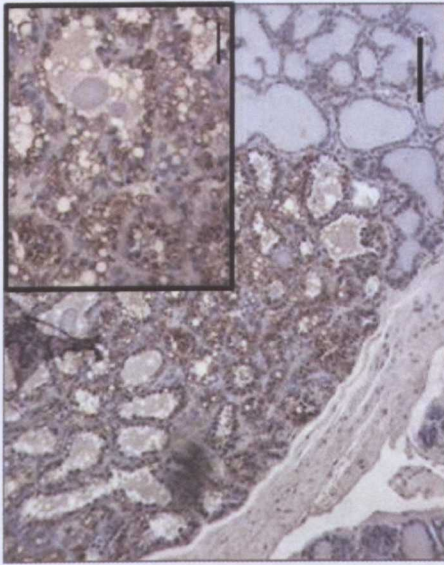
Case	Tumour Type	EGFR	HER2	HER3	HER4
4072979	Benign mixed mammary tumour	++	++	++	+
3391515	Benign mixed mammary tumour	++	++	++	+
3908976	Benign mixed mammary tumour	++	+	+++	+
3687104a*	Benign mixed mammary tumour	+	+	+++	+
3687104b*	Complex adenoma	+	+	++	+
3649008	Hyperplasia, fibroadenomatous	+	—	+ / ++	+
3915662	Benign mixed mammary tumour	—	—	++	+
CTUATL	Benign mixed mammary tumour	+	—	++	++
CTPASN	Benign mixed mammary tumour	+	+	+	++
CVVCJA	Carcinoma, tubular (low grade)	++	++	++ / +++	+
CRXBGMa*	Simple adenoma, lobular hyperplasia	++	+ / +++	++	+
CRXBGMb*	Sebaceous hyperplasia – non neoplastic	+++	+++	++	++
CTYAGN	Benign mixed mammary tumour	++	++	+ / ++	+

Tissues were scored on a qualitative scale based on the intensity of staining observed: negative (—); weakly positive (+); moderately positive (++); strongly positive (+++). In cases where multiple scores are separated by “/” this denotes the presence of different intensities of staining in separate areas of the tissue.

* These cases are those in which the tissue came from the same patient, however their disease presented two areas with distinct histopathologies.

Figure 5.1: Examples of benign complex adenoma of canine mammary cancer stained for the four members of the EGF receptor family.

All large images at 10x magnification. Bar = 10 microns. Inserts are at 40x magnification, where bar = 3 microns.



5.3.2. Determination of the EGF Receptor and Ligand Expression in Malignant Canine Mammary Cancers

Results for the staining carried out with the malignant specimens are summarised in Table 5.2, with examples of the stains visible in Figures 5.2 and 5.3.

As in the case of the benign samples, these malignant cases also displayed highly disorganised histologies, which (in combination with the prominent, enlarged nuclei and lack of defined structure) also tended to show regions of necrosis and some ductal infiltration which is typical of malignant, invasive disease. The reader may also observe (when studying the image library attached to this thesis as a DVD) that a number of untreated slides stained only with haematoxylin show regions of brown colouring. This is due to the presence of melanin within the patients' skin, and was taken into consideration when observing slides stained for the presence of receptors and ligands.

In the malignant cases, stains were also carried out to observe the levels of NRG1 and NRG2 present in the tissues, as these are the primary ligands which bind to HER2 and HER3 (the receptors which act as heterodimers and which are most often involved in aggressive disease in humans).

Unlike the benign cases, the malignant specimens showed a greater proportion of moderate to strong staining of the receptors, with a large number showing some strong staining. Notably, one case (168349) showed only low levels of staining for all the receptors and the ligands. Only one case (174475) appeared to show very strong staining for HER2, and this also showed strong staining for EGFR and HER3, with generally moderate staining of the ligands as well. HER2 generally showed moderate amounts of staining throughout the observed cases. Overall, it was observed that EGFR was the receptor which showed the most frequent strong staining, while HER4 showed the least, with no cases showing anything above moderate staining.

Interestingly, the ligands showed strong staining slightly more than the receptors, with 6 out of 9 (66%) showing some strong ligand staining of at least one ligand, compared to 5 out of 9 (55%) cases showing strong staining for at least one receptor.

Table 5.2 – Immunoreactivity of the EGF receptors and neuregulins 1 and 2 to samples of malignant canine mammary cancer

Case	Age	Breed	Diagnosis	EGFR	HER2	HER3	HER4	NRG1 α	NRG1 β	NRG2 α	NRG2 β
147347	5	MinDasch	Well-defined complex adenocarcinoma	++	++	++	++	++	++	+++	++
147498	13	Box	Well-defined papillary cystadenocarcinoma	+++	++	++	++	+++	+++	++	+
159707	11	Xbreed	Infiltrative papillary adenocarcinoma	++	++	++	++	++	++	+	+
162663	7	BrdCollie	Infiltrative tubular adenocarcinoma with lymphatic emboli	+++	+	+	++	++	++	++	+
168349	10	EngSprSpan	Infiltrative tubular adenocarcinoma with lymphatic emboli	+	+	+	+	+	+	+	+
174475	10	LabX	Infiltrative tubular adenocarcinoma	+ / +++	++ / +++	++ / +++	++	++	++	++	++ / +++
176930	10	StaffBTerr	Infiltrative tubular adenocarcinoma	++	++	++ / +++	++	++ / ++	+++	++	++
176931	10	EngSprSpan	Well-defined complex adenocarcinoma	+	+ / ++	+	++	++	++	++ / ++	+ / +++
182919	8	Lur	Well-defined complex adenocarcinoma	++ / +++	++	+ / ++	+ / ++	++	++ / +++	+ / +++	+

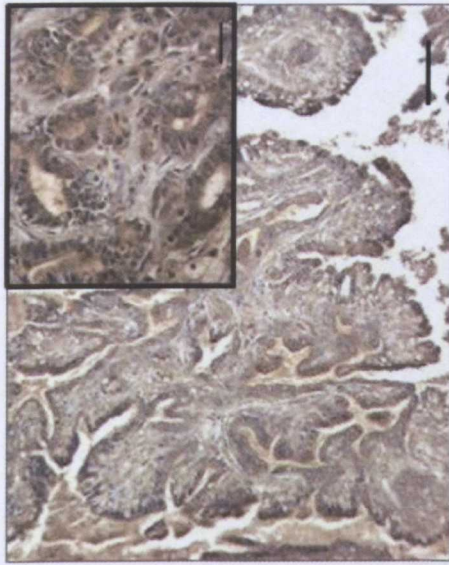
Tissues were scored on a semi-quantitative scale based on the intensity of staining observed: negative (—); weakly positive (+); moderately positive (++); strongly positive (+++). In cases where multiple scores are separated by “/” this denotes the presence of different intensities of staining in separate areas of the tissue.

Breeds: MinDasch = Miniature Dachshund; Box = Boxer; Xbreed = Crossbreed; BrdCollie = Border Collie; EngSprSpan = English Springer Spaniel; LabX = Labrador cross; StaffBTerrier = Staffordshire Bull Terrier; Lur = Lurcher.

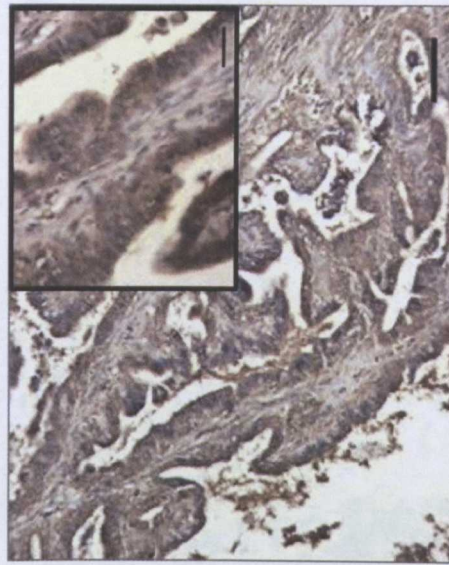
Figure 5.2: Examples of infiltrative papillary adenocarcinoma of the canine mammary gland of an 11 year old crossbreed dog. Samples were stained for the presence of the four members of the EGF receptor family.

All large images at 10x magnification. Bar = 10 microns. Inserts are at 40x magnification, where bar = 3 microns.

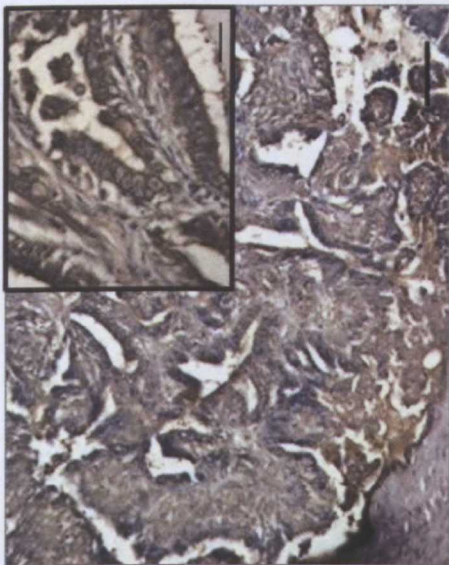
Note: Owing to problems which arose with the microscope on the occasion these images were recorded, the levels of the colours in this image and the brightness were adjusted with Jasc Paintshop Pro 7 to better demonstrate the true results in this thesis. Changes made were: colour balance levels in the midtones were adjusted to -26 (cyan/red), -9 (magenta/green) and -8 (yellow/blue); and brightness was increased to a score of +20.



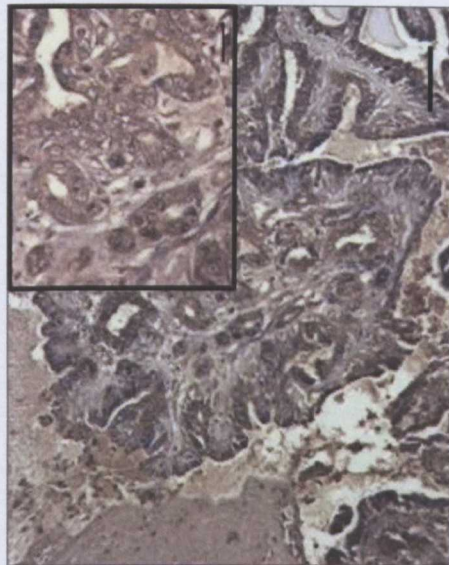
HER2



HER4



EGFR

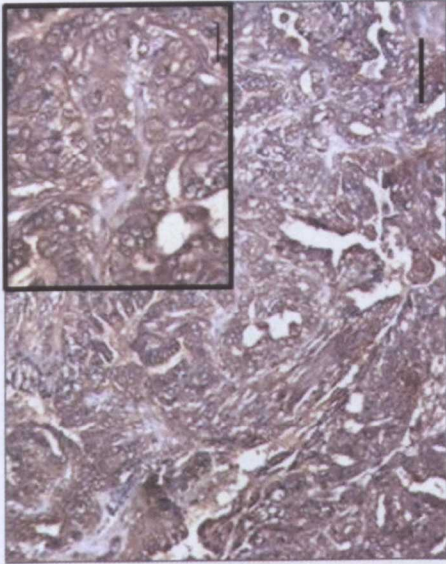


HER3

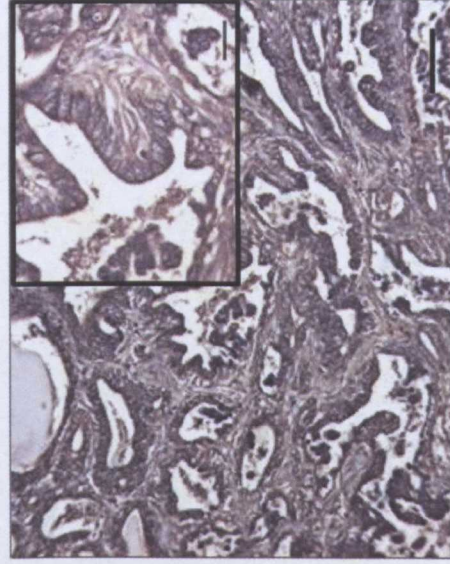
Figure 5.3: Examples of infiltrative papillary adenocarcinoma of the canine mammary gland of an 11 year old crossbreed dog. Samples were stained for the presence of NRG1 α , NRG1 β , NRG2 α and NRG2 β .

All large images at 10x magnification. Bar = 10 microns. Inserts are at 40x magnification, where bar = 3 microns.

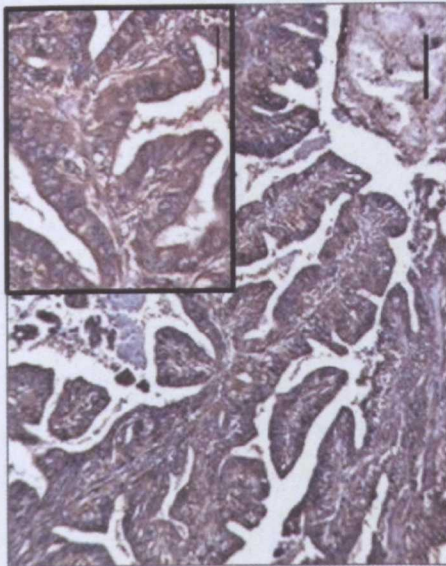
Note: Owing to problems which arose with the haematoxylin on the occasion these samples were stained, brightness was adjusted with Jasc Paintshop Pro 7 to better demonstrate the true results in this thesis. Changes made were: brightness was increased to a score of +20.



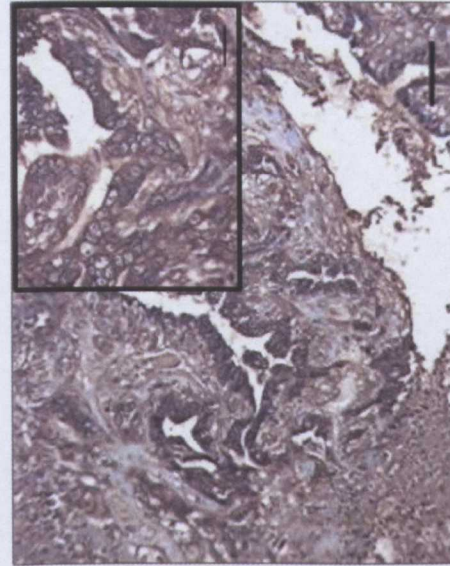
NRG1 β



NRG2 β



NRG1 α



NRG2 α

5.4. DISCUSSION

5.4.1. The Heterogeneity of Canine Mammary Cancer

Overall, it appears that the cases presented here indicate that the EGF receptors are present in canine mammary cancer at significant levels, as most samples showed either moderate or strong staining of the tissues. However, while it is easy to consider the receptors in each case individually, cancer is a disease which makes use of the heterogeneity of its receptor profile, and so the combinations of receptors should also be taken into account. HER2 and HER3 have often been documented to be strongly expressed together in human disease, owing to their preference to form heterodimers. In the cases observed here only one malignant case showed strong staining for both HER2 and HER3, with no benign cases showing such staining combinations. While there is a lack of strong staining for both receptors in many of these cases, it should be noted that a large proportion of cases showed moderate staining for both receptors (or a combination of moderate staining for HER2, with strong staining for HER3), which could perhaps indicate some relationship between these two receptors in the mechanisms behind these particular cases.

This heterogeneity is not limited to the molecular profiles of the disease displayed here, but is also evident in the morphology of each case. None of the cases studied in this project showed any great degree of normal mammary histology, with many displaying areas of disorganised cell structure, invasive regions of cancerous growth (into both the stroma and mammary ducts), regions of necrosis and morphologically altered cell nuclei. Little membranous staining (which is typically found in aggressive disease in humans) was observed in the course of this study for any of the receptors, although a number of cases did display strong staining of cellular cytoplasm. Overall, this study observed strong (3+) staining in only 11% of malignant cases (Table 5.3), and moderate (2+) staining in 78% of malignant cases. Similar studies in dog have found varying degrees of positive staining for HER2 in canine mammary cancer, ranging from 21% (Gama *et al.*, 2008) to 17.6% (Martín de las Mulas *et al.*, 2003) to 25.6% (of which 56.2% of cases were classified as 2+ and 7% were classified as 3+) (Dutra *et al.*, 2004). These figures show HER2 expression in canine mammary tumours to be roughly similar to that in breast cancer in humans (18-20% of human cases show HER2 over-expression), however many aggressive human cases show staining of the cell membranes, which was rarely observed in this study. The percent of

benign and malignant canine cases in this study which showed moderate (2+) and strong (3+) expression (for all 4 EGF receptors) are summarised in Table 5.3.

Table 5.3 – Percent of benign and malignant cases which showed strong (+++) and moderate (++) staining of the receptors.

Receptor	Strong staining benign cases*	Strong staining in malignant cases**	Moderate staining in benign cases*	Moderate staining in malignant cases**
EGFR	9%	44%	55%	44%
HER2	18%	11%	36%	78%
HER3	27%	22%	91%	66%
HER4	0%	0%	27%	89%

* n = 11; ** n = 9

Further studies into other molecular subtypes of these cases could not be carried out owing to time constraints and the limited amount of tissue available. However an investigation into the oestrogen receptor (ER) statuses of these cases may shed further light on the mechanisms behind disease progression in canine mammary cancer.

5.4.2. Statistical Analysis

Unfortunately, at the time this project was carried out, samples of diseased tissue were difficult to obtain and so only a small amount of material (either benign or malignant) was available for study. This resulted in insufficient data being available to carry out any reliable statistical analysis, and limited the numerical analysis to observing the percent of cases which showed significant expression (Table 5.3). Further studies using a greater number of cases would allow for more reliable and useful analysis, and could potentially highlight any heterogeneous relationship between different receptors and between receptor combinations and morphological subtypes. Information such as this could improve the understanding of disease progression and aggressiveness, thus improving the accuracy of prognoses.

CHAPTER SIX

Observing Small Molecule Inhibitor Efficacy using a Human EGFR/Rat HER2 Chimeric Receptor

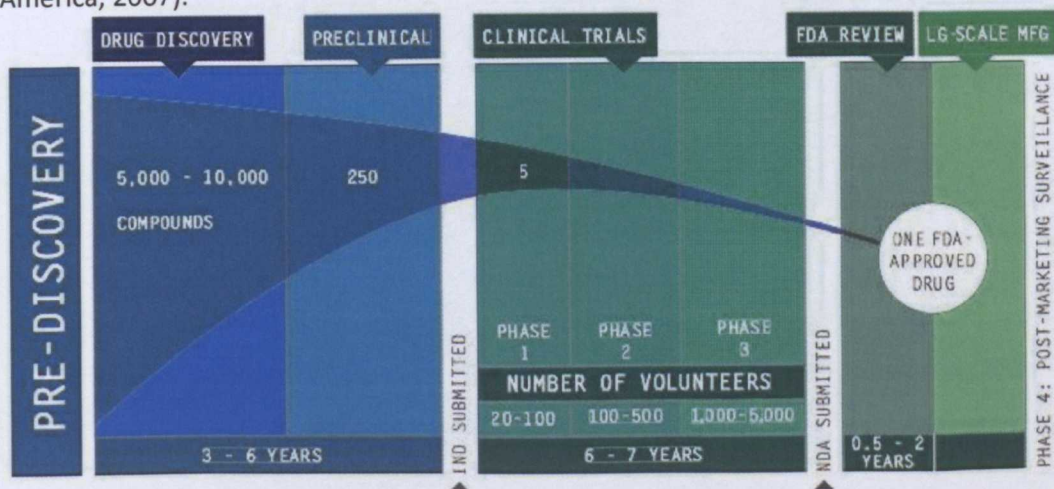
6.1. INTRODUCTION

6.1.1. Small Molecule Tyrosine Kinase Inhibitors and Drug Discovery

Recently, two SMTKIs have come to market specifically for use in dogs. These are Toleranib (Palladia) and Masitinib (Masivet) and both are aimed at treating canine mast cell tumours by targeting the split-kinase receptors involved in the angiogenesis of neoplasms (Pryer *et al.*, 2003; Hahn *et al.*, 2008). While this is an achievement, when the typical model of drug discovery is considered a somewhat different picture is painted.

The business model within the pharmaceutical industry is an unusual one (Figure 6.1): typically a company may begin with thousands of compounds following a drug discovery programme. Over the course of 10-15 years, these thousands of compounds go through various preclinical and clinical trials and are eventually narrowed down to one. This compound must then be approved by the national governing body before reaching the factory for large-scale production and distribution (with patients being monitored in Phase 4 Post-Marketing Surveillance).

Figure 6.1: Typical timeline of the evolution of a pharmaceutical compound, from pre-discovery to Phase 4 studies (Pharmaceutical Research and Manufacturers of America, 2007).



While this model has brought a number of successful drugs to the market, many thousands are removed from the development programme owing to factors such as unacceptable levels of adverse effects or insufficient target inhibition. In this thesis, I would propose that a number of these compounds could have some potential in a veterinary setting. The high degree of genetic similarity between humans and canines would indicate that these drugs could possibly serve a purpose in veterinary oncology – particularly when one considers that these drugs are often prescribed to animals in lower doses to minimise any adverse effects associated with them.

6.1.2. Using Human Small Molecule Tyrosine Kinase Inhibitors in Dogs

This chapter aims to determine if the drugs available for use in the laboratory were suitable inhibitors of HER2 phosphorylation. These tests were necessary as some drugs had been supplied to the laboratory several years earlier, and subsequently required testing to ensure they had not deteriorated to such an extent as to prevent inhibition of the HER2 kinase at reasonable dosages. Similarly, any drugs acquired more recently (either as gifts from Pfizer or purchased from laboratory suppliers) also required testing to determine their efficacy.

To accomplish this, the NEN-7 cell line was used (Pandiella *et al.*, 1989), which is composed of mouse fibroblasts which have been stably transfected to express a chimeric extracellular human EGFR/rat transmembrane and intracellular HER2 receptor (Figure 6.2).

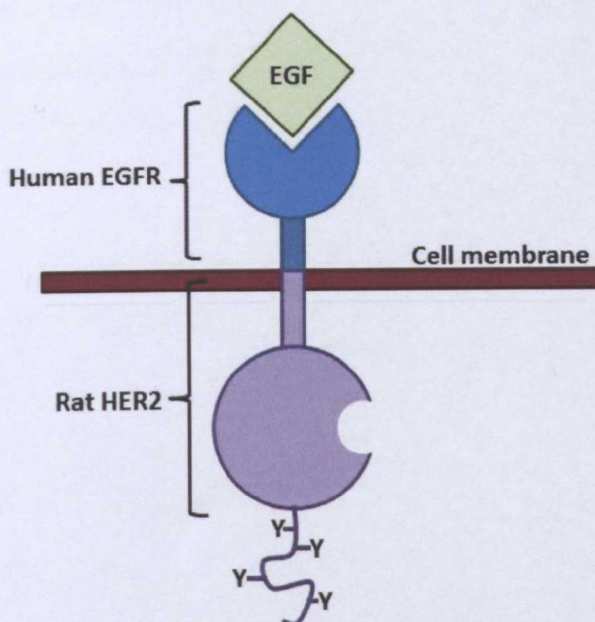


Figure 6.2: Cartoon depiction of the construct within the NEN-7 cell line. The chimera consists of extracellular human EGFR, and transmembrane and intracellular rat HER2.

This system allows for HER2 kinase activation to be strictly controlled by the addition of EGF to the cells, and also allows for a degree of specificity when observing the results (i.e. the effect on HER2 kinase can be reliably observed without concern that any detectable signal may have arisen from another receptor).

While this chimera is a useful tool in SMTKI investigations, an ideal system would consist of a chimera composed of human EGFR/dog HER2 receptor portions, as this would give an indication of both the suitability of the drugs (e.g. had they decayed whilst in storage) and if they were able to act directly on canine HER2 kinase. Attempts were made in this project to create such a chimera, however problems arose when attempting to amplify the full-length canine HER2 by PCR. Numerous adjustments and optimisation steps were made to the protocol in an attempt to amplify this canine HER2, but ultimately a decision was made to abandon these efforts in order to focus the limited time and resources on other aspects of the thesis which would also provide suitable data.

Some analysis, however, was carried out to determine the similarity of the rat portion of this chimera with its canine counterpart (Figure 6.3). In order to be sure that the rat and canine HER2 kinases were similar, Pfam analysis was performed on both species' protein sequence for HER2 to identify their kinase domains. The sequences for these domains were then extracted and compared by BLAST analysis. This showed that within the kinase domain, there were only two residues which differed between species, and that overall the sequences were 99% similar (figure 6.3a). One further analysis was performed to compare the human HER2 kinase domain with its canine equivalent. This was carried out as for the comparisons between rat and dog species, and it was found that in this instance four residues differed, with sequences being 98% similar overall (Figure 6.3b).

Figure 6.3: BLAST analysis of kinase domains (A) rat and dog and (B) human and dog HER2. Differing residues are highlighted with a red box, while the essential lysine residue of the catalytic site is highlighted with a blue box.

A: Rat (Query) vs dog (Sbjct)

Score = 522 bits (1344), Expect = 3e-153, Method: Compositional matrix adjust.
Identities = 252/254 (99%), Positives = 254/254 (100%), Gaps = 0/254 (0%)

```

Query 1   KVKVLGSGAFGTVYKGIWIPDGENVKI FVA[K]VLRRENTSPKANKEILDEAYVMAGVGSFY 60
Sbjct 1   KVKVLGSGAFGTVYKGIWIPDGENVKI FVA[K]VLRRENTSPKANKEILDEAYVMAGVGSFY 60

Query 61  VSRLLGICLTSTVQLVTQLMPYGCLLDHVREHRGRGRLGSQDLLNWCVQIAKGMSYLEDVRL 120
Sbjct 61  VSRLLGICLTSTVQLVTQLMPYGCLLDHVREHRGRGRLGSQDLLNWCVQIAKGMSYLEDVRL 120

Query 121 VHRDLAARNVVKSPNHVKITDFGLARLLDIDETEYHADGGKVPKWMAL[SE]LRRRFTH 180
Sbjct 121 VHRDLAARNVVKSPNHVKITDFGLARLLDIDETEYHADGGKVPKWMAL[SE]LRRRFTH 180

Query 181 QSDVWSYGVTVWELMTFGAKPYDGI PAREIPDLEKGERLPQPPICTIDVYMIMVKC[MI] 240
Sbjct 181 QSDVWSYGVTVWELMTFGAKPYDGI PAREIPDLEKGERLPQPPICTIDVYMIMVKC[MI] 240

Query 241 DSECRPRFREL[SE] 254
Sbjct 241 DSECRPRFREL[SE] 254

```

B: Human (Query) vs dog (Sbjct)

Score = 518 bits (1335), Expect = 4e-152, Method: Compositional matrix adjust.
Identities = 250/254 (98%), Positives = 254/254 (100%), Gaps = 0/254 (0%)

```

Query 1   KVKVLGSGAFGTVYKGIWIPDGENVKI FVA[K]VLRRENTSPKANKEILDEAYVMAGVGSFY 60
Sbjct 1   KVKVLGSGAFGTVYKGIWIPDGENVKI FVA[K]VLRRENTSPKANKEILDEAYVMAGVGSFY 60

Query 61  VSRLLGICLTSTVQLVTQLMPYGCLLDHVRE[HR]GRGRLGSQDLLNWC[Q]IAKGMSYLEDVRL 120
Sbjct 61  VSRLLGICLTSTVQLVTQLMPYGCLLDHVRE[HR]GRGRLGSQDLLNWC[Q]IAKGMSYLEDVRL 120

Query 121 VHRDLAARNVVKSPNHVKITDFGLARLLDIDETEYHADGGKVPKWMAL[SE]LRRRFTH 180
Sbjct 121 VHRDLAARNVVKSPNHVKITDFGLARLLDIDETEYHADGGKVPKWMAL[SE]LRRRFTH 180

Query 181 QSDVWSYGVTVWELMTFGAKPYDGI PAREIPDLEKGERLPQPPICTIDVYMIMVKC[MI] 240
Sbjct 181 QSDVWSYGVTVWELMTFGAKPYDGI PAREIPDLEKGERLPQPPICTIDVYMIMVKC[MI] 240

Query 241 DSECRPRFREL[SE] 254
Sbjct 241 DSECRPRFREL[SE] 254

```

Owing to these small differences (most of the differing residues were replaced with those with relatively similar structures and polarities) it was reasonably assumed that the rat portion of the chimera would be a suitable model for the experiments at hand. However, between the human and canine comparisons, there was one difference which could have caused problems: an asparagine (which possesses a polar, uncharged sidechain) was replaced with a histidine (which possesses a positively charged sidechain) at residue 93 of the alignment (residue 813 of full-length human HER2). While this would appear to be a significant change which may alter the structure of the canine HER2 kinase, this histidine also exists in the rat sequence, and experiments carried out in this chapter showed that this

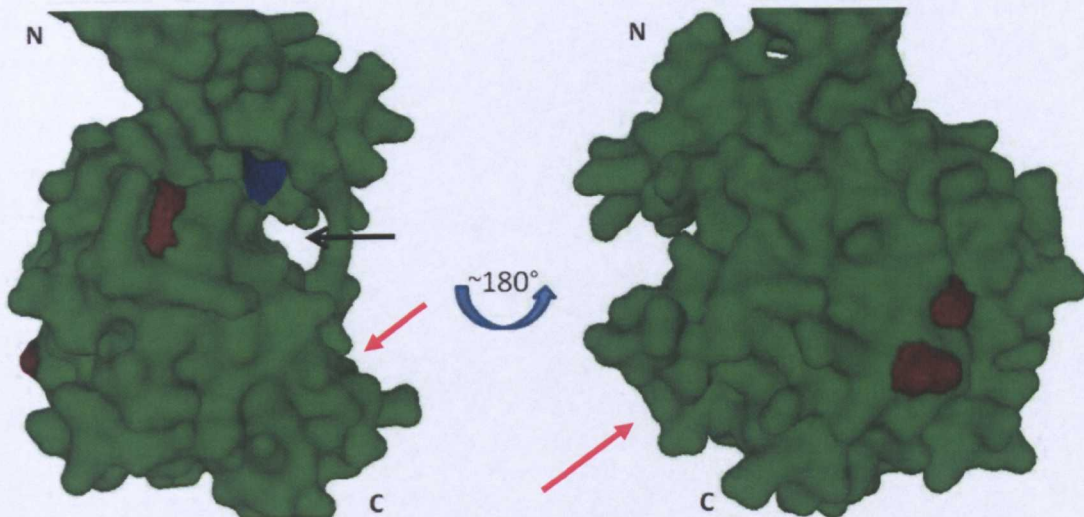


Figure 6.4: 3D mapping of substituted residues in intracellular canine HER2. The 3D protein shown here is a predicted structure of what canine HER2 would look like, as developed by I-TASSER. The catalytic pocket of the HER2 kinase is indicated with a black arrow. The residue highlighted in blue represents the essential lysine involved in receptor activity, which is conserved between human and canine species. Residues which differ between the canine and human protein (highlighted in more detail in Figure 6.3b) are highlighted in red, with the location of one substituted residue that is not clearly visible in these orientations indicated by a red arrow. It can be observed that none of these differences are within particularly close proximity to the catalytic pocket where many TKIs are predicted to bind.

had no observable effect on inhibitor binding to the protein. To further study what effect these changes could possibly have on any catalytic activity, a predicted structure of canine HER2 was developed using the I-TASSER (Iterative Threading ASSEmbly Refinement) server (Fabian *et al.*, 2005; Weigelt *et al.*, 2005; Minami *et al.*, 2007). The I-TASSER server allotted this model a score of 0.85 (where models are scored between -2 and 5, with higher numbers denoting higher levels of confidence), and using this it was possible to visualise the locations of the proteins substituted between canine and human species (Figure 6.4).

Results showed that the residues substituted were not particularly close to the catalytic pocket of the HER2 kinase domain (in fact, two were on the opposing side of the protein, while a third bordered the catalytic pocket and a fourth [not directly visible in Figure 6.4] was on the bottom-most surface of the protein, near the C-terminus), and were unlikely to pose a problem with regard to any TKI binding sites.

6.2. AIMS

1. To determine if the SMTKIs available for testing were suitable for use in this thesis and had not undergone any kind of degradation whilst in storage.
2. To determine the potencies of these SMTKIs.
3. To identify which SMTKIs were most suitable to take forward into experiments using canine mammary cancer cells.

6.3. RESULTS

6.3.1. Detecting Chimeric Receptor Phosphorylation in the NEN-7 Cell Line

In order to first determine if the NEN-7 cell line was suitable for observing the effect of SMTKIs on receptor phosphorylation, experiments were performed to determine what concentration of EGF was required to stimulate significant observable phosphorylation (Figure 6.5).

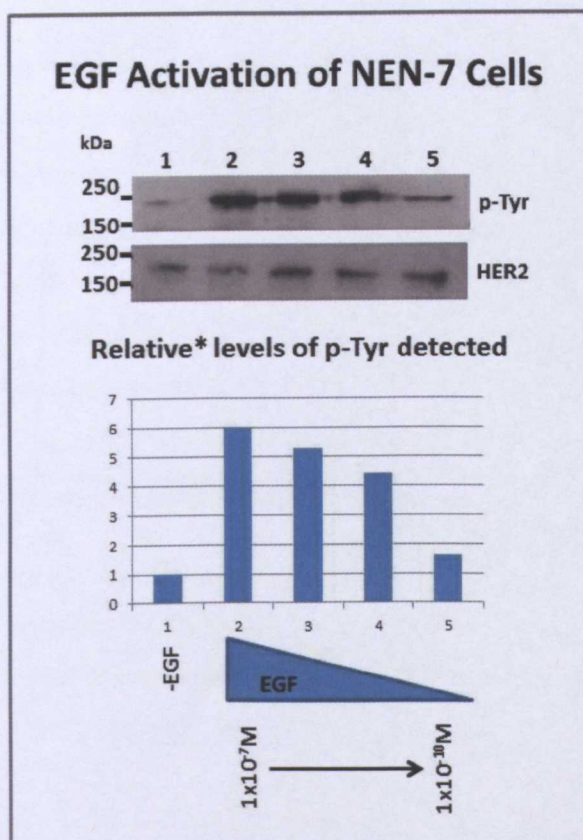


Figure 6.5: NEN-7 cells were stimulated with four different final concentrations of EGF: $1 \times 10^{-7} \text{M}$, $1 \times 10^{-8} \text{M}$, $1 \times 10^{-9} \text{M}$ and $1 \times 10^{-10} \text{M}$. Stimulation lasted for 5 minutes in each case.

Band densities were analysed using Image J Software, and the resulting values used to calculate band intensities *relative to the negative (unstimulated) control. These values were plotted on a histogram.

Lanes are, 1: Unstimulated (-EGF) control; 2-5: cells stimulated in varying final concentrations of EGF.

Results showed that there was an observable concentration dependent effect when adding varying concentrations of EGF to the cells. A final concentration of $1 \times 10^{-7} \text{M}$ was found to be suitable for future experiments, as this produced the strongest band upon blotting, which would provide a reliable signal for phosphorylation detection.

6.3.2. Determining the Suitability of SMTKIs

Results of NEN-7 blots with the available SMTKIs are shown in Figures 6.6a-g. It was observed that the SMTKIs applied to the cells caused a decrease in the amount of phosphorylation at the receptor's cytoplasmic domain, measured by probing the cell lysates for the presence of phosphotyrosine (p-Tyr). In each case, the amount of noticeable activation decreased with decreasing concentration of drug, suggesting there was a concentration dependent effect.

Figures 6.6 a-g (on following pages): Blots and histograms from NEN-7 cells treated with the available SMTKIs. In each case, the blots probed for phosphotyrosine (p-Tyr) were analyzed using Image J software, to determine the optical density of the bands observed. The data derived from this analysis was used to calculate the intensities observed relative to the positive activation controls (lane 3 on each blot), with the resulting values plotted as a histogram. Lanes are, 1: Unstimulated (-EGF), untreated control; 2: Stimulated (+EGF) control in the presence of drug vehicle (+DMSO*); 3: stimulated (+EGF), untreated cells; 4-7: Stimulated cells (+EGF), in the presence of varying concentrations of SMTKI (concentrations are: $1 \times 10^{-6} \text{M}$, $1 \times 10^{-7} \text{M}$, $1 \times 10^{-8} \text{M}$ and $1 \times 10^{-9} \text{M}$). In the case of stimulated cells, $1 \times 10^{-7} \text{M}$ EGF was applied to the cells. In the unstimulated control, this was substituted with an equal volume of 1x PBS.

*DMSO is required to solubilise the TKIs being tested here. While this is an effective means of delivering the drugs to the cells, drug vehicles can have non-specific toxic effects. The vehicle control is applied to ensure that any significant inhibition observed is not caused by this non-specific event.

*Phosphotyrosine levels were calculated relative to the untreated positive controls (Lane 3).

Figure 6.6b

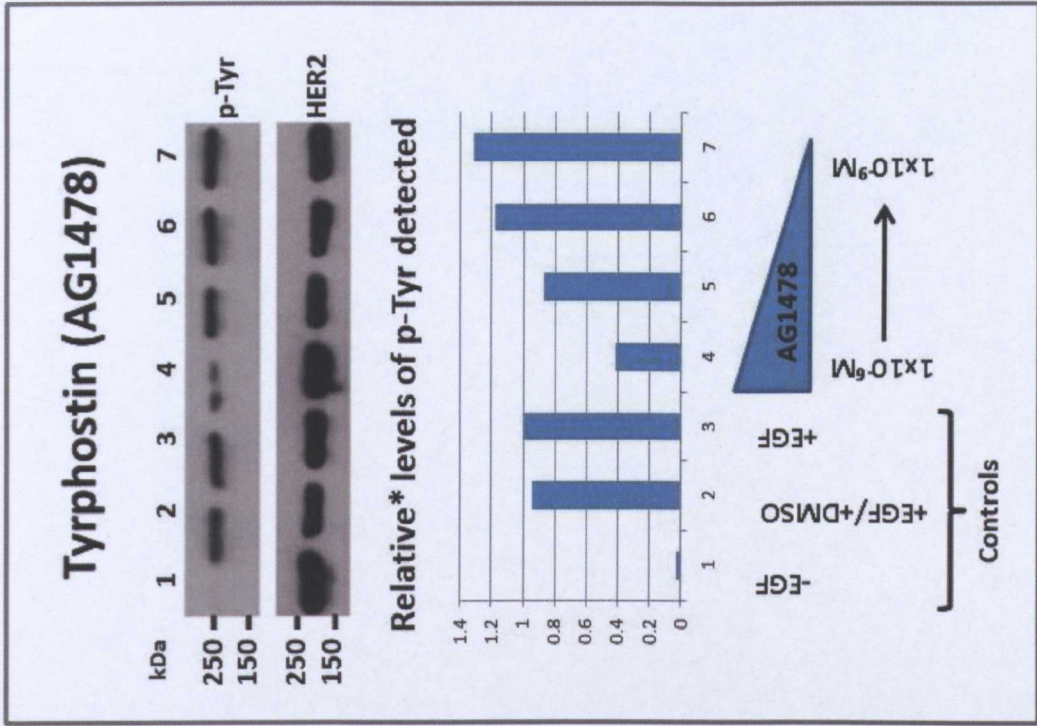
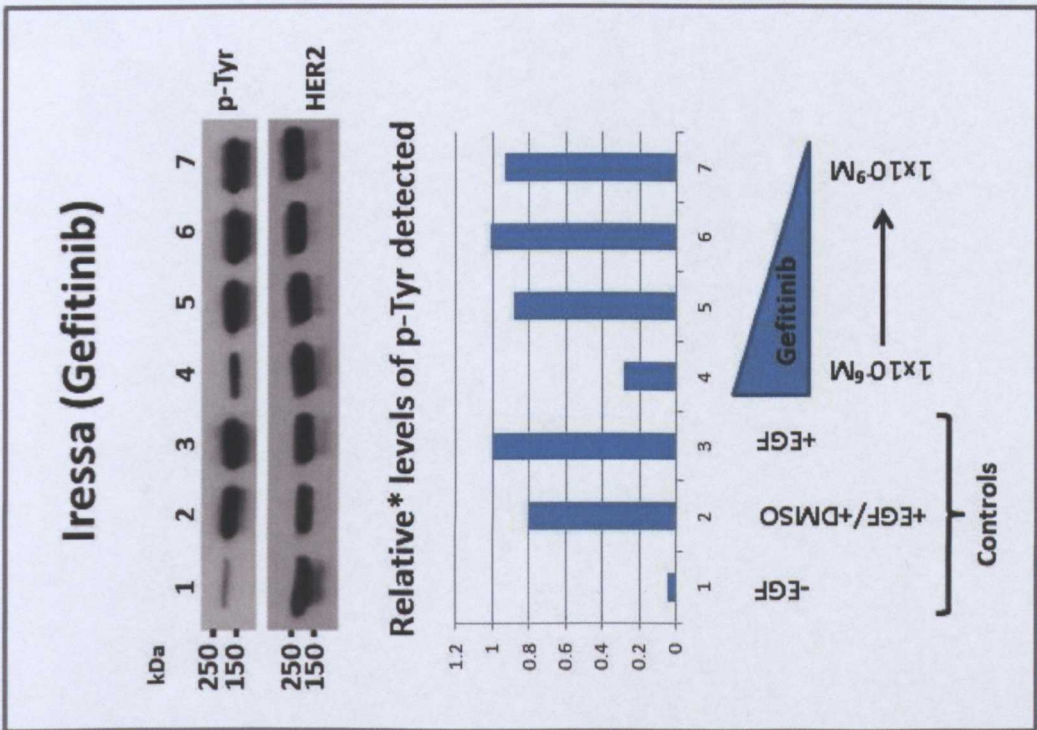


Figure 6.6a



*Phosphotyrosine levels were calculated relative to the untreated positive controls (Lane 3).

Figure 6.6d

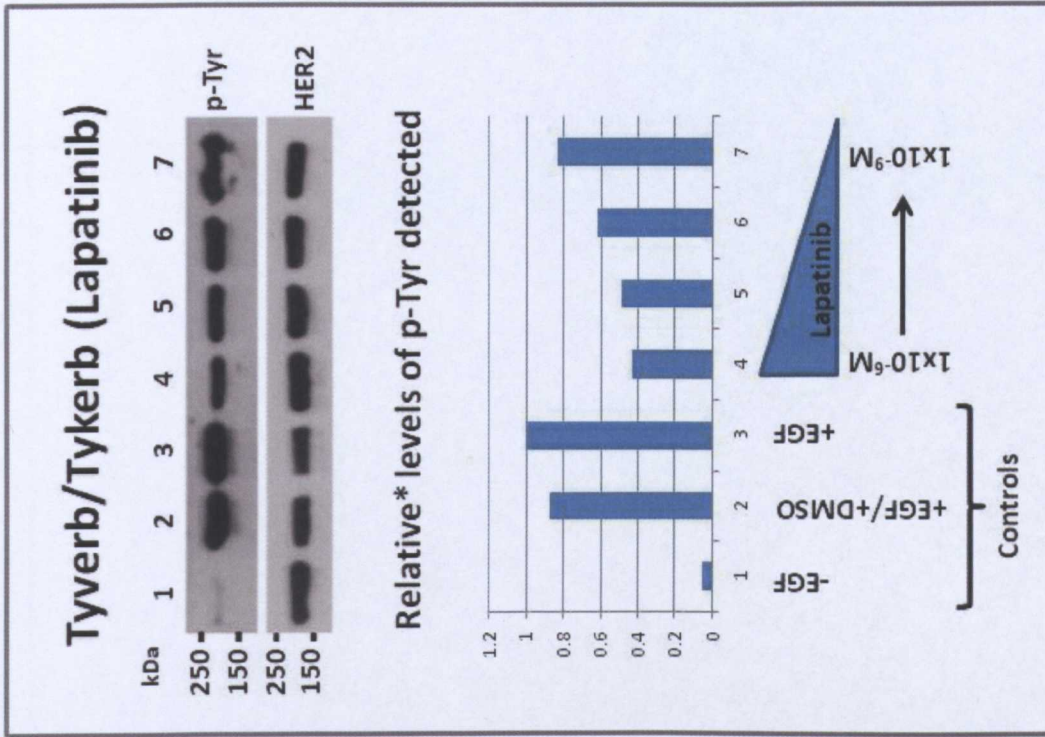
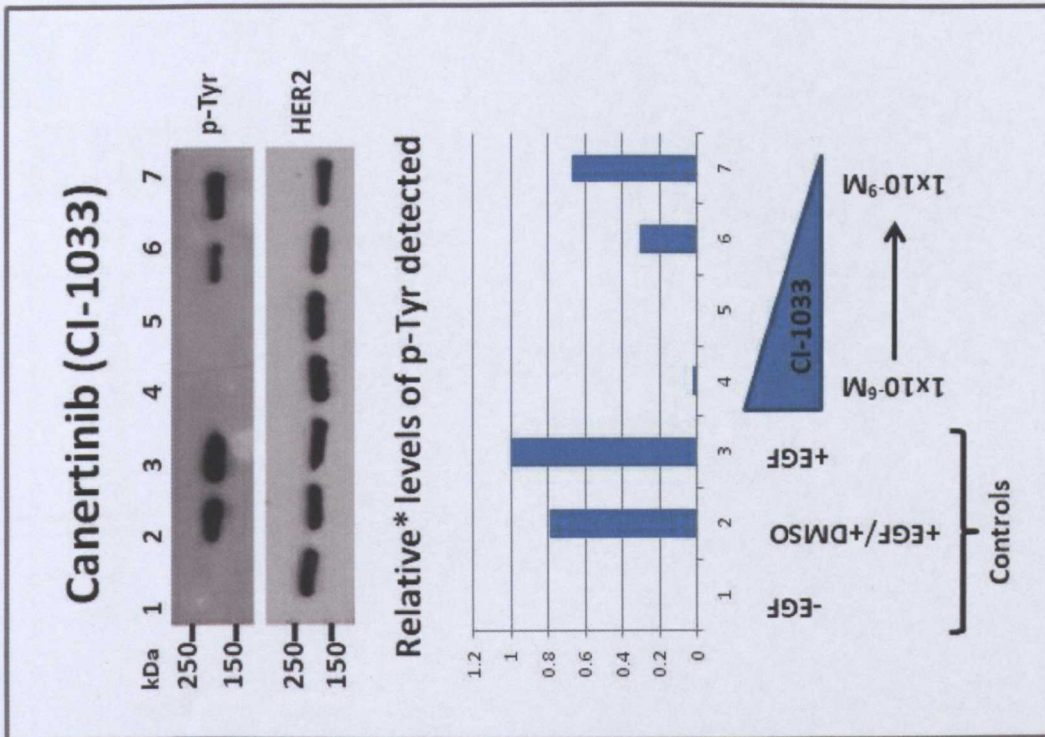


Figure 6.6c



*Phosphotyrosine levels were calculated relative to the untreated positive controls (Lane 3).

Figure 6.6f

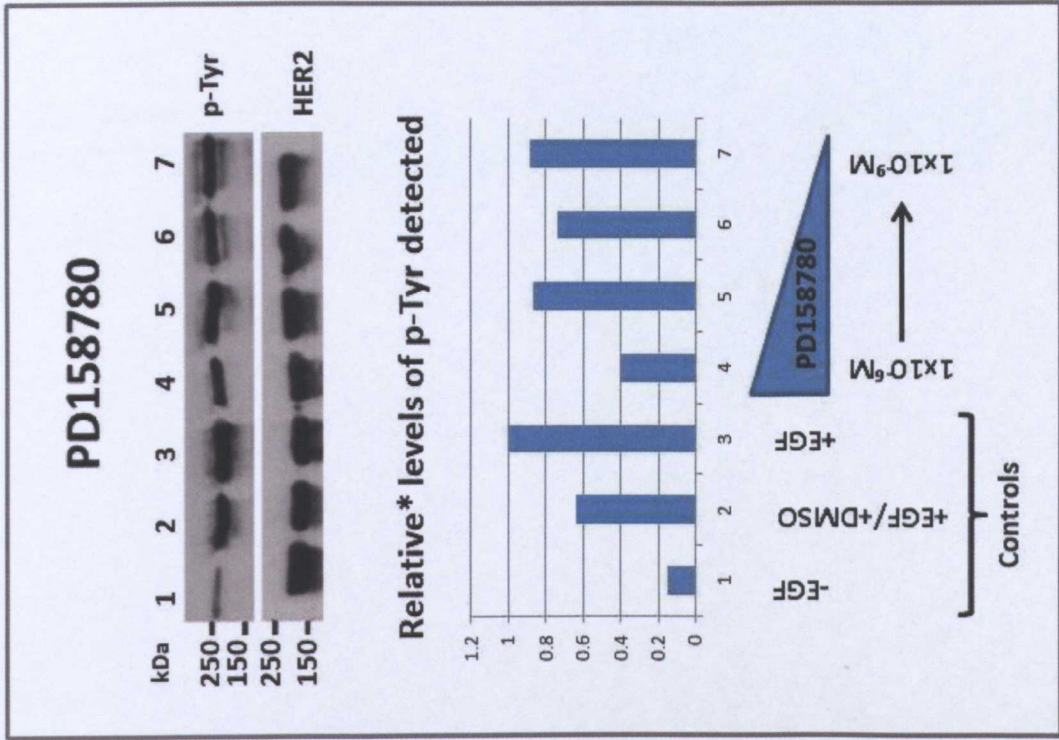
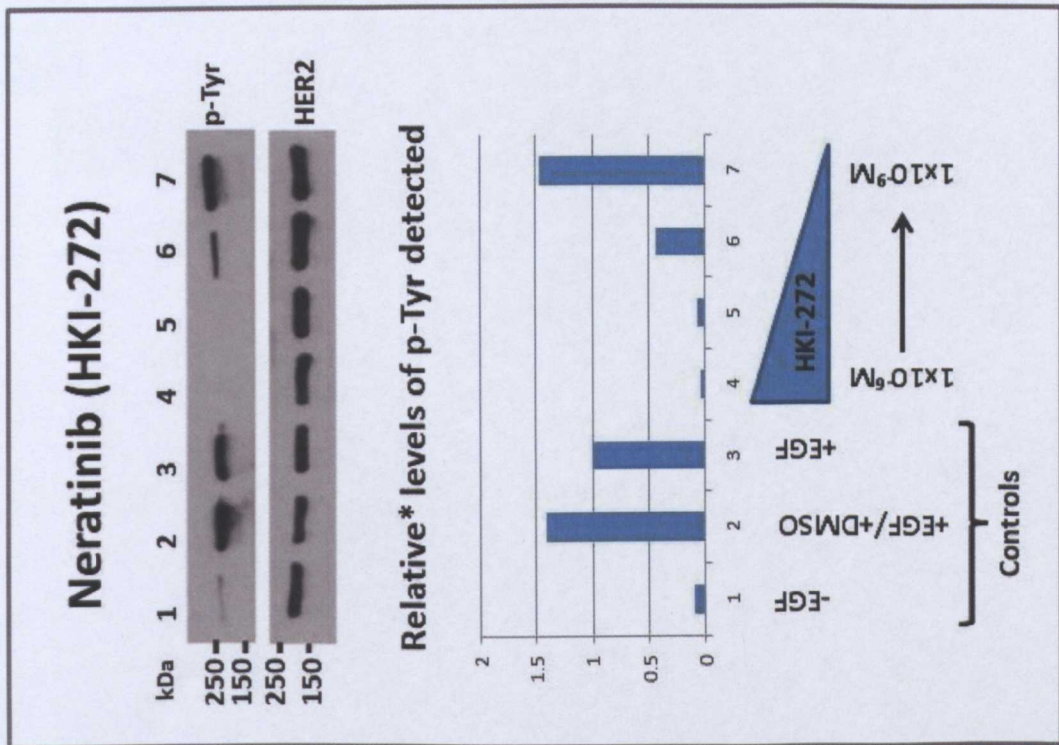
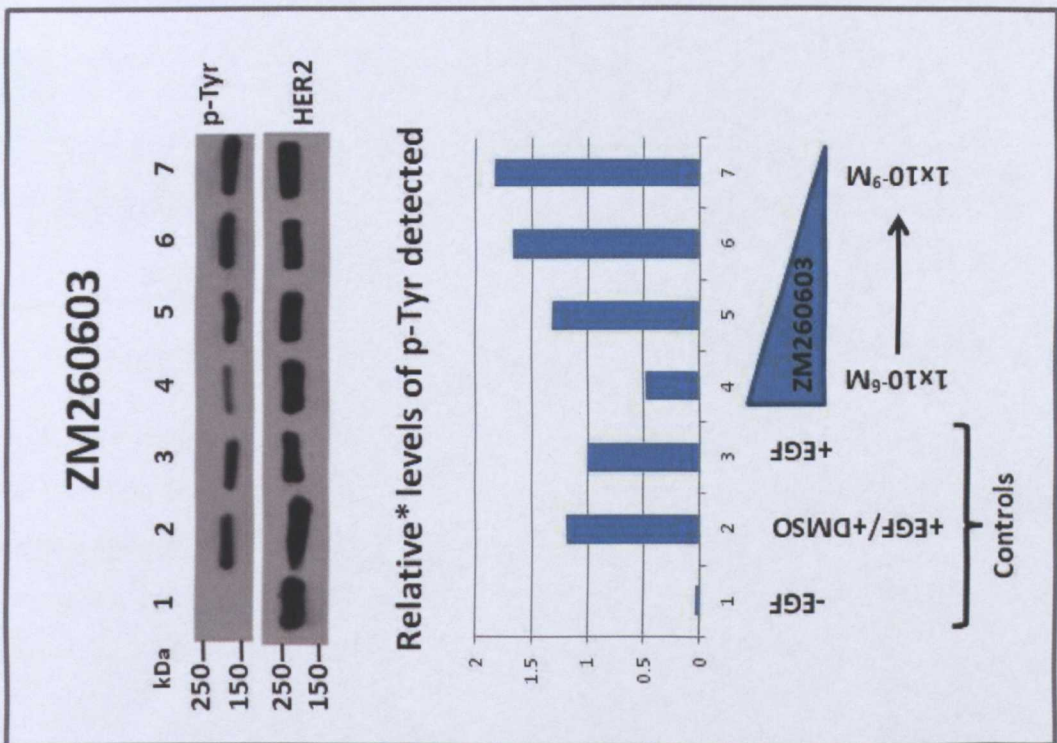


Figure 6.6e



*Phosphotyrosine levels were calculated relative to the untreated positive controls (Lane 3).

Figure 6.6g



6.3.3. Determining Relative Potencies of the Observed SMTKIs

Having carried out Western Blots to observe phosphorylation inhibition it was then possible to determine the concentrations at which 50% of inhibition occurs using the histograms presented in Figures 6.5a-g. The data for the positive control lanes (Lane 3 in each histogram) was compared to the data for the cells treated with SMTKIs (Lanes 4-7). The drug treatment lane which showed at least a 50% decrease in band intensity from the positive control was recorded in Table 6.1. From these results, it was possible to identify the most potent drugs as Lapatinib, Neratinib and Canertinib.

Drug	Concentration at which at least 50% inhibition of phosphorylation activity is observed
Canertinib (CI-1033)	$1 \times 10^{-8} \text{M}$
Iressa	$1 \times 10^{-6} \text{M}$
Lapatinib	$1 \times 10^{-7} \text{M}$
Neratinib (HKI-272)	$1 \times 10^{-8} \text{M}$
PD158780	$1 \times 10^{-6} \text{M}$
Tyrphostin (AG1478)	$1 \times 10^{-6} \text{M}$
ZM260603	$1 \times 10^{-6} \text{M}$

Despite its potency, Canertinib was not selected to take forward into cell proliferation experiments owing to its lack of specificity: it is a pan-ErbB inhibitor, while Lapatinib and Neratinib are highly specific for EGFR and HER2.

6.4. DISCUSSION

Overall, these experiments showed that all of the drugs tested here were suitable inhibitors of HER2 kinase at reasonable doses of at least $1 \times 10^{-6} \text{M}$, and could potentially be carried through into tests making use of canine mammary cancer cells (Chapter 7 in this thesis). There were some differences between the potencies of these drugs however, which can be explained by a number of factors including the nature of inhibitor binding.

6.4.1. Reversible versus Irreversible Inhibitors

One inhibitor proved to be much more efficient at inhibiting phosphorylation than any others: this was Neratinib, which was able to inhibit 50% of receptor phosphorylation at a concentration of $1 \times 10^{-8} \text{M}$ (with concentrations of $1 \times 10^{-6} \text{M}$ and $1 \times 10^{-7} \text{M}$ completely inhibiting phosphorylation), while most other inhibitors required the highest concentration of $1 \times 10^{-6} \text{M}$. This could in part be explained by the method with which the drug binds to its target. Neratinib is an irreversible inhibitor of EGFR and HER2, and this could cause it to have a more prolonged effect on the receptors than other reversible inhibitors. Similar results were observed with Canertinib – also an irreversible inhibitor – which showed 50% inhibition at a concentration of $1 \times 10^{-8} \text{M}$.

6.4.2. Pharmacokinetics versus Pharmacodynamics

One limitation of this portion of the study is that the activities of these drugs are only being observed in a closed, cell culture system. While this is beneficial in that it allows for a direct observation of inhibitor activity against target receptors (that is, the pharmacodynamics of the drugs), it does not give any indication of what effect a patient has on the drug in its system (the pharmacokinetics). Pharmacokinetic observations would allow for data to be gathered regarding any metabolic conversions that a drug may undergo, what the clearance rate of the drug is, along with any observable toxicities or off-target effects which may occur.

Such observations are particularly relevant when considering drugs such as Tamoxifen, a small molecule drug which blocks the action of estrogen in the treatment of breast cancers. Tamoxifen is technically a pro-drug, which undergoes a metabolic conversion by cytochrome P450 enzymes (specifically isoforms CYP2D6 and CYP3A4) into active metabolites 4-hydroxytamoxifen (Afimoxifene) and N-desmethyl-4-hydroxytamoxifen (Endoxifen) (Desta *et al.*, 2004) which have greatly increased activities (30 to 100-fold) against estrogen receptors compared to Tamoxifen itself (Borgna & Rochefort, 1981; Coezy *et al.*, 1982; Jordan, 1982; Robertson *et al.*, 1982). While this situation provides an obvious benefit to the patient, there always exists the possibility that such conversions could have unanticipated adverse effects that would not necessarily be accounted for when simply observing a drug itself.



Given that these drugs were designed for use in humans, little is known about how the canine metabolism would react to these compounds. However, the advent of inhibitors such as Palladia and Masivet shows that dogs do have the ability to respond to and metabolise small molecule drugs in a similar fashion to humans (utilizing hepatic enzymes such as P450) and to excrete the remaining metabolites successfully (Yancey *et al.*, 2010). This would lend confidence to the theory that human inhibitors may also be suitable in dogs (provided allowances were made for suitable dosage adjustments).

6.4.3. Taking SMTKIs into Tests with Canine Mammary Cancer Cells

Previous work carried out by another group (Fabian *et al.*, 2005) had determined the receptor targets against which a number of small molecule drugs were active (Figure 6.7). While many of these compounds had not been tested in the experiments described in this chapter, Lapatinib (GW-2016 in Figure 6.7) had.

These experiments showed that unlike many of the other drugs tested, Lapatinib had a very specific set of receptors against which it was active. These were EGFR and HER2 (both members of the EGF receptor family) and, importantly, only showed one relatively weak off-target effect against a creatine kinase. This specificity was important when considering what drugs to use against canine cells. While the CMT28 (canine mammary cancer) cells had undergone testing to determine their receptor profile with regard to the EGF receptor family, there was insufficient time to explore the presence of other receptors that they may have expressed. In order to determine if any drugs applied to the cells were affecting only the receptor system being studied in this thesis, it was important to select drugs which had high degrees of specificity. In addition to Lapatinib, the drug Neratinib was also selected for use with canine mammary cells. Similarly to Lapatinib, Neratinib had showed high specificity against HER2 and EGFR (Rabindran *et al.*, 2004) and so was considered a suitable drug to take forward in this study. While both these drugs showed similar specificities, they did differ in their binding: Lapatinib binds reversibly (Rusnak *et al.*, 2001) to its targets, while Neratinib binds irreversibly (Rabindran *et al.*, 2004). This difference would allow for an opportunity to observe any differences that mode of action may have on cell proliferation.

The next step in utilizing these drugs was to determine the receptor profile of the canine mammary cancer cell line, in order to determine if these therapies would have relevant targets upon which they could act.



Figure 6.7: The specificity profiles of 20 separate SMTKIs against the kinome taken from (Fabian *et al.*, 2005). Each red dot shows where the drug has been documented as having an effect, with larger dots representing a greater degree of off-target binding.

Studies showed that while many drugs showed activity against receptors other than their targets, Lapatinib (here, GW-2016) showed strong specificity, with there being only one off-target receptor to which it bound.

CHAPTER SEVEN

Characterising the CMT28 Cell Line and Determining the Role HER2 Plays in the Growth of Canine Mammary Cancer

7.1. INTRODUCTION

HER2 has long been known in human cancers as being a key player in the growth of carcinomas: the receptor is overexpressed in roughly 15%-20% of human breast cancers (Venter *et al.*, 1987), and has become a popular target for many current and emerging small molecule and antibody therapies. While comparatively little research has been carried out into the role of this receptor in a case of canine cancer, some evidence has been published suggesting it can be overexpressed in canine disease (Ahern *et al.*, 1996; Rungsipipat *et al.*, 1999; Martín de las Mulas *et al.*, 2003; Dutra *et al.*, 2004; Hsu *et al.*, 2009). These studies on HER2 in dogs, combined with the already well-established precedent in human disease, suggested that it was reasonable to explore this expression further. Chapters Four and Five of this thesis have already addressed this issue through immunohistochemical staining on normal tissues and benign and malignant canine mammary cancers, and the results found were in concordance with previously published literature. This chapter aims to explore the functional role of HER2 in canine mammary cancer through a cell culture model.

Cell culture is a well-established tool in biological research, which provides researchers with many different human, animal and insect cell lines that can be applied to many aspects of research. One area where cultured cells are highly valued is in drug discovery and development, where *in vitro* tests provide the basis of the evidence which will allow potential new therapies to progress into tests with animals or humans. For many years, a number of cell lines of human origin have been widely used in studies investigating cancer and the role that drugs play in fighting cancerous growth and other diseases. Such cell lines include SKBR3 cells (human breast cancer cell line which expresses high levels of HER2), A431 cells (cells from a vulval cancer, which express high levels of EGFR), 293-T cells (embryonic human kidney cells), and HeLa cells (the first human cells to be isolated and

successfully grown in culture – from a cervical cancer) to name but a few. Cell lines now exist from many different species, including dog. A search of the American Type Culture Collection (ATCC, <http://www.lgcstandards-atcc.org/>) of Cell Lines and Hybridomas for cell lines derived from *Canis familiaris* returns a total of 23 cell lines, many of which are derived from osteosarcomas, kidney or thymus. At the outset of this project, no canine mammary cell lines could be procured from any cell culture collection (although 5 now exist within the ATCC). This required that we identify cell culture resources from other groups.

A group from Auburn University in Alabama had isolated and cultured cells from a canine mammary tumour (named the CMT28 cell line) which reportedly expressed HER2 at levels 14.5 times higher than in a reference fibroblast cell line (Ahern *et al.*, 1996) as determined by dot-blot analysis. However this only demonstrated the presence of HER2 at the mRNA level, and there was no available information regarding the presence of any other members of the EGF receptor family at the protein level. It was important that this information be established prior to applying drugs to this cell line, as this project is primarily concerned with the role that HER2 (and, to a lesser extent, the receptors with which it forms dimers) plays in canine mammary cancer. With this information it is possible to investigate the possibility of utilizing human SMTKIs in veterinary oncology.

With this in mind, this chapter describes determining the receptor status of this cell line through Western Blotting and PCR, and also examines what role HER2 plays in the growth of these cells.

7.2. AIMS

1. To determine the complete EGF family receptor profile of the CMT28 cell line by Western Blotting and PCR.
2. To use this information (together with data obtained in Chapter Six) to choose SMTKIs to take forward into experiments with the CMT28 cells.
3. To determine to what extent HER2 is involved with the growth of canine mammary cancers through studies with:
 - a. Small molecule drugs
 - b. Herceptin
 - c. siRNA technology

7.3. RESULTS

7.3.1. Determining CMT28 Receptor Status by PCR

As no normal canine mammary cancer cell line could be procured at the time of this study, the MDCK cell line was used instead. This is a normal canine kidney cell line which has been studied in the past, and for which there was some literature available (Gaush *et al.*, 1966) for comparison of the results obtained here, which allowed for MDCK cells to be used as an experimental control.

PCR was carried out with primers described in Chapter Two (Materials and Methods). The Results showed that the MDCK cells appeared to express all receptors except HER4 (Figure 7.1a), while the CMT28 cell line expressed all four receptors (Figure 7.1b). It was noticed during the course of carrying out the PCR to amplify HER4 that 3 separate bands appeared in addition to the band of the expected size. Upon further scrutiny of the primer designs for this amplification, it was noticed that the primers spanned a splice site, which could explain these extra bands. HER4 is also known to exist (in humans) as four separate isoforms which are encoded by a number of different splice variants.

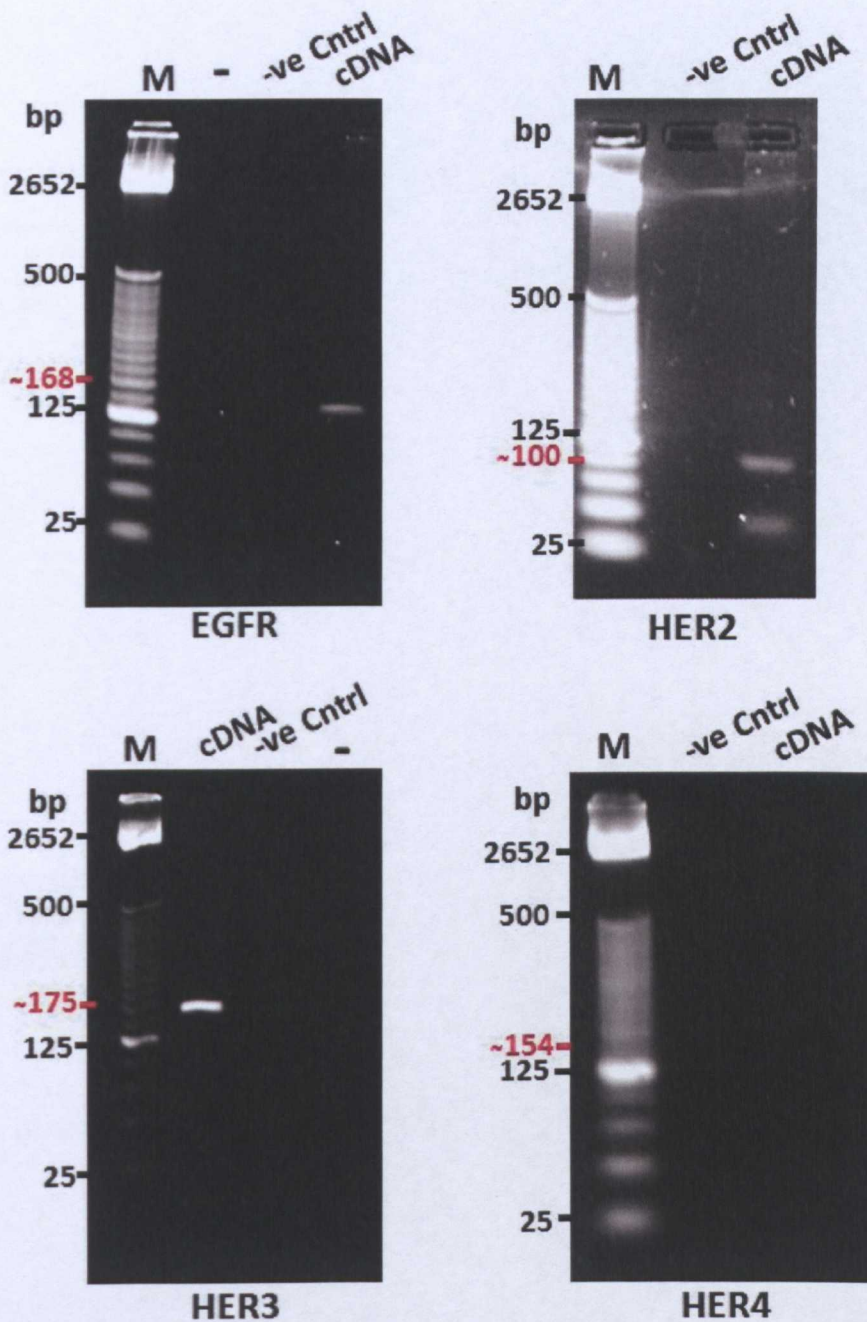


Figure 7.1a: PCR experiments to survey the expression of the members of the EGF receptor family in MDCK cells. Results showed that these cells expressed all members of the family with the exception of HER4. The reader should note that the PCRs for EGFR and HER2 were enhanced in PowerPoint (+40% brightness and +40% contrast) as the bands were difficult to see after printing.

Key: numbers in red indicate the expected size of the product; “-” denotes a lane left intentionally empty (typically to avoid possible contamination between lanes); “-ve Cntrl” denotes lanes in which the PCR was carried out without a cDNA template; “cDNA” denotes lanes in which cDNA was added to the PCR mix.

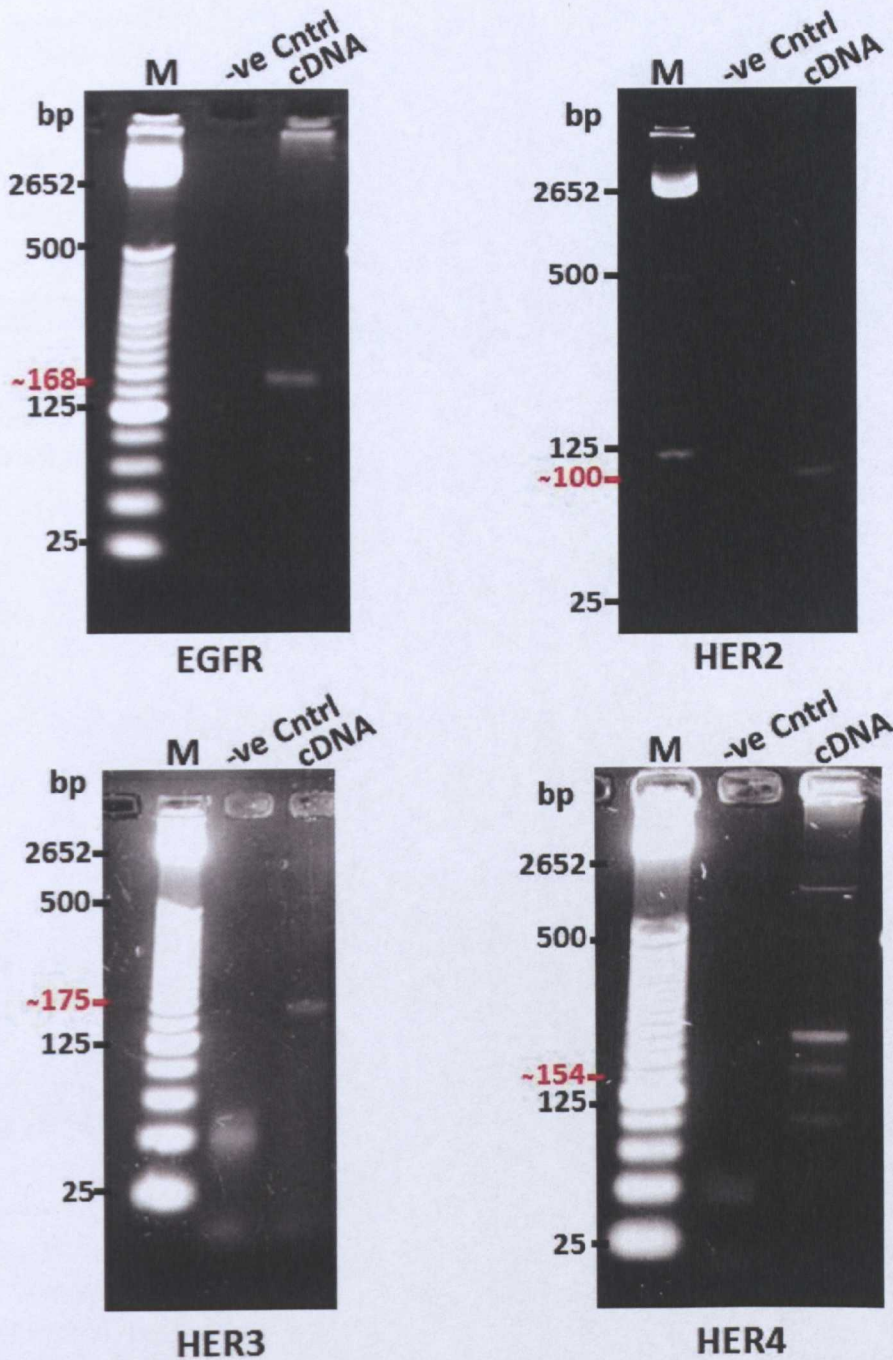


Figure 7.1b: PCR experiments to survey the expression of the members of the EGF receptor family in CMT28 cells. Results showed that these cells expressed all members of the family. Noticeably, the PCR for HER4 showed 4 distinct bands where only one was expected. The reader should note that the PCRs for HER3 and HER4 were enhanced in PowerPoint (+40% brightness and +40% contrast) as the bands were difficult to see after printing.

Key: numbers in red indicate the expected size of the product; “-” denotes a lane left intentionally empty (typically to avoid possible contamination between lanes); “-ve Cntrl” denotes lanes in which the PCR was carried out without a cDNA template; “cDNA” denotes lanes in which cDNA was added to the PCR mix.

7.3.2. Determining CMT28 Receptor Status by Western Blotting

Western Blots were able to detect HER2 and EGFR (although the signal for the latter was very weak, the PCR gave a strong result) (Figure 7.2). Problems arose when attempting to blot for HER3. Multiple bands appeared on the blots, even when probing lysates from cells which did not contain HER3. Many attempts were made to optimize the experiments to eradicate these problems (different blocking conditions, the use of specific protease inhibitors) however a reliable blot could not be produced in the time available.

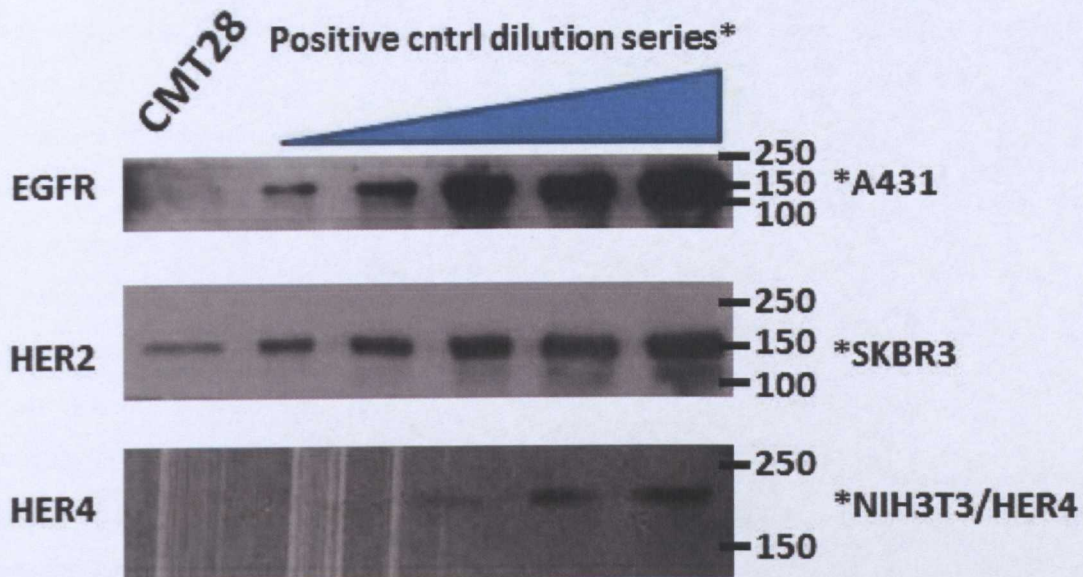


Figure 7.2: Western blots comparing lysate from CMT28 cells with lysates from positive control cell lines (for EGFR: A431 cells; for HER2 SKBR3 cells; for HER4: NIH3T3/HER4 cells). Results showed that CMT28 cells expressed HER2 in greatest abundance, along with some low levels of EGFR. Blots did not show any evidence of HER4 expression. Blots to check for the presence of HER3 were unsuccessful (data shown in appendix).

Note: In order to better emphasise the weak band seen when blotting for EGFR, the contrast levels of this blot were increased in Microsoft PowerPoint to 40%. Similarly, the brightness and contrast levels of the HER4 blot were increased to 20% and 40% respectively.

Using the blot to detect HER2, it was possible to estimate the number of HER2 receptors CMT28 cells have using Image J analysis (data not shown). It is known that SKBR3 cells have roughly 2×10^6 HER2 receptors per cell (Aguilar *et al.*, 1999). By comparing the intensity of the SKBR3 band with the CMT28 band, it can be estimated that CMT28 cells have in the order of 2×10^5 per cell – ten times fewer than SKBR3s. While this is obviously not as ideal a cell line for use as the SKBR3 cell line is, it must be remembered that the SKBR3 cell line is one human breast cancer cell line out of a very many, and that of those very many only two

(SKBR3 and BT474) are known to express very high levels of HER2. In the case of canine cell lines, a great deal fewer are available than there are in humans, and so it would be unlikely to find a cell which expresses HER2 at equally high levels.

7.3.3. Using Herceptin in Canine Mammary Cancer

Owing to the high sequence similarities observed between human and canine species, it is not unreasonable to assume that monoclonal antibody therapies may be useful in treating canine malignancies. Thus, along with observing the effects of small molecule drugs, the well-established antibody therapy Herceptin was also tested. Using an antibody directed against the C-terminal end of the HER2 receptor (20N) (Gullick *et al.*, 1987) it was possible to detect the presence of the receptor in both the human and canine cells. However attempts to apply an antibody targeted against a human extracellular epitope (N24) were less successful. While it was still possible to clearly detect the signal in the human cells, no signal could be detected with the canine cells. Similar results occurred when Herceptin was applied to each set of cells, with human cells giving a clear signal but canine cells giving none (Figure 7.3a). This indicated that Herceptin was unable to bind to the canine HER2 receptor. Given the high degree of similarity between the human and canine HER2 sequences, this inability of Herceptin to bind to the canine protein was unexpected and possible explanations for it were sought.

Previous work by another group (Cho *et al.*, 2003) had identified three particular loops within the structure of human HER2 which bound to Herceptin (Figure 7.3b). Using these results, it was possible to identify the residues involved in Herceptin/HER2 binding, and compare these between the two species (Table 7.1). These comparisons showed that while the residues in loop 2 were identical, there were some differences in loop 1 (a proline substituted for a serine) and loop 3 (a phenylalanine substituted for an alanine, and an alanine substituted for a threonine). While these differences may appear subtle, they could confer structural changes that could prevent Herceptin binding to the canine protein. In loop 1 for example, the amino acid proline is well-known for its conformational rigidity compared to other amino acids and its substitution to a serine may have an effect on the structure of the protein around it. Similarly in loop 3, the phenylalanine (substituted for an alanine) contains a benzene ring, which makes its structure considerably larger than its substitute, and further in this loop the alanine in the human structure is classed as having a

hydrophobic side chain, while its replacement (threonine) has a polar uncharged side chain. These differences may add up and alter the structure of canine HER2 in ways that could bring about steric hindrance, thus preventing the antibody from binding to the target.

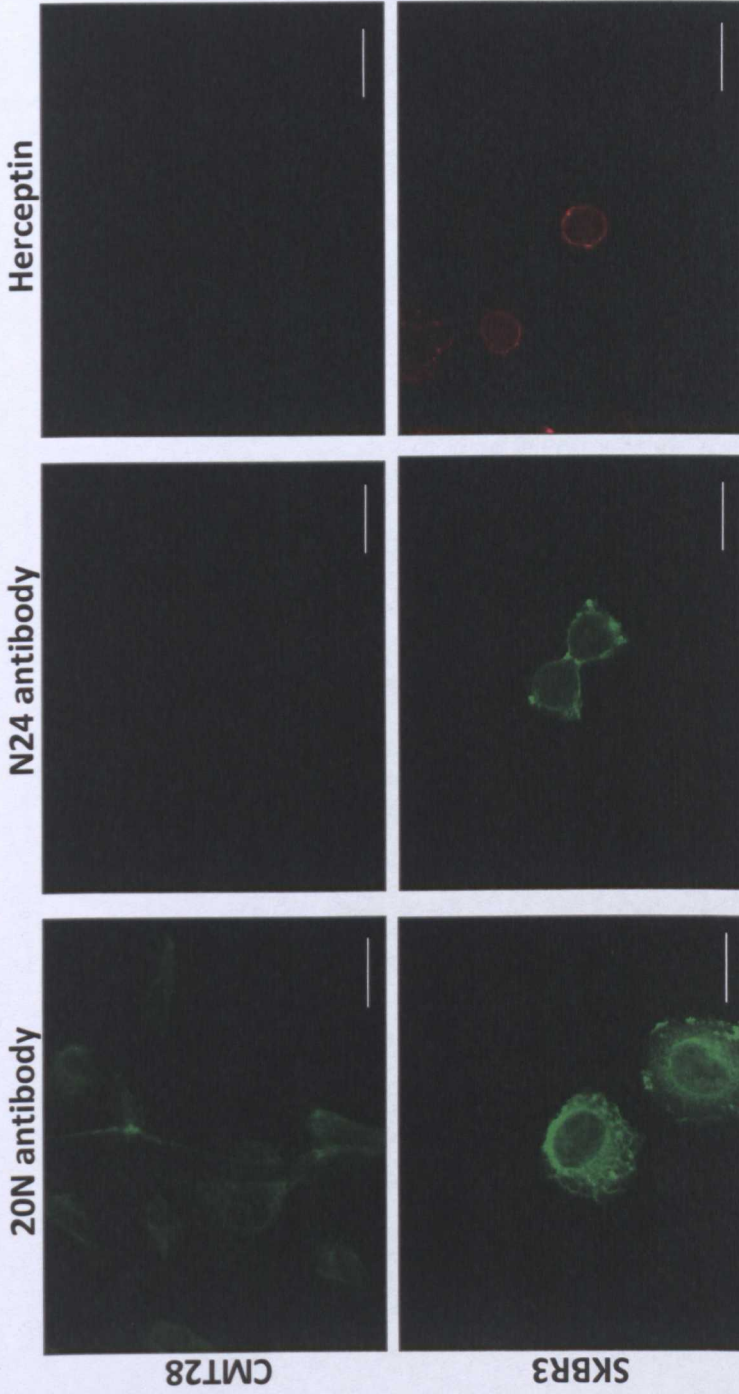


Figure 7.3a: Determining if Herceptin is able to bind to canine HER2. Using immunofluorescent staining, CMT28 and SKBR3 cells were probed with 20N (directed against the intracellular region of HER2), N24 and Herceptin (each directed against an extracellular human epitope). Using 20N it was possible to determine the presence of HER2 in both cell lines. However further experiments attempting to observe the binding of N24 and Herceptin antibodies gave no signals for the CMT28 cells, while SKBR3 positive controls showed strong positive signals.

All images at 63x magnification, bar = 3 μm . All images have the same exposure time. Cells which were treated with 20N were permeabilised, while those treated with N24 and Herceptin were not.

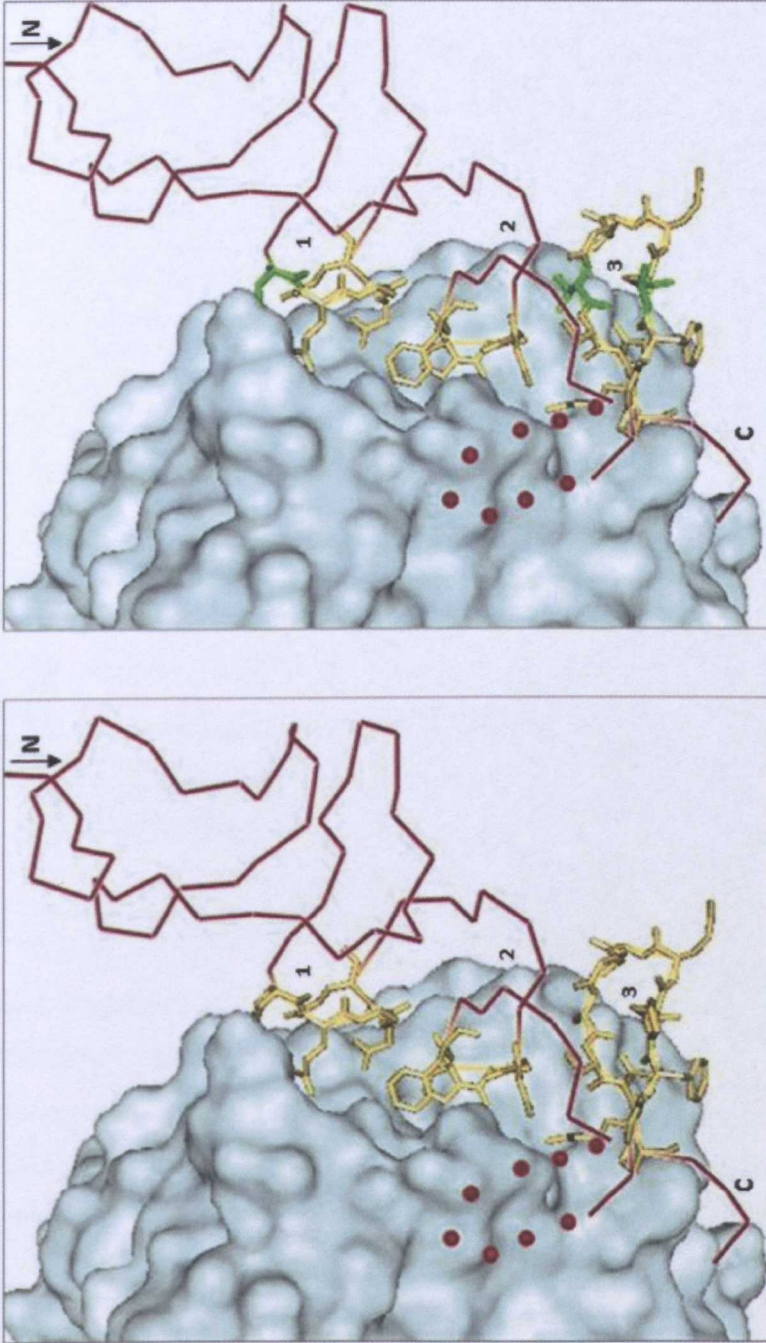


Figure 7.3b: Three dimensional structure of Herceptin Fab (cyan) in complex with human HER2 (red). The image on the left shows Herceptin as it normally binds to the human receptor, with the residues of the three binding loops shown in yellow. On the right, point mutations have been made in the structure (green) to reflect the differences in the canine receptor. The positions of the three loops are indicated (loop 1: residues 557-561, loop 2: residues 570-573, and loop 3: residues 593-603), as are the N and C termini of the regions displayed here. An eight residue loop of HER2 not visible in the structure (but which was described by Cho et al) is indicated with red dots.

Image adapted from Cho et al (Cho et al., 2003) using PDB reference 1N8Z, and edited using PyMol Software.

Table 7.1 – Comparison of HER2 binding residues between human and dog proteins

Loop 1	
Human	PEADQ
Dog	SEADQ
Loop 2	
Human	DPPF
Dog	DPPF
Loop 3	
Human	KFPDEEGACQP
Dog	KAPDEEGTCQP

7.3.4. Determining to What Extent Canine Mammary Cancer Relies on HER2

Note to the reader: details of the methods employed are given in the relevant sections of the Materials & Methods chapter.

7.3.4.1. Generating CMT28 Growth Curve

It was important to determine the optimum density of cells to seed for future cell proliferation experiments. Using the graph generated from the results of these experiments, the number of cells to be seeded for future experiments was taken from the observed log phase of growth –this was found to be 600 cells/well (Figure 7.4).

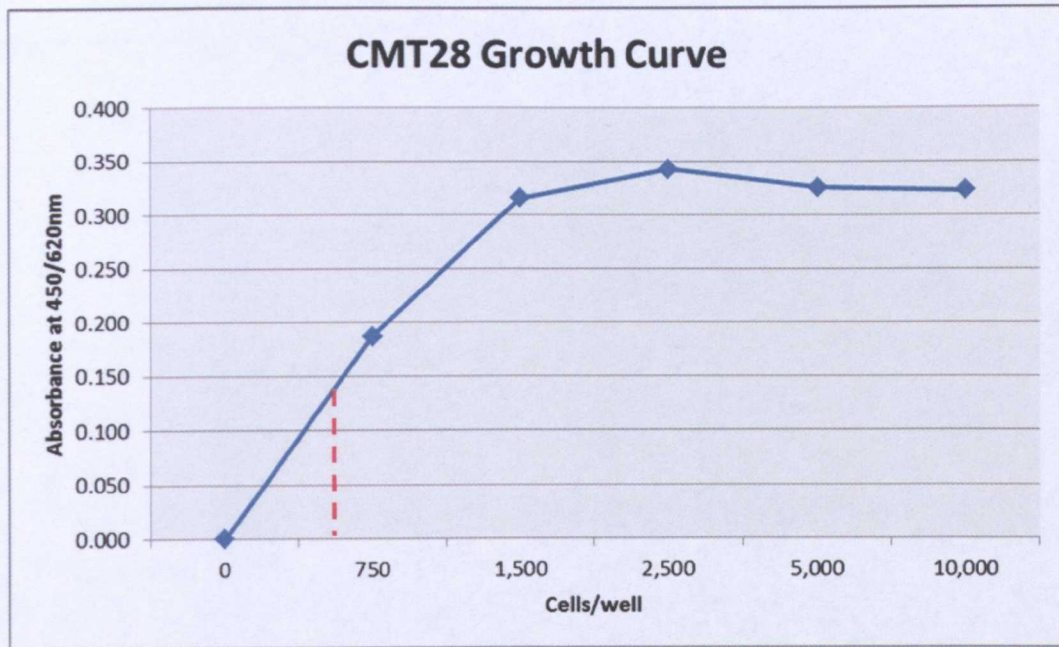
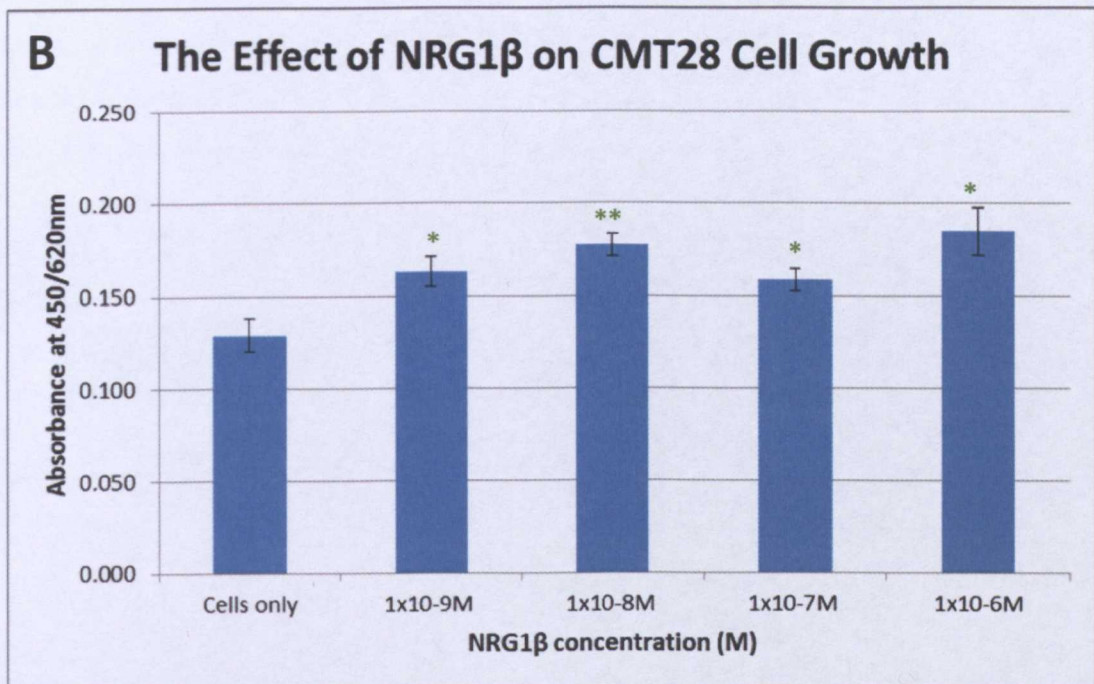
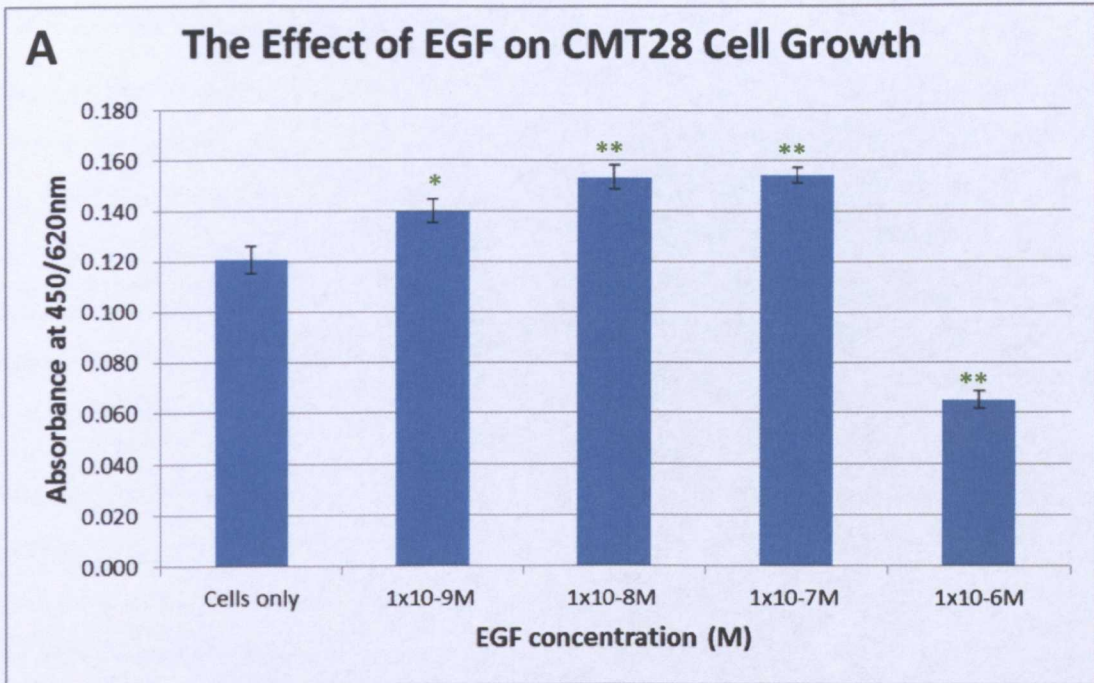


Figure 7.4: Growth curve generated for CMT28 cells. Cells were seeded at 750, 1500, 2500, 5000 and 10000 cell/well and allowed to grow over the course of 7 days. The results were plotted on a graph, and used to estimate the number of cell to seed (dotted red line - - - -). It was decided that 600 cells/well would be adequate for future experiments.

7.3.4.2. Stimulating CMT28 Growth by the Application of Growth Factors

Having shown that HER2 is expressed within CMT28 cells, it was necessary to show that the receptor was functional in the growth of these cells. In order to determine if HER2 activation stimulated cell growth, cells were seeded at 600 cells/well and treated with varying concentrations of EGF (Figure 7.5a) and NRG1 β (Figure 7.5b) as these ligands bind to EGFR and HER3 – binding partners of HER2 which are also present in the CMT28 cells. It was observed in the course of these experiments that EGF in particular was able to stimulate cell growth to a statistically significant level. A similar effect was observed when using NRG1 β although this appeared to level off beyond concentrations of ligand exceeding $1 \times 10^{-8} \text{M}$. Notably in experiments using EGF, there was a distinct decrease in observed cell growth at concentrations of $1 \times 10^{-6} \text{M}$ – indeed the results at this concentration dipped below those of the untreated cells, suggesting that cells were in fact undergoing cell death. A possible explanation for this is that the high quantities of ligand available to the cells stimulated them to burn through their stores of ATP rapidly, leaving them without sufficient resources to maintain a viable cell population. Similar experiments with A431 cells have also shown this effect when stimulated with EGF (Kawamoto *et al.*, 1983).



Figures 7.5a & b: Stimulating CMT28 cell growth by the application of ligands of the EGF family. It was found that the application of EGF to the cells caused a significant increase in cell growth, which dramatically decreased at its highest concentration. The application of NRG1 β to the cells also caused a statistically significant increase in cell growth, although in this case there appeared to be a levelling-off beyond ligand concentrations of 1x10⁻⁸M.

p \leq 0.05 = *; p \leq 0.01 = **; p \leq 0.001 = ***

7.3.4.3. Inhibiting CMT28 Growth by the Application of SMTKIs

One method to determine to what extent CMT28 cells rely on HER2 for their growth is to inhibit the receptor's activity by the application of specific small molecule drugs. Following on from the work carried out in Chapter Six, it was decided that the most appropriate inhibitors to use for these experiments would be Lapatinib (Tyverb/Tykern) and Neratinib (HKI-272) owing to both their high degrees of specificity and their differing binding natures: Lapatinib binds to its targets reversibly, while Neratinib binds irreversibly (more detail on this is available in the Discussion of Chapter Six).

The results (Figures 7.6a & b) showed that both drugs were capable of inhibiting cell growth in a concentration dependent manner at a statistically significant level. Overall Lapatinib showed the greatest inhibition at the highest concentration of drug ($1 \times 10^{-6} \text{M}$), however Neratinib showed greater amounts of inhibition at lower concentrations, and was able to inhibit half of the normal cell growth at the lowest concentration of $1 \times 10^{-9} \text{M}$ (whilst Lapatinib only achieved this at $1 \times 10^{-7} \text{M}$). This difference can possibly be explained by the binding natures of these two drugs: as Neratinib binds irreversibly, it has a more sustained effect on the cells than Lapatinib (which binds to its targets reversibly). These results would suggest that HER2 may play a role in the growth of these cells.

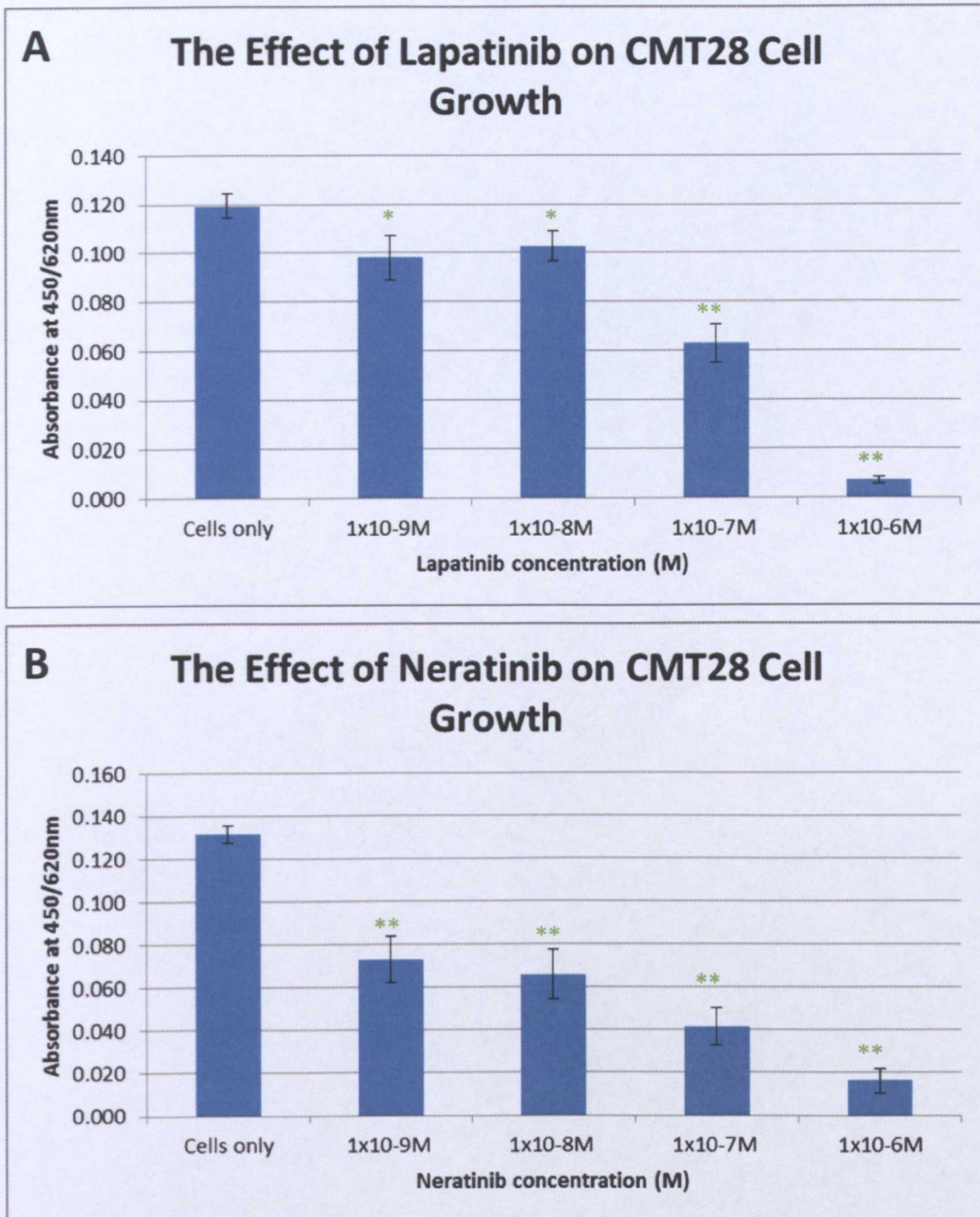


Figure 7.6a & b: Inhibiting CMT28 cell growth by the application of Lapatinib and Neratinib to cells. Results showed that both drugs were able to inhibit cell growth in a concentration dependant fashion. While both drugs were successful in this respect, Neratinib demonstrated more statistically significant inhibition at lower concentrations than Lapatinib. Both drugs were able to inhibit 50% of cell growth of reasonable concentrations (1×10^{-7} M in Lapatinib and 1×10^{-9} M in Neratinib). Data shown here is a combination of three replicates of the same experiment – experimental conditions remained consistent throughout each experiment.

$p \leq 0.05 = *$; $p \leq 0.01 = **$; $p \leq 0.001 = ***$

7.3.4.5. Inhibiting CMT28 Growth by the Application of siRNA & Establishing how siRNA Affects CMT28 Cell Growth

Inhibiting CMT28 Cell Growth with siRNA

Specific siRNAs were designed and applied to cells as described in the Materials & Methods chapter of this thesis. Results of an initial siRNA knockdown (Figure 7.7a) showed that the three specific siRNAs applied to the cells were capable of significantly reducing HER2 protein expression in CMT28 cells, whilst scrambled controls showed no deleterious effects on receptor expression. Having established that the siRNAs were viable in knockdown experiments, two were selected to take forward into experiments with cell proliferation experiments alongside the scrambled controls: siRNAs 1 and 3.

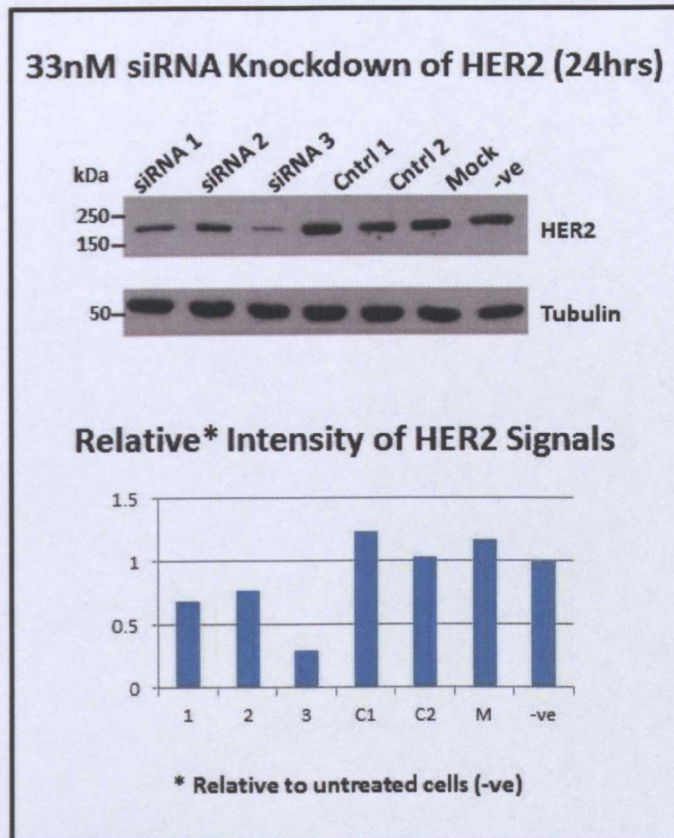


Figure 7.7a: Knockdown of canine HER2 using siRNA. siRNA (at a concentration of 33nM) was transfected into equal numbers of CMT28 cells, and left for 24 hours. HER2 knockdown was then assayed for by Western Blot, using the 20N antibody and an antibody to tubulin as a loading control. Image J was used to determine signal intensities. Results showed that the three specific siRNAs were capable of significantly reducing HER2 expression in CMT28 cells, while the scrambled control siRNAs and mock transfection had no effect on receptor expression.

When these siRNAs were applied in cell proliferation experiments (Figure 7.7b) over a seven day period, similar results were observed. Specific siRNAs 1 and 3 caused a decrease in cell growth (although this was only statistically significant in the case of siRNA3) while scrambled control 1 showed little effect on cell growth. Unexpectedly, scrambled control 2 repeatedly had a significant effect on cell growth, despite it not knocking down HER2 as evidenced by previous experiments (Figure 7.7a). siRNAs are known to occasionally cause unexpected and non-specific toxicities within cells. Unfortunately, it was not possible to design another control and have it synthesized in time to employ it in these experiments.

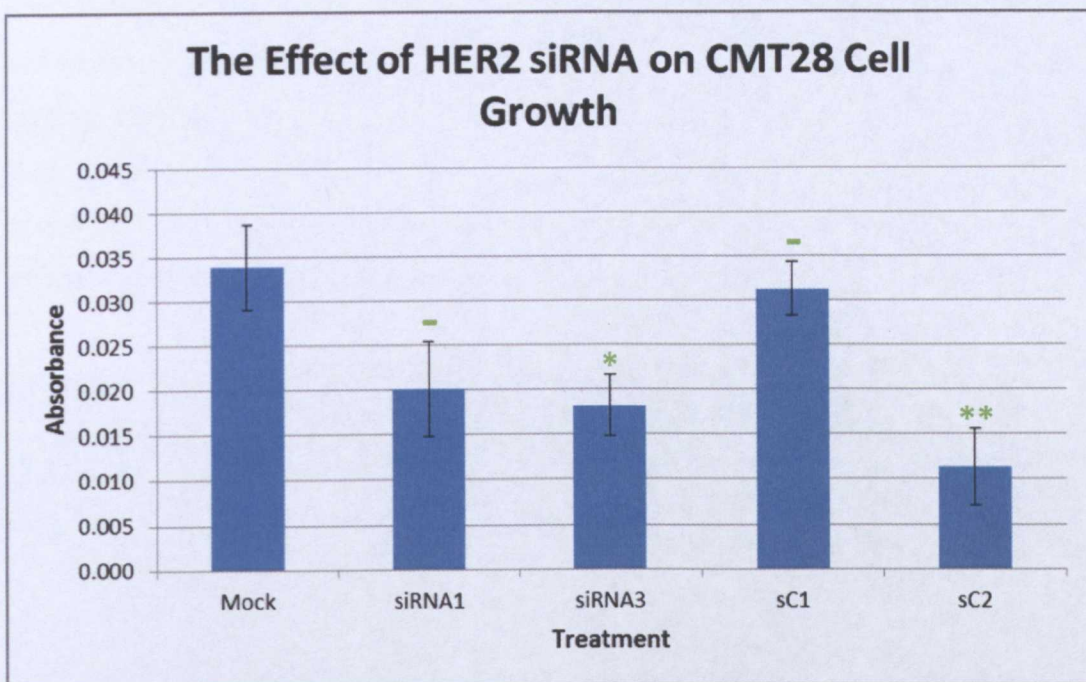


Figure 7.7b: The effect of HER2 specific siRNAs on CMT28 cell proliferation over 7 days. Results showed that knocking down HER2 with specific siRNAs caused a significant decrease in cell growth, whilst scrambled control 1 appeared to have little effect on cell growth. In all experiments, scrambled control 2 consistently caused significant inhibition of cell growth. siRNAs are known to occasionally have toxic effects for no obvious reasons, which is what was assumed was occurring here.

$p \leq 0.05 = *$; $p \leq 0.01 = **$; $p \leq 0.001 = ***$; $p > 0.05 = -$

Key: Mock = mock transfected cells (transfecting agent only); siRNA1/3 = specific siRNAs 1 or 3; sC1/2 = scrambled control siRNAs.

Note: All siRNAs were applied to cells at a concentration of 33nM.

Disregarding the results from scrambled control 2, it appeared that knocking down HER2 caused a decrease in cell growth. While some toxic effect was observed as a result of the transfection reagent, the siRNAs consistently showed a greater decrease in cell growth than in mock treated cells, supporting the hypothesis that HER2 could play some role in CMT28 cell growth.

Does siRNA Induce Apoptosis in CMT28 Cells?

Similar experiments in human SKBR3 cells where siRNAs were used to knockdown HER2 have shown that the decrease in cell growth is caused by apoptosis (Choudhury *et al.*, 2004; Faltus *et al.*, 2004). In order to determine if siRNA knockdown of HER2 was having a similar effect in CMT28 cells (and to attempt to determine why scrambled siRNA control 2 was having a non-specific inhibitory effect on CMT28 cell growth), propidium iodide was used to observe if the cells were undergoing apoptosis (Figure 7.8a). Propidium iodide binds to DNA within cells. Once the cells begin to undergo apoptosis their chromatin condenses – thus any nuclei stained with propidium iodide belonging to cells which are undergoing apoptosis display a bright condensed nucleus, whilst the nuclei of cells not

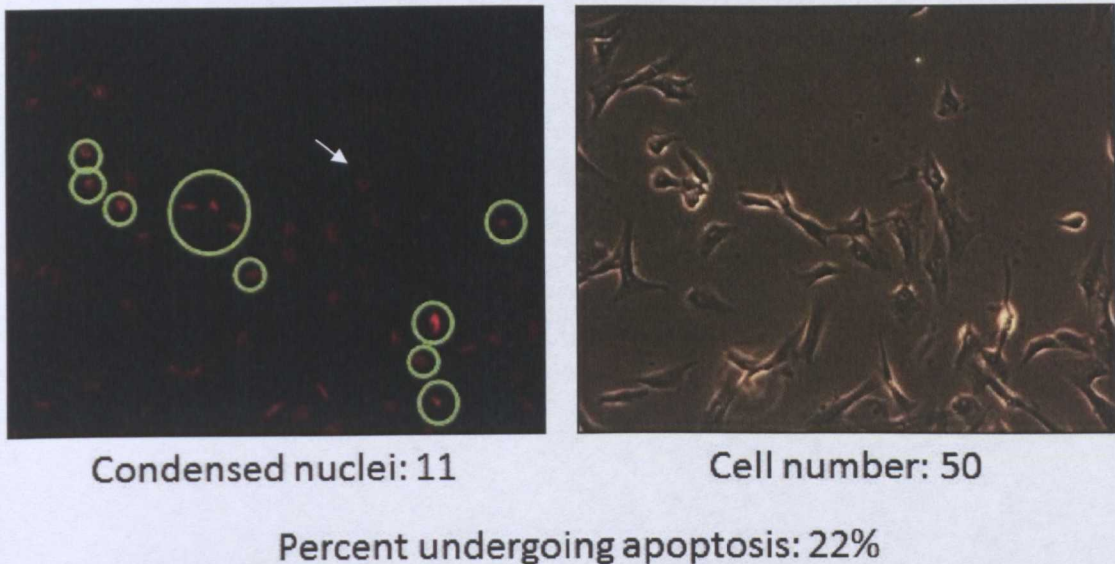


Figure 7.8a: Determining the number of CMT28 cells undergoing apoptosis following treatment with siRNA. Total number of cells were counted from the phase image, and the number of cells undergoing apoptosis (indicated by bright, condensed nuclei in green circles [an example of a diffuse nucleus is indicated with the white arrow]) were counted from the fluorescent image. In this example, the cells have been treated with siRNA1. From this data, the percent of cells undergoing apoptosis was determined. Results from each of the four coverslips carried out for each treatment were collated and recorded on the graph in Figure 7.9.

undergoing apoptosis remain diffuse. Cells were treated as described in the Materials & Methods section of this thesis, and then counted manually. Each treatment (untreated, mock transfected, siRNA1-3, and the two controls) was carried out on two coverslips, and five pictures were taken of each coverslip (in both phase and fluorescent states). This experiment was carried out twice, resulting in a total of four coverslips for each treatment (for an example of each treatment, see Figure 7.8b). From the phase pictures, the total number of cells in the field of view was counted, and the number of condensed nuclei were counted from the fluorescent image (Figure 7.8a). The percent of cells undergoing apoptosis was determined this way, and the results from each of the four coverslips was collated and plotted on the graph in Figure 7.9.

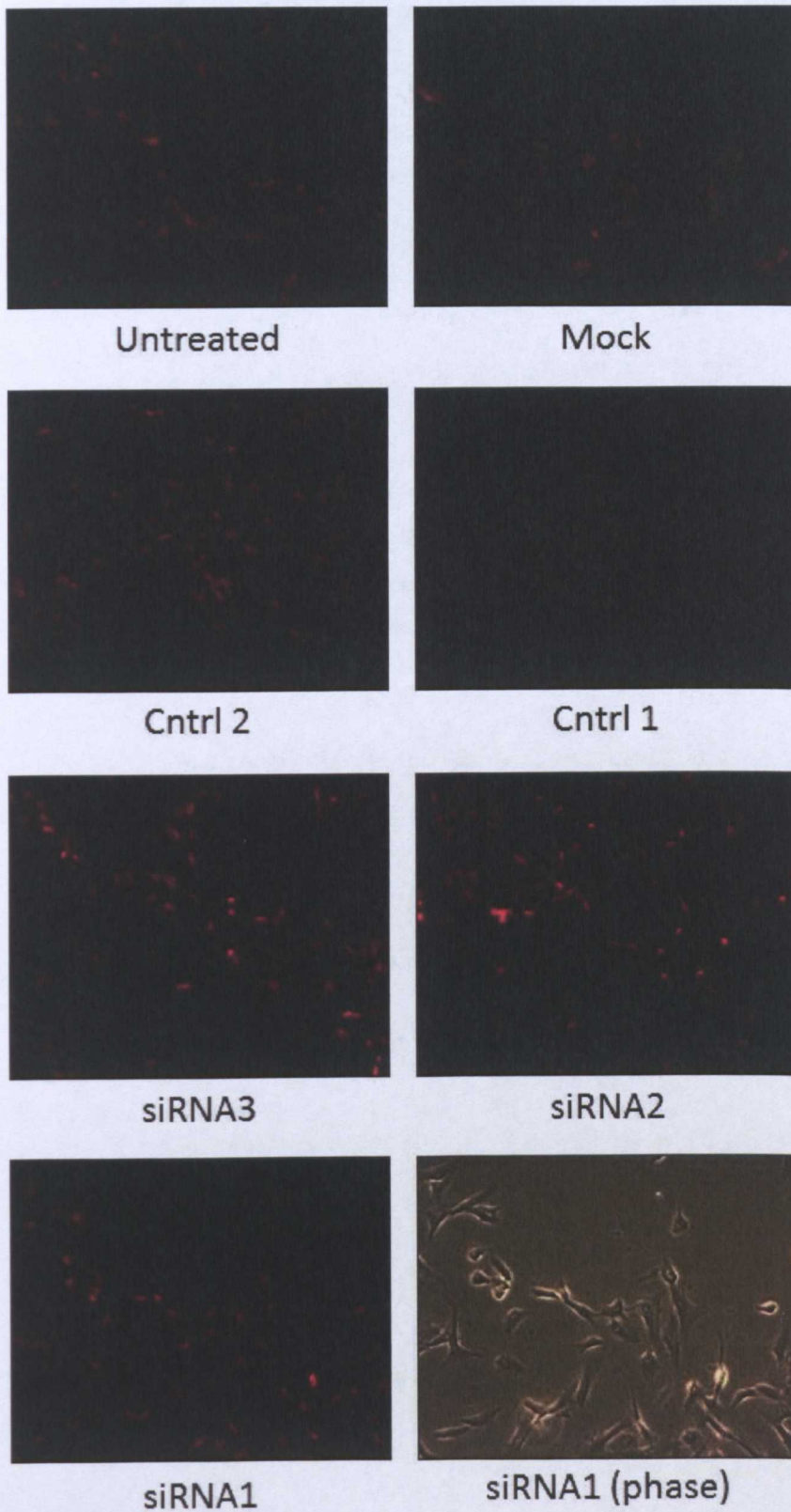


Figure 7.8b: Examples of fluorescent images (and one example of a complimentary phase image) obtained in the course of propidium iodide experiments. Cells displaying bright, condensed nuclei are undergoing apoptosis, whilst cells with diffuse, less sharp nuclei are normal.

These collated results showed that in the cases of the three test siRNAs, there was an increased level of apoptosis compared to the controls of mock transfected cells, untreated cells and cells transfected with scrambled control 1. Scrambled control 2 showed extremely high levels of apoptosis within the cells – levels which exceeded the apoptosis observed in even the most effective siRNA treatment (siRNA3). This was not entirely unexpected given the results observed in the cell proliferation experiments, however it did not provide an alternate explanation as to why this scrambled control was causing the cell growth to be inhibited (that is, the non specific toxic effect observed when using this control siRNA was causing cell death through the same mechanism as the other siRNAs).

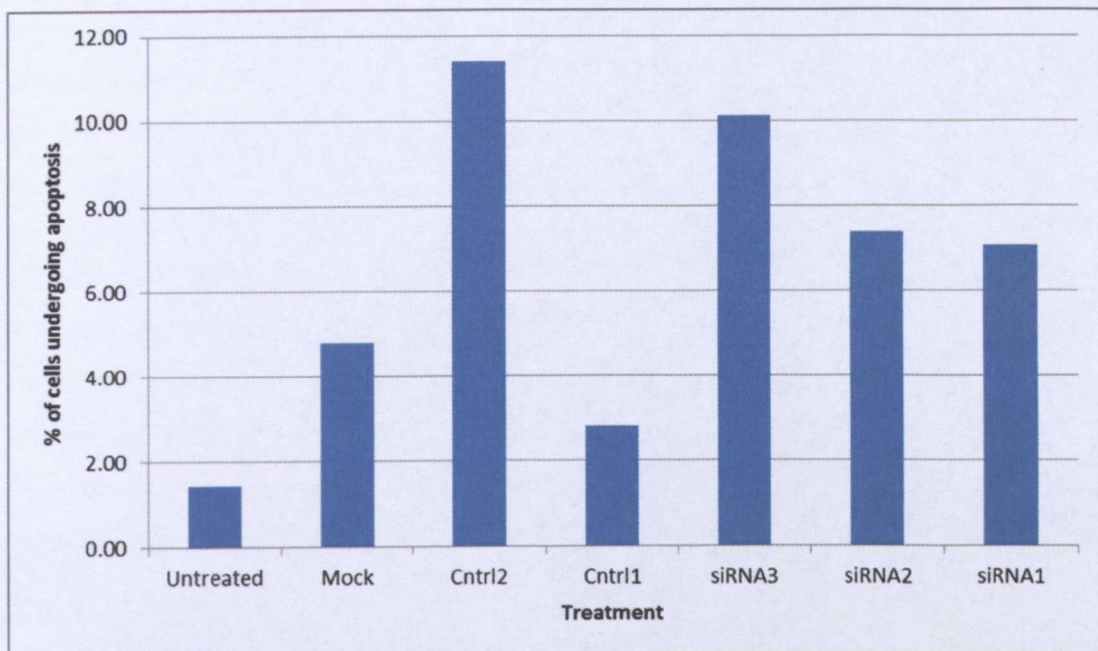


Figure 7.9: Graphical representation of results obtained from propidium iodide experiments. Results showed that the three test siRNAs were causing increased levels of apoptosis compared to the untreated, mock transfected cells and cells treated with scrambled control 1. Scrambled control 2 consistently showed high levels of apoptosis, which was consistent with the results gathered in the cell proliferation experiments using siRNA (where scrambled control 2 significantly decreased CMT28 cell growth). Data shown here is a combination of three replicates of the same experiment – experimental conditions remained consistent throughout each experiment.

7.4. DISCUSSION

This chapter aims to establish both the receptor expression profile of a canine mammary cancer, and to determine to what extent such a cell line relies on HER2 to maintain a malignant phenotype. Through PCR and Western Blotting, it has been possible to

determine that the CMT28 cell line used here seems to express all members of the EGF receptor family, including HER2 – a receptor that has been well studied in human cancer and which is implicated in more aggressive disease. Having established that this receptor was present, it was possible to carry out experiments to determine what role HER2 played in canine mammary cancer.

In the first instance, ligands of the EGF family which bind to receptors known to form heterodimers with HER2 (EGF binds to EGFR, while NRG1 binds to HER3 and HER4) were applied to CMT28 cells in culture. These ligands appeared to cause an increase in cell growth, perhaps suggesting that HER2 plays a role in stimulating cell growth. Further experiments which made use of specific tyrosine kinase inhibitors (to block HER2 phosphorylation) and specific siRNAs (to knockdown the receptor) caused a decrease in cell growth – further suggesting that HER2 is required to maintain the malignant phenotype of the CMT28 cells.

However a limitation arises when one considers that at the time this project was carried out, only one relevant cell line was available for study. Ideally, these experiments would have been carried out on a number of representative cell lines. Following on from this project, further work in this laboratory is currently aiming to carry out similar experiments using canine mammary cancer cell lines which have more recently become available from other groups. These studies are not only utilizing the experiments described here to determine the role of HER2 in other canine mammary cancer cell lines, but are also incorporating Boyden chambers and wound healing assays to observe the chemotactic effects of inhibitors and ligands on such cells.

With regard to the propidium iodide experiments to observe the effect of siRNA on apoptosis, it must be emphasized that these are only preliminary results which were conducted in the last days of this study. Should further time have been available, a number of experiments could have added to this data, for example:

- Western Blots probing for the presence of Annexin V and Caspases (among numerous other protein markers) involved in apoptosis.
- Fluorescent automated cell sorting (FACS) analysis making use of propidium iodide staining and staining for another marker to improve counting methods. FACS would

also help to eliminate any human error made in cell counting in the manual method described in this study.

- DNA laddering assays to observe the degradation of DNA between histones typically observed in apoptosis. This assay would also help to distinguish apoptosis from toxic cell death which may be caused by the transfecting agents involved in the application of siRNAs to cells.

CHAPTER EIGHT

Discussion

8.1. RESULTS OF THIS PROJECT

The role of the EGF family in human disease (particularly in cancers) is well established. This is perhaps best illustrated with the HER2 receptor, the role of which has been widely studied in breast cancer for many years. Consequently, a number of HER2 specific therapies have been developed for the treatment of cancers which overexpress this receptor. While this understanding has contributed extensively to human healthcare, the potential market in animal health has been somewhat overlooked, and our understanding of the EGF family in companion animals is limited. However the growing number of pet owners taking out pet insurance to help treat their pets is beginning to encourage pharmaceutical companies to develop animal-specific cancer therapies. This project aimed to address this gap in our knowledge with regard to canine cancer by exploring the role of the EGF family (in particular the HER2 receptor) in canine mammary cancer.

It is perhaps surprising that so little is known about the EGF family in dogs considering how similar humans and dogs are on a genetic level – dogs are more closely related to humans than mice (more widely used and studied models) are. The genes of the EGF family are highly conserved in mammals (Stein & Staros, 2006), and as such it may be reasonable to assume that similar protein products would be produced amongst mammalian species. Bioinformatical analysis carried out in this project sought to compare the HER2 gene and its protein products between our species and *Canis familiaris*. BLAST alignments of human and canine protein sequences showed that the sequences were highly similar, sharing greater than 90% identity. This similarity also extended to the structure of the protein as shown by Dot Plot analysis, which revealed that the canine structure shared a number of repeated protein sequences that corresponded to the cysteine rich extracellular regions of HER2. Analysis of cDNA sequences also showed a highly similar exon structure between species. Having determined that the receptor was so similar in its basic structure, attempts were also made to determine if similar splice variants also existed, as certain drug resistances have been related to the expression of truncated protein isoforms. While there was

evidence that the residue involved in the alternative initiation of the p95-HER2 isoform was conserved, EST library analysis failed to identify any variants of HER2. This may not be the complete picture however. While the canine genome has been sequenced, molecular study of the domestic dog is still in its early days when compared to humans. In years to come, further canine sequences may be added to the EST database which could perhaps identify splice variants and isoforms of HER2 in dogs, or further work could be carried out to identify such sequence tags, for example through rapid amplification of cDNA ends (RACE)-PCR.

Having established that the canine and human gene and protein products for HER2 are similar, the next step in the project was to compare HER2 expression (along with other members of the EGF family) in normal canine tissues with their human equivalents.

While several studies have explored the expression of EGFR and HER2 in canine mammary cancer (Nerurkar *et al.*, 1987; Rutteman *et al.*, 1994; Dutra *et al.*, 2004; Selvarajah *et al.*, 2012), and one study has observed the expression of EGFR in canine osteosarcoma (Selvarajah *et al.*, 2012) none appear to have addressed the levels of expression in normal tissues. While these studies have been of use in understanding canine cancer, they do not provide a base level which can be used to compare diseased tissues with their healthy counterparts. Knowledge of healthy tissue expression can also help to predict potential adverse effects of certain drugs, by identifying where high concentrations of the target are located within a healthy body.

Similar information has been gathered from mutant mice. Studies have shown that mice which have a null mutation of the TGF- α gene show distinctive waviness in their coats and whiskers and can develop corneal inflammation (Mann *et al.*, 1993). A further study showed that a point mutation in EGFR which reduced its phosphorylation activity by 90% gave rise to a "waved-2" (wa-2) phenotype which displayed similar abnormalities to the TGF- α deficient mice (Luetkeke *et al.*, 1994). The adverse effects of Herceptin (which, while famed for its effectiveness and low levels of adverse effects, does cause cardio toxicity in some patients) were predicted through knockout studies of HER2 in mice. Mice lacking HER2 showed early embryonic lethality from defective cardiac development owing to a lack of trabeculation within the heart (Gassmann *et al.*, 1995; Lee *et al.*, 1995; Meyer & Birchmeier, 1995). Immunohistochemical stains in this study have described this normal distribution and expression. These results showed that members of the EGF family were

widely distributed throughout the canine tissues, with tissues of the gastrointestinal tract showing strong expression of most proteins – perhaps due to the frequent sloughing of cells caused by eating and peristalsis, and the related repair processes in these tissues. Results showed HER2 was strongly to moderately expressed throughout many tissues in the dog, while studies in humans have shown that HER2 is generally less strongly expressed in normal tissues with EGFR, HER3 and HER4 being expressed more strongly throughout human tissues compared to HER2.

It is, however, difficult to make entirely fair comparisons between the results obtained in this project and the results from the other groups which were used for comparison. Variations exist in both the scientific method employed by others groups (for example, different antibodies, different methodologies and incubation times) and in the methods used in scoring and reporting the results from stains. There is no precise way to quantify the results from an immunohistochemical stain – the technique is enzyme based and as such non-linear, and there is no industry-standard method of measurement. As such, different groups interpret staining intensities differently, and difficulties also arise when attempting to draw cross-comparisons between my own individual stains – different antibodies may react differently with each antigen owing to their individual affinities.

Further immunohistochemical studies were carried out on both benign and malignant canine mammary cancer tissue samples. While stains on normal tissues observed both receptor and ligand expression, stains on the diseased samples initially aimed to observe receptor expression only, and stains for NRG1 and NRG2 were later carried out with the malignant samples, as these ligands bind to HER3 (the preferential binding partner of HER2). In the benign tissues, it was generally found that HER2 and HER3 showed the greatest levels of expression. Among these samples 18% showed strong expression for HER2 and 27% showed strong staining for HER3. In the malignant samples EGFR, HER2 and HER3 also generally showed moderate to strong expression levels. However, strong (3+) HER2 staining was observed in only 11% of cases, compared to 44% of cases showing strong EGFR staining and 22% of cases showing strong HER3 staining. It should be mentioned that much of the staining observed in these cancers was located in the cell cytoplasm, rather than in the membrane which is more typically seen in aggressive human disease. In addition to these immunohistochemical stains, it would have been beneficial to carry out gene amplification studies on canine samples. In human disease, the HER2

receptor is not considered a relevant therapeutic target unless gene amplification of HER2 is observed by FISH.

In the course of observing stains on cancerous tissues, it became apparent that the histology of these neoplasms was highly varied and disorganised – such pleomorphisms are less commonly seen in human disease, but are relatively common in canine mammary tumours (Dutra *et al.*, 2004). Regions of necrosis, invasion and morphologically altered cell nuclei were also present.

Further analysis of normal MDCK cells and canine mammary cancer (CMT28) cells (chosen as these showed the highest HER2 mRNA levels in the relevant literature) by RT-PCR and Western Blot was also carried out to survey receptors present in cultured canine cells. While CMT28 had previously been shown to express HER2 mRNA by dot-blot (Ahern *et al.*, 1996), this had not been confirmed through PCR or at the protein level. Results suggested that MDCK cells (used in this study as a positive control) expressed EGFR, HER2 and HER3 (which was in agreement with previous studies on the cell line) while the CMT28 cells expressed all receptors of the EGF family, although Western Blot analysis of this cell line showed that HER2 was the highest expressed of all the receptors.

Having determined that HER2 was present in the canine mammary cancer cells, we next sought to observe what effect this receptor has on cell growth. The application of EGF and NRG1 β (ligands to EGFR and HER3, each of which are HER2 binding partners) to CMT28 cells caused an increase in cell growth. This perhaps suggests that HER2 present in these cells plays a role in cell growth through its activation as part of a receptor heterodimer – although homodimers of EGFR and HER3 are likely also at play here. To test this hypothesis further, experiments were carried out to remove the effect that HER2 could be having on cell growth through two separate approaches: first, to inhibit the activation of the HER2 receptor through the application of SMTKIs; and second, to knockout the receptor using siRNA technologies.

Human SMTKIs Lapatinib and Neratinib (which had been shown by Western Blot with NEN-7 cell lysates to be efficient inhibitors of HER2 kinase) applied to CMT28 cells showed a concentration dependent inhibition of cell growth when applied over the course of seven days. This inhibitory effect was most noticeable with Neratinib, perhaps due to its irreversible binding nature (which Lapatinib does not share), which would prolong its inhibitory effects on cell receptors. It should be noted however, that these observations are

made on an *in vitro* system, rather than *in vivo*. Within an organism, both the pharmacokinetics and the pharmacodynamics of a drug must be considered, as factors such as metabolism and excretion can play a role in how effective a drug is – certain compounds undergo chemical changes in the body, which may alter their affinities. Such is the case with Tamoxifen – a prodrug which, after its administration, is metabolised to 4-hydroxytamoxifen and N-desmethyl-4-hydroxytamoxifen, each of which has significantly higher affinities for their targets than Tamoxifen itself (Desta *et al.*, 2004). Further experiments would be useful to determine the effects of these drugs in dogs *in vivo* as, while their pharmacokinetic and dynamic properties have been demonstrated in humans, little is known about them in dogs other than in data gathered from safety studies in which the animals are often disease-free.

While these drugs are highly specific, their targets are not exclusively HER2 and they are also able to bind EGFR. To more conclusively show that HER2 is involved in CMT28 cell growth, it was decided that the receptor should be knocked down to remove any effect it had on the cells. To this end, siRNA was used to knockdown HER2 in CMT28 cells. Following the application of siRNA, knockdown was assayed for after 24 hours by Western Blot and it was found that all three siRNAs designed were able to significantly knockdown receptor expression. Following on from this, siRNAs were applied to cell proliferation assays where one of the two tested showed a significant decrease in cell growth when compared to mock transfected cells. While one scrambled control siRNA showed a significant effect on cell growth, this is likely due to non-specific toxicities which are occasionally found in siRNAs (BLAST analysis carried out during siRNA design indicated no similarities between this toxic control and any other known gene), and had more time been available an alternative control would have been designed. Investigations into how siRNAs brought about the observed decreases in cell growth showed (through propidium iodide analysis) that a greater degree of apoptosis was occurring in cells treated with test siRNAs (and the aberrant scrambled control). Similar effects have been seen in human SKBR3 cells where HER2 has been knocked down using siRNA (Faltus *et al.*, 2004).

As few canine cell lines which express HER2 are currently available, further experiments could focus on stably transfecting canine HER2 into a cell line to study its overexpression, rather than removing it. These studies would focus more on observing an increase in cellular growth caused by the addition of the receptor, rather than observing any decrease caused by blocking it. Such studies have both advantages and disadvantages: they remove

any general non-specific toxic effects from the cells which may be caused by SMTKIs or transfecting agents, so any change in growth is likely down to the receptor itself and not an external cytotoxicity; however a stable transfection does not represent a “normal” situation – the cell line has not been cultured from a tumour expressing HER2 – and so is not entirely representative of the disease state.

8.2. THE FUTURE

While this project provides information to help bridge the gaps in the knowledge with regard to canine mammary cancer, it is only a very small piece of the puzzle. We cannot definitely prove that HER2 plays a significant role in the disease, although data gathered here thus far does support this. Future work would focus on expanding the study sample sizes, so that more tumour samples and relevant cell lines could be added to the data presented in this thesis. Indeed, work currently being carried out in the laboratory after this project was completed is striving to do just this, and is making use of another two cell lines which have recently become available. An increased number of tumour samples and cell lines would also allow for a greater analysis of HER2 expression in canine mammary cancers to be carried out, to better gauge the incidences of HER2 overexpression in the disease and to see if membrane staining can be observed in canine disease, in addition to studying the prevalence of gene amplification of HER2 in canine mammary cancer.

With these samples becoming more available, and with the dog becoming a more widely recognised model for study, it is likely that man’s best friend will play a significant role not only as a companion animal, but also as a useful piece in the puzzle of biomedical research – in particular cancer research.

REFERENCES

Aas T, Borresen A-L, Geisler S, Smith-Sorensen B, Johnsen H, Varhaug JE, Akslen LA & Lonning PE (1996). Specific P53 mutations are associated with de novo resistance to doxorubicin in breast cancer patients. *Nat Med*, **2**: 811-814.

Abe K (2000). Therapeutic Potential of Neurotrophic Factors and Neural Stem Cells Against Ischemic Brain Injury. *J Cereb Blood Flow Metab*, **20**: 1393-1408.

United States Food & Drug Administration (2006). *FDA Licenses New Vaccine for Prevention of Cervical Cancer and Other Diseases in Females Caused by Human Papillomavirus* [WWW Reference]. Available from: <http://www.fda.gov/NewsEvents/Newsroom/PressAnnouncements/2006/ucm108666.htm>

Aguilar Z, Akita RW, Finn RS, Ramos BL, Pegram MD, Kabbinavar FF, Pietras RJ, Pisacane P, Sliwkowski MX & Slamon DJ (1999). Biologic effects of heregulin/neu differentiation factor on normal and malignant human breast and ovarian epithelial cells. *Oncogene*, **18**: 6050-6062.

Agus DB, Akita RW, Fox WD, Lewis GD, Higgins B, Pisacane PI, Lofgren JA, Tindell C, Evans DP, Maiese K, Scher HI & Sliwkowski MX (2002). Targeting ligand-activated ErbB2 signaling inhibits breast and prostate tumor growth. *Cancer Cell*, **2**: 127-137.

Ahern TE, Bird RC, Bird AE & Wolfe LG (1996). Expression of the oncogene c-erbB-2 in canine mammary cancers and tumor-derived cell lines. *Am J Vet Res*, **57**: 693-696.

Albanell J, Codony J, Rovira A, Mellado B & Gascón P (2003). Mechanism of action of anti-HER2 monoclonal antibodies: scientific update on trastuzumab and 2C4. *Adv Exp Med Biol*, **532**: 253-268.

Alberti L, Carniti C, Miranda C, Roccato E & Pierotti MA (2003). RET and NTRK1 proto-oncogenes in human diseases. *J Cell Physiol*, **195**: 168-186.

Altschul SF, Madden TL, Schäffer AA, Zhang J, Zhang Z, Miller w & Lipman DJ (1997). Gapped BLAST and PSI-BLAST: a new generation of protein database search programs. *Nucleic Acids Res*, **25**: 3389-3402.

American Pet Products Association (2010). *Industry Statistics & Trends: Pet Ownership* [WWW Reference]. Last Accessed: 12th August, 2011. Available from: http://www.americanpetproducts.org/press_industrytrends.asp.

American Pet Products Association (2012). *Industry Statistics & Trends* [WWW Reference]. Last Accessed: 9th March, 2012. Available from: http://www.americanpetproducts.org/press_industrytrends.asp.

Anido J, Scaltriti M, Bech Serra JJ, Santiago Josef B, Todo FR, Baselga J & Arribas J (2006). Biosynthesis of tumorigenic HER2 C-terminal fragments by alternative initiation of translation. *EMBO J*, **25**: 3234-3244.

Anklesaria P, Teixidó J, Laiho M, Pierce JH, Greenberger JS & Massagué J (1990). Cell-cell adhesion mediated by binding of membrane-anchored transforming growth factor alpha to epidermal growth factor receptors promotes cell proliferation. *Proc Natl Acad Sci*, **87**: 3289-3293.

Aplin AE, Howe A, Alahari SK & Juliano RL (1998). Signal Transduction and Signal Modulation by Cell Adhesion Receptors: The Role of Integrins, Cadherins, Immunoglobulin-Cell Adhesion Molecules, and Selectins. *Pharmacol Rev*, **50**: 197-264.

Arman K (2007). A new direction for kennel club regulations and breed standards. *Can Vet J*, **48**: 953-965.

Australian Government: Department of Health and Ageing (2006). *Listing of Herceptin on the PBS* [WWW Reference]. Last Accessed: 20th September, 2010. Available from: <http://www.health.gov.au/internet/main/publishing.nsf/Content/herceptin-govtdecision.htm>.

Bagshawe KD, Sharma SK, Springer CJ & Rogers GT (1994). Antibody directed enzyme prodrug therapy (ADEPT). *Ann Oncol*, **5**: 879-891.

Bailey J (2008). An Assessment of the Role of Chimpanzees in AIDS Vaccine Research. *ATLA*, **36**: 381-428.

Barros CS, Calabrese B, Chamero P, Roberts AJ, Korzus E, Lloyd K, Stowers L, Mayford M, Halpain S & Müller U (2009). Impaired maturation of dendritic spines without disorganization of cortical cell layers in mice lacking NRG1/ErbB signaling in the central nervous system. *Proc Natl Acad Sci*, **106**: 4507-4512.

BBC News (2006) Woman loses Herceptin court bid. [News Article]. Last Accessed: 20th September 2010. Available from: <http://news.bbc.co.uk/1/hi/health/4715430.stm>

BBC News (2008) Pedigree dogs plagued by disease. [News Article]. Last Accessed: 5th March 2012. Available from: <http://news.bbc.co.uk/1/hi/uk/7569064.stm>

BBC News (2012) Cancer fear and denial 'is killing thousands'. [News Article]. Last Accessed: 12th March, 2012. Available from: <http://www.bbc.co.uk/news/health-17257900>

BBC News (2012) US spending on pets 'passes \$50bn'. [News Article]. Last Accessed: 9th March 2012. Available from: <http://www.bbc.co.uk/news/world-us-canada-17243094>

Pedigree Dogs Exposed, (22nd August 2008). Television documentary. Prod: J. Harrison, **BBC Television**. 60 mins.

Bergman PJ, Camps-Palau MA, McKnight JA, Leibman NF, Craft DM, Leung C, Liao J, Riviere I, Sadelain M, Hohenhaus AE, Gregor P, Houghton AN, Perales MA & Wolchok JD (2006). Development of a xenogeneic DNA vaccine program for canine malignant melanoma at the Animal Medical Center. *Vaccine*, **24**: 4582-4585.

Bergman PJ, McKnight J, Novosad A, Charney S, Farrelly J, Craft D, Wulderk M, Jeffers Y, Sadelain M, Hohenhaus AE, Segal N, Gregor P, Engelhorn M, Riviere I, Houghton AN &

- Wolchok JD (2003). Long-Term Survival of Dogs with Advanced Malignant Melanoma after DNA Vaccination with Xenogeneic Human Tyrosinase. *Clin Cancer Res*, **9**: 1284-1290.
- Birchmeier C (2009). ErbB receptors and the development of the nervous system. *Exp Cell Res*, **315**: 611-618.
- Bjorn MJ, Groetsema G & Scalapino L (1986). Antibody-Pseudomonas Exotoxin A Conjugates Cytotoxic to Human Breast Cancer Cells in Vitro. *Cancer Research*, **46**: 3262-3267.
- Borgna JL & Rochefort H (1981). Hydroxylated metabolites of tamoxifen are formed in vivo and bound to estrogen receptor in target tissues. *J Biol Chem*, **256**: 859-868.
- Boston University (2001). *Boston University Histology Learning System* [WWW Reference]. Last Accessed: 31st August, 2010. Available from: <http://www.bu.edu/histology/m/>.
- Bouyain S, Longo PA, Li S, Ferguson KM & Leahy DJ (2005). The extracellular region of ErbB4 adopts a tethered conformation in the absence of ligand. *Proc Natl Acad Sci U S A*, **102**: 15024-15029.
- Brachmann R, Lindquist PB, Nagashima M, Kohr W, Lipari T, Napier M & Derynck R (1989). Transmembrane TGF- β precursors activate EGF/TGF- β receptors. *Cell*, **56**: 691-700.
- Bradford MM (1976). A rapid and sensitive method for the quantitation of microgram quantities of protein utilizing the principle of protein-dye binding. *Anal Biochem*, **72**: 248-254.
- British Bulldog Club Inc (2011). *Bulldog of the Year* [WWW Reference]. Last Accessed: 8th March, 2012. Available from: <http://www.bulldog-inc.com/boy.html>.
- Bross PF, Beitz J, Chen G, Chen XH, Duffy E, Kieffer L, Roy S, Sridhara R, Rahman A, Williams G & Pazdur R (2001). Approval Summary: Gemtuzumab Ozogamicin in Relapsed Acute Myeloid Leukemia. *Clin Cancer Res*, **7**: 1490-1496.
- Buonanno A & Fischbach GD (2001). Neuregulin and ErbB receptor signaling pathways in the nervous system. *Curr Opin Neurobiol*, **11**: 287-296.
- Burgess AW, Cho H-S, Eigenbrot C, Ferguson KM, Garrett TPJ, Leahy DJ, Lemmon MA, Sliwkowski MX, Ward CW & Yokoyama S (2003). An Open-and-Shut Case? Recent Insights into the Activation of EGF/ErbB Receptors. *Mol Cell*, **12**: 541.
- Burriss HA, Rugo HS, Vukelja SJ, Vogel CL, Borson RA, Limentani S, Tan-Chiu E, Krop IE, Michaelson RA, Girish S, Amler L, Zheng M, Chu Y-W, Klencke B & O'Shaughnessy JA (2011). Phase II Study of the Antibody Drug Conjugate Trastuzumab-DM1 for the Treatment of Human Epidermal Growth Factor Receptor 2 (HER2) –Positive Breast Cancer After Prior HER2-Directed Therapy. *J Clin Oncol*, **29**: 398-405.
- Campo MS (2002). Animal models of papillomavirus pathogenesis. *Virus Res*, **89**: 249.

Cancer Research UK (2009). *Cancer survival rates - trends* [WWW Reference]. Last Accessed: 12th March, 2012. Available from: <http://info.cancerresearchuk.org/cancerstats/survival/fiveyear/>.

Cancer Research UK (2011). *Cancer incidence for common cancers - UK statistics* [WWW Reference]. Last Accessed: 12th March, 2012. Available from: <http://info.cancerresearchuk.org/cancerstats/incidence/commoncancers/>.

Cancer Research UK (2011). *Cancer Worldwide - the global picture* [WWW Reference]. Last Accessed: 12th March, 2012. Available from: <http://info.cancerresearchuk.org/cancerstats/world/the-global-picture/#source1>.

Cancer Research UK (2012). *Is cancer just a modern disease?* [WWW Reference]. Last Accessed: 12th March, 2012. Available from: <http://info.cancerresearchuk.org/cancerandresearch/all-about-cancer/what-is-cancer/is-cancer-a-modern-disease/iscanceramoderndisease>.

Cancer Research UK (2012). *Public ignorance and fear add thousands to annual cancer death toll: Press Release* [WWW Reference]. Last Accessed: 12th March, 2012. Available from: <http://info.cancerresearchuk.org/news/archive/pressrelease/2012-03-06-ignorance-adds-thousands-to-cancer-death-toll?view=n-and-r-homepage>.

CCOGC (2004). *Canine Comparative Oncology & Genomics Consortium* [WWW Reference]. Last Accessed: 4th April, 2012. Available from: <http://www.ccogc.net/index.html>.

Capasso LL (2005). Antiquity of cancer. *Int J Cancer*, **113**: 2-13.

Capra E & Capra G (1991). *Il Basset Hound* [Book]. De Vecchi.

Carter P (2001). Improving the efficacy of antibody-based cancer therapies. *Nat Rev Cancer*, **1**: 118-129.

Carter TA, Wodicka LM, Shah NP, Velasco AM, Fabian MA, Treiber DK, Milanov ZV, Atteridge CE, Biggs WH, Edeen PT, Floyd M, Ford JM, Grotzfeld RM, Herrgard S, Insko DE, Mehta SA, Patel HK, Pao W, Sawyers CL, Varmus H, Zarrinkar PP & Lockhart DJ (2005). Inhibition of drug-resistant mutants of ABL, KIT, and EGF receptor kinases. *Proc Natl Acad Sci U S A*, **102**: 11011-11016.

Castiglioni F, Tagliabue E, Campiglio M, Pupa SM, Balsari A & Ménard S (2006). Role of exon-16-deleted HER2 in breast carcinomas. *Endocr Relat Cancer*, **13**: 221-232.

Chambers AF & Matrisian LM (1997). Changing Views of the Role of Matrix Metalloproteinases in Metastasis. *J Natl Cancer Inst*, **89**: 1260-1270.

Chetboul V, Tissier R, Villaret F, Nicolle A, Déan E, Benalloul T & Pouchelon J-L (2004). Epidemiological, clinical, echo-doppler characteristics of mitral valve endocardiosis in Cavalier King Charles in France: a retrospective study of 451 cases (1995 to 2003). *Can Vet J*, **45**: 1012-1015.

- Chiavaras MM & Petrides M (2000). Orbitofrontal sulci of the human and macaque monkey brain. *J Comp Neurol*, **422**: 35-54.
- Cho H-S & Leahy DJ (2002). Structure of the extracellular region of HER3 reveals an interdomain tether. *Science*, **297**: 1330-1333.
- Cho H-S, Mason K, Ramyar KX, Stanley AM, Gabelli SB, Denney DW & Leahy DJ (2003). Structure of the extracellular region of HER2 alone and in complex with the Herceptin Fab. *Nature*, **421**: 756.
- Chobotova K, Spyropoulou I, Carver J, Manek S, Heath JK, Gullick WJ, Barlow DH, Sargent IL & Mardon HJ (2002). Heparin-binding epidermal growth factor and its receptor ErbB4 mediate implantation of the human blastocyst. *Mech Dev*, **119**: 137-144.
- Choudhury A, Charo J, Parapuram SK, Hunt RC, Hunt DM, Seliger B & Kiessling R (2004). Small interfering RNA (siRNA) inhibits the expression of the Her2/neu gene, upregulates HLA class I and induces apoptosis of Her2/neu positive tumor cell lines. *Int J Cancer*, **108**: 71-77.
- Christianson TA, Doherty JK, Lin YJ, Ramsey EE, Holmes R, Keenan EJ & Clinton GM (1998). NH2-terminally Truncated HER-2/neu Protein: Relationship with Shedding of the Extracellular Domain and with Prognostic Factors in Breast Cancer. *Cancer Res*, **58**: 5123-5129.
- Chun R, Garrett LD & Vail DM (2007). Cancer Chemotherapy. Withrow & McEwan's Small Animal Clinical Oncology, Saunders. 4th Ed. 163-192.
- Clynes RA, Towers TL, Presta LG & Ravetch JV (2000). Inhibitory Fc receptors modulate in vivo cytotoxicity against tumor targets. *Nat Med*, **6**: 443-446.
- Codony-Servat J, Albanell J, Lopez-Talavera JC, Arribas J & Baselga J (1999). Cleavage of the HER2 ectodomain is a pervanadate-activable process that is inhibited by the tissue inhibitor of metalloproteases-1 in breast cancer cells. *Cancer Res*, **59**: 1196-1201.
- Cozy E, Borgna J-L & Rochefort H (1982). Tamoxifen and Metabolites in MCF7 Cells: Correlation between Binding to Estrogen Receptor and Inhibition of Cell Growth. *Cancer Res*, **42**: 317-323.
- Cohen BD, Green JM & Fell HP (1996). HER4-mediated biological and biochemical properties in NIH 3T3 cells. Evidence for HER1-HER4 heterodimers. *J Biol Chem*, **271**: 4813-4818.
- Cohen S (1997). EGF and its receptor: historical perspective. Introduction. *J Mammary Gland Biol Neoplasia*, **2**: 93-96.
- Coussens LM & Werb Z (1996). Matrix metal loproteinases and the development of cancer. *Chem Biol*, **3**: 895-904.
- Czarnetzki A (1980). Pathological changes in the morphology of the young paleolithic skeletal remains from Stetten (south-west Germany). *J Hum Evol*, **9**: 15-17.

- Damjanov I, Mildner B & Knowles BB (1986). Immunohistochemical localization of the epidermal growth factor receptor in normal human tissues. *Lab Invest*, **55**: 588-592.
- David AR & Zimmerman MR (2010). Cancer: an old disease, a new disease or something in between? *Nat Rev Cancer*, **10**: 728-733.
- Desta Z, Ward BA, Soukhova NV & Flockhart DA (2004). Comprehensive Evaluation of Tamoxifen Sequential Biotransformation by the Human Cytochrome P450 System in Vitro: Prominent Roles for CYP3A and CYP2D6. *J Pharmacol Exp Ther*, **310**: 1062-1075.
- Díaz-Montes TP, Ji H, Smith-Sehdev AE, Zahurak ML, Kurman RJ, Armstrong DK & Bristow RE (2006). Clinical significance of Her-2/neu overexpression in uterine serous carcinoma. *Gynecol Oncol*, **100**: 139-144.
- Dorn CR, Taylor DO, Schneider R, Hibbard HH & Klauber MR (1968). Survey of animal neoplasms in Alameda and Contra Costa Counties, California. II. Cancer morbidity in dogs and cats from Alameda County. *40*, **2**.
- Dosztányi Z, Csizmók V, Tompa P & Simon I (2005). IUPred: web server for the prediction of intrinsically unstructured regions of proteins based on estimated energy content. *Bioinformatics*, **21**: 3433-3434.
- Dosztányi Z, Csizmók V, Tompa P & Simon I (2005). The Pairwise Energy Content Estimated from Amino Acid Composition Discriminates between Folded and Intrinsically Unstructured Proteins. *J Mol Biol*, **347**: 827-839.
- Dubchak I, Brudno M, Loots GG, Mayor C, Pachter L, E.M. R & K.A. F (2000). Active Conservation of Noncoding Sequences Revealed by 3-way Species Comparisons. *Genome Res*, **10**: 1304-1306.
- Dunn M, Sinha P, Campbell R, Blackburn E, Levinson N, Rampaul R, Bates T, Humphreys S & Gullick WJ (2004). Co-expression of neuregulins 1, 2, 3 and 4 in human breast cancer. *J Pathol*, **203**: 672-680.
- Dutra A, Granja N, Schmitt F & Cassali G (2004). c-erbB-2 expression and nuclear pleomorphism in canine mammary tumors. *Braz J Med Biol Res*, **37**: 1673-1681.
- Edwards PAW (2010). Fusion genes and chromosome translocations in the common epithelial cancers. *J Pathol*, **220**: 244-254.
- Embrace Pet Insurance (2009). *Facts & Statistics on the US Pet Insurance Industry* [WWW Reference]. Last Accessed: 9th March, 2012. Available from: <http://www.embracepetinsurance.com/about-us/press/pet-insurance-statistics.aspx>.
- Ensembl (2010). *BlastView* [WWW Reference]. Last Accessed: April 26th, 2010. Available from: <http://www.ensembl.org/Multi/blastview>.

Ensinger C, Prommegger R, Kendler D, Gabriel M, Spizzo G, Mikuz G & Kremser R (2003). Her2/neu expression in poorly-differentiated and anaplastic thyroid carcinomas. *Anticancer Res*, **23**: 2349-2353.

Esworthy RS & Neville DM (1984). A comparative study of ricin and diphtheria toxin-antibody-conjugate kinetics on protein synthesis inactivation. *J Biol Chem*, **259**: 11496-11504.

European Medicines Agency (2010). *Masivet (Masitinib)* [WWW Reference]. Last Accessed: 17th November, 2011. Available from: http://www.ema.europa.eu/ema/index.jsp?curl=pages/medicines/veterinary/medicines/000128/vet_med_000137.jsp&mid=WC0b01ac058001fa1c.

European Society of Veterinary Oncology (2010). *Information for Pet Owners* [WWW Reference]. Last Accessed: 25th March, 2010. Available from: <http://www.esvonc.org/PetownerbrnbspnbspnInformation/tabid/54/Default.aspx>.

Fabian MA, Biggs WH, Treiber DK, Atteridge CE, Azimioara MD, Benedetti MG, Carter TA, Ciceri P, Edeen PT, Floyd M, Ford JM, Galvin M, Gerlach JL, Grotzfeld RM, Herrgard S, Insko DE, Insko MA, Lai AG, Lélías JM, Mehta SA, Milanov ZV, Velasco AM, Wodicka LM, Patel HK, Zarrinkar PP & Lockhart DJ (2005). A small molecule-kinase interaction map for clinical kinase inhibitors. *Nat Biotechnol*, **23**: 329-336.

Falls DL (2003). Neuregulins and the neuromuscular system: 10 years of answers and questions. *J Neurocytol*, **32**: 619-647.

Falls DL (2003). Neuregulins: functions, forms, and signaling strategies. *Exp Cell Res*, **284**: 14-30.

Faltus T, Yuan J, Zimmer B, Krämer A, Loibl S, Kaufmann M & Strebhardt K (2004). Silencing of the HER2/neu gene by siRNA inhibits proliferation and induces apoptosis in HER2/neu-overexpressing breast cancer cells. *Neoplasia*, **6**: 786-795.

Ferguson KM, Berger MB, Mendrola JM, Cho H-S, Leahy DJ & Lemmon MA (2003). EGF Activates Its Receptor by Removing Interactions that Autoinhibit Ectodomain Dimerization. *Mol Cell*, **11**: 507.

Ferguson KM, Berger MB, Mendrola JM, Cho H-S, Leahy DJ & Lemmon MA (2003). EGF Activates Its Receptor by Removing Interactions that Autoinhibit Ectodomain Dimerization. *Mol Cell*, **11**: 507-517.

Ferlay J, Shin H-R, Bray F, Forman D, Mathers C & Parkin DM (2010). Estimates of worldwide burden of cancer in 2008: GLOBOCAN 2008. *Int J Cancer*, **127**: 2893-2917.

Fleck LM (2006). The Cost of Caring: Who Pays? Who Profits? Who Panders? *Hastings Cent Rep*, **36**: 13-17.

Flynn JF, Wong C & Wu JM (2009). Anti-EGFR Therapy: Mechanism and Advances in Clinical Efficacy in Breast Cancer. *J Oncol*, Epub ID: 526963 April 14th 2009.

- Frazer KA, Pachter L, Poliakov A, Rubin EM & Dubchak I (2004). VISTA: computational tools for comparative genomics. *Nucleic Acids Res*, **32**: W273-279.
- Fuller SJ, Sivarajah K & Sugden PH (2008). ErbB receptors, their ligands, and the consequences of their activation and inhibition in the myocardium. *J Mol Cell Cardiol*, **44**: 831.
- Gama A, Alves A & Schmitt F (2008). Identification of molecular phenotypes in canine mammary carcinomas with clinical implications: application of the human classification. *Virchows Archiv*, **453**: 123-132.
- Gassmann M, Casagrande F, Orioli D, Simon H, Lai C, Klein R & Lemke G (1995). Aberrant neural and cardiac development in mice lacking the ErbB4 neuregulin receptor. *Nature*, **378**: 390-394.
- Gassmann M, Casagrande F, Orioli D, Simon H, Lai C, Klein R & Lemke G (1995). Aberrant neural and cardiac development in mice lacking the ErbB4 neuregulin receptor. *Nature*, **378**: 390-394.
- Gaush CR, Hard WL & Smith TF (1966). Characterization of an established line of canine kidney cells (MDCK). *Proc Soc Exp Biol Med*, **122**: 931-935.
- Genentech (2009). *Herceptin - Historical Sales* [WWW Reference]. Last Accessed: 20th September, 2010. Available from: <http://www.gene.com/gene/about/ir/historical/product-sales/herceptin.html>.
- Genomics Division of Lawrence Berkeley National Laboratory (1997). *VISTA (Visualisation Tool for Alignments)* [WWW Reference]. Last Accessed: 18th August, 2010. Available from: <http://genome.lbl.gov/vista/index.shtml>.
- Gerlai R, Pisacane P & Erickson S (2000). Heregulin, but not ErbB2 or ErbB3, heterozygous mutant mice exhibit hyperactivity in multiple behavioral tasks. *Behavioural Brain Research*, **109**: 219-227.
- Gillies SD, Lan Y, Williams S, Carr F, Forman S, Raubitschek A & Lo K-M (2005). An anti-CD20-IL-2 immunocytokine is highly efficacious in a SCID mouse model of established human B lymphoma. *Blood*, **105**: 3972-3978.
- Gilmour LMR, Macleod KG, McCaig A, Gullick WJ, Smyth JF & Langdon SP (2001). Expression of erbB-4/HER-4 Growth Factor Receptor Isoforms in Ovarian Cancer. *Cancer Research*, **61**: 2169-2176.
- Girish S, Gupta M, Wang B, Lu D, Krop I, Vogel C, Burris iii H, LoRusso P, Yi J-H, Saad O, Tong B, Chu Y-W, Holden S & Joshi A Clinical pharmacology of trastuzumab emtansine (T-DM1): an antibody-drug conjugate in development for the treatment of HER2-positive cancer. *Cancer Chemother Pharmacol*: 1-12.
- Gollamudi M, Nethery D, Liu J & Kern JA (2004). Autocrine activation of ErbB2/ErbB3 receptor complex by NRG-1 in non-small cell lung cancer cell lines. *Lung Cancer*, **43**: 135-143.

- Goodman S & Check E (2002). Animal experiments: The great primate debate. *Nature*, **417**: 684-687.
- Gotoh N, Tojo A, Hino M, Yazaki Y & Shibuya M (1992). A highly conserved tyrosine residue at codon 845 within the kinase domain is not required for the transforming activity of human epidermal growth factor receptor. *Biochem Biophys Res Commun*, **186**: 768.
- Greenberg S, Chang P & Silverstein SC (1993). Tyrosine phosphorylation is required for Fc receptor-mediated phagocytosis in mouse macrophages. *J Exp Med*, **177**: 529-534.
- Greulich H, Chen T-H, Feng W, Jänne PA, Alvarez JV, Zappaterra M, Bulmer SE, Frank DA, Hahn WC, Sellers WR & Meyerson M (2005). Oncogenic Transformation by Inhibitor-Sensitive and -Resistant EGFR Mutants. *PLoS Med*, **2**: e313.
- Gullick WJ (2001). The Type 1 growth factor receptors and their ligands considered as a complex system. *Endocr Relat Cancer*, **8**: 75-82.
- Gullick WJ, Berger MS, Bennett PL, Rothbard JB & Waterfield MD (1987). Expression of the c-erbB-2 protein in normal and transformed cells. *Int J Cancer*, **40**: 246-254.
- Gullick WJ, Marsden JJ, Whittle N, Ward B, Bobrow L & Waterfield MD (1986). Expression of Epidermal Growth Factor Receptors on Human Cervical, Ovarian, and Vulval Carcinomas. *Cancer Res*, **46**: 285-292.
- Gusterson B, Cowley G, Smith JA & Ozanne B (1984). Cellular localization of human epidermal growth factor receptor. *Cell Biol Int Rep*, **8**: 649-658.
- Gusterson BA, Gullick WJ, Venter DJ, Powles TJ, Elliott C, Ashley S, Tidy A & Harrison S (1987). Immunohistochemical localization of c-erbB-2 in human breast carcinomas. *Mol Cell Probes*, **1**: 383-391.
- Hague AK, Syed S, Lele SM, Freeman DH & Adegboyega PA (2002). Immunohistochemical study of thyroid transcription factor-1 and HER2/neu in non-small cell lung cancer: strong thyroid transcription factor-1 expression predicts better survival. *Appl Immunohistochem Mol Morphol*, **10**: 103-109.
- Hahn KA, Ogilvie G, Rusk T, Devauchelle P, Leblanc A, Legendre A, Powers B, Leventhal PS, Kinet JP, Palmerini F, Dubreuil P, Moussy A & Hermine O (2008). Masitinib is safe and effective for the treatment of canine mast cell tumors. *J Vet Intern Med*, **22**: 1301-1309.
- Hanahan D & Folkman J (1996). Patterns and emerging mechanisms of the angiogenic switch during tumorigenesis. *Cell*, **86**: 353-364.
- Hanahan D & Weinberg RA (2000). The Hallmarks of Cancer. *Cell*, **100**: 57-70.
- Harbeck N, Ross JS, Yurdseven S, Dettmar P, Pölcher M, Kuhn W, Ulm K, Graeff H & Schmitt M (1999). HER-2/neu gene amplification by fluorescence in situ hybridization allows risk-group assessment in node-negative breast cancer. *Int J Oncol*, **14**: 663-671.

- Harris CC (1996). COMMENTARY: p53 Tumor suppressor gene: from the basic research laboratory to the clinic—an abridged historical perspective. *Carcinogenesis*, **17**: 1187-1198.
- Harris RC, Chung E & Coffey RJ (2003). EGF receptor ligands. *Exp Cell Res*, **284**: 2-13.
- Hayflick L (1997). Mortality and immortality at the cellular level. A review. *Biochemistry (Mosc)*, **62**: 1180-1190.
- Hellström I, Goodman G, Pullman J, Yang Y & Hellström KE (2001). Overexpression of HER-2 in Ovarian Carcinomas. *Cancer Res*, **61**: 2420-2423.
- Herbst RS (2004). Review of epidermal growth factor receptor biology. *Int J Radiat Oncol Biol Phys*, **59**: 21-26.
- Higashiyama S, Iwabuki H, Morimoto C, Hieda M, Inoue H & Matsushita N (2008). Membrane-anchored growth factors, the epidermal growth factor family: Beyond receptor ligands. *Cancer Sci*, **99**: 214-220.
- Higashiyama S, Nanba D, Nakayama H, Inoue H & Fukuda S (2011). Ectodomain shedding and remnant peptide signalling of EGFRs and their ligands. *J Biochem*, **150**: 15-22.
- Hsu W-L, Huang H-M, Liao J-W, Wong M-L & Chang S-C (2009). Increased survival in dogs with malignant mammary tumours overexpressing HER-2 protein and detection of a silent single nucleotide polymorphism in the canine HER-2 gene. *The Veterinary Journal*, **180**: 116-123.
- Huang X & Miller W (1991). A time-efficient, linear-space local similarity algorithm. *Adv. Appl. Math.*, **12**: 337-357.
- Hubbard SR, Mohammadi M & Schlessinger J (1998). Autoregulatory Mechanisms in Protein-tyrosine Kinases. *J Biol Chem*, **273**: 11987-11990.
- Hunt CR, Hale RJ, Armstrong C, Rajkumar, Gullick WJ & Buckley CH (1995). c-erbB-3 proto-oncogene expression in uterine cervical carcinoma. *Int J Gynecol Cancer*, **5**: 282-285.
- Ikemoto N, Kumar RA, Ling TT, Ellestad GA, Danishefsky SJ & Patel DJ (1995). Calicheamicin-DNA complexes: warhead alignment and saccharide recognition of the minor groove. *Proc Natl Acad Sci U S A*, **92**: 10506-10510.
- ISD Scotland Online (2011). *ISD Cancer Information Programme* [WWW Reference]. Last Accessed: 12th March, 2012. Available from: <http://www.isdscotlandarchive.scot.nhs.uk/isd/183.html>.
- Jackson JG, St. Clair P, Sliwkowski MX & Brattain MG (2004). Blockade of Epidermal Growth Factor- or Heregulin-Dependent ErbB2 Activation with the Anti-ErbB2 Monoclonal Antibody 2C4 Has Divergent Downstream Signaling and Growth Effects. *Cancer Res*, **64**: 2601-2609.
- Janmaat ML, Kruyt FAE, Rodriguez JA & Giaccone G (2003). Response to Epidermal Growth Factor Receptor Inhibitors in Non-Small Cell Lung Cancer Cells. *Clin Cancer Res*, **9**: 2316-2326.

- Jordan VC (1982). Metabolites of tamoxifen in animals and man: identification, pharmacology and significance. *Breast Cancer Res Treat*, **2**: 123-138.
- Jorissen RN, Walker F, Pouliot N, Garrett TPJ, Ward CW & Burgess AW (2003). Epidermal growth factor receptor: mechanisms of activation and signalling. *Exp Cell Res*, **284**: 31.
- Kainer RA & McCracken T (2002). *Dog Anatomy: A Colouring Atlas* [Book]. Teton NewMedia.
- Kameda T, Yasui W, Yoshida K, Tsujino T, Nakayama H, Ito M, Ito H & Tahara E (1990). Expression of ERBB2 in Human Gastric Carcinomas: Relationship between p185ERBB2 Expression and the Gene Amplification. *Cancer Res*, **50**: 8002-8009.
- Kaminski MS, Tuck M, Estes J, Kolstad A, Ross CW, Zasadny K, Regan D, Kison P, Fisher S, Kroll S & Wahl RL (2005). 131I-Tositumomab Therapy as Initial Treatment for Follicular Lymphoma. *New England Journal of Medicine*, **352**: 441-449.
- Karlsson EK & Lindblad-Toh K (2008). Leader of the pack: gene mapping in dogs and other model organisms. *Nat Rev Genet*, **9**: 713-725.
- Kawamoto T, Sato JD, Le A, Polikoff J, Sato GH & Mendelsohn J (1983). Growth stimulation of A431 cells by epidermal growth factor: identification of high-affinity receptors for epidermal growth factor by an anti-receptor monoclonal antibody. *Proc Natl Acad Sci*, **80**: 1337-1341.
- Kelsey JL, Moore AS & Glickman T (1998). Epidemiologic Studies of Risk Factors for Cancer in Pet Dogs. *Epidemiol Rev*, **20**: 204-217.
- Kennel Club (2009) Kennel Club Announces Healthy New Year Regulations for Pedigree Dogs. [News Article]. Last Accessed: 8th March 2012. Available from: <http://www.thekennelclub.org.uk/item/2234/23/5/3>
- Knize MG, Salmon CP & Felton JS (2003). Mutagenic activity and heterocyclic amine carcinogens in commercial pet foods. *Mutat Res*, **539**: 195.
- Knowles PP, Murray-Rust J, Kjær S, Scott RP, Hanrahan H, Santoro M, Ibañez CF & McDonald NQ (2006). Structure and Chemical Inhibition of the RET Tyrosine Kinase Domain. *J Biol Chem*, **281**: 33577-33587.
- Kobayashi K, Kumakura M, Yoshimura K, Nonaka K, Murayama T & Henneberg M (2003). Comparative morphological study of the lingual papillae and their connective tissue cores of the koala. *Anatomy and Embryology*, **206**: 247-254.
- Kroger Pet Insurance (2012). *History of Pet Insurance* [WWW Reference]. Last Accessed: 8th March, 2012. Available from: <http://www.savewithpetinsurance.com/pet-insurance-history>.
- Krüger S, Lange I, Kausch I & Feller AC (2005). Protein Expression and Gene Copy Number Analysis of Topoisomerase 2 α , HER2 and P53 in Minimally Invasive Urothelial Carcinoma of

the Urinary Bladder - a Multitissue Array Study with Prognostic Implications. *Anticancer Res*, **25**: 263-271.

Kwak EL, Sordella R, Bell DW, Godin-Heymann N, Okimoto RA, Brannigan BW, Harris PL, Driscoll DR, Fidias P, Lynch TJ, Rabindran SK, McGinnis JP, Wissner A, Sharma SV, Isselbacher KJ, Settleman J & Haber DA (2005). Irreversible inhibitors of the EGF receptor may circumvent acquired resistance to gefitinib. *Proc Natl Acad Sci U S A*, **102**: 7665-7670.

Kwong KY & Hung M-C (1998). A novel splice variant of HER2 with increased transformation activity. *Mol Carcinog*, **23**: 62-68.

Laemmli UK (1970). Cleavage of Structural Proteins during the Assembly of the Head of Bacteriophage T4. *Nature*, **227**: 680-685.

Lane HA, Beuvink I, Motoyama AB, Daly JM, Neve RM & Hynes NE (2000). ErbB2 Potentiates Breast Tumor Proliferation through Modulation of p27Kip1-Cdk2 Complex Formation: Receptor Overexpression Does Not Determine Growth Dependency. *Mol Cell Biol*, **20**: 3210-3223.

Latif Z, Watters AD, Dunn I, Grigor K, Underwood MA & Bartlett JMS (2004). HER2/neu gene amplification and protein overexpression in G3 pT2 transitional cell carcinoma of the bladder: a role for anti-HER2 therapy? *Eur J Cancer*, **40**: 56-63.

Lax I, Johnson A, Howk R, Sap J, Bellot F, Winkler M, Ullrich A, Vennstrom B, Schlessinger J & Givol D (1988). Chicken epidermal growth factor (EGF) receptor: cDNA cloning, expression in mouse cells, and differential binding of EGF and transforming growth factor alpha. *Mol Cell Biol*, **8**: 1970-1978.

Le Cesne A, Blay J-Y, Bui BN, Bouché O, Adenis A, Domont J, Cioffi A, Ray-Coquard I, Lassau N, Bonvalot S, Moussy A, Kinet J-P & Hermine O (2010). Phase II study of oral masitinib mesilate in imatinib-naïve patients with locally advanced or metastatic gastro-intestinal stromal tumour (GIST). *Eur J Cancer*, **46**: 1344-1351.

Lee K-F, Simon H, Chen H, Bates B, Hung M-C & Hauser C (1995). Requirement for neuregulin receptor erbB2 in neural and cardiac development. *Nature*, **378**: 394-398.

Lehväslaiho H, Lehtola L, Sistonen L & Alitalo K (1989). A chimeric EGF-R-neu proto-oncogene allows EGF to regulate neu tyrosine kinase and cell transformation. *EMBO J*, **8**: 159-166.

Lemoine NR, Jain S, Silvestre F, Lopes C, Hughes CM, McLelland E, Gullick WJ & Filipe MI (1991). Amplification and overexpression of the EGF receptor and c-erbB-2 proto-oncogenes in human stomach cancer. *Br J Cancer*, **64**: 79-83.

LeRoy BE & Northrup N (2009). Prostate cancer in dogs: Comparative and clinical aspects. *Vet J*, **180**: 149.

Linggi B & Carpenter G (2006). ErbB receptors: new insights on mechanisms and biology. *Trends Cell Biol*, **16**: 649.

- Liu X, Baker E, Eyre HJ, Sutherland GR & Zhou M (1999). Gamma-heregulin: a fusion gene of DOC-4 and neuregulin-1 derived from a chromosome translocation. *Oncogene*, **18**: 7110-7114.
- Lode HN, Xiang R, Becker JC, Gillies SD & Reisfeld RA (1998). Immunocytokines: a promising approach to cancer immunotherapy. *Pharmacol Ther*, **80**: 277-292.
- London CA, Hannah AL, Zadovoskaya R, Chien MB, Kollias-Baker C, Rosenberg M, Downing S, Post G, Boucher J, Shenoy N, Mendel DB, McMahon G & Cherrington JM (2003). Phase I Dose-Escalating Study of SU11654, a Small Molecule Receptor Tyrosine Kinase Inhibitor, in Dogs with Spontaneous Malignancies. *Clin Cancer Res*, **9**: 2755-2768.
- Lord LK, Yaissle JE, Marin L & Couto CG (2007). Results of a web-based health survey of retired racing Greyhounds. *J Vet Intern Med*, **21**: 1243-1250.
- Luetke NC, Phillips HK, Qiu TH, Copeland NG, Earp HS, Jenkins NA & Lee DC (1994). The mouse waved-2 phenotype results from a point mutation in the EGF receptor tyrosine kinase. *Genes Dev*, **8**: 399-413.
- Lupu R, Cardillo M, Cho C, Harris L, Hijazi M, Perez C, Rosenberg K, Yang D & Tang C (1996). The significance of heregulin in breast cancer tumor progression and drug resistance. *Breast Cancer Res Treat*, **38**: 57-66.
- Lyon E, Millson A, Lowery MC, Woods R & Wittwer CT (2001). Quantification of HER2/neu Gene Amplification by Competitive PCR Using Fluorescent Melting Curve Analysis. *Clin Chem*, **47**: 844-851.
- Lyon, France: International Agency for Research on Cancer (2010). *GLOBOCAN 2008 v1.2, Cancer Incidence and Mortality Worldwide: IARC CancerBase No. 10* [WWW Reference]. Last Accessed: 12th March, 2012. Available from: <http://globocan.iarc.fr/>.
- Määttä JA, Sundvall M, Junttila TT, Peri L, Laine VJO, Isola J, Egeblad M & Elenius K (2006). Proteolytic Cleavage and Phosphorylation of a Tumor-associated ErbB4 Isoform Promote Ligand-independent Survival and Cancer Cell Growth. *Mol Biol Cell*, **17**: 67-79.
- Mamot C, Drummond DC, Greiser U, Hong K, Kirpotin DB, Marks JD & Park JW (2003). Epidermal Growth Factor Receptor (EGFR)-targeted Immunoliposomes Mediate Specific and Efficient Drug Delivery to EGFR- and EGFRvIII-overexpressing Tumor Cells. *Cancer Res*, **63**: 3154-3161.
- Mann GB, Fowler KJ, Gabriel A, Nice EC, Williams RL & Dunn AR (1993). Mice with a null mutation of the TGF α gene have abnormal skin architecture, wavy hair, and curly whiskers and often develop corneal inflammation. *Cell*, **73**: 249-261.
- Marchini C, Gabrielli F, Iezzi M, Zenobi S, Montani M, Pietrella L, Kalogris C, Rossini A, Ciravolo V, Castagnoli L, Tagliabue E, Pupa SM, Musiani P, Monaci P, Menard S & Amici A (2011). The human splice variant Δ 16HER2 induces rapid tumor onset in a reporter transgenic mouse. *PLoS One*, **6**: e18727.

Martín de las Mulas J, Ordás J, Millán Y, Fernández-Soria V & Ramón y Cajal S (2003). Oncogene HER-2 in Canine Mammary Gland Carcinomas. *Breast Cancer Res Treat*, **80**: 363-367.

Mason WE (1915). *Dogs of All Nations* [Book]. Kessinger Publishing.

Matsubara H, Yamada Y, Naruse K, Nakamura K, Aoki S, Taki T, Tobiume M, Zennami K, Katsuda R & Honda N (2008). Potential for HER-2/neu molecular targeted therapy for invasive bladder carcinoma: comparative study of immunohistochemistry and fluorescent in situ hybridization. *Oncol Rep*, **19**: 57-63.

Mendoza N, Phillips GL, Silva J, Schwall R & Wickramasinghe D (2002). Inhibition of Ligand-mediated HER2 Activation in Androgen-independent Prostate Cancer. *Cancer Res*, **62**: 5485-5488.

Meng S, Tripathy D, Shete S, Ashfaq R, Haley B, Perkins S, Beitsch P, Khan A, Euhus D, Osborne C, Frenkel E, Hoover S, Leitch M, Clifford E, Vitetta E, Morrison L, Herlyn D, Terstappen LW, Fleming T, Fehm T, Tucker T, Lane N, Wang J & Uhr J (2004). HER-2 gene amplification can be acquired as breast cancer progresses. *Proc Natl Acad Sci*, **101**: 9393-9398.

The Merck Veterinary Manual. Merck, Edited by: C. M. Kahn. (2010). Merck, 9th edition.

Merlo DF, Rossi L, Pellegrino C, Ceppi M, Cardellino U, Capurro C, Ratto A, Sambucco PL, Sestito V, Tanara G & Bocchini V (2008). Cancer Incidence in Pet Dogs: Findings of the Animal Tumor Registry of Genoa, Italy. *J Vet Intern Med*, **22**: 976-984.

Meyer D & Birchmeier C (1995). Multiple essential functions of neuregulin in development. *Nature*, **378**: 386-390.

Minami Y, Shimamura T, Shah K, LaFramboise T, Glatt KA, Liniker E, Borgman CL, Haringsma HJ, Feng W, Weir BA, Lowell AM, Lee JC, Wolf J, Shapiro GI, Wong K-K, Meyerson M & Thomas RK (2007). The major lung cancer-derived mutants of ERBB2 are oncogenic and are associated with sensitivity to the irreversible EGFR/ERBB2 inhibitor HKI-272. *Oncogene*, **26**: 5023-5027.

Mintel Reports Summary (2008). *Pet Accessories and Healthcare - UK - September 2008* [Report]. Last Accessed: 8th March, 2012. Available from: <http://oxygen.mintel.com/sinatra/oxygen/display/id=227705>.

Mitra D, Brumlik MJ, Okamgba SU, Zhu Y, Duplessis TT, Parvani JG, Lesko SM, Brogi E & Jones FE (2009). An oncogenic isoform of HER2 associated with locally disseminated breast cancer and trastuzumab resistance. *Mol Cancer Ther*, **8**: 2152-2162.

Moelans CB, Milne AN, Morsink FH, Offerhaus GJA & van Diest PJ (2011). Low frequency of HER2 amplification and overexpression in early onset gastric cancer. *Cell Oncol*, **34**: 89-95.

Molina MA, Codony-Servat J, Albanell J, Rojo F, Arribas J & Baselga J (2001). Trastuzumab (herceptin), a humanized anti-Her2 receptor monoclonal antibody, inhibits basal and activated Her2 ectodomain cleavage in breast cancer cells. *Cancer Res*, **61**: 4744-4749.

Molina MA, Sáez R, Ramsey EE, Garcia-Barchino MJ, Rojo F, Evans AJ, Albanell J, Keenan EJ, Lluch A, García-Conde J, Baselga J & Clinton GM (2002). NH(2)-terminal truncated HER-2 protein but not full-length receptor is associated with nodal metastasis in human breast cancer. *Clin Cancer Res*, **8**: 347-353.

Morgan GE, Mikhail MS & Murray MJ (2005). *Clinical Anaesthesiology* [Book]. McGraw-Hill Professional.

Moscoso LM, Chu GC, Gautam M, Noakes PG, Merlie JP & Sanes JR (1995). Synapse-associated expression of an acetylcholine receptor-inducing protein, ARIA/heregin, and its putative receptors, ErbB2 and ErbB3, in developing mammalian muscle. *Dev Biol*, **172**: 158-169.

Motoyama AB, Hynes NE & Lane HA (2002). The Efficacy of ErbB Receptor-targeted Anticancer Therapeutics Is Influenced by the Availability of Epidermal Growth Factor-related Peptides. *Cancer Res*, **62**: 3151-3158.

Moutsatsou P & Papavassiliou AG (2007). The glucocorticoid receptor signalling in breast cancer. *J Cell Mol Med*, **12**: 145-163.

Munday JS & Kiupel M (2010). Papillomavirus-Associated Cutaneous Neoplasia in Mammals. *Vet Pathol*, **Epub ahead of print**.

Murray JK, Browne WJ, Roberts MA, Whitmarsh A & Gruffydd-Jones TJ (2010). Number and ownership profiles of cats and dogs in the UK. *Vet Rec*, **166**: 163-168.

Myers SM, Eng C, Ponder BA & Mulligan LM (1995). Characterization of RET proto-oncogene 3' splicing variants and polyadenylation sites: a novel C-terminus for RET. *Oncogene*, **16**: 2039-2045.

Nahta R & Esteva FJ (2006). Herceptin: mechanisms of action and resistance. *Cancer Lett*, **232**: 123-138.

Natarajan LC, Melott AL, Rothschild BM & Martin LD (2007). Bone cancer rates in dinosaurs compared with modern vertebrates. *Trans Kans Acad Sci*, **110**: 155-158.

NCBI (National Center for Biotechnology Information) (2010). *NCBI Entrez Protein* [WWW Reference]. Last Accessed: April 15th, 2010. Available from: <http://www.ncbi.nlm.nih.gov/protein>.

Neddens J & Buonanno A (2011). Expression of the Neuregulin Receptor ErbB4 in the Brain of the Rhesus Monkey (*Macaca mulatta*). *PLoS One*, **6**: e27337.

Nerurkar VR, Seshadri R, Mulherkar R, Ishwad CS, Lalitha VS & Naik SN (1987). Receptors for epidermal growth factor and estradiol in canine mammary tumors. *Int J Cancer*, **40**: 230-232.

Nicholls PK & Stanley MA (1999). Canine Papillomavirus--A Centenary Review. *J Comp Pathol*, **120**: 219.

Normanno N, Qi C, Gullick W, Persico G, Yarden Y, Wen D, Plowman G, Kenney N, Johnson G, Kim N, Brandt R, Martinezlacaci I, Dickson R & Salomon D (1993). Expression of amphiregulin, cripto-1, and heregulin-alpha in human breast-cancer cells. *Int J Oncol*, **2**: 903-911.

Northern Ireland Statistics and Research Agency (2008). *Online statistics: All Cancers* [WWW Reference]. Last Accessed: 12th March, 2012. Available from: <http://www.qub.ac.uk/research-centres/nicr/CancerData/OnlineStatistics/AllCancers/>.

Nuciforo PG, Pellegrini C, Fasani R, Maggioni M, Coggi G, Parafioriti A & Bosari S (2003). Molecular and immunohistochemical analysis of HER2/neu oncogene in synovial sarcoma. *Human pathology*, **34**: 639-645.

Office for National Statistics (2010). *Registrations of cancer diagnosed in 2008, England* [Report]. Last Accessed: 12th March, 2012. Available from: <http://www.ons.gov.uk/ons/index.html>.

Ohren JF, Chen H, Pavlovsky A, Whitehead C, Zhang E, Kuffa P, Yan C, McConnell P, Spessard C, Banotai C, Mueller WT, Delaney A, Omer C, Sebolt-Leopold J, Dudley DT, Leung IK, Flamme C, Warmus J, Kaufman M, Barrett S, Tecle H & Hasemann CA (2004). Structures of human MAP kinase kinase 1 (MEK1) and MEK2 describe novel noncompetitive kinase inhibition. *Nat Struct Mol Biol*, **11**: 1192-1197.

Olsen RJ, Lydiatt WM, Koepsell SA, Lydiatt D, Johansson SL, Naumann S, Bridge JA, Neff JR, Hinrichs SH & Tarantolo SR (2005). C-erb-B2 (HER2/neu) expression in synovial sarcoma of the head and neck. *Head & Neck*, **27**: 883-892.

Ostrander EA, Galibert F & Patterson DF (2000). Canine genetics comes of age. *Trends Genet*, **16**: 117.

Page K, Hava N, Ward B, Brown J, Guttery DS, Ruangpratheep C, Blighe K, Sharma A, Walker RA, Coombes RC & Shaw JA (2011). Detection of HER2 amplification in circulating free DNA in patients with breast cancer. *Br J Cancer*, **104**: 1342-1348.

Pandiella A, Lehvaslaiho H, Magni M, Alitalo K & Meldolesi J (1989). Activation of an EGFR/neu chimeric receptor: early intracellular signals and cell proliferation responses. *Oncogene*, **4**: 1299-1305.

Pao W, Miller V, Zakowski M, Doherty J, Politi K, Sarkaria I, Singh B, Heelan R, Rusch V, Fulton L, Mardis E, Kupfer D, Wilson R, Kris M & Varmus H (2004). EGF receptor gene mutations are common in lung cancers from "never smokers" and are associated with sensitivity of tumors to gefitinib and erlotinib. *Proc Natl Acad Sci U S A*, **101**: 13306-13311.

Pao W, Miller VA, Politi KA, Riely GJ, Somwar R, Zakowski MF, Kris MG & Varmus H (2005). Acquired resistance of lung adenocarcinomas to gefitinib or erlotinib is associated with a second mutation in the EGFR kinase domain. *PLoS Med*, **2**: e73.

Paoloni M & Khanna C (2008). Translation of new cancer treatments from pet dogs to humans. *Nat Rev Can*, **8**: 147-156.

Park JW, Hong K, Kirpotin DB, Colbern G, Shalaby R, Baselga J, Shao Y, Nielsen UB, Marks JD, Moore D, Papahadjopoulos D & Benz CC (2002). Anti-HER2 Immunoliposomes. *Clin Cancer Res*, **8**: 1172-1181.

Park JW, Kirpotin DB, Hong K, Shalaby R, Shao Y, Nielsen UB, Marks JD, Papahadjopoulos D & Benz CC (2001). Tumor targeting using anti-her2 immunoliposomes. *J Control Release*, **74**: 95-113.

Park SI & Press OW (2007). Radioimmunotherapy for treatment of B-cell lymphomas and other hematologic malignancies. *Curr Opin Hematol*, **14**: 632-638.

Parker JE, Knowler SP, Rusbridge C, Noorman E & Jeffery ND (2011). Prevalence of asymptomatic syringomyelia in Cavalier King Charles spaniels. *Vet Rec*, **168**: 667.

PetPages (2010). *Schizophrenia Can Strike Your Pet* [WWW Reference]. Last Accessed: 14th December, 2011. Available from: <http://www.floridapetpages.com/articles/SchizophreniaInPets.html>. (Information provided by Dr. Arthur Newman DVM (owner of Crossroads Veterinary Clinic, 5987 Pine Ridge Road, Naples, Florida, USA) to floridapetpages.com.)

Pharmaceutical Research and Manufacturers of America (2007). *Drug Discovery and Development: Understanding the R&D Process*. Page 12. [Pamphlet Reference]. Last Accessed: 6th January 2011. Available from: http://www.pfmr.org/sites/default/files/159/rd_brochure_022307.pdf.

Plowman GD, Whitney GS, Neubauer MG, Green JM, McDonald VL, Todaro GJ & Shoyab M (1990). Molecular cloning and expression of an additional epidermal growth factor receptor-related gene. *Proc Natl Acad Sci U S A*, **87**: 4905-4909.

Press MF, Cordon-Cardo C & Slamon DJ (1990). Expression of the HER-2/neu proto-oncogene in normal human adult and foetal tissues. *Oncogene*, **5**: 953-962.

Prigent SA & Gullick WJ (1994). Identification of c-erbB-3 binding sites for phosphatidylinositol 3'-kinase and SHC using an EGF receptor/c-erbB-3 chimera. *EMBO J*, **13**: 2831-2841.

Prigent SA, Lemoine NR, Hughes CM, Plowman GD, Selden C & Gullick WJ (1992). Expression of the c-erbB-3 protein in normal human adult and foetal tissues. *Oncogene*, **7**: 1273-1278.

Pruitt KD, Harrow J, Harte RA, Wallin C, Diekhans M, Maglott DR, Searle S, Farrell CM, Loveland JE, Ruef BJ, Hart E, Suner MM, Landrum MJ, Aken B, Ayling S, Baertsch R, Fernandez-Banet J, Cherry JL, Curwen V, Dicuccio M, Kellis M, Lee J, Lin MF, Schuster M, Shkeda A, Amid C, Brown G, Dukhanina O, Frankish A, Hart J, Maidak BL, Mudge J, Murphy MR, Murphy T, Rajan J, Rajput B, Riddick LD, Snow C, Steward C, Webb D, Weber JA, Wilming L, Wu W, Birney E, Haussler D, Hubbard T, Ostell J, Durbin R & Lipman D (2009). The consensus coding sequence (CCDS) project: Identifying a common protein-coding gene set for the human and mouse genomes. *Genome Res*, **19**: 1316-1323.

Pryer NK, Lee LB, Zadovaskaya R, Yu X, Sukbuntherng J, Cherrington JM & London CA (2003). Proof of Target for SU11654: Inhibition of KIT Phosphorylation in Canine Mast Cell Tumors. *Clin Cancer Res*, **9**: 5729-5734.

Rabindran SK, Discafani CM, Rosfjord EC, Baxter M, Floyd MB, Golas J, Hallett WA, Johnson BD, Nilakantan R, Overbeek E, Reich MF, Shen R, Shi X, Tsou H-R, Wang Y-F & Wissner A (2004). Antitumor Activity of HKI-272, an Orally Active, Irreversible Inhibitor of the HER-2 Tyrosine Kinase. *Cancer Res*, **64**: 3958-3965.

Rassnick KM, Moore AS, Williams LE, London CA, Kintzer PP, Engler SJ & Cotter SM (1999). Treatment of canine mast cell tumors with CCNU (lomustine). *J Vet Intern Med*, **16**: 601-605.

Mintel Reports Summary (2005). *Pet Insurance - UK - December 2005* [Report]. Last Accessed: 8th March, 2012. Available from: <http://reports.mintel.com/sinatra/reports/index/&letter=16/display/id=125533&anchor=a125533>.

Reuters (2007). *UPDATE 1-Glaxo prepares to launch Cervarix after EU okay* [WWW Reference]. Last Accessed: Available from: <http://www.reuters.com/article/idUSL2446805720070924>.

Rivenson A & Silverman J (1979). The prostatic carcinoma in laboratory animals: a bibliographic survey from 1900 to 1977. *Invest Urol*, **16**: 468-472.

Robertson DW, Katzenellenbogen JA, Long DJ, Rorke EA & Katzenellenbogen BS (1982). Tamoxifen antiestrogens: a comparison of the activity, pharmacokinetics and metabolic activation of the cis and trans isomers of tamoxifen. *J Steroid Biochem*, **16**: 1-13.

Rungsipipat A, Ateyama S, Yamaguchi R, Uchida K, Miyoshi N & Hayashi T (1999). Immunohistochemical Analysis of c-yes and c-erbB-2 Oncogene Products and p53 Tumor Suppressor Protein in Canine Mammary Tumors. *J Vet Med Sci*, **61**: 27-32.

Rusnak DW, Lackey K, Affleck K, Wood ER, Alligood KJ, Rhodes N, Keith BR, Murray DM, Glennon K, Knight WB, Mullin RJ & Gilmer TM (2001). The Effects of the Novel, Reversible Epidermal Growth Factor Receptor/ErbB-2 Tyrosine Kinase Inhibitor, GW2016, on the Growth of Human Normal and Tumor-derived Cell Lines in Vitro and in Vivo. *Mol Cancer Ther*, **1**: 85-94.

Rutteman GR, Foekens JA, Portengen H, Vos JH, Blankenstein MA, Teske E, Cornelisse CJ & Misdorp W (1994). Expression of epidermal growth factor receptor (EGFR) in non-affected and tumorous mammary tissue of female dogs. *Breast Cancer Res Treat*, **30**: 139-146.

Saeki T, Stromberg K, Qi C-F, Gullick WJ, Tahara E, Normanno N, Ciardiello F, Kenney N, Johnson GR & Salomon DS (1992). Differential Immunohistochemical Detection of Amphiregulin and Cripto in Human Normal Colon and Colorectal Tumors. *Cancer Res*, **52**: 3467-3473.

- Sáez R, Molina MA, Ramsey EE, Rojo F, Keenan EJ, Albanell J, Lluch A, García-Conde J, Baselga J & Clinton GM (2006). p95HER-2 predicts worse outcome in patients with HER-2-positive breast cancer. *Clin Cancer Res*, **12**: 424-431.
- Santin AD (2003). HER2/neu overexpression: has the Achilles' heel of uterine serous papillary carcinoma been exposed? *Gynecol Oncol*, **88**: 263-265.
- Santin AD, Bellone S, Siegel ER, Palmieri M, Thomas M, Cannon MJ, Kay HH, Roman JJ, Burnett A & Pecorelli S (2005). Racial differences in the overexpression of epidermal growth factor type II receptor (HER2/neu): A major prognostic indicator in uterine serous papillary cancer. *Am J Obstet Gynecol*, **192**: 813-818.
- Scaltriti M, Rojo F, Ocaña A, Anido J, Guzman M, Cortes J, Di Cosimo S, Matias-Guiu X, Ramon y Cajal S, Arribas J & Baselga J (2007). Expression of p95HER2, a Truncated Form of the HER2 Receptor, and Response to Anti - HER2 Therapies in Breast Cancer. *J Natl Cancer Inst*, **99**: 628-638.
- Schaefer G, Fitzpatrick VD & Sliwkowski MX (1997). Gamma-heregulin: a novel heregulin isoform that is an autocrine growth factor for the human breast cancer cell line, MDA-MB-175. *Oncogene*, **15**: 1385-1394.
- Schuhmacher J, Klivényi G, Matys R, Stadler M, Regiert T, Hauser H, Doll J, Maier-Borst W & Zöller M (1995). Multistep Tumor Targeting in Nude Mice Using Bispecific Antibodies and a Gallium Chelate Suitable for Immunoscintigraphy with Positron Emission Tomography. *Cancer Res*, **55**: 115-123.
- Selvarajah GT, Verheije MH, Kik M, Slob A, Rottier PJ, Mol JA & Kirpensteijn J (2012). Expression of epidermal growth factor receptor in canine osteosarcoma: Association with clinicopathological parameters and prognosis. *Vet J*, **Epub ahead of print**.
- Sequist LV (2007). Second-Generation Epidermal Growth Factor Receptor Tyrosine Kinase Inhibitors in Non-Small Cell Lung Cancer. *Oncologist*, **12**: 325-330.
- Shay JW & Bacchetti S (1997). A survey of telomerase activity in human cancer. *Eur J Cancer*, **33**: 787-791.
- She Q-B, Solit D, Basso A & Moasser MM (2003). Resistance to Gefitinib in PTEN-Null HER-Overexpressing Tumor Cells Can Be Overcome through Restoration of PTEN Function or Pharmacologic Modulation of Constitutive Phosphatidylinositol 3 γ -Kinase/Akt Pathway Signaling. *Clin Cancer Res*, **9**: 4340-4346.
- Shi F, Telesco SE, Liu Y, Radhakrishnan R & Lemmon MA (2010). ErbB3/HER3 intracellular domain is competent to bind ATP and catalyze autophosphorylation. *Proceedings of the National Academy of Sciences*, **107**: 7692-7697.
- Shigematsu H, Takahashi T, Nomura M, Majmudar K, Suzuki M, Lee H, Wistuba II, Fong KM, Toyooka S, Shimizu N, Fujisawa T, Minna JD & Gazdar AF (2005). Somatic Mutations of the HER2 Kinase Domain in Lung Adenocarcinomas. *Cancer Research*, **65**: 1642-1646.

- Shing Y, Christofori G, Hanahan D, Ono Y, Sasada R, Igarashi K & Foljman J (1993). Betacellulin: a mitogen from pancreatic beta cell tumors. *Science*, **259**: 1604-1607.
- Shiple DL, Spigel DR, Carrell DL, Dannaher C, Greco FA, Hainsworth JD, Markus TM, Thompson D, Rotman R & Dannaher C (2009). Rituximab plus short-duration chemotherapy followed by Yttrium-90 Ibritumomab tiuxetan as first-line treatment for patients with follicular non-Hodgkin lymphoma: a phase II trial of the Sarah Cannon Oncology Research Consortium. *Clin Lymphoma Myeloma*, **9**: 223-228.
- Shipp S (2007). Structure and function of the cerebral cortex. *Curr Biol*, **17**: R443-449.
- Shiraiwa H, Sekine T, Tobisu K-i, Kakizoe T & Koiso K (1991). A New Form of Specific Targeting Cancer Immunotherapy Using Anti-tumor Monoclonal Antibody-conjugated Lymphokine-activated Killer Cells. *Cancer Sci*, **82**: 621-623.
- Siegel PM, Ryan ED, Cardiff RD & Muller WJ (1999). Elevated expression of activated forms of Neu/ErbB-2 and ErbB-3 are involved in the induction of mammary tumors in transgenic mice: implications for human breast cancer. *EMBO J*, **18**: 2149-2164.
- Simon R, Atefy R, Wagner U, Forster T, Fijan A, Bruderer J, Wilber K, Mihatsch MJ, Gasser T & Sauter G (2003). HER-2 and TOP2A coamplification in urinary bladder cancer. *Int J Cancer*, **107**: 764-772.
- Singh RK, Gutman M, Bucana CD, Sanchez R, Llansa N & Fidler IJ (1995). Interferons alpha and beta down-regulate the expression of basic fibroblast growth factor in human carcinomas. *Proc Natl Acad Sci*, **92**: 4562-4566.
- Slamon DJ, Clark GM, Wong SG, Levin WJ, Ullrich A & McGuire WL (1987). Human breast cancer: correlation of relapse and survival with amplification of the HER-2/neu oncogene. *Science*, **235**: 177-182.
- Slichenmyer WJ, Elliott WL & Fry DW (2001). CI-1033, a pan-erbB tyrosine kinase inhibitor. *Semin oncol*, **28**: 80-85.
- Sonnhammer ELL, Eddy SR & Durbin R (1997). Pfam: A comprehensive database of protein domain families based on seed alignments. *Proteins: Structure, Function, and Bioinformatics*, **28**: 405-420.
- Sordella R, Bell DW, Haber DA & Settleman J (2004). Gefitinib-sensitizing EGFR mutations in lung cancer activate anti-apoptotic pathways. *Science*, **305**: 1163-1167.
- Sporn MB (1996). The war on cancer. *Lancet*, **347**: 1377-1381.
- Srinivasan R, Benton E, McCormick F, Thomas H & Gullick WJ (1999). Expression of the c-erbB-3/HER-3 and c-erbB-4/HER-4 growth factor receptors and their ligands, neuregulin-1 α , neuregulin-1 β , and betacellulin, in normal endometrium and endometrial cancer. *Clin Cancer Res*, **5**: 2877-2883.

Srinivasan S, Poulson R, Hurst HC & Gullick WJ (1998). Expression of the c-erbB-4/HER4 protein and mRNA in normal human fetal and adult tissues and in a survey of nine solid tumour types. *J Pathol*, **185**: 236-245.

Stefansson H, Petursson H, Sigurdsson E, Steinthorsdottir V, Bjornsdottir S, Sigmundsson T, Ghosh S, Brynjolfsson J, Gunnarsdottir S, Ivarsson O, Chou TT, Hjaltason O, Birgisdottir B, Jonsson H, Gudnadottir VG, Gudmundsdottir E, Bjornsson A, Ingvarsson B, Ingason A, Sigfusson S, Hardardottir H, Harvey RP, Lai D, Zhou M, Brunner D, Mutel V, Gonzalo A, Lemke G, Sainz J, Johannesson G, Andresson T, Gudbjartsson D, Manolescu A, Frigge ML, Gurney ME, Kong A, Gulcher JR & Stefansson K (2002). Neuregulin 1 and Susceptibility to Schizophrenia. *American journal of human genetics*, **71**: 877-892.

Stein R & Staros J (2006). Insights into the evolution of the ErbB receptor family and their ligands from sequence analysis. *BMC Evol Biol*, **6**: 79.

Sundvall M, Veikkolainen V, Kurppa K, Salah Z, Tvorogov D, van Zoelen EJ, Aqeilan R & Elenius K (2010). Cell Death or Survival Promoted by Alternative Isoforms of ErbB4. *Mol Biol Cell*, **21**: 4275-4286.

Takai N, Jain A, Kawamata N, Popoviciu LM, Said JW, Whittaker S, Miyakawa I, Agus DB & Koeffler HP (2005). 2C4, a monoclonal antibody against HER2, disrupts the HER kinase signaling pathway and inhibits ovarian carcinoma cell growth. *Cancer*, **104**: 2701-2708.

Taylor F, Gear R, Hoather T & Dobson J (2009). Chlorambucil and prednisolone chemotherapy for dogs with inoperable mast cell tumors: 21 cases. *J Small Anim Pract*, **50**: 284-289.

Thamm DH, Mauldin EA & Vail DM (1999). Prednisone and vinblastine chemotherapy for canine mast cell tumor--41 cases (1992-1997). *J Vet Intern Med*, **15**: 491-497.

The Basset Hound Club (2011). *Events and Fixtures* [WWW Reference]. Last Accessed: 8th March, 2012. Available from: <http://www.bassethoundclub.co.uk/events.htm>.

The British Dalmatian Club (2009). *Addition of Imported Dalmatian/Pointer Backcrosses to the Kennel Club Registration System* [Report]. Last Accessed: 8th March, 2012. Available from: <http://www.britishdalmatianclub.org.uk/downloads/Submission%20to%20KC.pdf>.

The Bull Terrier Club (2002). *The Bull Terrier Club Home Page* [WWW Reference]. Last Accessed: 8th March, 2012. Available.

The Independent (2006) Scientists 'should be allowed to test on apes'. [News Article]. Last Accessed: 9th March 2012. Available from: <http://www.independent.co.uk/news/science/scientists-should-be-allowed-to-test-on-apes-480902.html>

Tornabene's Bandogge Mastiffs and Performance Neapolitan Mastiffs (2011). *Chisulo "Sulo"* [WWW Reference]. Last Accessed: 8th March, 2012. Available from: <http://www.tornabenebandoggemastiffs.com/Galleries/Chisulo/indexChisulo.html>.

UK Neapolitan Mastiff Club (2005). *Championship Show Results 2005* [WWW Reference]. Last Accessed: 8th March, 2012. Available from: <http://www.uknmc.org.uk/newchampshows05.htm>.

United States Food & Drug Administration (2009). *October 16, 2009 Approval Letter - Cervarix* [WWW Reference]. Last Accessed: Available from: <http://www.fda.gov/BiologicsBloodVaccines/Vaccines/ApprovedProducts/ucm186959.htm>.

Vail DM & MacEwen EG (2000). Spontaneously occurring tumours of companion animals as models for human cancer. *Cancer Invest*, **18**: 781-792.

Veikkolainen V, Vaparanta K, Halkilahti K, Iljin K, Sundvall M & Elenius K (2011). Function of ERBB4 is determined by alternative splicing. *Cell Cycle*, **10**: 2647-2657.

Venter DJ, Tuzi NL, Kumar S & Gullick WJ (1987). Overexpression of the c-erbB-2 oncoprotein in human breast carcinomas: immunohistological assessment correlates with gene amplification. *Lancet*, **2**: 69-72.

Vita GD, Melillo RM, Carlomagno F, Visconti R, Castellone MD, Bellacosa A, Billaud M, Fusco A, Tsihchlis PN & Santoro M (2000). Tyrosine 1062 of RET-MEN2A Mediates Activation of Akt (Protein Kinase B) and Mitogen-activated Protein Kinase Pathways Leading to PC12 Cell Survival. *Cancer Research*, **60**: 3727-3731.

Vogel CL, Cobleigh MA, Tripathy D, Gutheil JC, Harris LN, Fehrenbacher L, Slamon DJ, Murphy M, Novotny WF, Burchmore M, Shak S, Stewart SJ & Press M (2002). Efficacy and Safety of Trastuzumab as a Single Agent in First-Line Treatment of HER2-Overexpressing Metastatic Breast Cancer. *J Clin Oncol*, **20**: 719-726.

Volpert OV, Dameron KM & Bouck N (1997). Sequential development of an angiogenic phenotype by human fibroblasts progressing to tumorigenicity. *Oncogene*, **14**: 1495-1502.

Wang SE, Narasanna A, Perez-Torres M, Xiang B, Wu FY, Yang S, Carpenter G, Gazdar AF, Muthuswamy SK & Arteaga CL (2006). HER2 kinase domain mutation results in constitutive phosphorylation and activation of HER2 and EGFR and resistance to EGFR tyrosine kinase inhibitors. *Cancer cell*, **10**: 25-38.

Wang XZ, Jolicoeur EM, Conte N, Chaffanet M, Zhang Y, Mozziconacci MJ, Feiner H, Birnbaum D, Pébusque MJ & Ron D (1999). γ -heregulin is the product of a chromosomal translocation fusing the DOC4 and HGL/NRG1 genes in the MDA-MB-175 breast cancer cell line. *Oncogene*, **18**: 5718-5721.

Ward C & Garrett T (2001). The relationship between the L1 and L2 domains of the insulin and epidermal growth factor receptors and leucine-rich repeat modules. *BMC Bioinformatics*, **2**: 4.

Waters DJ, Patronek GJ, Bostwick DG & Glickman LT (1996). Comparing the age at prostate cancer diagnosis in humans and dogs. *J Natl Cancer Inst*, **88**: 1686-1687.

- Weber LW, Bowne WB, Wolchok JD, Srinivasan R, Qin J, Moroi Y, Clynes R, Song P, Lewis JJ & Houghton AN (1998). Tumor immunity and autoimmunity induced by immunization with homologous DNA. *J Clin Invest*, **102**: 1258-1264.
- Weigelt B, Peterse JL & van 't Veer LJ (2005). Breast cancer metastasis: markers and models. *Nat Rev Can*, **5**: 591-602.
- Weinberg RA (1995). The retinoblastoma protein and cell cycle control. *Cell*, **81**: 323-330.
- Welsh Cancer Intelligence and Surveillance Unit (2011). *Cancer Incidence in Wales, 2005-2009* [WWW Reference]. Last Accessed: 12th March, 2012. Available from: <http://www.wales.nhs.uk/sites3/page.cfm?orgid=242&pid=51358>.
- Werb Z (1997). ECM and cell surface proteolysis: regulating cellular ecology. *Cell*, **91**: 439-442.
- Whitehead S, Viner B, Cuddy B & Sullivan K (1999). *The Complete Dog Guide* [Book]. Barnes & Noble Books.
- Wolchok JD, Livingston PO & Houghton AN (1998). Vaccines and other adjuvant therapies for melanoma. *Hematol Oncol Clin North Am*, **12**: 835-848.
- Wong ST, Winchell LF, McCune BK, Earp HS, Teixido J, Massague J, Herman B & Lee DC (1989). The TGF- β precursor expressed on the cell surface binds to the EGF receptor on adjacent cells, leading to signal transduction. *Cell*, **56**: 495-506.
- Woods A, Sherwin T, Sasse R, MacRae TH, Baines AJ & Gull K (1989). Definition of individual components within the cytoskeleton of *Trypanosoma brucei* by a library of monoclonal antibodies. *J Cell Sci*, **93**: 491-500.
- World Health Organisation (2009). *Human papillomavirus (HPV)* [WWW Reference]. Last Accessed: 4th March, 2011. Available from: <http://www.who.int/nuvi/hpv/en/>.
- Wright WE, Pereira-Smith OM & Shay JW (1989). Reversible cellular senescence: implications for immortalization of normal human diploid fibroblasts. *Mol Cell Biol*, **9**: 3088-3092.
- Wu S, Skolnick J & Zhang Y (2007). Ab initio modeling of small proteins by iterative TASSER simulations. *BMC Biol*, **5**: 17.
- Yancey MF, Merritt DA, Lesman SP, Boucher JF & Michels GM (2010). Pharmacokinetic properties of toceranib phosphate (Palladia™, SU11654), a novel tyrosine kinase inhibitor, in laboratory dogs and dogs with mast cell tumors. *J Vet Pharmacol Ther*, **33**: 162-171.
- Young BS, Lowe JS, Stevens A & Heath JW (2006). *Wheater's Functional Histology* [Book]. Churchill Livingstone Elsevier.
- Yun C-H, Mengwasser KE, Toms AV, Woo MS, Greulich H, Wong K-K, Meyerson M & Eck MJ (2008). The T790M mutation in EGFR kinase causes drug resistance by increasing the affinity for ATP. *Proc Natl Acad Sci*, **105**: 2070-2075.

Zhang B, Pan X, Cobb GP & Anderson TA (2007). microRNAs as oncogenes and tumor suppressors. *Dev Biol*, **302**: 1.

Zhang Y (2007). Template-based modeling and free modeling by I-TASSER in CASP7. *Proteins*, **69**: 108-117.

Zhang Y (2008). I-TASSER server for protein 3D structure prediction. *BMC Bioinformatics*, **9**: 40.

Zwick E, Bange J & Ullrich A (2001). Receptor tyrosine kinase signalling as a target for cancer intervention strategies. *Endocr Relat Cancer*, **8**: 161-173.

APPENDICES

APPENDIX I: EXAMPLES OF UNCROPPED PCR GEL IMAGES AND WESTERN BLOT AUTORADIOGRAPHS

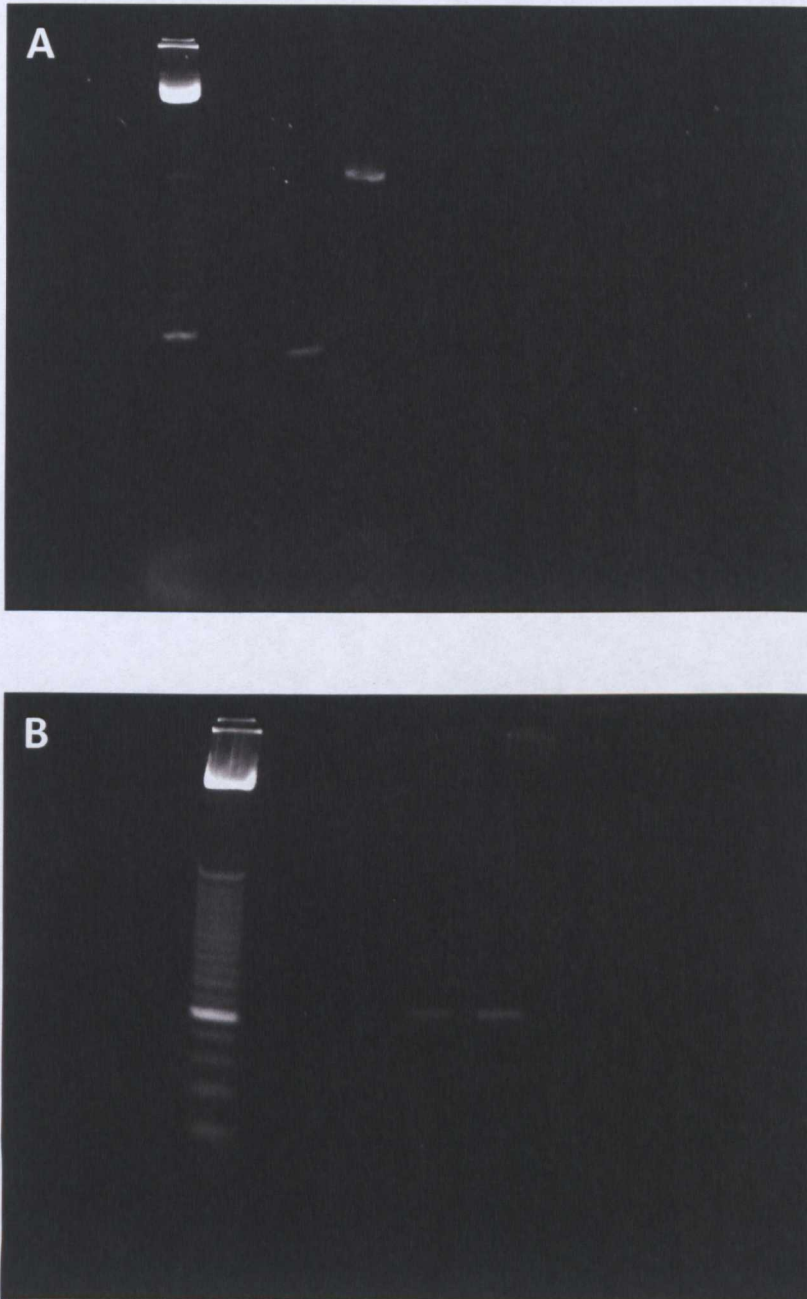


Figure A-1: Examples of uncropped PCR agarose gels. **A:** CMT28 cDNA with primers for HER2; **B:** MDCK cDNA with primers against EGFR. Gels were cropped to fit better on the page and to remove excess features such as empty wells or air bubbles.

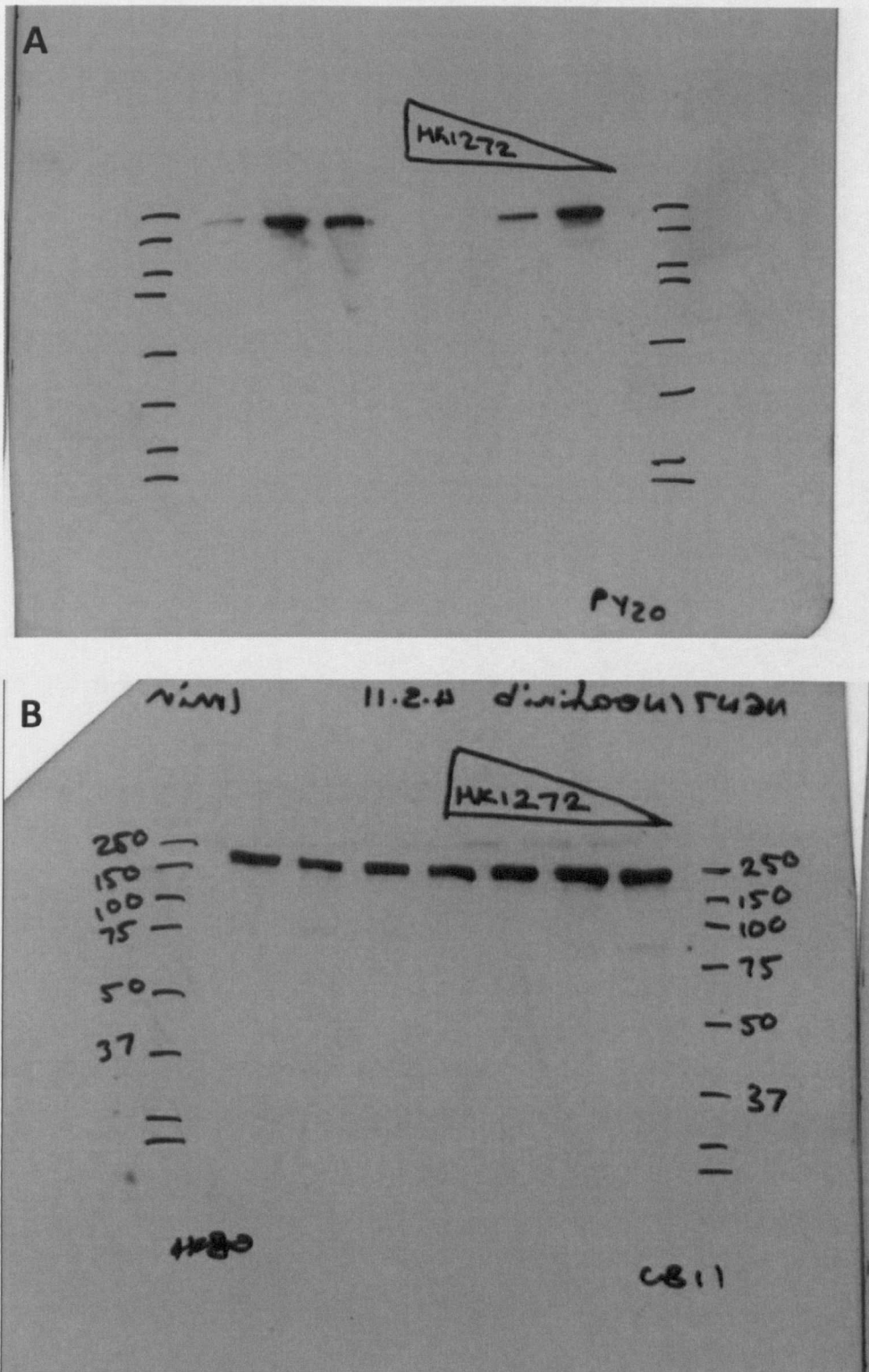


Figure A-2: Examples of uncropped Western Blot autoradiographs. Blots with NEN-7 lysates from cells which were treated with Neratinib. **A:** Blot probed with PY20 antibody (for phosphotyrosine); **B:** Blot probed with CB11 antibody (for HER2).

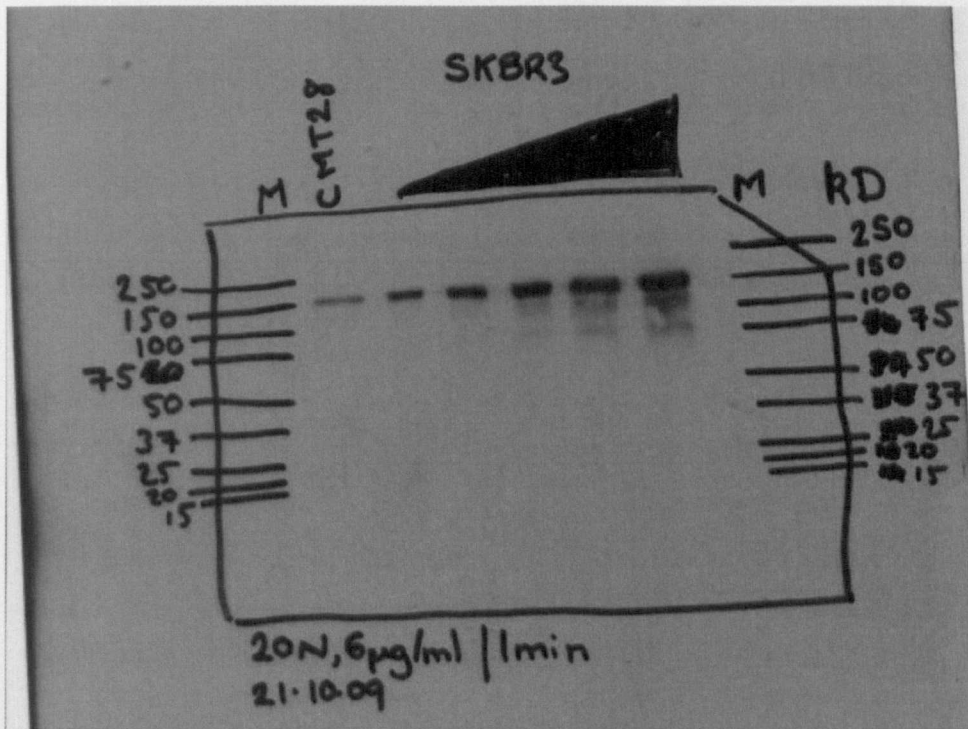


Figure A-3: Example of uncropped Western Blot where SKBR3 lysate was compared with CMT28 lysates and probed for HER2 with the 20N antibody. Blots were cropped to remove excess blank autoradiograph and hand-written annotations.

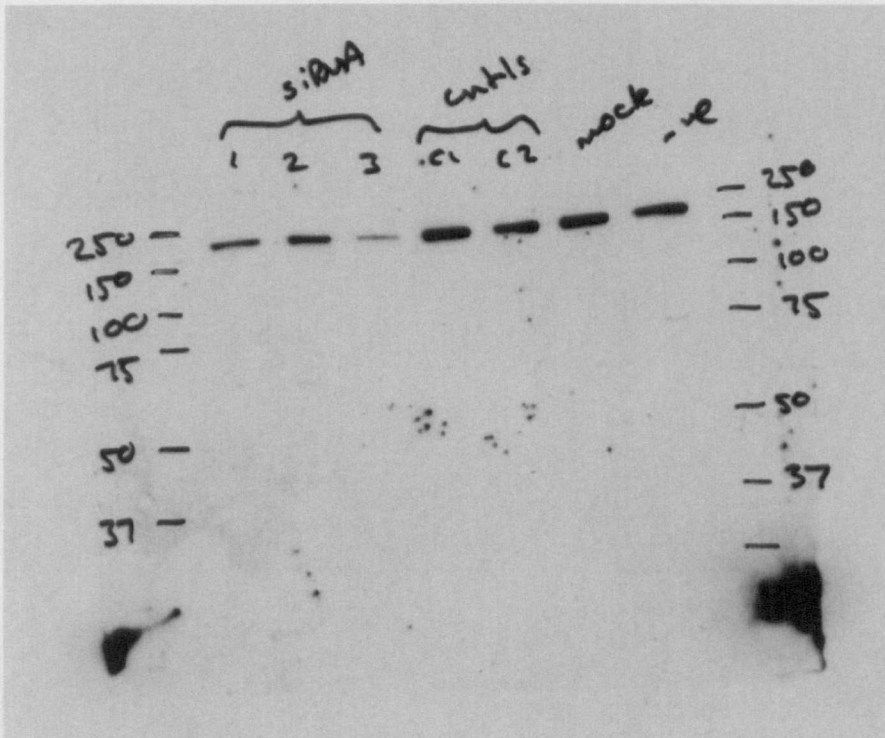


Figure A-4: Example of uncropped Western Blot where CMT28 cells were treated with siRNA and assayed for knockdown after 24 hours by probing for HER2 with the 20N antibody. Blots were cropped to remove excess blank autoradiograph and hand-written annotations.

**APPENDIX II: IMAGE CATALOGUE OF
IMMUNOHISTOCHEMICAL STAINS ON NORMAL AND
CANCEROUS CANINE TISSUES**

These results are presented as a DVD attached to the back cover of this thesis.

Please read the "READ ME" files with regard to scale bars and file nomenclature.

APPENDIX III: RAW DATA FROM CELL PROLIFERATION EXPERIMENTS

Raw data from cell proliferation experiments used to create the graphs presented in Chapter Seven.

The Effect of EGF on CMT28 cell growth

Column	CMT28 cells (600 cells/well) & EGF concentration					
	Blank (media only)	Cells only	1x10 ⁻⁹ M	1x10 ⁻⁸ M	1x10 ⁻⁷ M	1x10 ⁻⁶ M
2	0.121	0.271	0.252	0.289	0.282	0.206
3	0.144	0.268	0.293	0.299	0.294	0.181
4	0.127	0.258	0.274	0.292	0.271	0.193
5	0.128	0.251	0.290	0.291	0.283	0.199
6	0.149	0.274	0.273	0.280	0.298	0.183
7	0.134	0.246	0.269	0.280	0.285	0.218
8	0.132	0.247	0.273	0.281	0.277	0.188
9	0.124	0.232	0.243	0.267	0.301	0.193
10	0.123	0.227	0.266	0.249	0.273	0.184
11	0.113	0.226	0.260	0.301	0.273	0.201
AVERAGE	0.130	0.250	0.269	0.283	0.284	0.195
AVERAGE-media only	0.000	0.121	0.140	0.153	0.154	0.065
STDEV.P	0.010210289	0.0169115	0.014588	0.014815	0.010247	0.011038
SE	0.003228777	0.0053479	0.004613	0.004685	0.003241	0.003491

The Effect of NRG1β on CMT28 Cell Growth

Column	CMT28 cells (600 cells/well) & NRG1β concentration						
	Blank (media only)	Cells only	1x10 ⁻⁹ M	1x10 ⁻⁸ M	1x10 ⁻⁷ M	1x10 ⁻⁶ M	
2	0.111	0.275	0.226	0.250	0.293	0.282	
3	0.104	0.254	0.262	0.277	0.302	0.262	
4	0.105	0.253	0.283	0.278	0.277	0.215	
5	0.111	0.259	0.256	0.294	0.260	0.361	
6	0.115	0.259	0.285	0.288	0.265	0.292	
7	0.110	0.224	0.301	0.327	0.256	0.348	
8	0.109	0.213	0.270	0.284	0.243	0.295	
9	0.110	0.241	0.263	0.285	0.284	0.321	
10	0.106	0.174	0.257	0.280	0.246	0.267	
11	0.115	0.235	0.322	0.305	0.253	0.299	
AVERAGE	0.110	0.239	0.273	0.287	0.268	0.294	
AVERAGE-media only	0.000	0.129	0.163	0.177	0.158	0.185	
STDEV.P	0.003583295	0.02768	0.025319	0.018936	0.019154	0.040375	
SE	0.001133137	0.008753	0.008007	0.005988	0.006057	0.012768	

Combined Lapatinib Data

Date	Column	CMT28 cells (600 cells/well) & lapatinib concentration					
		Media only	Cells only	1x10 ⁻⁹ M	1x10 ⁻⁸ M	1x10 ⁻⁷ M	1x10 ⁻⁶ M
17.3.11	2	0.141	0.250	0.255	0.261	0.251	0.151
	3	0.133	0.274	0.266	0.263	0.231	0.153
	4	0.134	0.262	0.267	0.256	0.149	0.144
	5	0.141	0.250	0.273	0.276	0.141	0.132
	6	0.139	0.280	0.268	0.261	0.149	0.150
	7	0.140	0.302	0.276	0.283	0.147	0.133
	8	0.136	0.280	0.252	0.267	0.150	0.138
	9	0.139	0.273	0.281	0.257	0.142	0.132
	10	0.144	0.293	0.251	0.240	0.153	0.138
	11	0.149	0.280	0.267	0.271	0.138	0.144
28.3.11	2	0.137	0.214	0.132	0.190	0.181	0.138
	3	0.131	0.241	0.187	0.201	0.192	0.141
	4	0.145	0.251	0.172	0.196	0.185	0.140
	5	0.134	0.202	0.168	0.207	0.181	0.164
	6	0.159	0.243	0.164	0.192	0.187	0.144
	7	0.146	0.245	0.160	0.198	0.185	0.145
	8	0.137	0.250	0.165	0.193	0.182	0.139
	9	0.143	0.251	0.195	0.203	0.189	0.140
	10	0.137	0.221	0.177	0.193	0.188	0.137
	11	0.139	0.226	0.177	0.204	0.172	0.148
7.4.11	2	0.117	0.216	0.228	0.231	0.281	0.129
	3	0.119	0.242	0.285	0.235	0.254	0.141
	4	0.121	0.228	0.228	0.220	0.200	0.139
	5	0.132	0.220	0.215	0.227	0.229	0.136
	6	0.131	0.287	0.301	0.246	0.279	0.142
	7	0.133	0.248	0.252	0.244	0.214	0.140
	8	0.129	0.271	0.304	0.273	0.252	0.143
	9	0.094	0.239	0.220	0.294	0.205	0.147
	10	0.126	0.260	0.307	0.228	0.222	0.138
	11	0.126	0.313	0.279	0.302	0.285	0.133
AVERAGE		0.134	0.254	0.232	0.237	0.197	0.141
AVERAGE-media only		0.000	0.119	0.098	0.103	0.063	0.007
STDEV.P		0.01153 43	0.026997 4	0.050031 7	0.033391 5	0.043472 4	0.007085 9
SE		0.00210 586	0.004929	0.009134 5	0.006096 4	0.007936 9	0.001293 7

Combined Neratinib Data

Date	Column	CMT28 cells (600 cells/well) & neratinib concentration					
		Media only	Cells only	1x10 ⁻⁹ M	1x10 ⁻⁸ M	1x10 ⁻⁷ M	1x10 ⁻⁶ M
17.3.11	2	0.145	0.198	0.184	0.244	0.142	0.151
	3	0.140	0.236	0.244	0.204	0.176	0.144
	4	0.134	0.239	0.207	0.174	0.170	0.153
	5	0.140	0.255	0.193	0.196	0.177	0.145
	6	0.135	0.230	0.181	0.201	0.183	0.158
	7	0.138	0.247	0.182	0.217	0.192	0.160
	8	0.129	0.245	0.176	0.193	0.171	0.131
	9	0.136	0.243	0.141	0.188	0.197	0.132
	10	0.138	0.248	0.153	0.212	0.180	0.130
	11	0.140	0.236	0.198	0.144	0.184	0.144
28.3.11	2	0.118	0.292	0.186	0.157	0.160	0.151
	3	0.130	0.266	0.176	0.179	0.163	0.165
	4	0.138	0.256	0.186	0.177	0.156	0.166
	5	0.138	0.252	0.170	0.183	0.174	0.164
	6	0.148	0.266	0.186	0.179	0.167	0.168
	7	0.142	0.236	0.196	0.181	0.168	0.165
	8	0.140	0.252	0.173	0.186	0.169	0.160
	9	0.137	0.243	0.198	0.178	0.178	0.160
	10	0.141	0.254	0.175	0.184	0.184	0.159
	11	0.138	0.239	0.166	0.173	0.173	0.159
20.4.11	2	0.163	0.408	0.307	0.279	0.247	0.196
	3	0.186	0.364	0.343	0.298	0.244	0.216
	4	0.183	0.368	0.340	0.304	0.253	0.200
	5	0.184	0.375	0.386	0.274	0.241	0.195
	6	0.184	0.422	0.265	0.258	0.234	0.164
	7	0.185	0.388	0.291	0.286	0.247	0.236
	8	0.185	0.325	0.286	0.262	0.214	0.187
	9	0.183	0.340	0.299	0.289	0.234	0.200
	10	0.179	0.282	0.291	0.272	0.209	0.182
	11	0.182	0.297	0.270	0.265	0.222	0.206
AVERAGE		0.152	0.283	0.225	0.218	0.194	0.168
AVERAGE-media only		0.000	0.131	0.073	0.066	0.042	0.016
STDEV.P		0.021724 77	0.059458 4	0.064321 3	0.047060 5	0.031650 7	0.025553 5
SE		0.003966 38	0.010855 6	0.011743 4	0.008592	0.005778 6	0.004665 4

Combined Data for the Effect of siRNA on CMT28 Cell Growth

Date	Column	Treatment (33nM/well)				
		Media only	Mock	siRNA1 33nM	siRNA3 33nM	Cntrl1 33nM
11.4.11	2	0.112	0.253	0.356	0.282	0.197
	3	0.118	0.239	0.243	0.179	0.194
	4	0.114	0.217	0.343	0.201	0.199
	5	0.114	0.265	0.356	0.160	0.167
	6	0.117	0.294	0.237	0.187	0.182
	7	0.123	0.264	0.193	0.162	0.191
	8	0.118	0.253	0.192	0.169	0.165
	9	0.116	0.269	0.157	0.163	0.172
	10	0.124	0.248	0.163	0.158	0.175
	11	0.120	0.268	0.153	0.152	0.184
19.4.11	2	0.131	0.260	0.231	0.164	0.205
	3	0.128	0.372	0.157	0.164	0.244
	4	0.125	0.300	0.219	0.200	0.252
	5	0.139	0.253	0.152	0.158	0.196
	6	0.128	0.236	0.146	0.159	0.181
	7	0.139	0.213	0.153	0.167	0.166
	8	0.127	0.231	0.169	0.145	0.174
	9	0.132	0.192	0.160	0.164	0.230
	10	0.137	0.222	0.169	0.147	0.185
	11	0.133	0.183	0.133	0.148	0.180
4.5.11	2	0.165	0.196	0.191	0.185	0.165
	3	0.190	0.224	0.215	0.186	0.188
	4	0.165	0.196	0.188	0.212	0.191
	5	0.172	0.208	0.187	0.203	0.178
	6	0.177	0.181	0.193	0.187	0.190
	7	0.184	0.189	0.185	0.204	0.183
	8	0.177	0.187	0.176	0.214	0.186
	9	0.226	0.201	0.202	0.208	0.184
	10	0.183	0.193	0.215	0.190	0.191
	11	0.178	0.189	0.182	0.208	0.186
AVERAGE		0.144	0.233	0.201	0.181	0.189
AVERAGE-media only		0.000	0.089	0.057	0.037	0.046
STDEV.P		0.0293029	0.0424094	0.0573014	0.0282474	0.0204034
SE		0.00535	0.0077429	0.0104618	0.0051572	0.0037251

APPENDIX IV: WESTERN BLOTS FOR HER3

Attempts were made to blot for the presence of HER3 in CMT28 cells through comparison with HEK293-HER3 cells, although numerous bands repeatedly appeared when using both CMT28 lysates and HEK293-HER3 lysates.

An experiment making use of proteasome inhibitor MG132 appeared to increase the strength of the band at the expected size, but we were unable to resolve one reliable band.

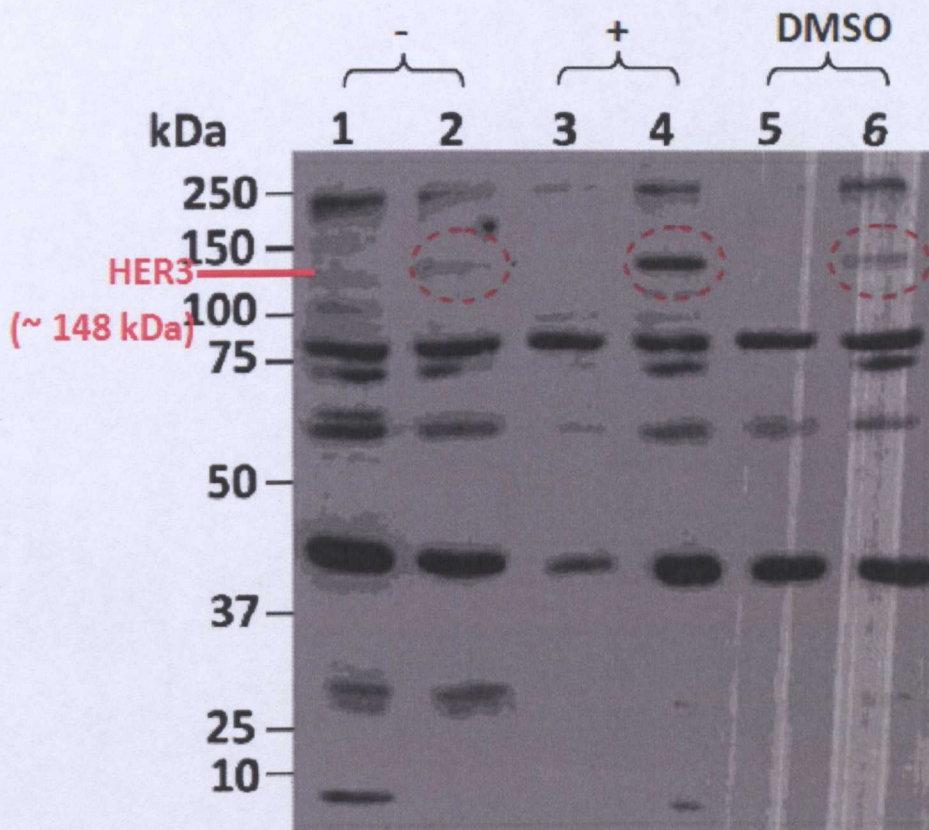


Figure A-5: Experiment to investigate the effect of adding proteasome inhibitor MG132 to HEK-293 and HEK293/HER3 cells on the number of bands visible after probing for HER3. **Lanes 1 & 2:** HEK-293 and HEK-293/HER3 cells (respectively) treated with PBS as a negative control; **Lanes 3 & 4:** HEK-293 and HEK-293/HER3 cells (respectively) treated with 20 μ M of MG132 proteasome inhibitor. The HEK-293/HER3 cells showed an increase in the intensity of the band at the expected size of HER3, following the addition of this inhibitor (highlighted with red circle); **Lanes 5 & 6:** HEK-293 and HEK-293/HER3 cells (respectively) treated with inhibitor vehicle only (DMSO).